Bacterial Immunotherapy: Redirecting the Immune System for Antibacterial Therapeutics

Brianna Elizabeth Dalesandro

B.S. Chemistry, DeSales University, 2017

A Dissertation

Presented to the Graduate Faculty of the University of Virginia in Candidacy for the

Degree of Doctor of Philosophy

Department of Chemistry

University of Virginia

November 2022

Abstract

Bacterial resistance has posed an immense threat to healthcare worldwide. Within the last year, nearly 2 million people were identified as having a drug resistant bacterial infection, and approximately 23,000 of these infections had a fatal outcome. The Centers for Disease Control and Prevention attributes this exponential increase in drug resistance to overuse of antibiotics resulting from over administration and improper prescribing. In the presence of antibiotics, a bacterium can undergo a mutation that induces drug resistance. Continued dosing of the antibiotic effectively eliminates the susceptible bacteria while the resistant phenotype rapidly divides, resulting in increased pathogenicity. Therefore, the development of new methods to treat this increasing number of resistant infections is crucial. Tailoring an immune response as a therapeutic modality has seen much success within the past several years, especially for the treatment of cancer. Interesting, oncological therapeutics such as preventative vaccines, monoclonal antibodies, and chimeric antigen receptor T cell therapy (CAR-T) are all FDA approved cancer treatments despite cancerous cells and healthy cells exhibiting high chemical and physical similarities. To this end, the bacterial cell surface is composed of structural modalities that are inherently unique from that of the host cell, ultimately increasing therapeutic specificity while limiting off target cytotoxicity. With this in mind, the focus of this thesis will be on applying immunotherapeutic applications to aid and enhance the immune system in response to bacterial infections.

Understanding the mechanisms of bacterial resistance is essential for developing new therapeutic measures to combat such pathogens. Chapter 1 will describe the history of antibiotics, their targets, and specific methods of resistance. The details of the bacterial cell envelope, the peptidoglycan (PG) layer in particular, will be described, as it is a primary target of antibiotics of which structural changes to the PG are a major contributing factor to antibiotic resistance. Additionally, the bacterial cell wall is the principal stimulating factor of both innate and adaptive immune responses against infection. As such, Chapter 2 will describe the host recognition and defensive mechanisms directed

toward invading bacterial pathogens, along with a comprehensive review of the advances to date in immunotherapies targeted at bacteria pathogens.

Chapters 3 describes the use of a novel synthetic PG stem peptide mimic tagged with a hapten to re-direct an immune response against drug resistant bacteria. To date, immune modulation of bacterial cells utilizing metabolic processes has been limited to mimics of natural substrates that require millimolar concentrations for effective labeling, such as single D-amino acids. The synthetic nature of the PG stem peptide mimics enabled a large degree of bacterial cell labeling due to high substrate recognition and specificity by PG crosslinking enzymes. As a result, relatively low concentrations of the hapten modified PG stem peptide mimic were needed to induce antibody recognition and enhanced phagocytotic uptake of drug resistant pathogens.

The innate immune system employs many mechanisms to detect bacterial pathogens. Taking inspiration from natural bacterial binding proteins, Chapter 4 describes the tagging of bacterial PG with a peptide fragment derived from the immune system of ticks. Modification of this peptide with a hapten enabled specific binding of bacterial cell surfaces, and effectively directed an immune response against pathogenic *Enterococci* species. Additionally, it was demonstrated that both exogenous and endogenous haptens can be installed on the PG binding peptide to effectively target bacterial cells for clearance by the immune system.

Bacteria have evolved several means of immune evasion and pressure from antibiotics. One of which involves transitioning from existing extracellularly to being able to survive within the intracellular host environment. Chapter 5 aims to examine intracellular *Staphylococcus aureus* in regard to avoiding antibiotic pressure. *S. aureus* is a pathogenic bacterium that has evolved to evade immune detection by proliferating intracellularly within host and immune cells. A challenge with treating such infections lies within the ability to uncover if decreased antibiotic efficacy is a result of poor antibiotic permeation into the host cytosolic compartments or phenotypic changes to the bacterium in response to immune defense. We described the use of a PG tag to covalently anchor

a biorthogonal click handle to the surface of *S. aureus* PG and assess the ability of azide modified antibiotics to react with the available click handle. We envisioned that comparing the reactions of the antibiotic between extracellular and intracellular *S. aureus* will give insight towards the permeability of antibiotics versus antibiotic efficacy within host cells.

Acknowledgements

I would like to dedicate this dissertation to my parents, Amy and Brian, for their continued love and support throughout my journey in becoming a Doctor of Philosophy.

Table of Contents

Chapter 1 Introduction

1.1 Discovery of Antibiotics

Bacteria were first identified in the 1670s by Antoni von Leeuwenhoek; however, it was not until two centuries later that the critical correlation between bacteria and disease was observed. Interestingly, this discovery not only spurred a flux in research regarding how bacteria are the causative modality of many diseases, but also in how to kill, inhibit, or slow the growth of these pathogenic bacteria.[1] Prior to the discovery of antibiotics, society faced waves of epidemics such as cholera, tuberculosis, plague, typhoid fever, syphilis, and leprosy.[2] Although epidemics still exist today, the discovery of antibiotics significantly improved the percentage of infection related deaths, and is considered to be one of the most successful medicinal discoveries in history.

In 1909, Paul Ehrlich identified the first synthetic sulfa drug, arsphenamine (salvarsan), that was used to treat syphilis only a few months after its discovery.[1, 3] Soon after, salvarsan was replaced with a sulfonamide prodrug, Prontosil, discovered by Gerhard Domagk, for which he was awarded a Nobel Prize in Medicine in 1939. Domagk continued the work of Ehrlich to develop sulfonamides as the first successful synthetic, broad-spectrum antimicrobial chemotherapy.[4]

In 1928, Alexander Fleming discovered the first natural antibiotic when he noticed inhibition of *Staphylococcus* growth by a secreted fluid from mold on a petri dish. He found that this 'mould juice,' of which he called penicillin, was effective against all Gram-positive pathogens; therefore, in 1940, penicillin began mass production for use during WWII.[2, 3] Concurrently, Selman Waksman, a researcher of soil-derived bacterium, coined the term 'antibiotic' as a chemical compound generated by a microorganism that is used for inhibition or destruction of microbes.[3] Waksman discovered that soil-derived streptomyces produced compounds with inherent antimicrobial activity. In a similar manner to Fleming, this unanticipated discovery triggered the development of a systematic screening process for the identification of naturally derived antimicrobial

molecules, known as the 'Waksman platform'. One of these molecules was streptomycin, the first aminoglycoside antibiotic, that exhibits potent activity against tuberculosis (TB).[5]
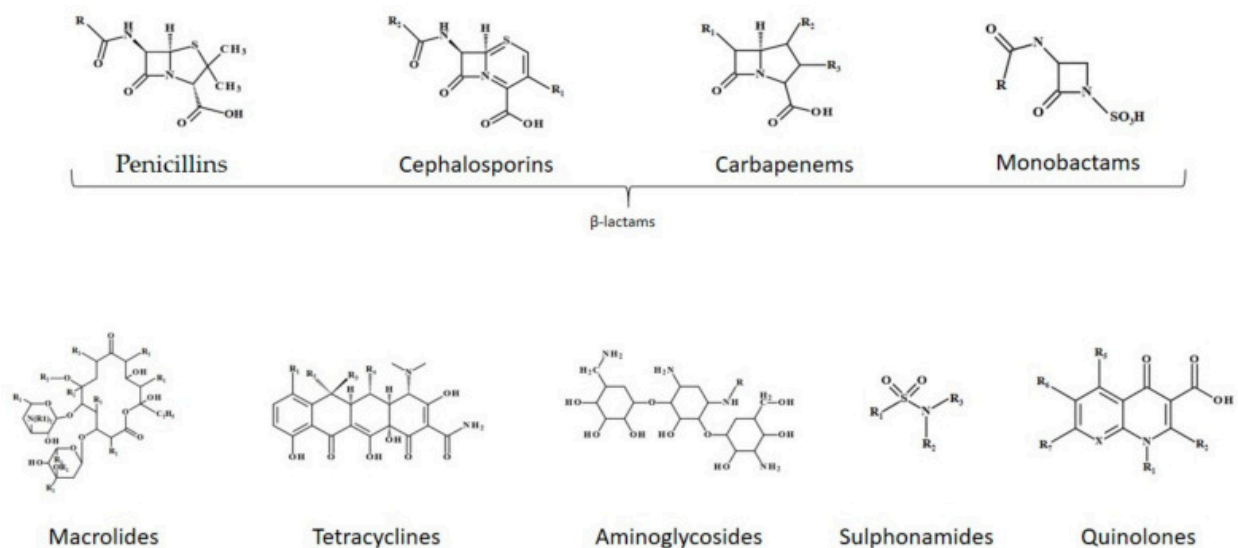
Figure 1.1 *Structures of the main classes of antibiotics.*

Reproduced with permission from[1].

Over the next 20 years, the 'Golden Age of Antibiotics' was attributed with the discovery of several major classes of natural and synthetic antibiotics that are currently used for clinical use today.[2] Such antibiotics include 1) natural antibiotics isolated from actinomycetes such as glycopeptides, tetracyclines, macrolides, aminoglycosides, and amphenicols, 2) fungal origin antibiotics such as penicillins and cephalosporins, and 3) synthetic antibiotics such as sulfones, quinolones, and azoles. The 1980s gave rise to additional β-lactam antibiotics: carbapenems and monobactams, and the 2000s improved upon the synthetic antibiotic classes: quinolone and oxazolidinone (Figure 1.1).[1]

1.2 Antibiotic Targets

Antibiotics are classified based on their mechanism of action in which they impart antibacterial effects. Antibiotics act in one of two ways: those that directly kill bacteria

(bactericidal) or those that inhibit bacterial cell growth (bacteriostatic). Examples of bactericidal antibiotics include aminoglycosides, β-lactams, and glycopeptides while examples of bacteriostatic antibiotics include macrolides, tetracyclines, linezolid, chloramphenicol, and oxazolidinones.[6] Although antibiotics function as either bactericidal or bacteriostatic, the antibiotics can be further categorized based on their cellular target and mechanism of killing/ inhibition. These categories include cell wall targeting antibiotics, inhibitors of protein biosynthesis, inhibitors of DNA replication, and folic acid metabolism inhibitors.[7]

Antibiotics that target the cell wall are categorized as bactericidal. The cell wall maintains the physical and chemical stability of the cell; therefore, antibiotics that aim to disrupt this essential component mechanistically function *via* direct killing of the microbe. β-lactams and glycopeptides inhibit cell wall synthesis enzymes, of such results in cell lysis and death. The first discovered natural antibiotic, penicillin, is a β-lactam that primarily targets penicillin binding proteins (PBPs), critical PG biosynthesis enzymes. Similarly, the glycopeptide, vancomycin, prevents cell wall synthesis enzymes from binding to cell wall precursors, hence inhibiting cell wall synthesis.[1, 7]

Inhibitors of protein biosynthesis function by targeting one of the two bacterial 70S ribosomal subunits, the 30S or 50S subunits, to effectively halt protein expression and lead to cell death. Inhibitors of the 30S subunit include aminoglycosides (AGs) and tetracyclines.[7] AGs are typically positively charged molecules that electrostatically bind to the outer membrane (in the case of Gram- negative) that result in the formation of large pores within the membrane to enable antibiotic permeation into the periplasmic space. Further, the antibiotic passes through the cytoplasmic membrane *via* an active proton motive force to reach the intended target of cytosolic ribosomes. For this reason, AGs can act synergistically with cell wall biosynthesis inhibitors, as such will cause membrane disruption, enabling greater uptake of AGs into the cytosol at a lower energy cost. Upon the intracellular accumulation of AGs, the AGs will hydrogen bond with the 16S ribosomal RNA (rRNA) near the A site of the 30S subunit, leading to misreading, error prone protein synthesis, and premature termination of the messenger RNA (mRNA).[8] Tetracycline is a

protein synthesis inhibiting antibiotic that functions by preventing the attachment of the aminoacyl-transfer RNA (tRNA) to the acceptor site (A site) of the 30S subunit. When this process is inhibited, protein synthesis halts; therefore, preventing bacterial cell growth. For this reason, tetracycline is categorized as a bacteriostatic antibiotic.[7, 9] Inhibitors of the 50S subunit include chloramphenicol, macrolides, and oxazolidinones. Chloramphenicol prevents protein chain elongation by inhibiting the peptidyl transferase of the ribosome by binding to a specific sequence of the 23S rRNA of the 50S subunit.[10] Macrolides, similar to chloramphenicol, function by preventing chain elongation; however, they also inhibit ribosomal translocation by targeting the peptidyl transferase of the 50S subunit.[11] Linezolid is an oxazolidinone (a novel class of entirely synthetic antibiotics) that blocks the initiation of protein production by binding the 23S rRNA on the 50S subunit to prevent formation of the 70S initiation complex, thereby preventing protein expression and bacterial division.[12]

Inhibitors of DNA replication include the quinolone class of antibiotics. Quinolones directly kill bacteria (bactericidal) by acting on enzymes essential for DNA replication such as bacterial type II topoisomerases, DNA gyrase, and topoisomerase IV to inhibit their function. Inhibition of such proteins triggers double stranded breaks to the bacterial chromosomal DNA, resulting in bacterial cell death. For example, fluoroquinolones (FQ) inhibit DNA gyrase, an enzyme responsible for maintaining excess supercoiling of DNA at the replication fork. Inhibition of DNA gyrase by FQ interferes with the strand cutting and resealing ability of the enzyme; therefore, stalling DNA replication.[13, 14]

Folic acid is essential for bacterial cell growth and survival; therefore, molecules that interfere with folic acid synthesis are employable as antibiotics. Examples of current antibiotics that inhibit folic acid metabolism are sulfonamide and trimethoprim. Each inhibits a distinct step in folic acid metabolism. Sulfonamides inhibit dihydropteroate synthesis by competitive binding over its natural substrate, p-amino benzoic acid (PABA); whereas trimethoprim acts at a later stage in the pathway by inhibiting the dihydrofolate reductase enzyme that reduces dihydrofolic acid to tetrahydrofolic acid. Both of which

inhibit the synthesis of folic acid and result in bacterial cell death in a bacteriostatic manner.[15]

It is becoming increasingly important to understand the mechanisms by which antibiotics target and kill bacterial cells. However, pivotal to the development of new antibiotics is the importance in understanding not only the biophysical entities of the bacterial cell, but also the chemical composition and mechanisms that comprise the bacterial cell wall.

1.3 Bacterial Cell Wall

Microbes have many structural and chemical entities that encourage virulence and pathogenicity. One of the most crucial aspects of the microbe is the cell wall, which is responsible for protecting the bacteria from external threats and maintaining osmotic stability. Physical disruption to the cell wall typically results in cell lysis due to osmotic instability; therefore, cell wall integrity is essential for survival of the pathogen. Owning to the importance of the cell wall, bacteria are categorized into classes based on the composition and chemical makeup of their cell wall. The three main classes of bacteria include Gram- positive, Gram- negative, and Mycobacteria.[16]

The main distinctions between Gram- positive and Gram- negative bacteria are the presence of an outer membrane (OM) and the thickness of the peptidoglycan (PG) layer.[17] Gram- negative bacteria have both an OM and an inner membrane (IM). The OM provides protection against threats and harsh environments and is a key proponent toward regulation of what can and cannot permeate the cell wall. The OM is an asymmetrical membrane composed of phospholipids within the inner leaflet and lipopolysaccharide (LPS) in the outer leaflet. LPS plays an important role in the structural stability of the cell, but also in the pathogenicity of the microbe. LPS has three distinct structural units: lipid A, an inner and outer polysaccharide core, and a hydrophilic O-antigen. Lipid A contains a lipid moiety that physically anchors the polysaccharide core into the OM. The inner core is highly conserved and contains the sugars 3-deoxy-D-manno-octulosonic acid (Kdo) and heptose sugars. The outer core of LPS displays high

species variability in polysaccharide composition. The O-antigen is made up of varying lengths polysaccharides and has high implication towards virulence of the pathogen. LPS harbors an overall negative charge due to the presence of several phosphates; however, to prevent electrostatic repulsion, the LPS is stabilized by tight binding to divalent Mg^{2+} and Ca^{2+} cations.[18] The OM also contains various membrane proteins such as porins, efflux pumps, and transport proteins, all of which play a critical role in stability and integrity of the cell.[19] Lipoproteins, which are important for cellular homeostasis and division, connect the outer membrane to a thin (only a few nm) PG layer.[17, 20] This thin layer of PG resides in the periplasmic space between an inner, phospholipid membrane, and the OM. The periplasmic space is a compartment separate from the cytoplasm that has a distinctive reducing environment to enable more efficient protein folding and quality control. Additionally, the periplasmic space contributes to withstanding turgor pressure by providing structural support to the cell in concert with the OM.[21]

Gram-positive bacteria have a thick layer (30-100 nm) of peptidoglycan surrounding an inner membrane.[17] Displayed on the surface of Gram-positive bacteria are families of glycopolymers that play a key role in maintaining the integrity of the cell wall. Wall teichoic acids (WTAs) are covalently linked to an *N*-acetylmuramic acid (MurNAc) unit in the PG through a highly conserved disaccharide linkage, *N*-acetylmannosamine-*N*-acetylglucoasmine-1-phosphate, *via* a phosphodiester bond. WTAs are 20-40 unit long, negatively charged, polyol phosphate polymeric chains of glycerol or ribitol repeats. Although the backbone of WTA is negatively chare, the polymer is overall zwitterionic due to the presence of positively charged D-alanine esters modified to the polyol phosphate backbone.[22] Interestingly, bacteria can execute several chemical modifications to the WTAs in response to antibiotics and other external stimuli in an effort to decrease antibiotic susceptibility, increase virulence, and improve their survival.[23] A second group of glycopolymers found in Gram-positive bacteria are Lipoteichoic Acids (LTAs). LTAs are anchored in the cytoplasmic membrane by a glycolipid and extend through the peptidoglycan to the extracellular space. LTAs are composed of amphiphilic polymeric chains of glycerol phosphate and are essential for maintaining the placement of the peptidoglycan to retain its construction and integrity.[24]

a Gram-negative bacteria

b Gram-positive bacteria
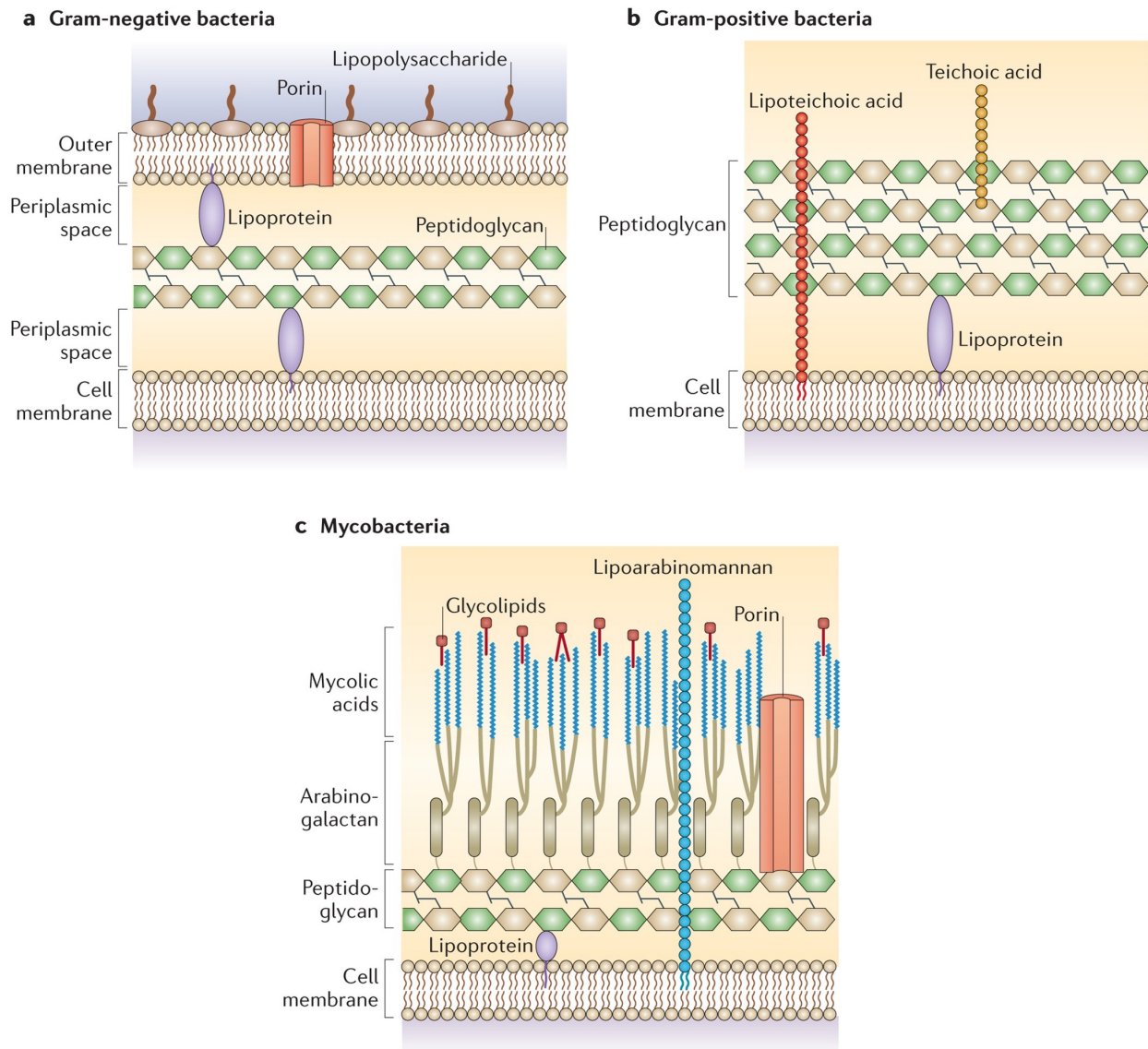
c Mycobacteria

Figure 1.2 *Cellular envelope of (a) Gram- negative, (b) Gram- positive,*

and (c) Mycobacteria. Reproduced with permission from[16].

The mycobacterial cell wall has components of both Gram- negative and Gram- positive; however, there are several distinguishing features unique to mycobacteria. The cell wall consists of an inner, cytoplasmic membrane, surrounded by an essential core cell wall that contains three layers: 1) a thin PG layer, 2) an arabinogalactan layer, and 3) a mycolic acid layer. The inner membrane is composed of phospholipids and is linked to the PG *via*

lipoproteins. The inner membrane also contains long glycolipids that extend the entirety of the cell wall called lipoarabinomannan (LAM). LAM is characterized by three distinct regions: a phosphatidylinositol anchor, a mannan backbone, and several arabinan antennas that attach to the mannan backbone.[25, 26] Unique to mycobacteria are the arabinogalactan and mycolic acid layers. The arabinogalactan layer is comprised of galactose and arabinose sugar residues in the furanose ring form and is connected to the PG *via* a single linker. The mycolic acid layer consists of long chains of α-alkyl-β-hydroxy fatty acid, also known as mycolic acids, and are attached to the arabinogalactan layer.[27]

The bacterial cell wall is composed of many structural motifs that are essential for maintaining cell wall integrity; however, much of the cell wall is comprised of non-essential components that contribute to virulence and pathogenicity rather than entirely structural stability. For instance, the presence of teichoic acids on the Gram- positive cell wall of *Staphylococcus aureus* (*S. aureus*) aids in host colonization, facilitates toxin release, and imparts a significant permeability barrier to the PG and cytosol; however, cell survival was still observed in the absence of WTA.[28-30] Additionally, the LPS layer of Gram- negative bacteria is traditionally considered an essential component of the OM; however, several strains have been identified to survive in the absence of LPS. Certain strains of *Neisseria,* for example, have demonstrated that in absence of the first biosynthetic enzyme of LPS, upregulation of capsular polysaccharide production served to maintain cell wall integrity.[31] *Acinetobacter baumannii* (*A. baumanni*) can also induce an LPS-deficient phenotype that is resistant to LPS targeting antibiotics and can escape recognition from Toll-like receptors on immune cells for increased survival.[32]

1.4 PG biosynthesis and crosslinking

The PG layer is an essential component of the bacterial cell wall regardless of Gram-type. The PG is a network of polymeric molecules crosslinked in a lattice structure that encapsulates the bacterial cell. The backbone of the peptidoglycan, which is highly conserved across bacterial species, consists of repeating disaccharides N-acetylglucosamine (GlcNAc) and N-acetylmuramic acid (MurNAc), that are joined

together by transglycosylases in a β(1-4) linkage. MurNAc is a variant of GlcNAc that has a D-lactate attached to C-3 through an ether bond. Linked to the lactyl group *via* an amide linkage is a short "stem peptide" that is unique to bacteria because it contains alternating L- and D- isomer amino acids. This pentapeptide is composed of amino acid residues L-alanine, D-glutamic Acid, L-lysine, D-alanine, and D-alanine. The sequence of the stem peptide is generally conserved; however, some variation is observed at the 3rd position. For example, many Gram-positive species contain an L-Lysine, such as *S. aureus*, while other Gram- positive and most Gram- negative species contain a *meso*-diaminopimelic acid (*m*-DAP), such as *Bacillus subtilis* (*B. subtilis*) and *Escherichia coli* (*E. coli*).[33]

PG biosynthesis occurs in three stages: the cytoplasmic stage, the membrane-associated stage, and the exocytoplasmic stage. Within the cytoplasmic stage, activated nucleotide precursors, uridine diphosphate-*N*-acetylglucosamine (UDP-GlcNAc) and UDP-*N*-acetylmuramyl pentapeptide, are synthesized and assembled.[34] UDP-GlcNAc is converted to UDP-*N*-acetylmuramic acid (UDP-MurNAc) by MurA and MurB enzymes. The amino acid ligases, MurC, MurD, and MurE, utilize ATP to successively attach the first three amino acids L-ala, L-glu and L-lys/*m*-dap to UDP-MurNAc.[35] Independently, Alr or DadX converts L-ala to D-ala where then DdlA conjugates two D-ala residues together to form the dipeptide D-ala-D-ala. MurF uses ATP to conjugate D-ala-D-ala to the existing UDP-MurNAc-L-ala-D-glu-L-lys/*m*-dap, resulting in the formation of UDP-MurNAc-pepntapeptide.[36]

The membrane associated step begins with a membrane anchored undecaprenol phosphate (C_{55}-P) displacing uridine monophosphate (UMP) from UDP-MurNAc-pentapeptide to create a membrane anchored PG precursor, known as Lipid I. This step is catalyzed by the glycosyltransferase (GTase), MraY. A second GTase, MurG, then catalyzes the attack of a UDP-GlcNAc to MurNAc on Lipid I, forming Lipid II.[37] A flippase enzyme (FtsW, RodA, MurJ) facilitates the transition from the membrane-associated stage to the exocytoplasmic stage by flipping Lipid II across the cytoplasmic membrane to the periplasmic side of the membrane.[38] It is at this point that GTases cleave the PG

backbone from the lipid anchor to begin the exocytoplasmic stage of PG biosynthesis where the newly synthesized PG strand is covalently stitched into the existing PG scaffold.[39]
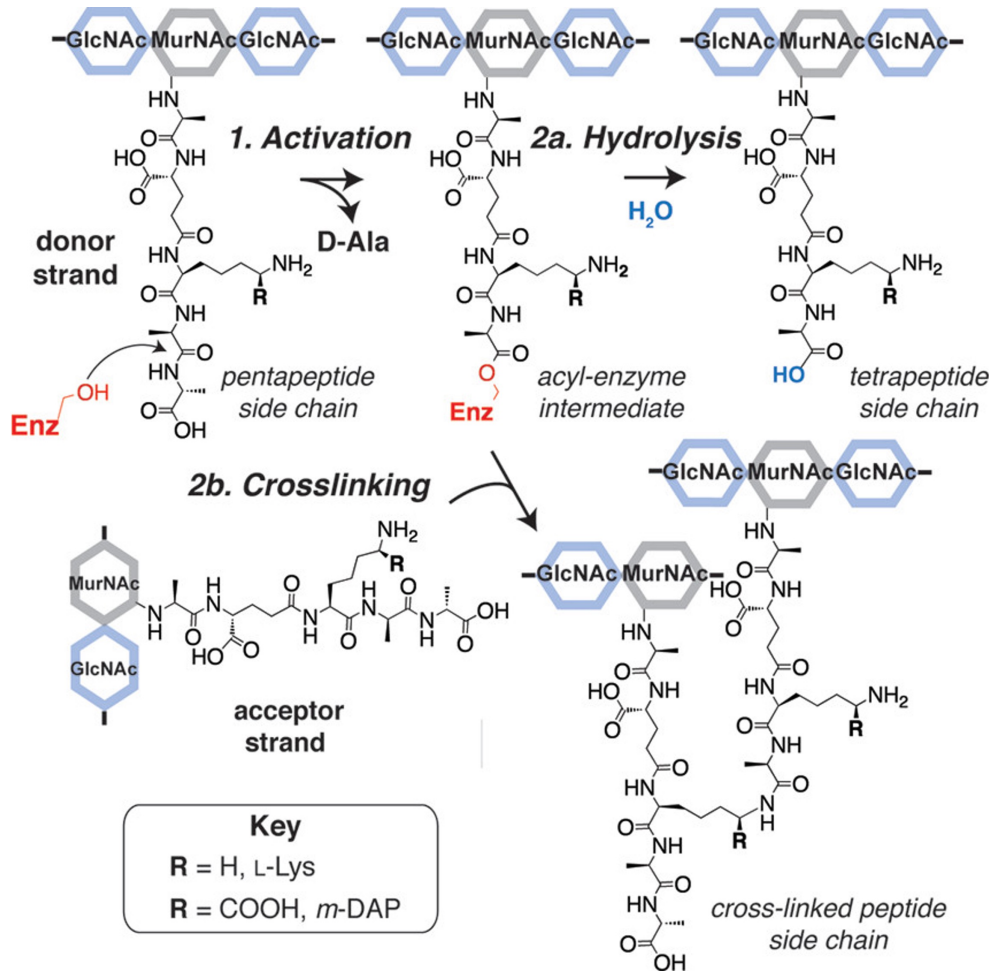
Figure 1.3 *Stepwise mechanism of peptidoglycan (PG) transpeptidases (TPs). Reproduced with permission from[39].*

Step 1. TPs activate PG donor strands resulting in release of terminal D-Ala and formation of an acyl-enzyme intermediate. Step 2. (a) Either hydrolysis of this activated donor or (b) peptide cross-linking to an acceptor strand can then occur.[40]

The extracellular processing of PG is executed by GTases, which link together the repeating units of disaccharides (GlcNAc-MurNAc), and transpeptidases (TPs), that crosslink nascent stem peptide strands to create the mesh-like scaffold that is PG.

Penicillin binding proteins (PBPs), also known as D,D-transpeptidases (Ddts), are TPs that create crosslinks between two adjacent stem peptide strands.[41] Ddts will only recognize pentapeptide strands, as the enzyme has specificity for the two D-stereocenters of the terminal D-ala- D-ala. Upon enzyme binding, sacrifice of the terminal D-ala results in the formation of the acyl- enzyme intermediate between the Ddt active site serine with the carboxy terminus of the stem peptide strand (known as the acyl donor). A reactive L-Lys or *m*-DAP on a neighboring strand (known as the acyl acceptor) displaces the acyl-enzyme intermediate to generate a covalent 4-3 crosslink between the acyl donor and acyl acceptor.[40]

L,D-transpeptidases (Ldts) are a newer class of TPs that, like Ddts, creates crosslinks between nascent stem peptide strands; however, unlike Ddts, Ldts have specificity for tetrapeptide donor strands where the two terminal residues contain an L- and D-stereocenter. Pentapeptide strands are often subject to hydrolysis of the terminal D-ala residue by TPs for the generation of tetrapeptide strands. Upon binding of the tetrapeptide donor strand by Ldts, the acyl-enzyme intermediate forms between the active site cysteine residue of the Ldts and the carboxy terminus of the donor strand, resulting in the sacrifice of the terminal D-ala. A reactive amine of L-lys/*m*-DAP on a neighboring acceptor stand displaces the Ldt to generate a 3-3 crosslink.[42, 43]

TPs are a main target of antibiotics because PG biosynthesis is an essential component of bacterial cell survival, and inhibition of crosslinking enzymes effectively halts cell growth and division. For instance, β-lactam antibiotics mimic directly inhibit TPs by mimicking the D-ala-D-ala substrate of the stem peptide. β-lactams function by forming an irreversible, covalent bond with the TP active site, thereby preventing crosslinking, and resulting in cell death.[44]

1.5 *Bacterial Resistance Mechanisms*

Bacteria have evolved many mechanisms of antibiotic resistance. According to the Centers for Disease Control and Prevention (CDC), antibiotic resistant bacterial infections killed nearly 5 million people globally in 2019. In the US alone, nearly 2.8 million people acquire and antibiotic resistant infection that resulted in around 35,000 fatalities.[45, 46] Antibiotic resistance mechanisms fall into four main categories: 1) inactivating a drug, 2) modifying a drug target, 3) active drug efflux, and 4) limiting drug uptake.

Inactivation of a drug can occur *via* two mechanisms: degradation of the drug molecule or modification of the drug to inactivate its activity. β-lactamases are a class of enzymes produced by bacteria that effectively degrade β-lactam antibiotics, rendering them ineffective. β-lactam antibiotics mimic the chemical structure of D-ala-D-ala, inhibiting PBPs from crosslinking; however, in response to β-lactams, bacteria start expressing β-lactamases that will hydrolyze the β-lactam ring of the antibiotic, inactivating it before prior to its inhibition of PBPs.[47] Additionally, inactivation of an antibiotic by modification with a chemical group is most commonly done with acetylation, phosphorylation, and adenylation. For instance, acetylation to aminoglycosides, chloramphenicol, and fluroquinolones has been demonstrated to reduce antibiotic efficacy.[48]

Modifying the drug target is a major mechanism of antibiotic resistance that occurs in almost all drug target modalities. Most primarily in the class of cell wall synthesis inhibitors. In addition to inactivation of β-lactams by β-lactamases, β-lactams can induce resistance mechanisms such as expression of PBPs with lower affinity to β-lactams and bypassing crosslinking steps *via* Ldts. Another example of modifying the drug target occurs with resistance to vancomycin, which the CDC also indicates as a top priority threat.[49] More specifically, *Enterococcus* species can induce several mechanisms of resistance in response to vancomycin, of which has high affinity for the D-ala-D-ala motif on Lipid II, inhibiting transglycosylation and transpeptidation.[50] The VanA and VanB clusters of genes are expressed upon recognition of vancomycin by membrane bound

sensors (VanR and VanS). As a result, PG precursors are synthesized to end in a depsidipeptide of D-ala-D-lactate (D-lac). This reduces the affinity of vancomycin for its target by 1000- fold. Additionally, both *vanA* and *vanB* clusters encode for a D,D-carboxypeptidase (VanY) that cleaves the terminal D-ala from the stem peptide, further contributing to vancomycin resistance.[51]

Two additional mechanisms of resistance include increasing efflux of the antibiotic and limiting permeation of the antibiotic into the cell. Many chromosomally expressed efflux pumps have been identified to get overexpressed under pressure of antibiotics. For example, Mex efflux pumps of *Pseudomonas aeruginosa* (*P. aeruginosa*) target several classes of antibiotics such as β-lactams, carbapenems, fluoroquinolones, tetracyclines, chloramphenicol, macrolides, and sulphonamides; moreover, drug-resistant clinical isolates have been identified to overexpress this resistance-nodulation-division (RND) pump.[52] Additionally, Gram- negative bacteria have exhibited OM remodeling in response to antibiotics. The OM is highly impermeable due to the presence of the LPS-phospholipid barrier; therefore, permeation of antibiotics is thought to occur via Outer Membrane Porins (Omps). The World Health Organization (WHO) and CDC have identified that all Gram-negative pathogens that feature as urgent threats utilize major porins for nutrient and drug entry into the cell.[53] However, studies done on *E. coli* demonstrated that expression of two major porins (OmpF and OmpC) are controlled by carbapenems and tetracycline, where in response to these antibiotics, OmpF expression is turned on and OmpC expression is turned off.[54] Similar responses have been observed by *Klebsiella pneumoniae* (*K. pneumoniea*) where the outer membrane has remodeled to express no major porin in response to carbapenems.[55]

Although the Golden Age of antibiotics gave rise to many classes of effective antibiotics, resistance started to develop as early as the 1950s. This triggered the modification of existing antibiotic scaffolds to improve their efficacy, but near the end of the 1900s, the development of new antibiotics started to decline while the percent of antibiotic resistant strains, such as methicillin-resistant *Staphylococcus aureus* (MRSA), vancomycin-

resistant *Enterococci* (VRE), and fluoroquinolone-resistant *Pseudomonas aeruginosa* (FQRP), started to increase. To this day, the WHO identifies that the development of new antibacterial treatments is inadequate to address the threat of antibiotic resistance. In a 2021 report, only 12 antibiotics have been approved since 2017 and 10 of which belong to classes of antibiotics that already exhibit antimicrobial resistance. As a result, novel methods to combat bacterial infections must continue to be explored.

1.6 Summary and Future Outlook

Chapter 1 details the discovery and development of different classes of antibiotics and their drug targets, the biology of the bacterial cell wall, and the mechanisms of antimicrobial resistance. To develop effective therapeutic modalities, it is essential to understand the underlying physical and chemical motifs that encompass the bacterial cell. Most importantly, it is critical to understand the chemical entities that comprise the metabolic mechanisms which provide the bacterial cell with the essential components to remain structurally and functionally sound. As such, a significant amount of work within the past several decades has revealed the structural and mechanistic details of a majority of cell wall synthesis enzymes.[56] From this comprehensive characterization, developing antibiotics that have specificity for early-stage enzymes may provide an additional mechanism to treat drug-resistant bacteria. In fact, several inhibitors of early-stage PG biosynthesis enzymes, MraY and MurG, have been identified, but little have entered clinical development. It has been reported this can be attributed to limited cellular permeability of the inhibitors, limited success *in vivo*, and potential cytotoxicity.[57] However, continued efforts to address these associated shortcomings can theoretically be used to potentiate existing antibiotics that act against more common drug targets for synergistic effects. In fact, a study conducted in 2018 revealed that utilizing higher-order drug combinations lead to increased synergy and lower toxicity in some combinations against *E. coli*.[58] Of note, random combinations of drugs may create a myriad of problems; however, formulating an 'antibiotic cocktail' that consists of antibiotics with highly characterized, specified, and varied drug targets may provide a possible solution for treatment of bacterial species that induce rapid drug resistance.

1.7 *References*

1. Pancu, D.F. *et al.* Antibiotics: Conventional Therapy and Natural Compounds with Antibacterial Activity-A Pharmaco-Toxicological Screening. *Antibiotics-Basel* **10** (2021).

2. Cook, M.A. & Wright, G.D. The past, present, and future of antibiotics. *Sci Transl Med* **14** (2022).

3. Peterson, E. & Kaur, P. Antibiotic Resistance Mechanisms in Bacteria: Relationships Between Resistance Determinants of Antibiotic Producers, Environmental Bacteria, and Clinical Pathogens. *Front Microbiol* **9** (2018).

4. Otten, H. Domagk and the Development of the Sulfonamides. *J Antimicrob Chemoth* **17**, 689-690 (1986).

5. Lewis, K. Platforms for antibiotic discovery. *Nat Rev Drug Discov* **12**, 371-387 (2013).

6. Nemeth, J., Oesch, G. & Kuster, S.P. Bacteriostatic versus bactericidal antibiotics for patients with serious bacterial infections: systematic review and meta-analysis. *J Antimicrob Chemoth* **70**, 382-395 (2015).

7. Kapoor, G., Saigal, S. & Elongavan, A. Action and resistance mechanisms of antibiotics: A guide for clinicians. *J Anaesthesiol Clin Pharmacol* **33**, 300-305 (2017).

8. Krause, K.M., Serio, A.W., Kane, T.R. & Connolly, L.E. Aminoglycosides: An Overview. *Csh Perspect Med* **6** (2016).

9. Chopra, I. & Roberts, M. Tetracycline antibiotics: Mode of action, applications, molecular biology, and epidemiology of bacterial resistance. *Microbiol Mol Biol R* **65**, 232-+ (2001).

10. Dinos, G.P. *et al.* Chloramphenicol Derivatives as Antibacterial and Anticancer Agents: Historic Problems and Current Solutions. *Antibiotics-Basel* **5** (2016).

11. Dinos, G.P. The macrolide antibiotic renaissance. *Brit J Pharmacol* **174**, 2967-2983 (2017).

12. Hashemian, S.M., Farhadi, T. & Ganjparvar, M. Linezolid: a review of its properties, function, and use in critical care. *Drug Des Dev Ther* **12**, 1759-1767 (2018).

13. Aldred, K.J., Kerns, R.J. & Osheroff, N. Mechanism of Quinolone Action and Resistance. *Biochemistry-Us* **53**, 1565-1574 (2014).

14. Reece, R.J. & Maxwell, A. DNA Gyrase - Structure and Function. *Crit Rev Biochem Mol* **26**, 335-375 (1991).

15. Smith, C.L. & Powell, K.R. Review of the sulfonamides and trimethoprim. *Pediatr Rev* **21**, 368-371 (2000).

16. Brown, L., Wolf, J.M., Prados-Rosales, R. & Casadevall, A. Through the wall: extracellular vesicles in Gram-positive bacteria, mycobacteria and fungi. *Nat Rev Microbiol* **13**, 620-630 (2015).

17. Silhavy, T.J., Kahne, D. & Walker, S. The Bacterial Cell Envelope. *Csh Perspect Biol* **2** (2010).

18. Simpson, B.W. & Trent, M.S. Pushing the envelope: LPS modifications and their consequences. *Nat Rev Microbiol* **17**, 403-416 (2019).

19. Ruiz, N., Kahne, D. & Silhavy, T.J. Advances in understanding bacterial outer-membrane biogenesis. *Nat Rev Microbiol* **4**, 57-66 (2006).

20. El Rayes, J., Rodriguez-Alonso, R. & Collet, J.F. Lipoproteins in Gram-negative bacteria: new insights into their biogenesis, subcellular targeting and functional roles. *Curr Opin Microbiol* **61**, 25-34 (2021).

21. Miller, S.I. & Salama, N.R. The gram-negative bacterial periplasm: Size matters. *PLoS Biol* **16**, e2004935 (2018).

22. Brown, S., Maria, J.P.S. & Walker, S. Wall Teichoic Acids of Gram-Positive Bacteria. *Annu Rev Microbiol* **67**, 313-336 (2013).

23. Auer, G.K. & Weibel, D.B. Bacterial Cell Mechanics. *Biochemistry-Us* **56**, 3710-3724 (2017).

24. Percy, M.G. & Grundling, A. Lipoteichoic Acid Synthesis and Function in Gram-Positive Bacteria. *Annual Review of Microbiology, Vol 68* **68**, 81-100 (2014).

25. Chan, J., Fan, X.D., Hunter, S.W., Brennan, P.J. & Bloom, B.R. Lipoarabinomannan, a possible virulence factor involved in persistence of Mycobacterium tuberculosis within macrophages. *Infect Immun* **59**, 1755-1761 (1991).

26. De, P. *et al.* Structural implications of lipoarabinomannan glycans from global clinical isolates in diagnosis of Mycobacterium tuberculosis infection. *J Biol Chem* **297**, 101265 (2021).

27. Abrahams, K.A. & Besra, G.S. Mycobacterial cell wall biosynthesis: a multifaceted antibiotic target. *Parasitology* **145**, 116-133 (2018).

28. Brignoli, T. *et al.* Wall Teichoic Acids Facilitate the Release of Toxins from the Surface of Staphylococcus aureus. *Microbiol Spectr* **10**, e0101122 (2022).

29. Ferraro, N.J., Kim, S., Im, W. & Pires, M.M. Systematic Assessment of Accessibility to the Surface of Staphylococcus aureus. *ACS Chem Biol* **16**, 2527-2536 (2021).

30. van Dalen, R., Peschel, A. & van Sorge, N.M. Wall Teichoic Acid in Staphylococcus aureus Host Interaction. *Trends Microbiol* **28**, 985-998 (2020).

31. Zhang, G., Meredith, T.C. & Kahne, D. On the essentiality of lipopolysaccharide to Gram-negative bacteria. *Curr Opin Microbiol* **16**, 779-785 (2013).

32. Moffatt, J.H. *et al.* Lipopolysaccharide-deficient Acinetobacter baumannii shows altered signaling through host Toll-like receptors and increased susceptibility to the host antimicrobial peptide LL-37. *Infect Immun* **81**, 684-689 (2013).

33. Vollmer, W., Blanot, D. & de Pedro, M.A. Peptidoglycan structure and architecture. *Fems Microbiol Rev* **32**, 149-167 (2008).

34. Egan, A.J.F., Errington, J. & Vollmer, W. Regulation of peptidoglycan synthesis and remodelling. *Nat Rev Microbiol* **18**, 446-460 (2020).

35. El Zoeiby, A., Sanschagrin, F. & Levesque, R.C. Structure and function of the Mur enzymes: development of novel inhibitors. *Mol Microbiol* **47**, 1-12 (2003).

36. Sobral, R.G., Ludovice, A.M., de Lencastre, H. & Tomasz, A. Role of murF in cell wall biosynthesis: isolation and characterization of a murF conditional mutant of Staphylococcus aureus. *J Bacteriol* **188**, 2543-2553 (2006).

37. Bouhss, A., Trunkfield, A.E., Bugg, T.D. & Mengin-Lecreulx, D. The biosynthesis of peptidoglycan lipid-linked intermediates. *Fems Microbiol Rev* **32**, 208-233 (2008).

38. Ruiz, N. Lipid Flippases for Bacterial Peptidoglycan Biosynthesis. *Lipid Insights* **8**, 21-31 (2015).

39. Buynak, J.D. Cutting and stitching: the cross-linking of peptidoglycan in the assembly of the bacterial cell wall. *ACS Chem Biol* **2**, 602-605 (2007).

40. Lupoli, T.J. *et al.* Transpeptidase-mediated incorporation of D-amino acids into bacterial peptidoglycan. *J Am Chem Soc* **133**, 10748-10751 (2011).

41. Sauvage, E., Kerff, F., Terrak, M., Ayala, J.A. & Charlier, P. The penicillin-binding proteins: structure and role in peptidoglycan biosynthesis. *Fems Microbiol Rev* **32**, 234-258 (2008).

42. Mainardi, J.L. *et al.* A novel peptidoglycan cross-linking enzyme for a beta-lactam-resistant transpeptidation pathway. *J Biol Chem* **280**, 38146-38152 (2005).

43. Aliashkevich, A. & Cava, F. LD-transpeptidases: the great unknown among the peptidoglycan cross-linkers. *FEBS J* **289**, 4718-4730 (2022).

44. Nikolaidis, I., Favini-Stabile, S. & Dessen, A. Resistance to antibiotics targeted to the bacterial cell wall. *Protein Sci* **23**, 243-259 (2014).

45. CDC (Atlanta, Georgia; 2019).

46. Solomon, S.L. & Oliver, K.B. Antibiotic resistance threats in the United States: stepping back from the brink. *Am Fam Physician* **89**, 938-941 (2014).

47. Zeng, X. & Lin, J. Beta-lactamase induction and cell wall metabolism in Gram-negative bacteria. *Front Microbiol* **4**, 128 (2013).

48. Reygaert, W.C. An overview of the antimicrobial resistance mechanisms of bacteria. *AIMS Microbiol* **4**, 482-501 (2018).

49. Muhlberg, E. *et al.* Renaissance of vancomycin: approaches for breaking antibiotic resistance in multidrug-resistant bacteria. *Can J Microbiol* **66**, 11-16 (2020).

50. Selim, S. Mechanisms of gram-positive vancomycin resistance (Review). *Biomed Rep* **16**, 7 (2022).

51. Arthur, M. & Quintiliani, R., Jr. Regulation of VanA- and VanB-type glycopeptide resistance in enterococci. *Antimicrob Agents Chemother* **45**, 375-381 (2001).

52. Pourakbari, B. *et al.* Evaluation of efflux pumps gene expression in resistant Pseudomonas aeruginosa isolates in an Iranian referral hospital. *Iran J Microbiol* **8**, 249-256 (2016).

53. Rosas, N.C. & Lithgow, T. Targeting bacterial outer-membrane remodelling to impact antimicrobial drug resistance. *Trends Microbiol* **30**, 544-552 (2022).

54. Chetri, S. *et al.* Transcriptional response of OmpC and OmpF in Escherichia coli against differential gradient of carbapenem stress. *BMC Res Notes* **12**, 138 (2019).

55. Rocker, A. *et al.* Global Trends in Proteome Remodeling of the Outer Membrane Modulate Antimicrobial Permeability in Klebsiella pneumoniae. *mBio* **11** (2020).

56. Gautam, A., Vyas, R. & Tewari, R. Peptidoglycan biosynthesis machinery: a rich source of drug targets. *Crit Rev Biotechnol* **31**, 295-336 (2011).

57. Liu, Y. & Breukink, E. The Membrane Steps of Bacterial Cell Wall Synthesis as Antibiotic Targets. *Antibiotics (Basel)* **5** (2016).

58. Tekin, E. *et al.* Prevalence and patterns of higher-order drug interactions in Escherichia coli. *NPJ Syst Biol Appl* **4**, 31 (2018).

Chapter 2 Bacteria and the Immune System

2.1 Bacterial Recognition by the Immune System

The emergence of multi-antibiotic resistant bacteria has encouraged researchers to expand the realm of possible treatment techniques to combat pathogenic bacterial infections. Drawing inspiration from our body's natural defense mechanisms can aid in combating these pathogens. However, the ability to develop and treat such bacteria relies extensively on having a thorough understanding of how the immune system recognizes and kills invading bacterial cells.

There are two different arms of the immune system that are activated in response to an invading microbe: innate and adaptive (Figure 2.1).[1] An innate immune response is characterized by the identification of unique components on the invading bacterial pathogen, often known as pattern recognition. Host immune cells have many broadly specific pattern recognition receptors (PRRs) expressed on their cell surface that enable the detection of pattern- associated molecular patterns (PAMPs), which are exclusively present on the surface of the bacterial cell.[2] This key feature employs immune cells to differentiate between self versus non-self cells. Additionally, PAMPs include structural features that are often invariant between bacterial species, which allows for broad spectrum specificity of PRRs. Furthermore, such motifs are typically considered essential components to the overall fitness of the microbe, ultimately reducing the likelihood of mutation as an immune evasion mechanism.[1] Bacterial PAMPs include, but are not limited to, components of the bacterial cell wall such as peptidoglycan (PG) and lipopolysaccharide (LPS).[3, 4] Two main classes of PRRs that are responsible for detection of PG and LPS are nucleotide-binding oligomerization domain (NOD) proteins and Toll-like receptors (TLR), respectively. The NOD proteins, NOD1 and NOD2, each recognize a distinct fragment of PG that upon binding, result in the production of pro-inflammatory cytokines and chemokines, along with the recruitment of macrophages and neutrophils (often referred to as phagocytes) to the infection site.[1, 3] TLRs are membrane bound receptors found on the surface of phagocytes that recognize common structural patterns

of microbial molecules. There are 10 known TLRs expressed by humans, where each TLR has a distinct binding target. For example, TLR2 recognizes lipoproteins or lipopeptides while TLR4 recognizes LPS.[2-6] Upon activation of TLRs, several pro-inflammatory and antibacterial responses are initiated such as the production of a systemic inflammatory response (via tumor necrosis factor (TNF) and interleukins) and the production of antibacterial proteins and peptides by macrophages.[2, 3, 5, 6]
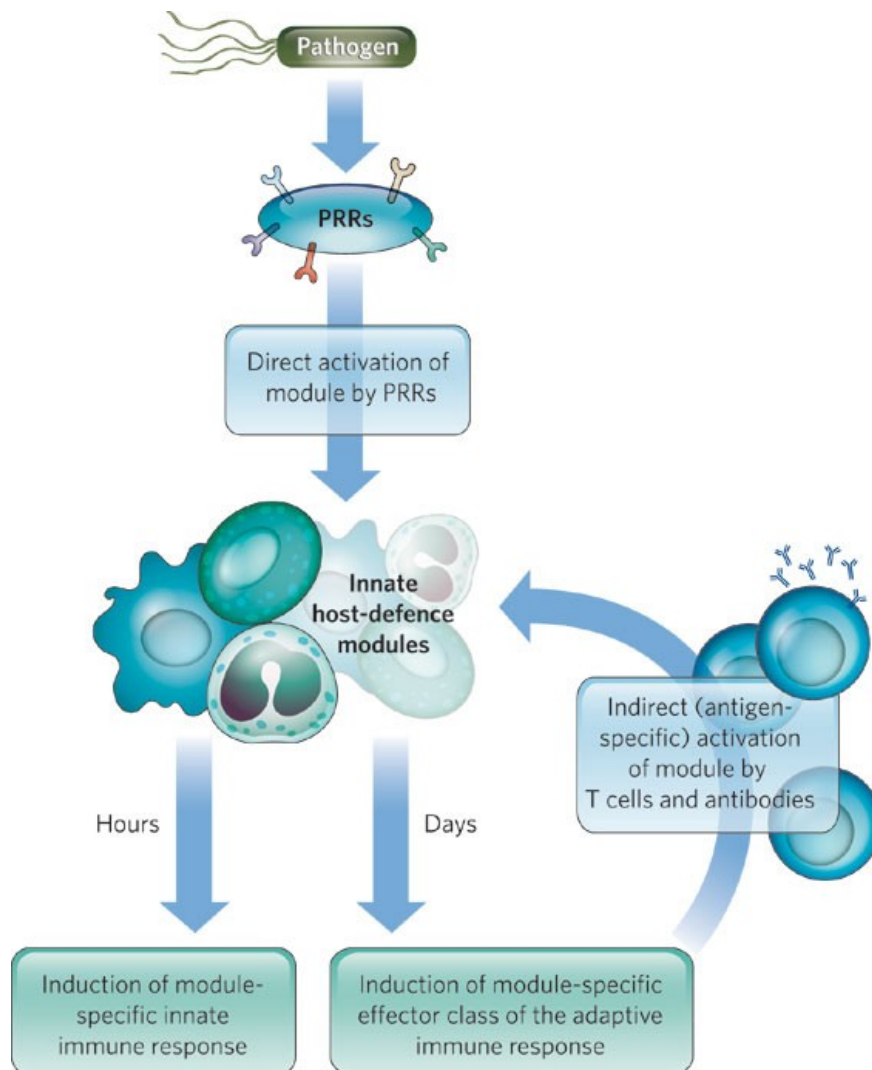

Figure 2.1 *Summary of innate and adaptive immune responses to bacterial pathogens. Reproduced with permission from[1].*

An adaptive immune response to bacterial pathogens is mediated by two types of antigen receptors: B cell receptors (BCRs) and T-cell receptors (TCRs) present on B and T lymphocytes.[1, 7, 8] The receptors present on both B and T cells are limited to one target antigen per cell, rather than having many receptors with multiple targets. The antigen receptors on each conventional lymphocyte are also not predetermined; therefore, they are assembled primarily at random upon encounter with an antigen.[1, 8] Being that B and T cells need to be primed with their specificity, an adaptive immune response typically occurs over the course of days post infection, rather than within hours as seen by an innate immune response. Upon infection, the innate arm of the immune system will be responsible for taking up the microbe into antigen presenting cells (APCs), which are then transported via the lymphatic system to the lymph nodes.[9] Once the APCs reach the lymph nodes, they will encounter conventional lymphocytes. Since B and T lymphocytes do not have a predetermined specificity, they must rely on signals transmitted from APCs within the innate immune response to distinguish the origin of the antigen they recognize.[8, 9] For B cells, this interaction occurs by a physical linkage between the PRR and BCR. When a B cell encounters an antigen on an APC, the mature B cells proliferate into either short-lived plasmablasts that rapidly secrete antibodies specific to that particular antigen or differentiate into memory B cells that present the antigen-specific molecules directly on the cell surface.[1, 7-9] For T cells, APCs will activate a T cell response *via* antigen loaded major histocompatibility complex (MHC). The T cells will proliferate to have antigen specificity that will recognize other infected cells displaying that specific antigen loaded MHC, resulting in a cytotoxic effect to the cell.[1, 7-9]

2.2 Bacterial Clearance by the Immune System

Within the adaptive immune response, the production of antigen specific antibodies by B cells is known as humoral immunity. A humoral immune response utilizes the B cell produced antibodies to circulate the extracellular space with the goal of eliminating the pathogenic bacteria. Antibody mediated clearance of bacterial pathogens occurs *via* three distinct mechanisms: neutralization, activation of the complement system, or opsonization-mediated phagocytosis.[7, 8] The most common modality for bacterial

elimination within the humoral immune response is the complement system (Figure 2.2).[10, 11] There are about 25 complement proteins circulating in the blood that upon initiation will work simultaneously to destroy bacteria.[12] The classical complement system is activated upon a recognition event between the C1 complex and a pathogen-bound antibody. Binding of C1 to the antibody triggers the cleavage of C4 and C2, which results in deposition of the C3 convertase enzyme onto the surface of the bacteria. This enzyme is responsible for the conversion of C3 into C3b, which is subsequently deposited onto the cell surface. When high levels of C3b are detected, C3 convertase transforms into C5 convertase, where the enzyme now utilizes C5 as a substrate. C5 convertase then cleaves C5 into C5a and C5b.[8, 10, 11] The deposition of C5b promotes the association of C6, C7, C8, and multiple C9 molecules to form a lytic membrane attack complex (MAC). The MAC is a pore that disrupts the outer membrane of Gram- negative bacteria.[12] This membrane perturbation results in cell death via osmotic instability to the cell. Although the complement cascade is effective at eliminating pathogens, instances of evasion strategies have been identified such as capsule production, modification of LPS, production of proteases that cleave complement proteins, and bacterial production of complement inhibitory molecules.[11]
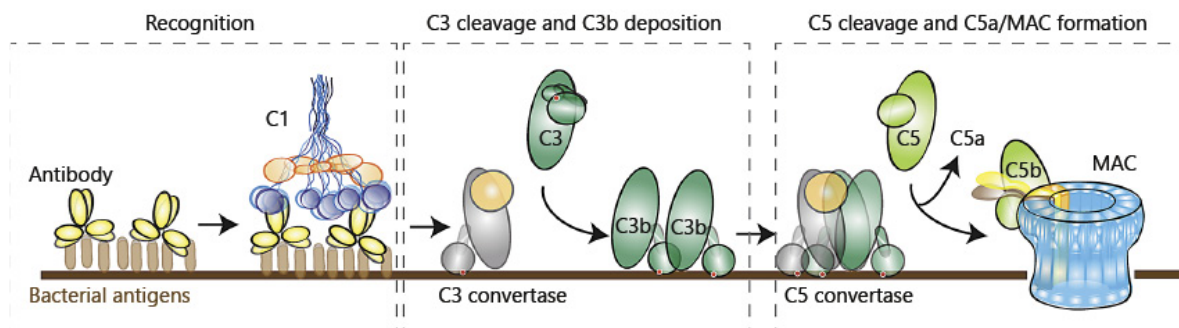
Figure 2.2 *Cartoon representation of the complement cascade. Reproduced with permission from[11].*

A second arm for immune clearance of bacterial infections is comprised by antibody-dependent cellular cytotoxicity (ADCC) and antibody-depended cellular phagocytosis

(ADCP) (Figure 2.3). The initiation of both ADCC/ ADCP is opsonization of the bacterial cell with antibodies, like as with complement. However, unlike complement, ADCC/ ADCP require an interaction with effector immune cells (macrophages, neutrophils, dendritic cells, and natural killer (NK) cells) for pathogen elimination. The effector immune cells will recognize and bind to opsonized bacterial cells *via* an interaction between the Fc region of the surface bound IgG and FcgR.[13] In the case of ADCC, this interaction triggers the phosphorylation of the FcgR, resulting in receptor signaling and secretion of cytotoxic substances, such as granzyme, perforin, and TNF, that mediate cell destruction in a non-phagocytotic manner.[14] For ADCP, initiation occurs in a similar manner to ADCC; however, the binding interaction between the antibody Fc and FcR occurs with a specific FcR, FcgRIIa for macrophages, to signal phagocytic uptake of the pathogen. Upon engulfment of the bacterial cell into a phagosome, the bacterial cell is then degraded by mechanisms such as acidification, production of reactive oxygen and nitrogen species, and the production of antibacterial proteins and peptides such as lysozyme and cathelicidins, respectively.[15] However, several instances of immune evasion and resistance to phagosomes have been identified. For example, it has been evidenced that in response to the phagosomal environment, *Staphylococcus aureus* (*S. aureus*) alters its cell wall structure to become resistant to antibacterial proteins and peptides, and increases expression of proteins that neutralize the effects of ROS.[15]
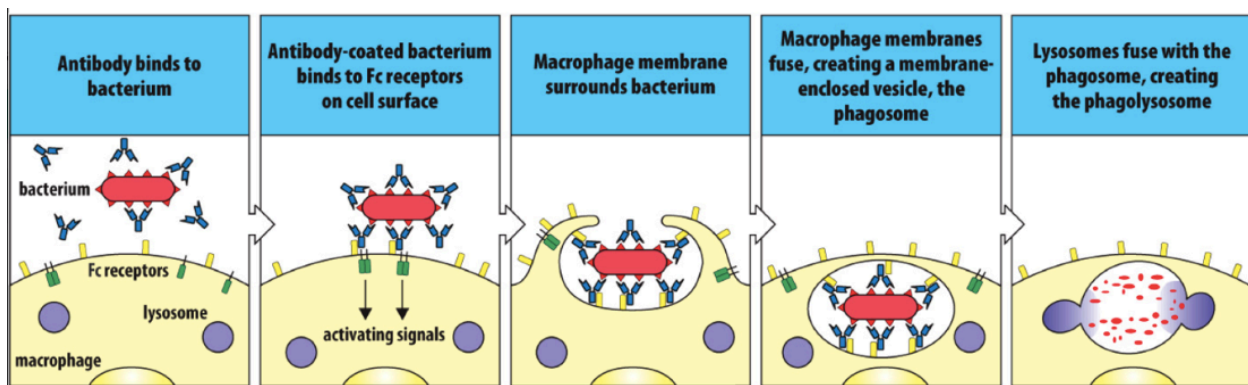
Figure 2.3 *Cartoon representation of antibody dependent cellular phagocytosis.*

2.3 Bacterial Immunotherapy

The use of immunotherapy for treatment of bacterial infections was demonstrated as early as the 1800s. In 1890, Emil von Behring developed a cure for diphtheria toxin by immunizing rats, guinea pigs, and rabbits with an attenuated form of the infectious agent and collecting the serum. The serum was subsequently injected into non-immunized animals harboring fully virulent diphtheria, to which treatment with the convalescent serum resulted in complete clearance of the infection.[16] In 1891, Behring's serum treatment (known today as convalescent serum therapy, CST) was successfully administered to a child for treatment of diphtheria, which ultimately awarded him the first Nobel Prize in Medicine in 1901, and gave him the title, "the savior of children."[17] Taking inspiration from CST and the idea of utilizing the immune system to combat bacterial infections, Dr. Pearl Kendrick and Grace Eldering developed a vaccine therapy in 1953 for the treatment of Pertussis, also known as whooping cough. Pertussis is a highly contagious respiratory tract infection caused by the bacterial species *Bordetella pertussis*.[18] Dr. Kendrick and Dr. Eldering were accredited with successfully generating the first vaccine based therapy for treatment of bacterial infections, for which they were granted induction into the Michigan Women's Hall of Fame.[19] Seminal work done by von Bering, Kendrick, and Eldering demonstrated the power of enhancing and utilizing an immune response for treatment against bacterial infections.

In the years following, the discovery of Penicillin fueled a large influx in using small molecules to treat bacterial infections. As a result, antibiotics quickly became the go-to treatment option for both acute and severe bacterial infections. However, in recent years, incidences of drug- resistant pathogens quickly began to rise as the development of new antibiotics lagged behind.[20, 21] This alarming trend served as motivation for developing alternative strategies to combat drug- resistant bacterial pathogens, including drawing inspiration from the early work by von Behring that focused on harnessing the patient's own immune system for bacterial clearance.[22, 23] The findings by von Behring served as foundational precedence to the development of modern anti-bacterial immunotherapeutic

agents, which can provide additional options for patients who are unresponsive to conventional antibiotics.

Modulating a target immune response has been extensively demonstrated within the past several decades as a viable option for treating a range of cancers. Interestingly, the same approach has not been as widely adopted for treatment of acute, drug-resistant bacterial infections, despite bacterial cells being inherently different in cell wall structure compared to mammalian cells, rendering this approach advantageous for limiting off target effects and cytotoxicity. However, several key groups have paved the way for immunotherapy against bacterial infections and this review will summarize the milestones achieved for combating bacterial pathogens by re-directing an immune response.

2.3.1 Receptor Based Targeting

Bacteria have many unique proteins and receptors located on the cell surface that are inherent to prokaryotic cells. One of which is the mannose- specific receptor that is located on the surface of bacterial pili and is used to aid in host adhesion and infectivity.[24] Taking inspiration from immunotherapeutic concepts to treat cancer, Bertozzi and Bednarski were the first to develop bifunctional molecules that can (1) bind to the bacterial cell surface and (2) elicit an immune response.[25] They synthesized a biotinylated C-glycoside mannose to target the mannose- specific receptor on the surface of *Escherichia coli* (*E. coli*) (Figure 2.4A). Upon incubation with *E. coli,* the biotin handle was displayed on the surface of the bacterial cell *via* the interaction between the mannose ligand and the mannose- specific receptor. The biotin moiety was then subject to binding with high affinity to avidin and followed by the recruitment of anti-avidin antibodies. The increased opsonization of *E. coli* in the presence of the bifunctional molecule led to bacterial cell killing *via* CDC.
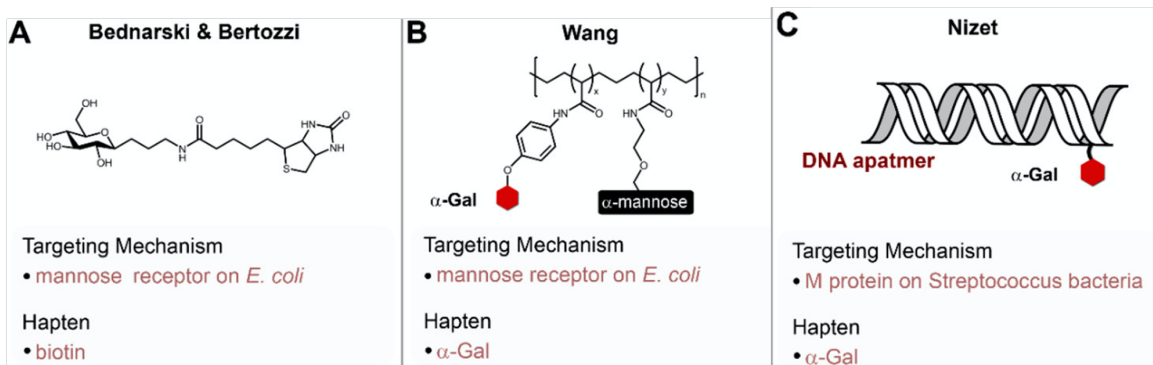
Figure 2.4 *Methods described to graft haptens onto the surface of pathogens via non-covalent associations. Reproduced with permission from[22].*

The mannose- specific receptor as a targeting moiety for homing to the surface of *E. coli* was further utilized to expand upon the seminal work by Bertozzi and Bednarski. Wang and coworkers synthesized an acrylamide-based polymer that displayed both α-mannosyl motifs and a small molecule hapten, α-Gal (Gala1$\rightarrow$3Gal) (Figure 2.4B).[26] Antibodies against α-Gal naturally make up 1% of the human antibody pool[27]; therefore, with this design, the need for supplementation of exogenous antibodies was eliminated. The deviation from Bertozzi and Bednarski's original design of a monomeric α-mannosyl to a polymeric display was rationalized by the low binding affinity observed between a monomeric α-mannosyl and a mannose- specific receptor. Increasing the number of α-mannosyl groups interacting with the cell surface significantly increased the avidity of the scaffold compared to the monomeric carbohydrate. Additionally, the inclusion of several α-Gal motifs within the polymeric scaffold promoted the opsonization of *E. coli* with multiple anti-Gal antibodies in an α-mannosyl mediated manner. Wang and co-workers demonstrated *in vitro* that the polymeric scaffold displaying both α-mannosyl and α-Gal was bound by anti-Gal antibodies as read out by ELISA.

2.3.2 Aptamer Based Targeting

The inclusion of multiple a-mannosyl motifs significantly improved binding affinity to the bacterial cell surface; however, the target therapy lacked bacterial cell specificity, as mannose receptors are also expressed on the surface of immune cells, such as macrophages and dendritic cells, to aid in host defense.[28] Additionally, synthetic challenges are associated with the synthesis of polymeric scaffolds in terms of controlled length and reproducibility. In response to these challenges, bacterial immunotherapy exhibited a shift towards utilizing biomacromolecules for the purpose of directing an immune response against bacterial cells. Nizet and co-workers developed an immune modulator of bacterial cells based on directed cell binding with a DNA aptamer.[29] Nucleic acid aptamers are short, single stranded oligonucleotides, of either RNA or DNA, that bind to a molecular target with high affinity and specificity based on their unique three-dimensional structure. Aptamers are innately advantageous for use as a cell binding moiety because they are easily synthesizable in large quantities, show low batch-to-batch variation, can be easily functionalized, are relatively small in size (10-30 kDa), and demonstrate high stability in biologically relevant mediums.[30] In the work done by Nizet and co-workers, a DNA aptamer with high specificity for a surface protein on Group A *Streptococcus* (GAS) bacteria was conjugated with α-Gal, termed 'alphamer', for the recruitment of endogenous anti-Gal antibodies (Figure 2.4C). Here, it was demonstrated that opsonization of GAS with anti-Gal antibodies was dependent on the presence of the alphamer and led to phagocytosis and killing of the pathogen. Additionally, the alphamer was able to reduce the replicability of GAS in human blood *in vitro,* demonstrating that this approach may be used as a passive immunization technique for the treatment of GAS.

2.3.3 Macrocyclic Peptide Based Targeting

Macrocyclic peptides are showing increasing popularity as a viable drug modality due to inherent advantageous pharmaceutical characteristics compared to other well-established therapeutic molecule classes. Like small molecules, macrocyclic peptides are easily synthetically obtained and can be tuned to improve biophysical properties. For example, cyclization of the peptide can improve the solubility, binding affinity and

specificity, and proteolytic stability compared to the linear counterpart. Additionally, several different screening techniques often yield high affinity macrocyclic peptides that have high specificity for a target protein.[31] In fact, Idso and co-workers applied a combinatorial protein-catalyzed capture agent (PCC) technology to identify macrocyclic peptide ligands with high affinity and specificity for a surface protein, MrkA, of the pathogen *Klebsiella pneumoniae (K. pneumoniae)*.[32] MrkA is a highly conserved surface protein that retains expression in the incidence of carbapenem resistance; therefore, Idso and co-workers utilized the top-preforming ligand of the PCC screen to develop an antibody-recruiting protein-catalyzed capture agent (AR-PCC) to immuno-modulate carbapenem-resistant *K. pneumoniae* (CRKP). The lead ligand cy(LLFFF) was conjugated to a 2,4-dinitrophenol (DNP) hapten and effectively demonstrated opsonization of anti-DNP antibodies to the surface of CRKP, leading to phagocytosis by macrophages, and subsequent opsonophagocytic killing (Figure 2.5).
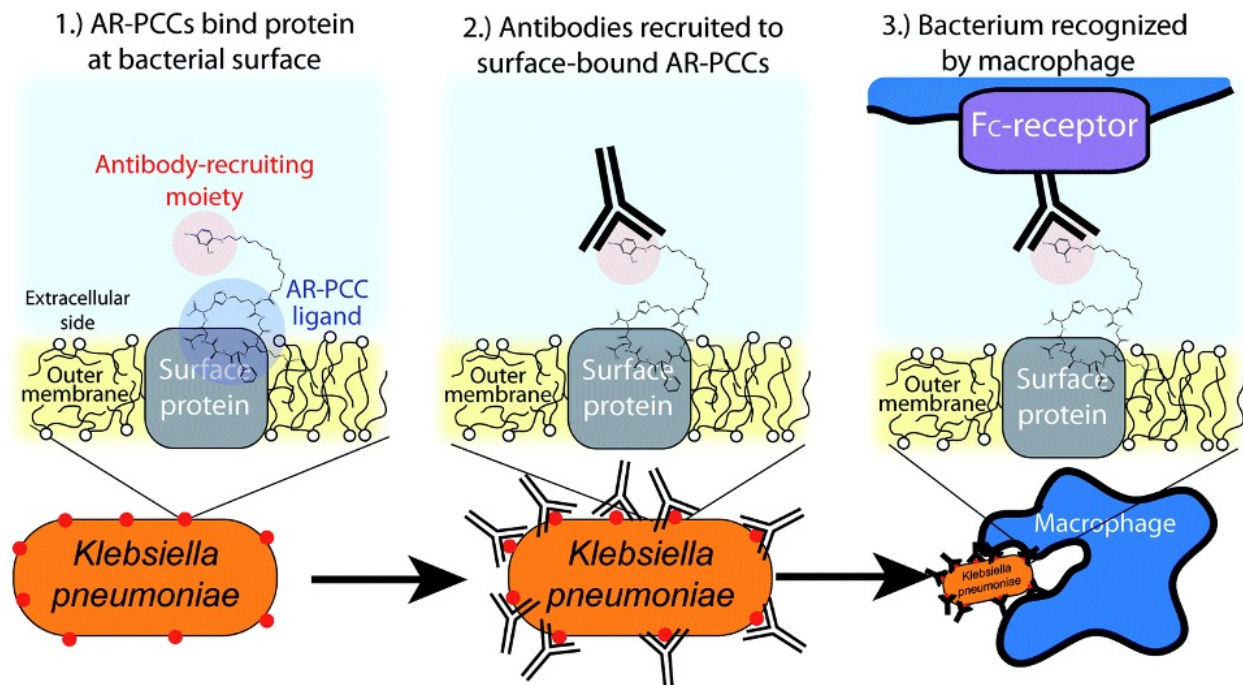
Figure 2.5 *Schematic depicting the mode-of-action of AR-PCCs against antibiotic-resistant Klebsiella pneumoniae. Reproduced with permission from[32].*

AR-PCC molecules (1) bind to a surface protein on a *K. pneumoniae* bacterium, then (2) recruit antibodies that opsonize the bacterium, which leads to (3) recognition and phagocytosis of the bacterium by immune cells (e.g., macrophages).

2.3.4 Antibiotic Based Targeting

Immunotherapeutic approaches directed against bacteria thus far have been focused on targeting the cell *via* bacterial surface proteins, which are often variant between bacterial species or have overlapping specificity with host cells. A differing approach lies within targeting motifs that are 1) exclusive to the bacterial cell wall and 2) broadly expressed between bacterial cell species. The peptidoglycan (PG) layer within the cell wall has a composition that is completely unique to bacterial cells. The PG consists of repeating disaccharide units that display a stem peptide with the composition of L-ala-D-glu-L-lys-D-ala-D-ala. Two neighboring stem peptides are crosslinked together by transpeptidase enzymes to create a mesh-like scaffold that maintains the physical and chemical stability of the cell. PG is often the target of many antibiotics as it is an essential component of the bacterial cell wall, and molecules that target the PG will exhibit low off-target cytotoxicity due to limited overlapping motifs with mammalian cells.

Whitesides and co-workers were the first to utilize an antibiotic for bacterial cell killing by means of immunotherapy. The antibiotic vancomycin was primarily used as a PG binding motif for hapten display on the bacterial cell surface.[33] In a similar approach to Wang, Whitesides synthesized a bifunctional polyacrylamide scaffold that displayed both a bacterial homing moiety, vancomycin, and the hapten fluorescein, termed pA-V-F (Figure 2.6A). Vancomycin has affinity ($K_d \sim$ mM) for the terminal D-ala-D-ala motif within the PG stem peptide. Traditionally, binding of vancomycin to D-ala-D-ala prevents further processing of PG precursors for maturation and results in cell death;[34, 35] however, Whitesides demonstrated that by incubating bacterial cells with sub- inhibitory concentrations of pA-V-F, cell labeling was achieved rather than cell death.[36] This design revolutionized the use of antibiotics solely for the purpose of bacterial cell binding. Additionally, polyvalency of pA-V-F significantly improved the binding avidity of

vancomycin to D-ala-D-ala, further exploiting the binding properties, rather than antibacterial properties of vancomycin. pA-V-F exhibited binding to the surface of three Gram- positive bacterial species: *Staphylococcus aureus* (*S. aureus*), *Staphylococcus epi* (*S. epi*), and *Streptococcus pneumoniae* (*S. pneumoniae*). Further, incubation of exogenous anti-fluorescein antibodies with pA-V-F tagged *S. aureus* resulted in opsonization and antibody- mediated phagocytosis into J774 macrophages. This approach by Whitesides and co-workers was foundational in the application of using antibiotics for hapten display rather than antibacterial activity.

The use of vancomycin for hapten display was further developed by Sabulski and co-workers.[37] Their design featured a unique modification to vancomycin that improved both bacterial cell tagging and specificity. Vancomycin was modified on the C-terminus with a substrate peptide sequence for *S. aureus* sortase A (srtA). SrtA transpeptidase is a surface bound enzyme that catalyzes the covalent linkage of proteins onto the PG of *S. aureus*. The transpeptidase recognizes a signaling peptide present within bacterial proteins (LPXTG, where X is any amino acid) to catalyze the acyl-transfer of the protein onto lipid II. As the lipid II unit is matured into crosslinked PG, the anchored protein will remain within the PG scaffold.[38-40] Therefore, modification of vancomycin, of which targets D-ala-D-ala on lipid II, with DNP tagged LPMTG, termed Sort3, enabled a covalent display of DNP onto the PG of *S. aureus* (Figure 2.6B).[41] SrtA is exclusively expressed by *S. aureus*; therefore, minimal cell labeling was observed for other bacterial species tested. It was demonstrated that overnight labeling of Sort3 with *S. aureus* led to the recruitment of anti-DNP antibodies from both pooled human serum and a purified antibody sample. Additionally, phagocytosis of *S. aureus* into J774 macrophages was significantly improved in the presence of both Sort3 and anti-DNP antibodies.

A

B

DNP

C

PDn, where n = number of PEG units
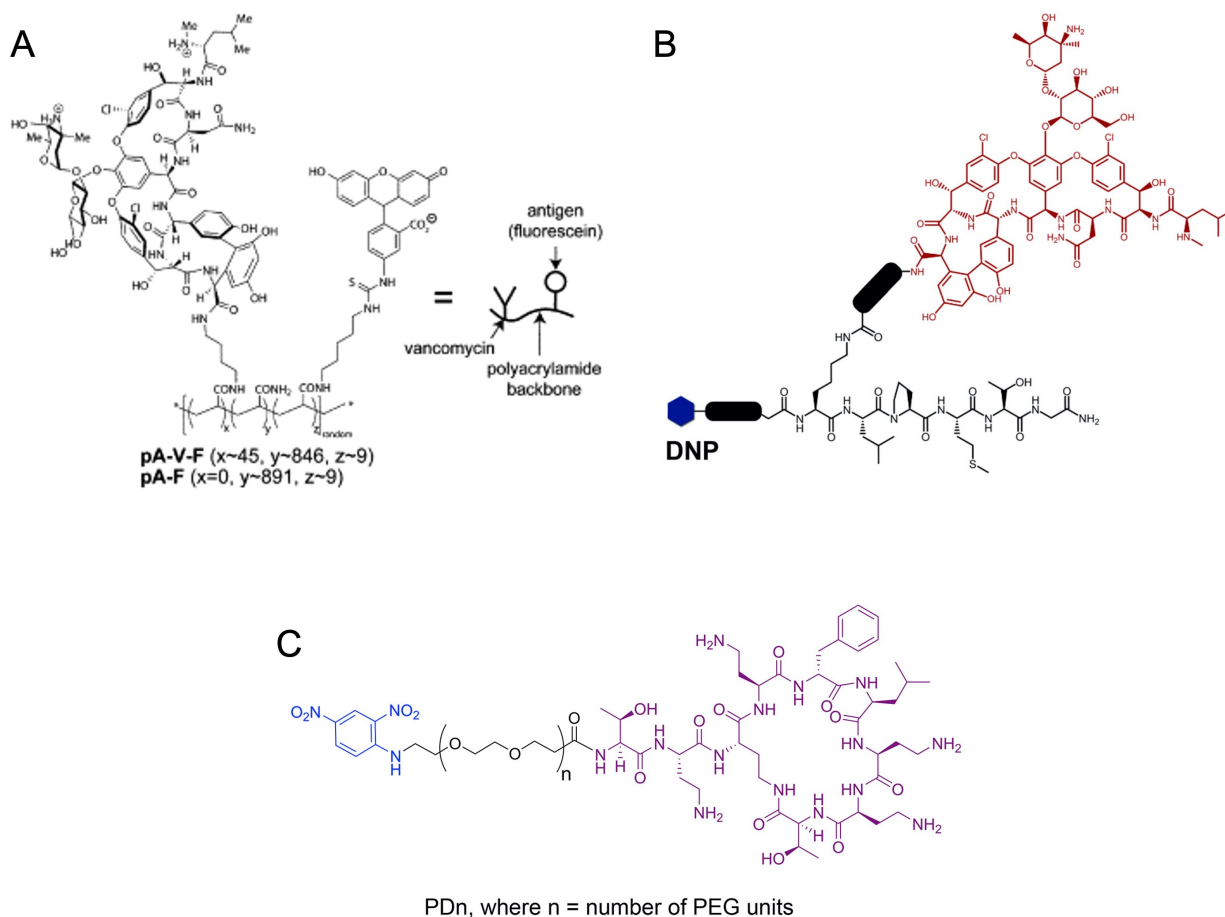
Figure 2.6 *Methods described to graft haptens onto the surface of pathogens via antibiotic targeting. Reproduced with permission from[33,37,42].*

(A) Whitesides and co-workers conjugated fluorescein onto a polymeric vancomycin scaffold for recruitment of anti-FITC antibodies to Gram- positive pathogens.[33] (B) Sabulski and co-workers conjugated a hapten, DNP, and a SrtA sorting signal, LPMTG, to vancomycin to covalently tag *S. aureus* with DNP for phagocytotic uptake.[37] (C) Sabulski and co-workers modified PMB with DNP for targeted immune clearance of Gram- negative pathogens.[42]

Sabulski and co-workers also adapted a similar approach for the treatment of Gram-negative pathogens.[42] In this study, polymyxin B (PMB) was tagged with the endogenous hapten, DNP, for labeling of Gram- negative bacterial cell surfaces and recruitment of anti-DNP antibodies (Figure 2.6C). PMBs are cationic cyclic lipodecapeptides that disrupt

the outer membrane of Gram- negative bacteria by displacing the calcium and magnesium bridges that stabilize lipopolysaccharides (LPS).[43] An important component of antibody recruitment to bacterial cells is optimizing the linker length between the bacterial cell binding moiety and the hapten. Here, it was demonstrated that the chemical spacer between PMB and DNP was of critical importance, as only the 3-polyethylene glycol (PEG) unit linker (PD3) induced significant anti-DNP binding to wild type *Escherichia coli* (*E. coli*). However, when the panel of PMB-DNP linkers was assessed for anti-DNP recruitment towards pathogenic *Pseudomonas aeruginosa* (*P. aeruginosa*), the 6-PEG unit linker (PD6) exhibited the most significant antibody labeling. Further, PD6 enhanced the killing of WT *E. coli via* CDC.

Antibiotic manipulation for immunotherapy against bacterial pathogens is not limited to hapten modification for recruitment of hapten specific antibodies. Work done by Tsubery and co-workers demonstrated that conjugation of an antibiotic to a moiety recognizing specific receptors on phagocytotic cells may promote opsonic activity toward bacterial cells. [44] In the study done by Tsubery, a Gram- negative targeting antibiotic, PMB, was conjugated with a chemoattractant that will directly activate an immune response *via* neutrophil receptor binding. PMB was covalently linked to a short chemotactic peptide, fMLF (fMet-Leu-Phe), also known as a formylated peptide (fPep). fPeps are N-terminal fragments of bacterial proteins derived from invading pathogens that contain an N-terminal formyl methionine (fMet), as fMet initiates protein synthesis in bacteria.[45] fPeps are pathogen-associated chemoattractants that are short in length (3-5 amino acids) and will induce chemotaxis and phagocytosis of bacteria upon recognition by neutrophil formyl peptide receptors (FPR). Tsubery and co-workers demonstrated that the conjugates consisting of PMB covalently linked with fMLF acted as opsonins in promoting phagocytotic killing of the Gram- negative pathogens *Klebsiella pneumoniae* (*K. pneumoniae*) and *P. aeruginosa.*
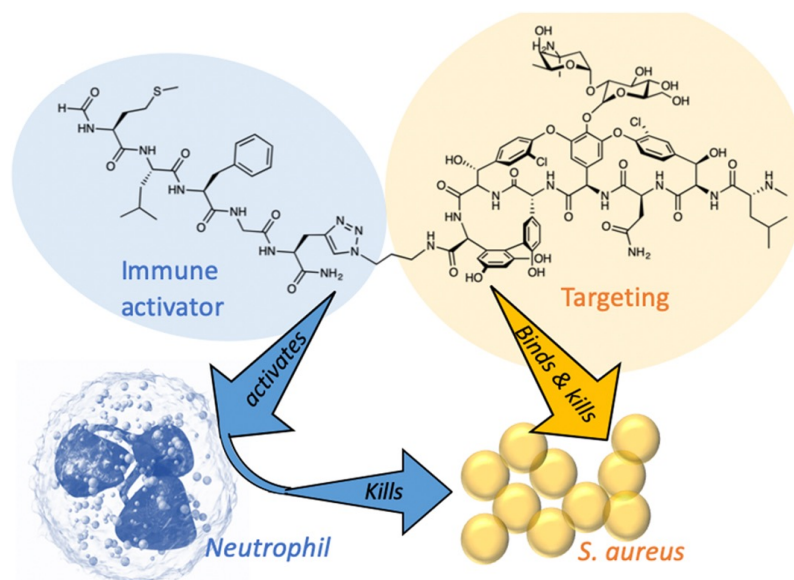
Figure 2.7 *Method described by Payne and co-workers that labels the bacterial cell directly with a neutrophil activating motif. Reproduced with permission from[46].*

Payne and co-workers adapted the work done by Tsubery and co-workers to apply to Gram-positive pathogens, in which vancomycin was modified with fPeps.[46] In this work, the C-terminus of vancomycin was conjugated to a library of formylated peptides (fPep) (Figure 2.7). Using infection-on-a-chip technology, neutrophils demonstrated enhanced recognition, phagocytosis, and killing of *S. aureus* in the presence of the vanc-fPep conjugates. Additionally, an *in vivo* mouse MRSA pneumonia model had a reduced bacterial load and exhibited improved lung pathology in response to treatment with vanc-fPep.

2.3.5 Cell Targeting *via* Antibody Conjugates

In early work done by Drabick and co-workers, polymyxin was conjugated non-specifically to human immunoglobulins (IgG) as a treatment for sepsis.[47] This foundational work set the stage for the development of antibody-antibiotic conjugates (AACs) active against bacterial related illnesses. Lehar and co-workers took inspiration from this work to develop an AAC that targeted intracellular *S. aureus*.[48] *S. aureus* readily evades

traditional antibiotic therapy and immune responses by invading and surviving inside of mammalian cells, often resulting in a recurring or chronic infection. With the goal of ablating intracellular *S. aureus,* Lehar and co-workers developed a novel therapeutic that is specifically activated only upon uptake into macrophages harboring intracellular *S. aureus*. A THIOMAB (antibody engineered to contain free cysteines) with specificity for *S. aureus* wall teichoic acids (anti-WTA) was covalently modified, *via* its reactive cysteines, with a phagolysosomal protease cleavable linker and the antibiotic rifalogue (Figure 2.8A). The AAC exhibited minimal antibacterial effects prior to *S. aureus* infection into macrophages; however, when AAC opsonized *S. aureus* were phagocytosed, intracellular proteases cleaved the linker to release the active form of rifalogue, resulting in a significant reduction in bacterial load. The AAC was able to eradicate *S. aureus* USA 300 in culture and in a mouse model. Additionally, treatment with the AAC was superior compared to both vancomycin and rifalogue alone. Due to the poor permeability of both anti-WTA and antibiotics individually through the mammalian cell membrane, treatment of intracellular *S. aureus* would be ineffective without opsonization mediated uptake of the bacterial pathogen for release of the antibiotic.

In a similar approach, Kajihara and co-workers developed a novel AAC that targets Gram-negative *P. aeruginosa*.[49] This group previously developed an antibiotic G2637 (an analogue of arylomycin) that has moderate activity against *P. aeruginosa*; moreover, they hypothesized that conjugation of G2637 to a monoclonal antibody (mAb) specific for a lipopolysaccharide O-antigen on the surface of *P. aeruginosa* would significantly improve antibiotic efficacy against intracellular *P. aeruginosa* infections (Figure 2.8B). The O-antigen specific THIOMAB was covalently modified with a lysosomal cathepsin-cleavable linker (cBuCit) and G2637, to yield a drug-to-antibody ratio of approximately 6. It was demonstrated that the AAC opsonized *P. aeruginosa* was readily phagocytosed into macrophages, which resulted in a significant decrease of bacterial survival compared to when treated with G2637 alone. Like Drabick's work, this approach emphasized that antibody mediated delivery of antibiotics inside macrophages created a high local antibiotic concentration for the killing of intracellular pathogens.
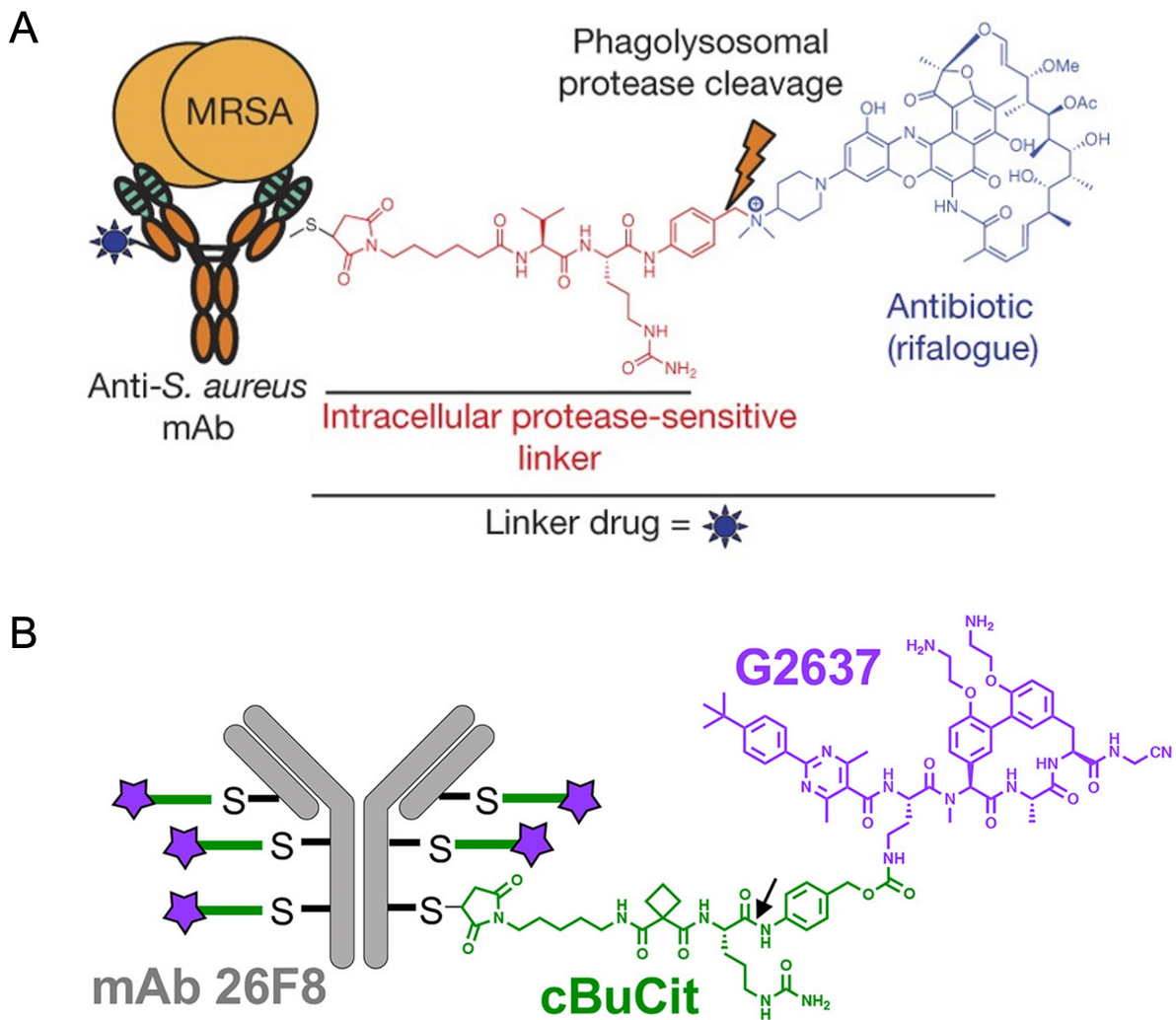
Figure 2.8 *Methods described to enhance antibiotic efficacy via immune modulation with human IgG. Reproduced with permission from[48,49].*

(A) Lehar and co-workers conjugated the antibiotic, rifalogue, *via* a protease cleavable linker to an anti-*S. aureus* antibody for treatment of intracellular *S. aureus*.[48] (B) Kajihara and co-workers described the site-selective modification of an anti-*P. aeruginosa* antibody with an antibiotic *via* a cathepsin-cleavable linker for treatment of intracellular *P. aeruginosa* infections.[49]

The concept of polyvalent antibiotic binding was utilized by Katzenmeyer and co-workers by the development of a polymeric vancomycin scaffold conjugated to a purified human IgG Fc.[50] Antibodies are composed of two primary regions, variable and non-variable.

The variable region comprises the antigen specificity, where the non-variable region maintains the same chemical entity and structure between all human IgGs. IgG recognition by immune cells is dependent solely on the interaction between the non-variable (or Fc) region and a surface bound Fc receptor.[51] Therefore, Katzenmeyer and co-workers' design features bacterial specificity mediated by polyvalent vancomycin binding and phagocyte recognition *via* the conjugated human IgG Fc (termed an artificial opsonin). This work demonstrated that the artificial opsonin mediated a 2-fold increase in neutrophil phagocytosis of *S. epidermis* RP62A, a methicillin-resistant bacterial pathogen implicated in biofilm formation. There was also an exhibited 2-3-fold increase in neutrophil secretion of IL-8 and a 20% increase in neutrophil reactive oxygen species generation.

2.3.6 Cell Targeting *via* Carbohydrate Binding Proteins

Therapeutic antibodies for treatment against bacterial pathogens remain an elusive goal. Many of the currently utilized mAb's target bacterial virulence factors that exist as either bound or secreted proteins. However, antibodies that directly target conserved bacterial epitopes on the cell surface are still being explored.[52, 53] A conserved motif within the bacterial cell wall is surface carbohydrates. The sugar backbone of the PG is comprised of repeating disaccharide units, GlcNAc and MurNAc, and are typically the target of many PG binding proteins and enzymes.[54] For instance, several classes of bacterial proteins implicated in cell wall synthesis and remodeling, such as muramidases, hydrolases, and endolysins, typically contain a cell wall carbohydrate epitope binding domain, often known as a lysin motif (LysM) domain.[55, 56] Being that surface carbohydrates are highly conserved and the targets of several sugar binding moieties, they may appear as attractive targets for the generation of mAb's; however, GlcNAc and MurNAc are T-cell independent antigens, rendering them poorly immunogenic.[57, 58]
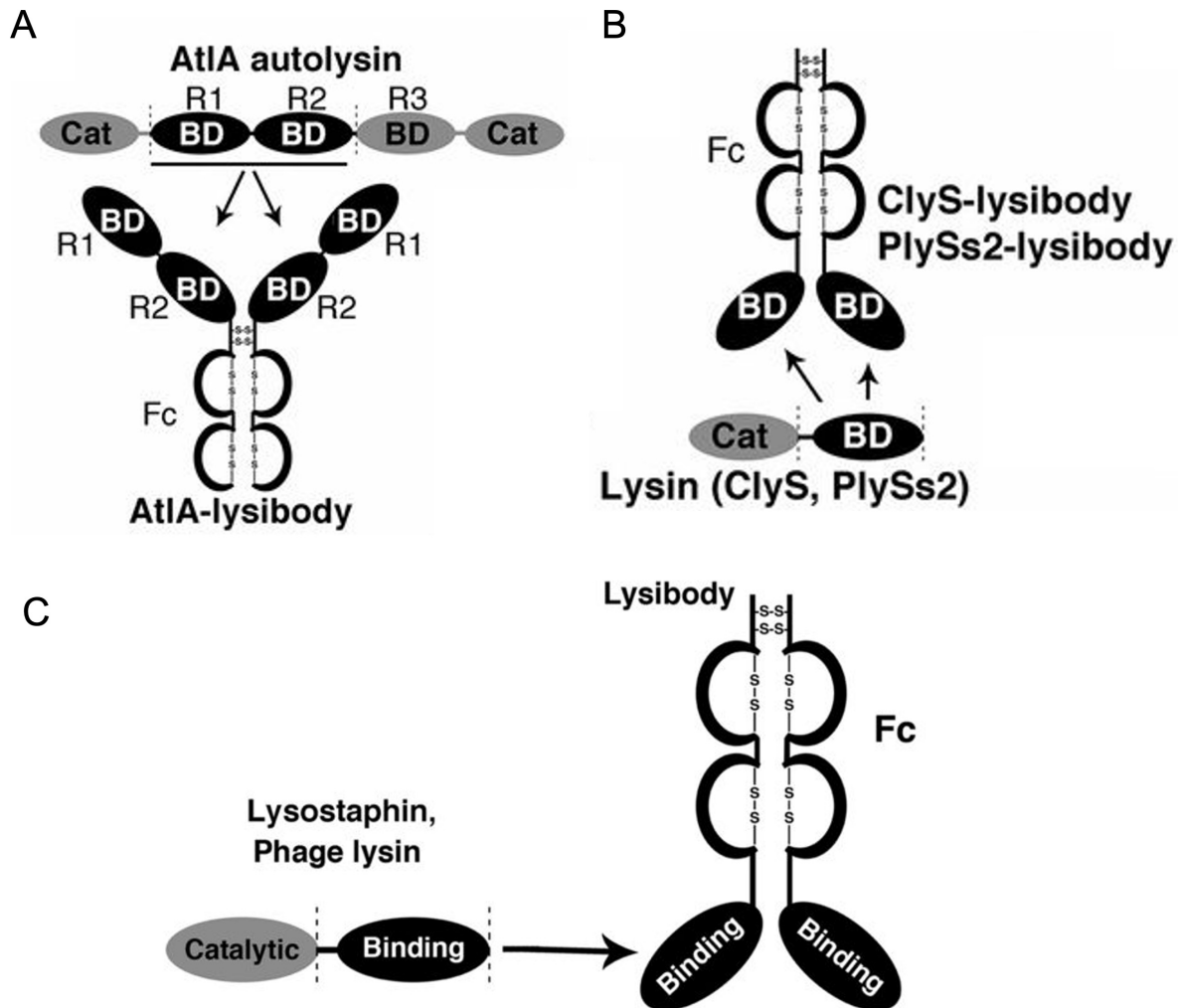
Figure 2.9 *Design of various 'lysibodies' by Raz and co-workers utilizing binding domains from (A) autolysins, (B) lysins, and (C) lysostaphin conjugated to human IgG Fc domains for immune mediated bacterial clearance. Reproduced with permission from*[59, 60]*.*

To address this, Raz and co-workers developed IgG Fc fusions with the carbohydrate binding domains of different cell wall hydrolases, creating 'lysibodies' that simultaneously target conserved regions of the bacterial cell wall and FCR's on immune cell surfaces.[59, 60] Several different lysibodies were constructed using varying cell binding domains that have specificity for methicillin-resistant *S. aureus* (MRSA) cell wall carbohydrates (Figure 2.9A-C). Cell binding of all lysibodies promoted an increase in complement deposition,

phagocytosis into both macrophages and neutrophils, and demonstrated protection against MRSA in a mouse model. Here it was demonstrated that lysibodies successfully cleared MRSA infections utilizing several different domains of cell wall binding proteins; therefore, this concept should be easily translated for the treatment of many different Gram-positive pathogens *via* implementing the corresponding species-specific cell wall binding domain into the lysibody scaffold.

2.3.7 Cell Targeting *via* Peptidoglycan Binding Proteins

PG binding proteins are found throughout both the bacterial and mammalian genome. For bacteria, it is essential that classes of proteins have inherent PG specificity to conduct processes involved in PG biosynthesis and remodeling. Alternatively, it is imperative that the host system also has protein classes of which detect and recognize bacterial PG to signal host defense mechanisms. Typically, such proteins are found within the immune system. Dalesandro and Pires took advantage of the PG specificity of a protein found within the innate immune system of *Ixodes scapularis* ticks called *Ixodes scapularis* antifreeze glycoprotein (IAFGP).[61] It was recently found that IAFGP binds to the D-alanine residue within the PG of the bacterial cell wall. Moreover, a fragment of this protein – called P1 – retained its ability to bind to the surface of the bacteria (Figure 2.10B).[62] Therefore, Dalesandro and Pires reasoned that conjugation of the exogenous hapten, fluorescein, onto P1 (P1fl) would label the bacterial to induce recruitment of anti-FITC antibodies (Figure 2.10A,C). It was demonstrated that P1fl mediated opsonization to the surface of vancomycin-resistant (VR) *Enterococci faecalis* (*E. faecalis*) preferentially over a vancomycin- sensitive strain. Additionally, phagocytotic uptake into macrophages was dependent on P1fl mediated bacterial cell binding, as minimal cell uptake was observed in the presence of a scramble peptide, P1fls. It was also shown that modifying the hapten on P1 still resulted in the recruitment of the cognate antibodies, for instance, utilizing the hapten DNP rather than FITC (Figure 2.10C).
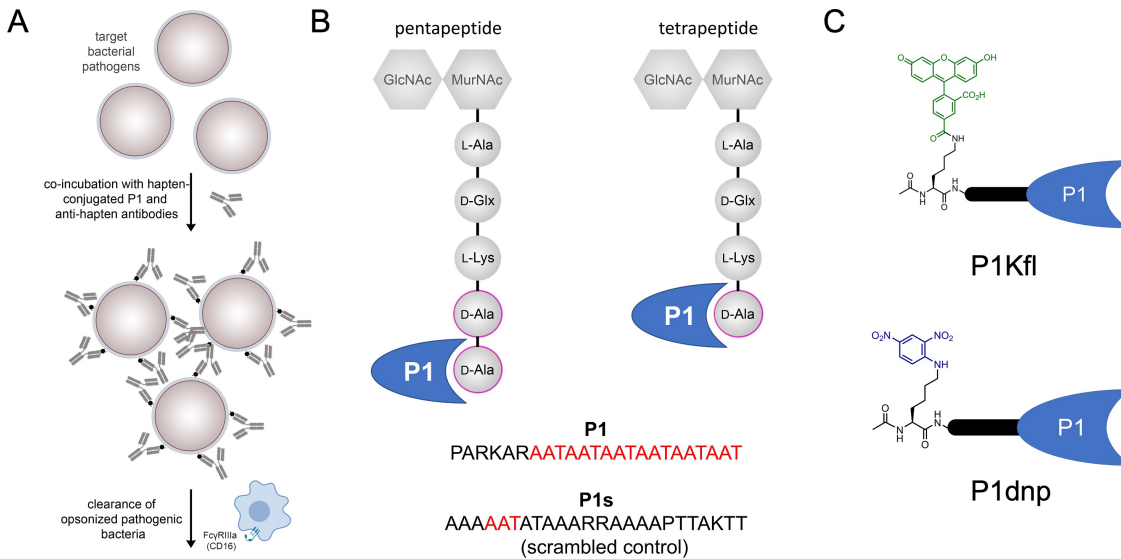
Figure 2.10 *Design of hapten conjugated PG binding peptide by Dalesandro and Pires for targeted bacterial immunotherapy. Reproduced with permission from[61].*

(A) General representation of hapten-P1 conjugates tagging the surface of bacteria followed by a specific immune response directed by the hapten. (B) Amino acid sequences of P1 and P1s with a cartoon representation of P1 binding to the D-Ala residue of a pentapeptide or tetrapeptide within the PG of the bacterial cell wall. D-iGlx refers to D-isoGln or D-isoGlu. (C) Chemical structures of modifications to P1 peptides.

2.3.8 Cell Targeting *via* Bacterial Biomacromolecule Binding Proteins

A major component of the bacterial cell wall is large biomacromoleules that are covalently anchored in the PG of Gram- positive bacteria and within the outer membrane of Gram-negative bacteria. As these biomacromolecules encompass most of the host exposed region of the bacterial cell, the immune system has evolved proteins that have specificity against such motifs. For example, the outer leaflet of the outer membrane in Gram-negative bacteria is comprised entirely of LPS; therefore, it is a main target of Toll-like

Receptors on immune cells. More specifically, a protein, CD14, has known affinity for LPS and is involved in recognition and signaling for Toll-like Receptor 4 (TLR4).[63] Drawing inspiration from bacterial binding immune proteins, Vida and co-workers developed a protein fusion consisting of CD14 and human IgG Fc to selectively target Gram- negative bacterial species for enhanced uptake into immune cells.[64] The artificial opsonin preferentially bound to the surface of Gram- negative bacteria and exhibited minimal binding to the Gram- positive bacteria, *Listeria monocytognenes.* The artificial opsonin increased uptake into neutrophils, macrophages, and dendritic cells, and phagocytosis was dependent on the human IgG Fc binding as uptake was inhibited by the FCR competitor, CD16.

2.3.9 Cell Binding *via* Enzymatic Mechanisms

A distinct approach in bacterial cell targeting for immunotherapy lies within hijacking the metabolic processes of the cell to covalently display the immune modulating moiety. Over the past several decades, it has been demonstrated that utilizing synthetic mimics of natural building blocks can be used to study enzyme tolerability and cellular processes within several biological systems. In bacterial systems, for example, synthetic analogs have been used to study the biosynthesis of lipids, proteins, nucleic acids, and metabolites.[65] The demonstrated promiscuity of these enzymes has enabled not only the mechanistic study of such processes, but also the development of immunotherapeutics that can be metabolic incorporated into live bacterial cells. Metabolic labeling of the target cell is advantageous because 1) the immune-modulator is irreversibly incorporated into the bacterial surface matrix, enabling longer persistence of the therapeutic modality compared to a non-covalent molecule and 2) mimicking natural, essential building blocks lessens the probably of developing therapeutic resistance.

Spiegel and co-workers applied a metabolic labeling strategy to bacterial cell surfaces by utilizing the promiscuity of SrtA.[66] Their work featured the conjugation of the SrtA sorting signal, LPXTG, to non-native small molecules to be covalently displayed on the PG of *S. aureus.* As a proof of concept, the LPXTG conjugates contained functional molecular

handles such as biotin, biorthogonal click handles, and fluorescein. It was demonstrated that covalent incorporation of the fluorescein motif into the PG scaffold of *S. aureus* by SrtA enabled the recruitment of anti-FITC antibodies (Figure 2.11A). This work was the first example of cell wall engineering of any pathogenic Gram- positive bacteria that can be used as precedence for further utility.
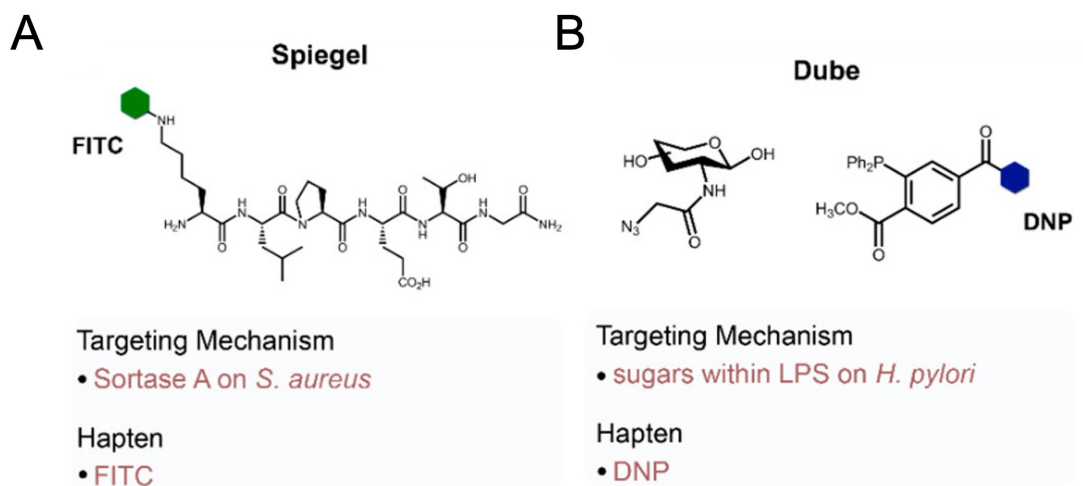
Figure 2.11 *Methods described to graft haptens onto the surface of pathogens via enzymatic reactions. Reproduced with permission from[22].*
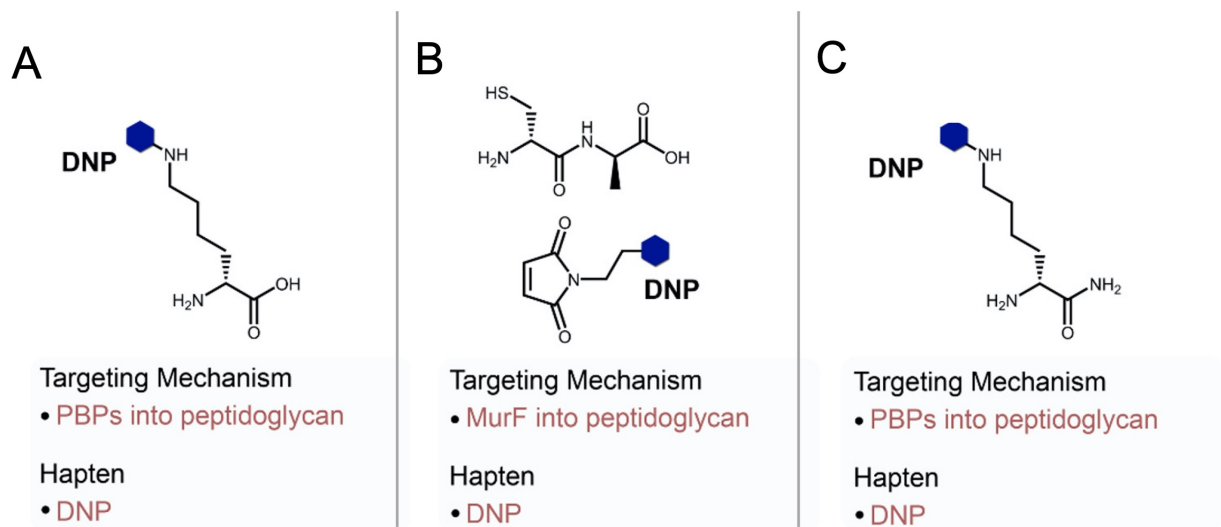
In a similar manner, Bertozzi, Reutter, and co-workers developed methods that hijack glycan synthesis pathways to metabolically label the surface of mammalian and bacterial cells. Metabolic oligosaccharide engineering (MOE) involves the installation of click handles on synthetic sugar substrates implemented in glycoconjugate synthesis.[67, 68] Dube and co-workers utilized this strategy to metabolically label the LPS of *Helicobacter pylori* (*Hp*) for the display of an immunogenic agent.[69] Glycans are an attractive target of *Hp* as they contribute to the overall pathogenicity of the species. The exterior of *Hp* is protected by an outer membrane of LPS that uniquely contains an unusual glycan core consisting of $_{DD}$-heptose, fucose, and N-acetylglucosamine (GlcNAc). Their design featured the incorporation of an azide handle onto a synthetic peractylated GlcNAc (Ac$_4$GlcNAz). Upon incubation with Ac$_4$GlcNAz, *Hp* metabolically displayed the azide

molecule onto the surface of the cell within the LPS structure. Since GlcNAc is unique to bacterial cells, treatment of mammalian cells with $Ac_4GlcNAz$ resulted in no labeling of extracellular glycans. Following surface display of the azide handle, a phosphine modified DNP was orthogonally reacted with the azide *via* a Staudinger ligation (Figure 2.11B). Finally, in a DNP dependent manner, effector cells induced damage to *Hp* when opsonized by anti-DNP antibodies as demonstrated by a bacterial viability assay.

To this point, enzymes involved in surface protein incorporation and biosynthetic glycan pathways have been exploited for hapten installation; however, one of the most critical pathways within the bacterial cell is the PG biosynthesis pathways. The Pires research lab was the first to utilize the promiscuity of PG transpeptidases to install immune modulators with the bacterial cell wall. Pires and others have demonstrated that the PG transpeptidase enzymes, DD- and LD-transpeptidases (Ddt and Ldt, respectively), are responsible for maintaining the integrity of the PG by catalyzing crosslinks to form between neighboring stem peptide strands. This is an essential and highly conserved process across all Gram-negative and Gram-positive bacteria. The Pires lab[70, 71] and others[72-74] have demonstrated that incubation of unnatural D-amino acids within the culture medium of growing bacterial cells, this unnatural D-amino acid will be metabolically installed within the PG stem peptide in place of the terminal D-alanine, in a process referred to D-amino acid swapping.

Fura and co-workers used this concept to metabolically incorporate haptens into the growing PG scaffold, referred to as D-amino acid antibody recruitment therapy (DART).[75] The hapten, DNP, was modified onto the g amine of D-lysine and added to the cell culture media of *Bacillus subtilis* (*B. subtilis*) and *S. aureus* (Figure 2.12A). Following metabolic incorporation of D-Lys(DNP) into the PG, flow cytometry analysis revealed that both DNP-tagged *B. subtilis* and *S. aureus* were able to bind both purified anti-DNP antibodies and anti-DNP antibodies from human serum. Additionally, opsonization of DNP tagged *B. subtilis* with anti-DNP antibodies from human serum led to enhanced phagocytic uptake into macrophages. Fura and Pires also probed to improve retention of the D-amino acid immune modulator within the PG by rendering the tag resistant to carboxypeptidase

activity and processing by crosslinking enzymes.[76] D-amino acid swapping naturally competes with crosslinking from a neighboring stem peptide amino group; therefore, Fura and Pires developed D-amino acid probes that have an amidated C-terminus, or a carboxamide, to better mimic the incoming nucleophile on the neighboring stem peptide, resulting in a more effective competition for the PBP acyl-intermediate (Figure 2.12B). They demonstrated that the carboxamide DNP derivative (DK-amide) drastically improved anti-DNP recruitment from human serum over the carboxylic acid DNP derivative (DK-acid) against *B. subtilis* and *E. faecalis*.


A

Targeting Mechanism
• PBPs into peptidoglycan

Hapten
• DNP

B

Targeting Mechanism
• MurF into peptidoglycan

Hapten
• DNP

C

Targeting Mechanism
• PBPs into peptidoglycan

Hapten
• DNP

Figure 2.12 *Designs described by the Pires laboratory in metabolically modifying bacterial cell surfaces with DNP epitopes. Reproduced with permission from[22].*

Another method developed by Fura and co-workers for targeted immunotherapy against bacterial cells hijacks the intracellular PG biosynthesis.[77] The advantage of targeting an earlier step in the PG biosynthetic pathway is the retention of the immune stimulant as mature PG is constantly being synthesized and remodeled.[78] Two processes that can potentially act to remove a D-amino acid label are carboxypeptidases and transpeptidases. Ddt mediated crosslinking involves hydrolysis of the terminal amino acid for activation of the acyl-donor intermediate. DD-carboxypeptidases catalyze the hydrolysis of the terminal residue for truncation into tetrapeptides to be further crosslinked

by LD-transpeptidases or partake in D-amino acid swapping by PBPs.[79] The intracellular enzyme, MurF, is responsible for ligating the terminal D-ala-D-ala motif to the newly synthesized PG precursor. Taking advantage of the promiscuity of MurF, Fura and co-workers synthesized a synthetic dipeptide, D-cys-D-ala, to take advantage of a dipeptide-based labeling strategy (Figure 2.12C). The D-cys was installed on the N-terminus for retention of the reactive moiety even in instance of hydrolysis to the C-terminal residue. Installation of the DNP hapten was achieved by reacting a maleimide-modified DNP with the reactive thiols embedded within the PG scaffold. Further, anti-DNP antibodies were recruited to the surface of *B. subtilis* in a DNP dependent manner.

Honing to target another class of bacterial enzymes, transpeptidases, for metabolic labeling of bacterial cells with immune tags, Dalesandro and Pires developed immune modulating synthetic analogs of peptidoglycan stem peptides for the recruitment of endogenous antibodies to the surface of vancomycin-resistant *E. faecalis*.[80] The Pires lab[81, 82] and others[83-86] demonstrated that synthetic PG analogs are tolerated by transpeptidase enzymes to metabolically label the PG of live bacterial cells. To capitalize on this enzyme promiscuity, their design featured a DNP-modified stem peptide (K(DNP)-Tetra) that can act as either an acyl-donor by Ldts or acyl-acceptor by both Ldts and Ddts to be crosslinked into the PG scaffold (Figure 2.13A,D). Metabolic incorporation of K(DNP)-Tetra into vancomycin-resistant *E. faecium* PG resulted in opsonization of anti-DNP antibodies and increased phagocytosis into macrophages in the presence of human serum (Figure 2.13B,C).
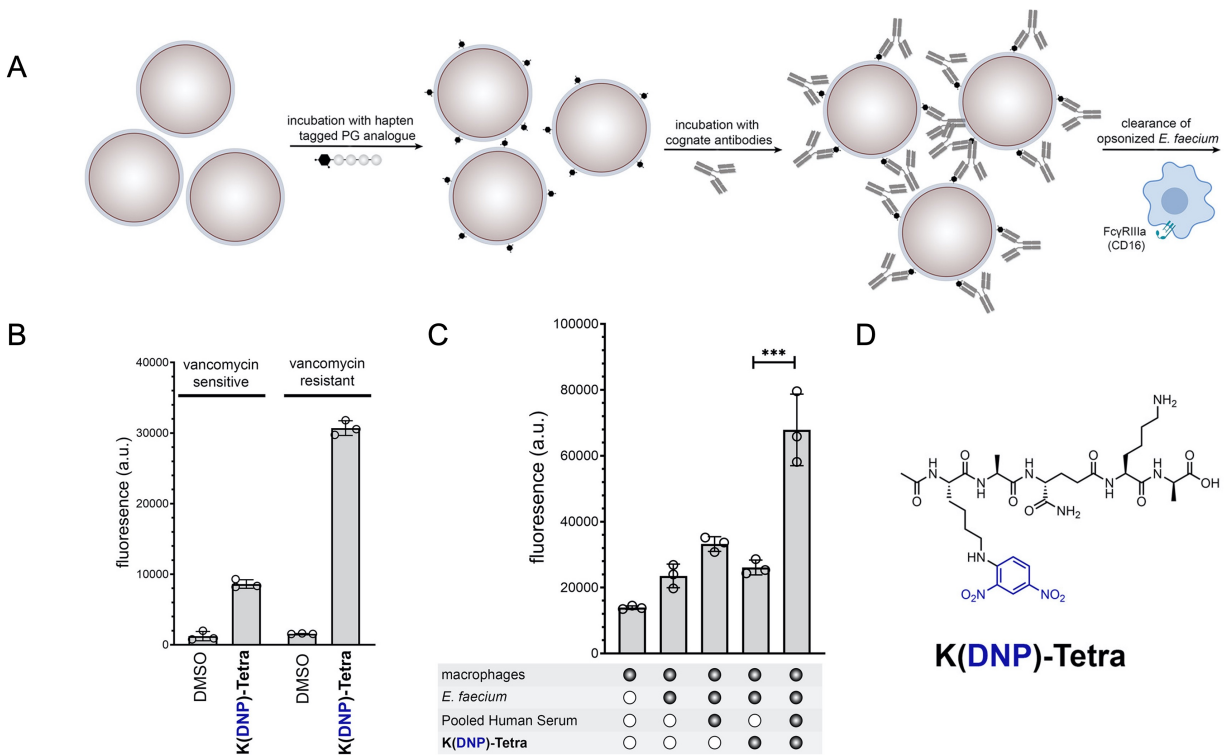
Figure 2.13 *Design of hapten conjugated PG binding peptide by Dalesandro and Pires for targeted bacterial immunotherapy. Reproduced with permission from[80].*

(A) General representation of hapten conjugates tagging the surface of *E. faecium* followed by a specific immune response. (B) Flow cytometry analysis of *E. faecium* (vancoymycin-sensitive and resistant strains) treated overnight with 100 µM K(DNP)-Tetra followed by incubation with Alexa Flour 488- conjugated anti-DNP antibodies. (C) Phagocytosis of bacterial cells was evaluated by incubating *E. faecium*(vancoymycin-resistant) in the presence or absence of 100 µM of K(DNP)-Tetra overnight and subsequently incubated with PBS or 15% PHS. J774A.1 macrophages were incubated for 20 min in the presence or absence of calcien-AM labeled *E. faecium* cells and measured by flow cytometry. Filled in circles indicate that those conditions were present in the assay arm. (D) Chemical structures of a PG analogue modified with the hapten DNP.

2.4 Conclusion

Within the past ten years, the field of bacterial immunotherapy has greatly expanded. Mechanisms to incorporate haptens for a directed antibody response range from non-covalent associations to covalent metabolic labels. Additionally, the repurposing of antibiotics for bacterial cell targeting have been implicated into antibody conjugates and immune receptor stimulating molecules that target both Gram- positive and Gram-negative bacterial pathogens. Drawing inspiration from the immune system, protein motifs that have high affinity for PG, surface carbohydrates, and surface polymers have been modified to drive phagocytotic uptake of bacterial pathogens in antibody-mediated and receptor-mediated manners. Although many challenges still exist in harnessing an immune response against bacterial pathogens, the progress made thus far in terms of therapeutic development and understanding bacteria-host interactions has a tremendous impact in the fight towards treating drug-resistant bacterial infections.

2.5 Summary and Future Outlook

The discovery and development of effective treatment options against drug resistant bacteria is declining dramatically. As a result, it is generally accepted that antibiotic therapy may never be the solution for combating drug resistant pathogens. Therefore, the development of novel therapeutic approaches to overcome the ever-evolving mechanisms that multidrug-resistant bacteria use to evade current treatments is critical. Chapter 2 describes the advances made to date in terms of applying immunotherapeutic techniques to target bacterial infections. A benefit to such therapy lies within utilizing pre-existing bacterial clearance mechanisms already in place by the immune system, ultimately enhancing the antibacterial effects. By installing immune modulators onto the bacterial cell, it will re-direct components of the immune system to once again target bacterial cells that may have undergone immune evasion mechanisms, circumventing resistance. It may be the case that bacterial immunotherapy may not completely solve the ever-growing problem of resistance; however, it is believed that only a multidisciplinary approach will enable the combat of the urgent threat of antimicrobial

resistance. Therefore, perhaps a combination therapy of antibiotic treatment and reinforced immune stimulation to the bacterial cell may provide as an effective modality to combat high priority infections.

2.6 References

1.   Medzhitov, R. Recognition of microorganisms and activation of the immune response. *Nature* **449**, 819-826 (2007).

2.   Akira, S., Uematsu, S. & Takeuchi, O. Pathogen recognition and innate immunity. *Cell* **124**, 783-801 (2006).

3.   Kubelkova, K. & Macela, A. Innate Immune Recognition: An Issue More Complex Than Expected. *Front Cell Infect Microbiol* **9**, 241 (2019).

4.   Finlay, B.B. & McFadden, G. Anti-immunology: evasion of the host immune system by bacterial and viral pathogens. *Cell* **124**, 767-782 (2006).

5.   Philpott, D.J. & Girardin, S.E. The role of Toll-like receptors and Nod proteins in bacterial infection. *Mol Immunol* **41**, 1099-1108 (2004).

6.   Park, B.S. & Lee, J.O. Recognition of lipopolysaccharide pattern by TLR4 complexes. *Exp Mol Med* **45**, e66 (2013).

7.   Alberts, B. *Molecular biology of the cell*, Edn. 4th. (Garland Science, New York; 2002).

8.   Janeway, C. *Immunobiology : the immune system in health and disease*, Edn. 6th. (Garland Science, New York; 2005).

9.   Marshall, J.S., Warrington, R., Watson, W. & Kim, H.L. An introduction to immunology and immunopathology. *Allergy Asthma Clin Immunol* **14**, 49 (2018).

10.   Dunkelberger, J.R. & Song, W.C. Complement and its role in innate and adaptive immune responses. *Cell Res* **20**, 34-50 (2010).

11.   Heesterbeek, D.A.C., Angelier, M.L., Harrison, R.A. & Rooijakkers, S.H.M. Complement and Bacterial Infections: From Molecular Mechanisms to Therapeutic Applications. *J Innate Immun* **10**, 455-464 (2018).

12.   Serna, M., Giles, J.L., Morgan, B.P. & Bubeck, D. Structural basis of complement membrane attack complex formation. *Nature Communications* **7** (2016).

13.   Nimmerjahn, F. & Ravetch, J.V. Fcgamma receptors as regulators of immune responses. *Nat Rev Immunol* **8**, 34-47 (2008).

14.   Zahavi, D., AlDeghaither, D., O'Connell, A. & Weiner, L.M. Enhancing antibody-dependent cell-mediated cytotoxicity: a strategy for improving antibody-based immunotherapy. *Antib Ther* **1**, 7-12 (2018).

15.   Uribe-Querol, E. & Rosales, C. Control of Phagocytosis by Microbial Pathogens. *Front Immunol* **8**, 1368 (2017).

16.   Winau, F. & Winau, R. Emil von Behring and serum therapy. *Microbes Infect* **4**, 185-188 (2002).

17.   Kaufmann, S.H.E. Remembering Emil von Behring: from Tetanus Treatment to Antibody Cooperation with Phagocytes. *Mbio* **8** (2017).

18.   Shapiro-Shapin, C.G. Pearl Kendrick, Grace Eldering, and the Pertussis Vaccine. *Emerg Infect Dis* **16**, 1273-1278 (2010).

19.   Marks, H.M. The Kendrick-Eldering-(Frost) pertussis vaccine field trial. *J Roy Soc Med* **100**, 242-247 (2007).

20.   Cook, M.A. & Wright, G.D. The past, present, and future of antibiotics. *Sci Transl Med* **14** (2022).

21.   Blair, J.M., Webber, M.A., Baylay, A.J., Ogbolu, D.O. & Piddock, L.J. Molecular mechanisms of antibiotic resistance. *Nat Rev Microbiol* **13**, 42-51 (2015).

22.   Feigman, M.J.S. & Pires, M.M. Synthetic Immunobiotics: A Future Success Story in Small Molecule-Based Immunotherapy? *Acs Infect Dis* **4**, 664-672 (2018).

23.   Motley, M.P., Banerjee, K. & Fries, B.C. Monoclonal antibody-based therapies for bacterial infections. *Curr Opin Infect Dis* **32**, 210-216 (2019).

24.   Sharon, N., Eshdat, Y., Silverblatt, F.J. & Ofek, I. Bacterial adherence to cell surface sugars. *Ciba Found Symp* **80**, 119-141 (1981).

25.   Bertozzi, C. & Bednarski, M. C-glycosyl compounds bind to receptors on the surface of Escherichia coli and can target proteins to the organism. *Carbohydr Res* **223**, 243-253 (1992).

26.   Li, J. *et al.* Bacteria targeted by human natural antibodies using alpha-Gal conjugated receptor-specific glycopolymers. *Bioorg Med Chem* **7**, 1549-1558 (1999).

27.   Rother, R.P. & Squinto, S.P. The alpha-galactosyl epitope: a sugar coating that makes viruses and cells unpalatable. *Cell* **86**, 185-188 (1996).

28.	Apostolopoulos, V. & McKenzie, I.F. Role of the mannose receptor in the immune response. *Curr Mol Med* **1**, 469-474 (2001).

29.	Kristian, S.A. *et al.* Retargeting pre-existing human antibodies to a bacterial pathogen with an alpha-Gal conjugated aptamer. *J Mol Med* **93**, 619-631 (2015).

30.	Kolm, C. *et al.* DNA aptamers against bacterial cells can be efficiently selected by a SELEX process using state-of-the art qPCR and ultra-deep sequencing. *Sci Rep-Uk* **10** (2020).

31.	Vinogradov, A.A., Yin, Y.Z. & Suga, H. Macrocyclic Peptides as Drug Candidates: Recent Progress and Remaining Challenges. *J Am Chem Soc* **141**, 4167-4181 (2019).

32.	Idso, M.N. *et al.* Antibody-recruiting protein-catalyzed capture agents to combat antibiotic-resistant bacteria. *Chem Sci* **11**, 3054-3067 (2020).

33.	Krishnamurthy, V.M. *et al.* Promotion of opsonization by antibodies and phagocytosis of Gram-positive bacteria by a bifunctional polyacrylamide. *Biomaterials* **27**, 3663-3674 (2006).

34.	Ge, M. *et al.* Vancomycin derivatives that inhibit peptidoglycan biosynthesis without binding D-Ala-D-Ala. *Science* **284**, 507-511 (1999).

35.	Roy, R.S. *et al.* Direct interaction of a vancomycin derivative with bacterial enzymes involved in cell wall biosynthesis. *Chem Biol* **8**, 1095-1106 (2001).

36.	Arimoto, H., Nishimura, K., Kinumi, T., Hayakawa, I. & Uemura, D. Multi-valent polymer of vancomycin: enhanced antibacterial activity against VRE. *Chem Commun*, 1361-1362 (1999).

37.	Sabulski, M.J., Pidgeon, S.E. & Pires, M.M. Immuno-targeting of Staphylococcus aureus via surface remodeling complexes. *Chem Sci* **8**, 6804-6809 (2017).

38.	Hendrickx, A.P.A., Budzik, J.M., Oh, S.Y. & Schneewind, O. Architects at the bacterial surface - sortases and the assembly of pili with isopeptide bonds. *Nature Reviews Microbiology* **9**, 166-176 (2011).

39.	Marraffini, L.A., DeDent, A.C. & Schneewind, O. Sortases and the art of anchoring proteins to the envelopes of gram-positive bacteria. *Microbiol Mol Biol R* **70**, 192-+ (2006).

40.	Mazmanian, S.K., Liu, G., Hung, T.T. & Schneewind, O. Staphylococcus aureus sortase, an enzyme that anchors surface proteins to the cell wall. *Science* **285**, 760-763 (1999).

41.   Popp, M.W., Antos, J.M., Grotenbreg, G.M., Spooner, E. & Ploegh, H.L. Sortagging: a versatile method for protein labeling. *Nat Chem Biol* **3**, 707-708 (2007).

42.   Feigman, M.S. *et al.* Synthetic Immunotherapeutics against Gram-negative Pathogens. *Cell Chem Biol* **25**, 1185-+ (2018).

43.   Brown, P. & Dawson, M.J. Development of new polymyxin derivatives for multi-drug resistant Gram-negative infections. *J Antibiot* **70**, 386-394 (2017).

44.   Tsubery, H. *et al.* Neopeptide antibiotics that function as opsonins and membrane-permeabilizing agents for gram-negative bacteria. *Antimicrob Agents Ch* **49**, 3122-3128 (2005).

45.   Zhuang, Y.W. *et al.* Molecular recognition of formylpeptides and diverse agonists by the formylpeptide receptors FPR1 and FPR2. *Nature Communications* **13** (2022).

46.   Payne, J.A.E. *et al.* Antibiotic-chemoattractants enhance neutrophil clearance of Staphylococcus aureus. *Nature Communications* **12** (2021).

47.   Drabick, J.J. *et al.* Covalent polymyxin B conjugate with human immunoglobulin G as an antiendotoxin reagent. *Antimicrob Agents Ch* **42**, 583-588 (1998).

48.   Lehar, S.M. *et al.* Novel antibody-antibiotic conjugate eliminates intracellular S. aureus. *Nature* **527**, 323-+ (2015).

49.   Kajihara, K.K. *et al.* Potent Killing of Pseudomonas aeruginosa by an Antibody-Antibiotic Conjugate. *Mbio* **12** (2021).

50.   Katzenmeyer, K.N., Szott, L.M. & Bryers, J.D. Artificial opsonin enhances bacterial phagocytosis, oxidative burst and chemokine production by human neutrophils. *Pathog Dis* **75** (2017).

51.   Chiu, M.L., Goulet, D.R., Teplyakov, A. & Gilliland, G.L. Antibody Structure and Function: The Basis for Engineering Therapeutics. *Antibodies* **8** (2019).

52.   Bebbington, C. & Yarranton, G. Antibodies for the treatment of bacterial infections: current experience and future prospects. *Curr Opin Biotechnol* **19**, 613-619 (2008).

53.   Casadevall, A., Dadachova, E. & Pirofski, L. Passive antibody therapy for infectious diseases. *Nature Reviews Microbiology* **2**, 695-703 (2004).

54.   Weidenmaier, C. & Peschel, A. Teichoic acids and related cell-wall glycopolymers in Gram-positive physiology and host interactions. *Nature Reviews Microbiology* **6**, 276-287 (2008).

55. Buist, G., Steen, A., Kok, J. & Kuipers, O.R. LysM, a widely distributed protein motif for binding to (peptido)glycans. *Mol Microbiol* **68**, 838-847 (2008).

56. Vollmer, W., Joris, B., Charlier, P. & Foster, S. Bacterial peptidoglycan (murein) hydrolases. *Fems Microbiol Rev* **32**, 259-286 (2008).

57. Mond, J.J., Lees, A. & Snapper, C.M. T-Cell-Independent Antigens Type-2. *Annu Rev Immunol* **13**, 655-692 (1995).

58. Snapper, C.M. & Mond, J.J. A model for induction of T cell-independent humoral immunity in response to polysaccharide antigens. *J Immunol* **157**, 2229-2233 (1996).

59. Raz, A. *et al.* Lysibodies are IgG Fc fusions with lysin binding domains targeting Staphylococcus aureus wall carbohydrates for effective phagocytosis. *Proc Natl Acad Sci U S A* **114**, 4781-4786 (2017).

60. Raz, A., Serrano, A., Thaker, M., Alston, T. & Fischetti, V.A. Lysostaphin Lysibody Leads to Effective Opsonization and Killing of Methicillin-Resistant Staphylococcus aureus in a Murine Model. *Antimicrob Agents Ch* **62** (2018).

61. Dalesandro, B.E. & Pires, M.M. Immuno-targeting of Gram-positive Pathogens via a Cell Wall Binding Tick Antifreeze Protein. *bioRxiv*, 2022.2009.2002.506389 (2022).

62. Abraham, N.M. *et al.* Pathogen-mediated manipulation of arthropod microbiota to promote infection. *P Natl Acad Sci USA* **114**, E781-E790 (2017).

63. Antal-Szalmas, P. Evaluation of CD14 in host defence. *Eur J Clin Invest* **30**, 167-179 (2000).

64. Vida, A. *et al.* Fusion of the Fc part of human IgG1 to CD14 enhances its binding to gram-negative bacteria and mediates phagocytosis by Fc receptors of neutrophils. *Immunol Lett* **146**, 31-39 (2012).

65. Siegrist, M.S., Swarts, B.M., Fox, D.M., Lim, S.A. & Bertozzi, C.R. Illumination of growth, division and secretion by metabolic labeling of the bacterial cell surface. *Fems Microbiol Rev* **39**, 184-202 (2015).

66. Nelson, J.W. *et al.* A Biosynthetic Strategy for Re-engineering the Staphylococcus aureus Cell Wall with Non-native Small Molecules. *Acs Chem Biol* **5**, 1147-1155 (2010).

67. Luchansky, S.J. *et al.* Constructing azide-labeled cell surfaces using polysaccharide biosynthetic pathways. *Method Enzymol* **362**, 249-272 (2003).

68.   Prescher, J.A., Dube, D.H. & Bertozzi, C.R. Chemical remodelling of cell surfaces in living animals. *Nature* **430**, 873-877 (2004).

69.   Kaewsapsak, P., Esonu, O. & Dube, D.H. Recruiting the Host's Immune System to Target Helicobacter pylori's Surface Glycans. *Chembiochem* **14**, 721-726 (2013).

70.   Fura, J.M., Kearns, D. & Pires, M.M. D-Amino Acid Probes for Penicillin Binding Protein-based Bacterial Surface Labeling. *J Biol Chem* **290**, 30540-30550 (2015).

71.   Pidgeon, S.E. & Pires, M.M. Cell Wall Remodeling of Staphylococcus aureus in Live Caenorhabditis elegans. *Bioconjugate Chem* **28**, 2310-2315 (2017).

72.   Kuru, E. *et al.* In Situ Probing of Newly Synthesized Peptidoglycan in Live Bacteria with Fluorescent D-Amino Acids. *Angew Chem Int Edit* **51**, 12519-12523 (2012).

73.   Shieh, P., Siegrist, M.S., Cullen, A.J. & Bertozzi, C.R. Imaging bacterial peptidoglycan with near-infrared fluorogenic azide probes. *P Natl Acad Sci USA* **111**, 5456-5461 (2014).

74.   Siegrist, M.S. *et al.* D-Amino Acid Chemical Reporters Reveal Peptidoglycan Dynamics of an Intracellular Pathogen. *Acs Chem Biol* **8**, 500-505 (2013).

75.   Fura, J.M., Sabulski, M.J. & Pires, M.M. D-Amino Acid Mediated Recruitment of Endogenous Antibodies to Bacterial Surfaces. *Acs Chem Biol* **9**, 1480-1489 (2014).

76.   Fura, J.M. & Pires, M.M. D-Amino Carboxamide-Based Recruitment of Dinitrophenol Antibodies to Bacterial Surfaces via Peptidoglycan Remodeling. *Biopolymers* **104**, 351-359 (2015).

77.   Fura, J.M., Pidgeon, S.E., Birabaharan, M. & Pires, M.M. Dipeptide-Based Metabolic Labeling of Bacterial Cells for Endogenous Antibody Recruitment. *Acs Infect Dis* **2**, 302-309 (2016).

78.   Typas, A., Banzhaf, M., Gross, C.A. & Vollmer, W. From the regulation of peptidoglycan synthesis to bacterial growth and morphology. *Nature Reviews Microbiology* **10**, 123-136 (2012).

79.   Popham, D.L., Gilmore, M.E. & Setlow, P. Roles of low-molecular-weight penicillin-binding proteins in Bacillus subtilis spore peptidoglycan synthesis and spore properties. *J Bacteriol* **181**, 126-132 (1999).

80.   Dalesandro, B.E. & Pires, M.M. Induction of Endogenous Antibody Recruitment to the Surface of the Pathogen Enterococcus faecium. *Acs Infect Dis* **7**, 1116-1125 (2021).

81.   Apostolos, A.J., Pidgeon, S.E. & Pires, M.M. Remodeling of Cross-bridges Controls Peptidoglycan Cross-linking Levels in Bacterial Cell Walls. *Acs Chem Biol* **15**, 1261-1267 (2020).

82.   Pidgeon, S.E. *et al.* L,D-Transpeptidase Specific Probe Reveals Spatial Activity of Peptidoglycan Cross-Linking. *Acs Chem Biol* **14**, 2185-2196 (2019).

83.   Gautam, S. *et al.* An Activity-Based Probe for Studying Crosslinking in Live Bacteria. *Angew Chem Int Edit* **54**, 10492-10496 (2015).

84.   Gautam, S., Kim, T. & Spiegel, D.A. Chemical Probes Reveal an Extraseptal Mode of Cross-Linking in Staphylococcus aureus. *J Am Chem Soc* **137**, 7441-7447 (2015).

85.   Ngadjeua, F. *et al.* Critical Impact of Peptidoglycan Precursor Amidation on the Activity of L,D-Transpeptidases from Enterococcus faecium and Mycobacterium tuberculosis. *Chem-Eur J* **24**, 5743-5747 (2018).

86.   Welsh, M.A. *et al.* Identification of a Functionally Unique Family of Penicillin-Binding Proteins. *J Am Chem Soc* **139**, 17727-17730 (2017).

Chapter 3 Induction of Endogenous Antibody Recruitment to the Surface of the Pathogen *Enterococcus faecium*

3.1 Abstract

For the foreseeable future, conventional small molecule antibiotics will continue to be the predominant treatment option due to wide patient coverage and low costs. Today, however, there is already a significant portion of patients that fail to respond to small molecule antibiotics and, according to the Centers for Disease Control and Prevention, this number is poised to increase in the coming years. Therefore, this rise in drug resistant bacteria must be countered with the development of nontraditional therapies. We propose a measure based on the re-engagement of the immune system toward pathogenic bacteria by grafting bacterial cell surfaces with immunogenic agents. Herein, we describe a class of cell wall analogues that selectively graft bacterial cell surfaces with epitopes that promote their opsonization. More specifically, synthetic analogues of peptidoglycan conjugated to haptens were designed to be incorporated by the cell wall biosynthetic machinery into live *Enterococcus faecium. E. faecium* is a formidable human pathogen that poses a considerable burden to healthcare and often results in fatalities. We showed that treatment of *E. faecium* and vancomycin-resistant strains with the cell wall analogues led to the display of haptens on the cell surface, which induced the recruitment of antibodies existing in the serum of humans. These results demonstrate the feasibility in using cell wall analogues as the basis of a class of bacterial immunotherapies against dangerous pathogens.

3.2 Introduction

Enterococci bacteria are microorganisms found in many diverse environments such as water, plants, soil, food, and the gastrointestinal tract (GI) of humans and animals. Recently, enterococci have been used as probiotics for the treatment or prevention of

irritable bowel syndrome and chronic intestinal disease.[1, 2] Although some enterococci exhibit health promoting benefits, other members of the same genus have evolved to be among the leading causative agents of nosocomial infections due to the emergence of several drug-resistance strains.[3, 4] As enterococci commonly exist as part of the gut microbiota, patient treatment with antibiotics can result in dysbiosis, thus precipitating the gut colonization of drug-resistant enterococci. The pathogen *Enterococcus faecium* is one of the more difficult enterococci infections to treat as it has developed resistance to several β-lactam antibiotics and the last-resort antibiotic, vancomycin. The Centers for Disease Control and Prevention (CDC) has identified vancomycin-resistant enterococci (VRE) as a serious threat level pathogen, as treatment options for this organism are becoming limited.[3, 5, 6] With the rise of incident VRE infections, it is clear that developing new treatment options is critical.

The human immune system is primed to identify infectious agents by means of recognition of pathogen associated molecular patterns (PAMPs). Upon an encounter with pathogenic bacteria, PAMP detection orchestrates an immune response to fend off bacterial colonization.[7-9] An example of this process includes the activation of toll-like receptors by bacterial cell wall fragments, which signals for the secretion of cytokines and induces the recruitment of effector cells (i.e., macrophages) for pathogen elimination.[10-12] Bacterial cells have developed mechanisms to evade immune responses or the challenge of antibiotics. For example, pathogens chemically modify the molecular structure of their PAMPs to avoid such detection.[13-15] For VRE, a prominent mechanism of drug resistance involves the chemical modification of cell wall components to circumvent recognition by vancomycin.[16, 17] To combat VRE, we set out to build agents that, instead of recognizing components of the cell wall, chemically reprogram the surface of bacterial pathogens to redirect the immune system toward *E. faecium* for enhanced clearance (Figure 3.1).
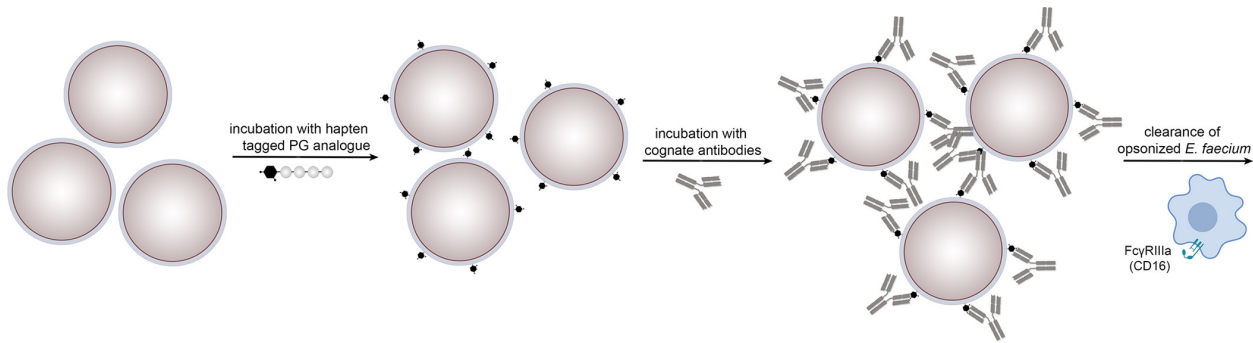
Figure 3.1 *General representation of hapten conjugates tagging the surface of E. faecium followed by a specific immune response.*

Recently, a number of highly successful immunotherapies have been described with the goal of engineering a guided immune response to target diseased cells. In the area of cancer therapy, two vastly different classes of agents (checkpoint blockers and the chimeric antigen receptor T-cells) have completely altered the therapeutic landscape by demonstrating the power of using a patient's own immune system to target cancer cells.[18-21] Another modality of cancer immunotherapy is centered on grafting small molecule haptens on the surface of malignant cells to induce antibody recruitment, followed by tumor clearance.[22-28] For example, Low and co-workers have developed several pioneering clinical candidates utilizing this approach to target cells that overexpress cancer biomarkers.[29-32] Immunotherapy for treatment of cancer has been successful for selectively targeting cancer cells over healthy cells, despite the two cell types exhibiting high level of similarity in surface composition. In contrast to cancer cells, bacterial cells have vast differences in composition compared to human cells, which in fact are already exploited by our immune system. Our group[32-35] and others[36, 37] have taken advantage of this feature to design amino acid agents that tag the surface of bacterial pathogens with small molecule haptens to induce their opsonization, leading to enhanced destruction by components in the immune system.

We identified peptidoglycan (PG) as a suitable biomacromolecule to target for recognition by the immune system due to its exposure to the extracellular space in Gram-positive bacteria. PG is a major component of the bacterial cell wall, and it provides

physical and chemical stability to the bacterial cell. PG is a mesh-like scaffold found on the outside of the cytoplasmic membrane and is essential for maintaining cell wall integrity.[38-40] The primary structure of PG is composed of repeating disaccharide units, *N*-acetyl-glucosamine (GlcNAc) and *N*-acetyl-muramic acid (MurNAc), with a pentapeptide chain (stem peptide) attached to MurNAc. The sequence of the stem peptide is generally conserved between bacterial species and contain the amino acids ʟ-Ala-ᴅ-Glx-(ʟ-Lys/*m*-DAP)-ᴅ-Ala-ᴅ-Ala (where *m*-DAP is *meso*-diaminopimelic acid). Once attached to the existing PG scaffold, nascent stem peptide chains are cross-linked together by two classes of transpeptidases: penicillin binding proteins (PBP) and ʟ,ᴅ-transpeptidases (Ldts) that create 4→3 cross-links and 3→3 cross-links, respectively (Figure 3.2A).[41-44] PG cross-linking is vital to bacterial survival as demonstrated by a large number of antibiotics that inhibit PG cross-linking.
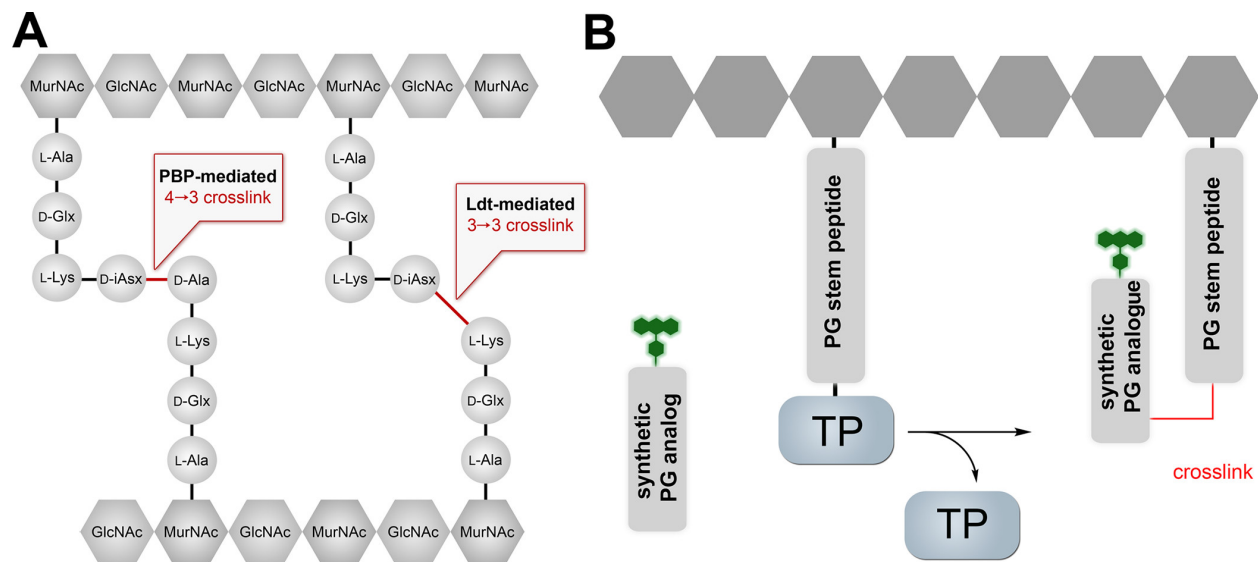
Figure 3.2 *Crosslinking in E. faecium*

(A) Schematic of PG cross-linking in *E. faecium* showing the two types of cross-links. (B) Diagram showing how the fluorescently tagged PG analogues covalently cross-linked into bacterial PG scaffold. D-iAsx refers to D-isoAsn or D-isoAsp. D-iGlx refers to D-isoGln or D-isoGlu

Realizing that some types of VRE involve the alteration of stem peptide biosynthesis[45-47] by the hydrolysis of the pentamer chain to a tetramer to escape recognition by vancomycin, we reasoned that we could build analogues of PG tetramers to gain entry into the cross-linking step during PG maturation. Recently, our lab[48, 49] and others,[50-53] have demonstrated that synthetic mimics of the stem peptide can be used to label the PG of live bacteria cells. More specifically, our group showed that tetrapeptide analogues of PG were incorporated into the PG scaffold of several bacterial strains. Herein, we have applied these observations to design novel tetrapeptide PG analogues that are conjugated to a DNP hapten through a lysine spacer, incorporated to enhance surface presentation. These agents hijack the cell wall machinery of *E. faecium* to metabolically install haptens on to the surface of Gram-positive bacteria for the recruitment of endogenous antibodies (Figure 3.2B). We anticipate that this design will (1) increase the display of haptens on the surface of pathogenic bacteria by utilization of a PG substrate and (2) covalently anchor haptens, by means of cross-linking, within the PG of VRE.

3.3 Results and Discussion

3.3.1 FITC modified tetrapeptide analogs to label the cell wall of E. faecium

To test our hypothesis that stem peptide mimics will efficiently tag the surface of bacterial cells to display non-native epitopes, a library of stem peptide analogues was designed and synthesized. All peptides included a fluorescein (Fl) handle attached to an amino group, which can be used to measure tagging efficiency (Figure 3.3A). We initially built four molecules (a single d-amino acid, one tripeptide, and two tetrapeptides) that were intended to be metabolically incorporated into the PG scaffold of *E. faecium* (Figure 3.3B). The simple supplementation of single unnatural d-amino acids to culture media results in their covalent incorporation into the PG scaffold, a feature that has been exploited by our group and others to label PG.[54-60] Likewise, we and others have also demonstrated that analogues of PG stem peptides can be cross-linked into the growing PG scaffold of live cells.
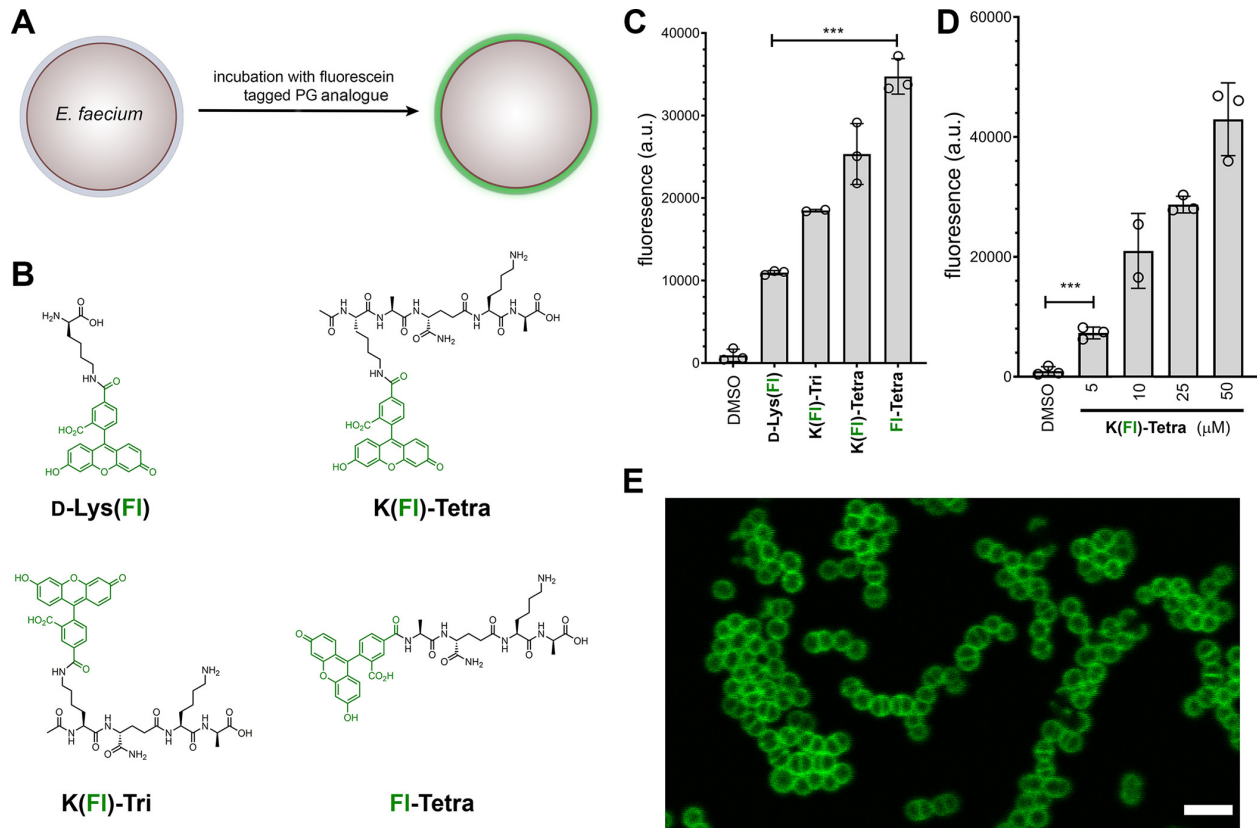
Figure 3.3 *Labeling of FITC tetrapeptide analogues of live E. faecium*

(A) Representation of the assay to measure incorporation of PG analogues. (B) Chemical structures of four initial PG analogues modified with Fl. (C) Flow cytometry analysis of *E. faecium* treated overnight with 100 μM of PG analogues. (D) Flow cytometry analysis of *E. faecium* treated overnight with varying concentrations of K(Fl)-Tetra. Data are represented as ± SD (n = 3). P-values were determined by a two- tailed t-test (*p < 0.05, **p < 0.01, ***p < 0.001, ns = not significant). (E) Confocal microscopy of E. faecium treated overnight with 100 μM K(Fl)-Tetra. Scale bar = 3 μm.

Bacterial cells were incubated with individual synthetic PG analogues and fluorescence levels were measured by flow cytometry, which should correlate with PG incorporation into live cells (Figure 3.3C). As expected, cell treatment with the single amino acid **D-Lys(Fl)** resulted in increased cellular fluorescence levels that were ~12-fold higher than untreated cells, which is consistent with the swapping of the terminal d-alanine with the

exogenous unnatural ᴅ-amino acid. The other three PG analogues evaluated were either tri- (**K(Fl)-Tri**) or tetra- (**K(Fl)-Tetra** and **Fl-Tetra**) stem peptides that were predicted to get incorporated by transpeptidases by acting as acyl-donor and/or -acceptors to get covalently linked into the PG scaffold (Figure 3.2A). We had previously used **Fl-Tetra** to dissect transpeptidase activity in live bacterial cells.[49] With the idea of providing better surface presentation of the hapten, we explored the inclusion of a lysine spacer that naturally includes an additional spacer unit. Satisfyingly, we found that all three stem peptide analogues led to higher tagging levels compared to ᴅ-**Lys(Fl)**. Moreover, these results are consistent with our previous work that showed high levels of incorporation of tetrapeptide analogues. Localization was revealed by confocal microscopy and it showed that incorporation of **K(Fl)-Tetra** was displayed on the surface of cells, as expected (Figure 3.3E). Next, *E. faecium* cells were treated with increasing concentrations of **K(Fl)-Tetra** and analyzed by flow cytometry (Figure 3.3D). Significant levels of cellular tagging were observed at concentrations as low as 5 µM. Due to increased incorporation efficiency of our fluorescent stem peptide mimics over single d-amino acids, we hypothesize that utilizing such analogues for hapten display will elicit an enhanced immune response at lower, more physiologically relevant concentrations.

3.3.2 DNP modified tetrapeptide analogs to opsonize live E. faecium

Based on our finding that stem peptide analogues were readily cross-linked into the cell wall, we expected that they could also be used to graft haptens for detection by antibodies. Therefore, we set out to build a stem peptide analogue that displayed a hapten to induce the recruitment of endogenous antibodies to the surface of *E. faecium* cells. We chose the hapten 2,4-dinitrophenol (DNP), as there is a naturally high abundance of anti-DNP antibodies in human serum and we have previously demonstrated surface grafted DNP epitopes can guide the recruitment of antibodies to Gram-negative and -positive pathogens.[27, 61, 62] The existence of an endogenous antibody pool eliminates the need for preimmunization against DNP. We anticipated that antibody recruitment to the surface of bacterial pathogens would be controlled by two major factors, namely level of

incorporation of PG analogues within the existing scaffold and the accessibility of the haptens to antibodies. Incorporation levels dictate the total amount of haptens imbedded within the entire scaffolds. It is expected that incorporation efficiency relates to the proper mimicry of PG substrates by synthetic analogues. The second major factor is related to hapten accessibility. Given the matrix-like structure of PG, not all haptens installed by synthetic PG analogues would be available to interact with antibodies. In fact, it is likely that only the most surface exposed haptens would be accessible to cognate antibodies to form a fruitful interaction.
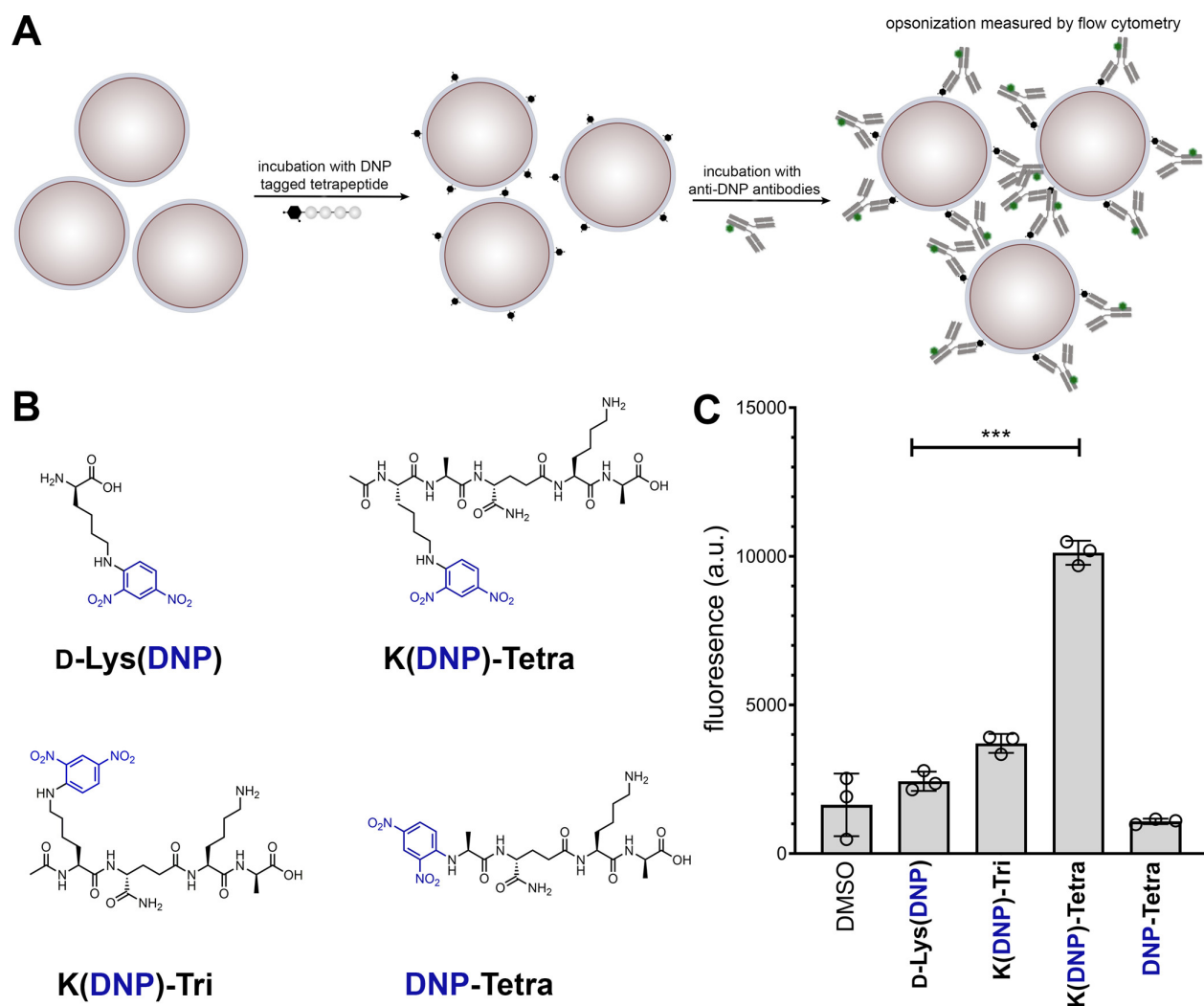
Figure 3.4 *Anti-DNP recruitment to the surface of live E. faecium*

(A) Cartoon representation of the assay to measure opsonization by anti-DNP. (B) Chemical structures of PG analogues modified with the hapten DNP. (C) Flow cytometry analysis of E. faecium treated overnight with 100 µM of PG analogues followed by incubation with Alexa Flour 488- conjugated anti-DNP antibodies. Data are represented as mean ± SD (n = 3). P-values were determined by a two-tailed t-test (*p < 0.05, **p < 0.01, ***p < 0.001, ns = not significant).

To evaluate antibody recruitment, *E. faecium* was treated with individual stem peptide analogues overnight followed by an incubation period with fluorescently labeled anti-DNP antibodies (Figure 3.4A,B). Fluorescence levels were subsequently measured by flow cytometry, and we expected that fluorescence levels should correlate with opsonization of anti-DNP antibodies. Of the four PG analogues evaluated, treatment with **K(DNP)-Tetra** led to the highest opsonization levels (Figure 3.4C). Bacterial opsonization was observed when cells were treated with **K(DNP)-Tetra** at concentrations as low as 10 µM, well below concentrations required in similar experiments conducted with smaller hapten conjugates tested previously by our group (data not shown). These results confirmed that PG analogues can effectively tag and induce antibody recruitment to *E.* faecium cells in a concentration dependent manner. Strikingly, in contrast to the incorporation levels measured by Fl derivatives, **DNP-Tetra** treated bacterial cells did not induce opsonization of bacterial cells. We attribute these results to the potential contribution of the moieties adjacent to the DNP hapten, which would be consistent with a previous study that showed a 1000-fold range in dissociation constant of anti-DNP antibodies based on the chemical entities flanking the DNP hapten.[63] Treatment with the single amino acid agent **D-Lys(DNP)** did not promote opsonization despite anticipation of robust levels of incorporation. We interpreted this result to mean that hapten accessibility may play a pivotal role in its recognition.

3.3.3 *Optimizing hapten display for anti-DNP recognition*

To explore hapten display further, a series of stem peptide analogues containing linkers of various compositions and lengths were designed. We utilized three different

compositions of linkers: glycine-serine, proline, and hydroxyproline (Figure 3.5A). Glycine-serine links possess high solubility and flexibility. In contrast, polyproline linkers are essentially rigid and offer a good test for potential increased hapten availability. To increase the hydration of the linker, we turned to hydroxyproline linkers. Interestingly, our work appears to be the first use of a hydroxyproline linker described in the literature, although individual residues have been modified to decorate the helix face for cell penetrating peptides.[64, 65] Two series of linkers (tetrameric and octameric) were synthesized and modified with Fl to first measure PG incorporation (Figure 3.5B). As before, *E. faecium* cells were treated with the PG analogues and PG incorporation was measured by flow cytometry. The decrease in incorporation with an increase in linker length may be a result of poorer permeation of these molecules to the site of the PG transpeptidases or a lack of tolerance by these enzymes toward them. Having seen that PG incorporation can deviate from opsonization levels, we set out to empirically evaluate the potential trade-off between incorporation level and hapten availability. We reasoned that although there was a decrease in incorporation for the longer linkers, this could be compensated by better hapten display to anti-DNP antibodies. The same set of linkers that were modified with Fl were instead conjugated to the hapten DNP (Figure 3.5A). Our results showed that increasing the linker length between the PG stem peptide analogue fragment and the DNP epitope led to decreasing levels of antibody recruitment (Figure 3.5C).
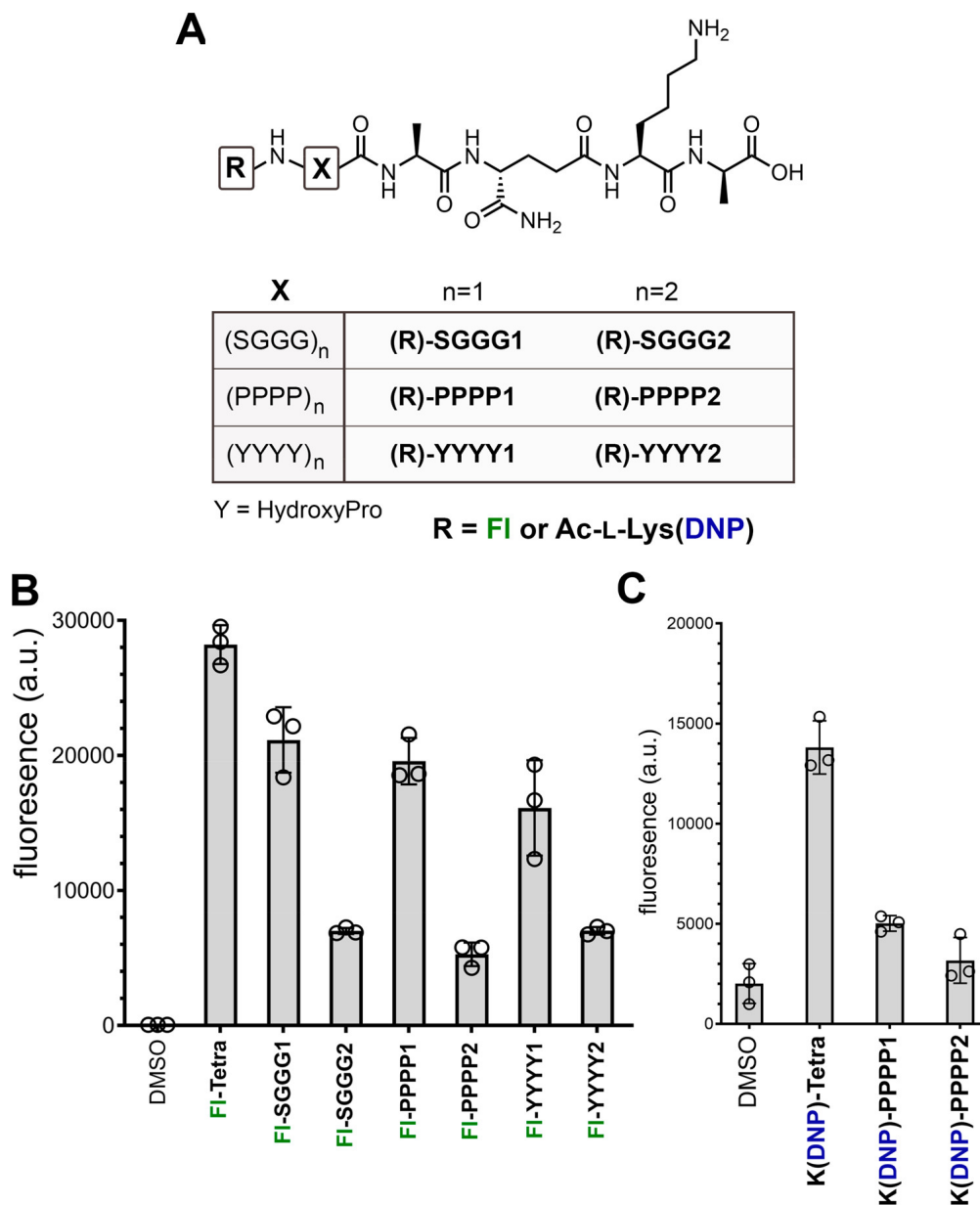
**Figure 3.5** *FITC and DNP modified tetrapeptide linker library*

(A) Chemical structures of PG analogues of variable linkers conjugated to either DNP or Fl. (B) Flow cytometry analysis of E. faecium treated overnight with 100 µM of PG analogues and (C) followed by incubation with Alexa Flour 488-conjugated anti-DNP antibodies. Data are represented as mean ± SD (n = 3).

3.3.4 Anti-DNP recruitment to live vancomycin-resistant E. faecium

Next, we set out to target drug resistant strains of *E. faecium*. Indeed, vancomycin-resistant enterococci infections are a major challenge in hospital settings.[66] An important modality of vancoymycin-resistant enterococci involves the bypass of PG transpeptidation by PBPs.[67, 68] Ldts incorporate a tetrapeptide stem lacking a terminal D-Ala that does not interact with vancomycin. Consistent with this idea, we showed that tetrameric PG analogues are incorporated more readily in *E. faecium* relative to pentameric PG analogues.[49] We confirmed these results by treating vancomycin-resistant *E. faecium* with **K(Fl)-Tetra** and found increased levels of PG incorporation (Figure 3.6A). Satisfyingly, cellular treatment with **K(DNP)-Tetra** similarly resulted in high levels of anti-DNP recruitment (Figure 3.6B) and the deposition of antibodies was visualized using confocal microscopy (Figure 3.6C). Most importantly, these results show that vancomycin-resistant strains are more prone to being labeled by our metabolic tags than drug-sensitive strains, as evidenced by a near 3-fold increase in antibody recruitment in vancoymycin-sensitive and vancomycin resistance strains (Figure 3.6B).

3.3.5 Immune cell uptake of DNP labeled live E. faecium

We then demonstrated that bacteria treated with **K(DNP)-Tetra** could be opsonized directly using human sera, which is expected to have a pool of native anti-DNP antibodies (Figure 3.6D). Finally, we set out to determine if grafting haptens onto the surface of *E. faecium* would increase the recognition and subsequent phagocytosis of the bacterial cell by macrophages, as this is one of the primary mechanisms for clearance of bacterial infections by the immune system. Bacterial cells were treated with **K(DNP)-Tetra** followed by calcein-AM staining to allow tracking of bacterial uptake into macrophages. The cells were then opsonized with human sera, incubated with J774A.1 macrophages, and analyzed for bacterial cell phagocytosis by flow cytometry. We observed that **K(DNP)-Tetra** treated bacterial cells in the presence of antibodies promoted greater uptake into macrophages over those untreated with **K(DNP)-Tetra** or lacking antibodies from human sera (Figure 3.6E).
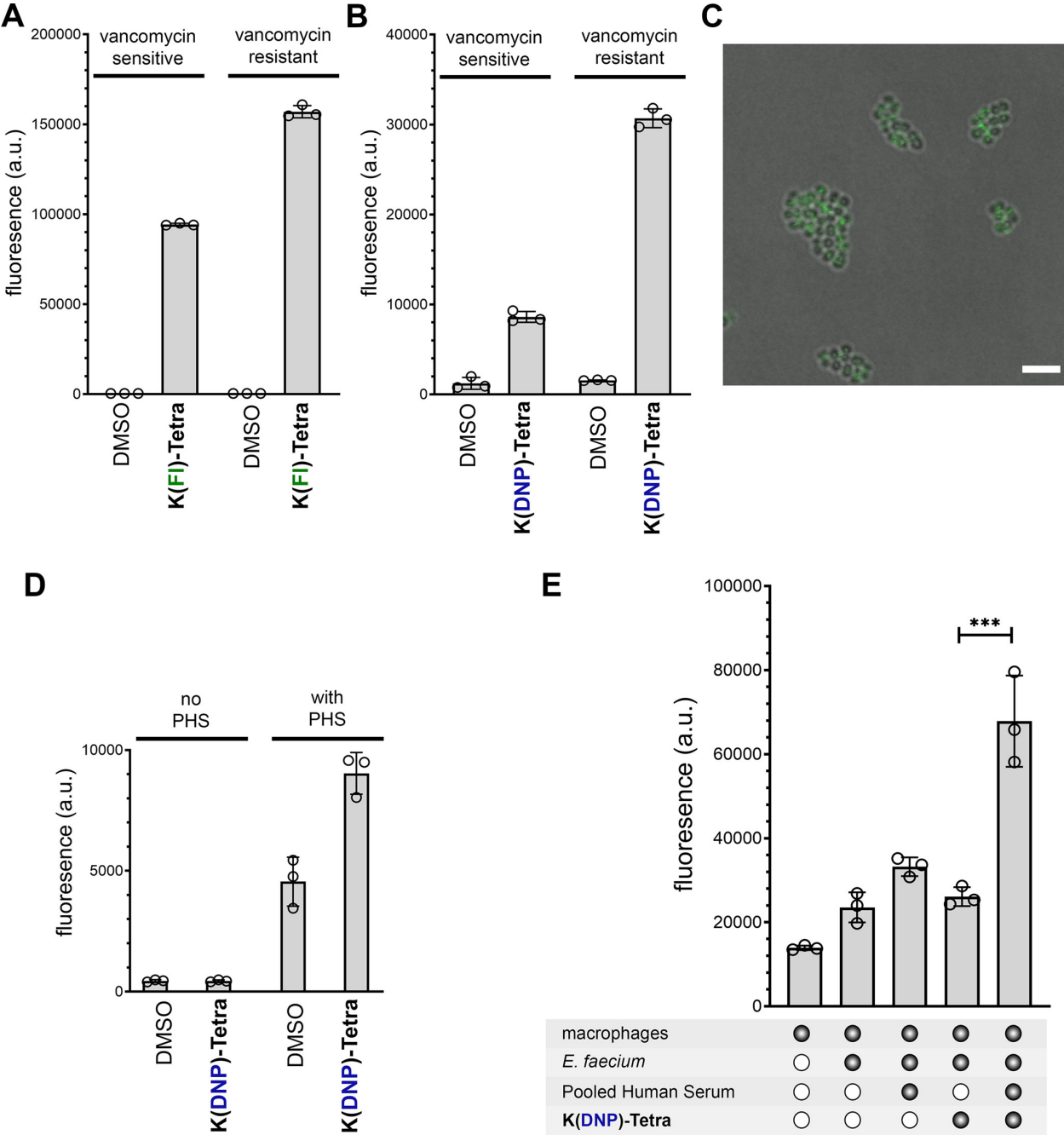
Figure 3.6 *Anti-DNP and immune cell recognition of live*

vancomycin-resistant E. faecium

(A) Flow cytometry analysis of E. faecium (vancoymycin-sensitive and resistant strains) treated overnight with 100 µM **K(Fl)-Tetra** and (B) treated overnight with

100 μM **K(DNP)-Tetra** followed by incubation with Alexa Flour 488- conjugated anti-DNP antibodies. (C) Confocal microscopy of vancoymycin-resistant E. faecium treated overnight with 100 μM of **K(DNP)-Tetra** followed by incubation with Alexa Fluor 488- conjugated anti-DNP antibodies. Scale bar = 3 μm. (D) E. faecium (vancoymycin-resistant) were treated overnight with 100 μM of **K(DNP)-Tetra**, incubated in the presence or absence of 15% pooled human serum (PHS), followed by incubation with FITC-conjugated anti-human IgG antibodies, and analyzed by flow cytometry. (E) Phagocytosis of bacterial cells was evaluated by incubating E. faecium (vancoymycin-resistant) in the presence or absence of 100 μM of **K(DNP)-Tetra** overnight and subsequently incubated with PBS or 15% PHS. J774A.1 macrophages were incubated for 20 min in the presence or absence of calcien-AM labeled E. faecium cells and measured by flow cytometry. Filled in circles indicate that those conditions were present in the assay arm. Data are represented as mean ± SD (n = 3). P-values were determined by a two-tailed t-test (*$p < 0.05$, **$p < 0.01$, ***$p < 0.001$, ns = not significant).

3.4 Conclusion

In conclusion, we have designed and synthesized a novel class of hapten conjugated stem peptide mimics that were readily cross-linked into the PG scaffold of the human pathogen *E. faecium*. We showed that surface bound haptens led to the recruitment of endogenous antibodies at low concentrations. Most significantly, this design achieved greater antibody recruitment compared to previously identified single d-amino acid antibody recruitment therapy. Finally, we showed that this opsonization led to increased bacterial cell uptake by macrophages. In the future, we will evaluate other endogenous antigens or expand to exogenous antigens to potentially provide greater temporal control on opsonization. We will continue to improve on the opsonization profile of pathogenic bacteria to refine our strategy, which we envision will give rise to a lead agent that could potentially show therapeutic activity in live animal models.

3.5 *Summary and Future Outlook*

In chapter 3, we describe novel immune-modulators that tag and direct the bacterial pathogen, *Enterococcus faecium,* for phagocytotic uptake by macrophages. Herein, a synthetic tetrapeptide analog modified with a hapten, 2,4- dinitrophenol (DNP), was covalently linked into the growing peptidoglycan scaffold of live *E. faecium*. Surface decoration of the pathogenic bacteria with an immune stimulating molecule enhanced recognition, opsonization, and phagocytotic activity of macrophages in culture. This approach was extensively dependent on understanding the chemical entities within the bacterial cell wall, bacterial metabolic processing, and the biology of host-pathogen interactions. The development of alternative therapies for the treatment of bacterial pathogens is critical, especially in terms of targeting multi-drug resistant phenotypes.

Here, we aimed to further improve upon the immunotherapy concepts directed towards bacterial pathogens developed previously in the Pires Lab. Prior work demonstrated the use of hapten modified D-amino acids to label bacterial PG and elicit an immune response for enhanced bacterial cell uptake. Although this work was pivotal to the field, a reoccurring drawback was the necessity of millimolar concentrations of the probe to achieve effective probe labeling, of which is not clinically applicable. The transition from a single D-amino acid to a synthetic mimic of the PG stem peptide enabled higher substrate specificity for TPs; therefore, higher degrees of labeling at lower, more physiologically relevant concentrations.

To further expand this work, one area of investigation could lie within minimizing the number of non-covalent interactions between the bacterial cell and the immune cell to further enhance phagocytosis levels. For instance, an antibody-antigen interaction typically has an equilibrium dissociation constant (K_d) that ranges from low micromolar (10^{-6}) to nanomolar (10^{-7}- 10^{-9}). Additionally, the interaction between the IgG Fc region and an Fc receptor (FcR) on an immune cell has a K_d value typically within same range; however, changes have been demonstrated to occur in response to pH, such as within the phagosomal environment.[69, 70] Therefore, the propensity of all three components, i.e.

the bacterium, the antibody, and the immune cell, being bound together for optimal bacterial cell uptake relies extensively on the K_d values of the associated binding partners. To address this shortcoming, a biorthogonal click handle can be modified onto the PG stem peptide mimic for display of a reactive moiety within the PG of the bacterium. Additionally, installation of the corresponding reactive partner onto the antibody will enable a covalent display of antibodies on the surface of the bacterial cell for opsonization dependent complement or binding by FcRs, effectively reducing the equilibrium to one set of non-covalent interactions. Covalent display of antibodies on cell surfaces has been successfully demonstrated for treatment of cancers[71]; therefore, transitioning this approach to apply towards bacterial cells may provide another novel advancement in bacterial immunotherapy.

3.6 Materials and Methods

Materials. All peptide related reagents and protected amino acids were purchased from Chem-Impex. 5, 6-carboxyfluorescein and 2,4-dinitrofluorobenzene were purchased from Chem-Impex. Antibody reagents were purchased from Thermo Fischer Scientific Inc. Pooled Human Serum was purchase from Sigma Aldrich. Dulbecco's Modified Eagle's Medium (DMEM) was purchased from VWR. Fetal Bovine Serum (FBS) was purchased from R&D Systems. Penicillin-Streptomycin was purchased from Sigma-Aldrich. All other organic chemical reagents were purchased from Fisher Scientific or Sigma Aldrich and used without further purification.

Bacteria Cell Culture. Bacterial cells were cultured in specified media in an aerobic environment while shaking at 250 rpm at 37 °C. *E. faecium* ATCC BAA 2127 (vancoymycin- sensitive) and *E. faecium* ATCC BAA 2317 (vancoymycin- resistant) were grown in Trypticase Soy Broth (TSB). BLS2 organisms should be manipulated using proper protective equipment.

Mammalian Cell Culture. J774A.1 cells were cultured in Dulbecco's modified Eagle's medium (DMEM) supplemented with 10% FBS, 50 IU/mL penicillin, 50 ug/mL streptomycin, and 2 mM L-glutamine in a humidified atmosphere of 55 CO_2 at 37 °C.

Fluorescent Labeling with PG Analogues. *E. faecium* ATCC BAA 2127 or ATCC BAA 2317 were grown to stationary phase in TSB while shaking (250 rpm) at 37 °C. Bacterial cells from the overnight growth were used to inoculate TSB (1:100) supplemented with fluorescein conjugated PG analogues (100 µM or designated concen- tration) and incubated at 37 °C with shaking (250 rpm) for 16 h. The bacteria were harvested, washed three times with 1× phosphate buffered saline (PBS), fixed with 2% formaldehyde solution, and analyzed using the CytoFLEX Flow Cytometer (Beckman Coulter) equipped with a 488 nm laser and 525/40 nm bandpass filter. The data were analyzed using CytEXPERT software.

Antibody Binding in *E. faecium.* *E. faecium* ATCC BAA 2127 or ATCC BAA 2317 were grown to stationary phase in TSB while shaking (250 rpm) at 37 °C. Bacterial cells from the overnight growth were used to inoculate TSB (1:100) supplemented with DNP conjugated PG analogues (100 µM or designated concentration) and incubated at 37 °C with shaking (250 rpm) for 16 h. The bacteria were harvested and washed three times with 1× PBS. Approximately 2×10^6 colony forming units (CFU) were then incubated in 100 µL of PBS containing 10% (v/v) FBS and 0.04 mg/mL of Alexa Fluor 488-conjugated rabbit anti-dinitrophenol KHL (Thermo Fischer #A-11097) and incubated at 37 °C for 1 h with shaking (250 rpm) protected from light. Samples were washed twice with 1× PBS, fixed in a 2% formaldehyde solution and analyzed by flow cytometry (as described above).

Confocal Microscopy Analysis of *E. faecium.* *E. faecium* ATCC BAA 2317 were grown to stationary phase in TSB while shaking (250 rpm) at 37 °C. Bacterial cells from the overnight growth were used to inoculate TSB (1:100) supplemented with 100 µM **K(Fl)-Tetra** or **K(DNP)-Tetra** and incubated at 37 °C with shaking at 250 rpm for 16 h as previously described. For K(Fl)-Tetra treated cells, the cells were washed with 1× PBS and fixed in a 2% formaldehyde solution. For **K(DNP)-Tetra** treated cells, the cells were opsonized with Alexa Fluor 488-conjugated anti-dinitrophenol KHL as described above, washed with 1× PBS, and fixed in a 2% formaldehyde solution. Both **K(Fl)-Tetra** and **K(DNP)-Tetra** treated cells were washed to remove the formaldehyde and analyzed using the Leica SP5X Imaging System provided by the W. M. Keck Center for Cellular Imaging.

E. faecium Opsonization with Pooled Human Serum. *E. faecium* ATCC BAA 2127 or ATCC BAA 2317 were grown to stationary phase in TSB while shaking (250 rpm) at 37 °C. Bacterial cells from the overnight growth were used to inoculate TSB (1:100) supplemented with 100 µM **K(DNP)-Tetra** and incubated at 37 °C with shaking (250 rpm) for 16 h. The bacteria were harvested and washed three times with 1× PBS. Pooled human serum (Sigma-Aldrich #H4522) was diluted to 25% in PBS and incubated with bentonite for 20 min at 37 °C to deactivate the lysozyme. The serum supernatant was obtained and diluted to 15% in PBS solution with 10% (v/v) FBS and incubated with the bacteria for 20 min on ice. The opsonized bacteria were then washed two times with 1× PBS and approximately 2×10^6 colony forming units (CFU) were incubated with FITC-conjugated anti-human IgG (Sigma-Aldrich #F9512) diluted 1:1000 in PBS containing 10% (v/v) FBS at 4 °C for 30 min protected from light. The cells were washed twice with 1× PBS and fixed in 2% formaldehyde solution. Samples were then analyzed by flow cytometry (as described above).

Phagocytosis of Opsonized *E. faecium*. *E. faecium* ATCC BAA 2317 were grown to stationary phase in TSB while shaking (250 rpm) at 37 °C. Bacterial cells from the overnight growth were used to inoculate TSB (1:100) supplemented with 100 µM **K(DNP)-Tetra** and incubated at 37 °C with shaking (250 rpm) for 16 h. The bacteria were harvested and washed three times with 1× PBS. The cells were resuspended in PBS containing 10 µM calcein-AM and incubated for 30 min at 37 °C then washed three times with 1× PBS. Pooled human serum (Sigma-Aldrich #H4522) was diluted to 25% in PBS and incubated with bentonite for 20 min at 37 °C to deactivate the lysozyme. The serum supernatant was obtained and diluted to 15% in PBS solution with 10% (v/v) FBS and incubated with the bacteria for 20 min on ice. The opsonized bacteria were washed twice with 1× PBS. J774A.1 cells were cultured as described previously. On the day of the experiment, J774A cells were washed twice with Hank's Balanced Salt Solution (HBSS) by centrifuging 5 min at 500 rpm. The washed J774A cells were then mixed with opsonized E. faecium in a ratio 1:3 and incubated in HBSS. The cell mixtures were then rotated at 37 °C for 20 min to induce phagocytosis, washed three times with cold HBSS,

and fixed for 30 min in PBS with 2% formaldehyde. Samples were then analyzed by flow cytometry as described above.

3.7 *References*

1. Wisplinghoff, H. *et al.* Nosocomial bloodstream infections in US hospitals: Analysis of 24,179 cases from a prospective nationwide surveillance study. *Clin Infect Dis* **39**, 309-317 (2004).

2. Buffie, C.G. & Pamer, E.G. Microbiota-mediated colonization resistance against intestinal pathogens. *Nat Rev Immunol* **13**, 790-801 (2013).

3. Murray, B.E. Drug therapy: Vancomycin-resistant enterococcal infections. *New Engl J Med* **342**, 710-721 (2000).

4. Arias, C.A. & Murray, B.E. The rise of the Enterococcus: beyond vancomycin resistance. *Nat Rev Microbiol* **10**, 266-278 (2012).

5. CDC Antibiotic Resistance Threats in the United States. *U.S. Department of Health and Human Services* **CDC** (2019).

6. Cetinkaya, Y., Falk, P. & Mayhall, C.G. Vancomycin-resistant enterococci. *Clin Microbiol Rev* **13**, 686-+ (2000).

7. Bell, J.K. *et al.* Leucine-rich repeats and pathogen recognition in Toll-like receptors. *Trends Immunol* **24**, 528-533 (2003).

8. Diacovich, L. & Gorvel, J.P. Bacterial manipulation of innate immunity to promote infection. *Nat Rev Microbiol* **8**, 117-128 (2010).

9. Kawai, T. & Akira, S. Pathogen recognition with Toll-like receptors. *Curr Opin Immunol* **17**, 338-344 (2005).

10. Aderem, A. & Ulevitch, R.J. Toll-like receptors in the induction of the innate immune response. *Nature* **406**, 782-787 (2000).

11. Akira, S., Takeda, K. & Kaisho, T. Toll-like receptors: critical proteins linking innate and acquired immunity. *Nat Immunol* **2**, 675-680 (2001).

12. Takeuchi, O. *et al.* Differential roles of TLR2 and TLR4 in recognition of gram-negative and gram-positive bacterial cell wall components. *Immunity* **11**, 443-451 (1999).

13. Boneca, I.G. *et al.* A critical role for peptidoglycan N-deacetylation in Listeria evasion from the host innate immune system. *P Natl Acad Sci USA* **104**, 997-1002 (2007).

14. Guan, R.J. & Mariuzza, R.A. Peptidoglycan recognition proteins of the innate immune system. *Trends Microbiol* **15**, 127-134 (2007).

15. Wolf, A.J. & Underhill, D.M. Peptidoglycan recognition by the innate immune system. *Nat Rev Immunol* **18**, 243-254 (2018).

16. Arthur, M. & Courvalin, P. Genetics and Mechanisms of Glycopeptide Resistance in Enterococci. *Antimicrob Agents Ch* **37**, 1563-1571 (1993).

17. Bugg, T.D.H. *et al.* Molecular-Basis for Vancomycin Resistance in Enterococcus-Faecium Bm4147 - Biosynthesis of a Depsipeptide Peptidoglycan Precursor by Vancomycin Resistance Proteins Vanh and Vana. *Biochemistry-Us* **30**, 10408-10415 (1991).

18. Brower, V. Checkpoint Blockade Immunotherapy for Cancer Comes of Age. *Jnci-J Natl Cancer I* **107** (2015).

19. June, C.H., O'Connor, R.S., Kawalekar, O.U., Ghassemi, S. & Milone, M.C. CAR T cell immunotherapy for human cancer. *Science* **359**, 1361-1365 (2018).

20. Mellman, I., Coukos, G. & Dranoff, G. Cancer immunotherapy comes of age. *Nature* **480**, 480-489 (2011).

21. Rosenberg, S.A. Cancer immunotherapy comes of age. *Nat Clin Pract Oncol* **2**, 115-115 (2005).

22. Carlson, C.B., Mowery, P., Owen, R.M., Dykhuizen, E.C. & Kiessling, L.L. Selective tumor cell targeting using low-affinity, multivalent interactions. *Acs Chem Biol* **2**, 119-127 (2007).

23. Dubrovska, A. *et al.* A Chemically Induced Vaccine Strategy for Prostate Cancer. *Acs Chem Biol* **6**, 1223-1231 (2011).

24. Murelli, R.P., Zhang, A.X., Michel, J., Jorgensen, W.L. & Spiegel, D.A. Chemical Control over Immune Recognition: A Class of Antibody-Recruiting Small Molecules That Target Prostate Cancer. *J Am Chem Soc* **131**, 17090-+ (2009).

25. Popkov, M., Gonzalez, B., Sinha, S.C. & Barbas, C.F., 3rd Instant immunity through chemically programmable vaccination and covalent self-assembly. *Proc Natl Acad Sci U S A* **106**, 4378-4383 (2009).

26. Rader, C., Sinha, S.C., Popkov, M., Lerner, R.A. & Barbas, C.F., 3rd Chemically programmed monoclonal antibodies for cancer therapy: adaptor immunotherapy

based on a covalent antibody catalyst. *Proc Natl Acad Sci U S A* **100**, 5396-5400 (2003).

27.   Sheridan, R.T., Hudon, J., Hank, J.A., Sondel, P.M. & Kiessling, L.L. Rhamnose glycoconjugates for the recruitment of endogenous anti-carbohydrate antibodies to tumor cells. *Chembiochem* **15**, 1393-1398 (2014).

28.   Wehr, J. *et al.* pH-Dependent Grafting of Cancer Cells with Antigenic Epitopes Promotes Selective Antibody-Mediated Cytotoxicity. *J Med Chem* **63**, 3713-3722 (2020).

29.   Lu, Y. & Low, P.S. Folate targeting of haptens to cancer cell surfaces mediates immunotherapy of syngeneic murine tumors. *Cancer Immunol Immunother* **51**, 153-162 (2002).

30.   Lu, Y. & Low, P.S. Targeted immunotherapy of cancer: development of antibody-induced cellular immunity. *J Pharm Pharmacol* **55**, 163-167 (2003).

31.   Lu, Y. *et al.* Folate-targeted dinitrophenyl hapten immunotherapy: effect of linker chemistry on antitumor activity and allergic potential. *Mol Pharm* **4**, 695-706 (2007).

32.   Feigman, M.S. *et al.* Synthetic Immunotherapeutics against Gram-negative Pathogens. *Cell Chem Biol* **25**, 1185-1194 e1185 (2018).

33.   Fura, J.M., Pidgeon, S.E., Birabaharan, M. & Pires, M.M. Dipeptide-Based Metabolic Labeling of Bacterial Cells for Endogenous Antibody Recruitment. *ACS Infect Dis* **2**, 302-309 (2016).

34.   Fura, J.M. & Pires, M.M. D-amino carboxamide-based recruitment of dinitrophenol antibodies to bacterial surfaces via peptidoglycan remodeling. *Biopolymers* **104**, 351-359 (2015).

35.   Fura, J.M., Sabulski, M.J. & Pires, M.M. D-amino acid mediated recruitment of endogenous antibodies to bacterial surfaces. *Acs Chem Biol* **9**, 1480-1489 (2014).

36.   Kaewsapsak, P., Esonu, O. & Dube, D.H. Recruiting the host's immune system to target Helicobacter pylori's surface glycans. *Chembiochem* **14**, 721-726 (2013).

37.   Kristian, S.A. *et al.* Retargeting pre-existing human antibodies to a bacterial pathogen with an alpha-Gal conjugated aptamer. *J Mol Med (Berl)* **93**, 619-631 (2015).

38. Vollmer, W., Blanot, D. & de Pedro, M.A. Peptidoglycan structure and architecture. *FEMS Microbiol Rev* **32**, 149-167 (2008).

39. Vollmer, W. & Bertsche, U. Murein (peptidoglycan) structure, architecture and biosynthesis in Escherichia coli. *Biochim Biophys Acta* **1778**, 1714-1734 (2008).

40. Typas, A., Banzhaf, M., Gross, C.A. & Vollmer, W. From the regulation of peptidoglycan synthesis to bacterial growth and morphology. *Nat Rev Microbiol* **10**, 123-136 (2011).

41. Macheboeuf, P., Contreras-Martel, C., Job, V., Dideberg, O. & Dessen, A. Penicillin binding proteins: key players in bacterial cell cycle and drug resistance processes. *FEMS Microbiol Rev* **30**, 673-691 (2006).

42. Magnet, S. *et al.* Identification of the L,D-transpeptidases responsible for attachment of the Braun lipoprotein to Escherichia coli peptidoglycan. *J Bacteriol* **189**, 3927-3931 (2007).

43. Mainardi, J.L., Villet, R., Bugg, T.D., Mayer, C. & Arthur, M. Evolution of peptidoglycan biosynthesis under the selective pressure of antibiotics in Gram-positive bacteria. *FEMS Microbiol Rev* **32**, 386-408 (2008).

44. Sauvage, E., Kerff, F., Terrak, M., Ayala, J.A. & Charlier, P. The penicillin-binding proteins: structure and role in peptidoglycan biosynthesis. *FEMS Microbiol Rev* **32**, 234-258 (2008).

45. Arthur, M., Depardieu, F., Snaith, H.A., Reynolds, P.E. & Courvalin, P. Contribution of VanY D,D-carboxypeptidase to glycopeptide resistance in Enterococcus faecalis by hydrolysis of peptidoglycan precursors. *Antimicrob Agents Chemother* **38**, 1899-1903 (1994).

46. de Jonge, B.L., Handwerger, S. & Gage, D. Altered peptidoglycan composition in vancomycin-resistant Enterococcus faecalis. *Antimicrob Agents Chemother* **40**, 863-869 (1996).

47. Gutmann, L. *et al.* Inducible carboxypeptidase activity in vancomycin-resistant enterococci. *Antimicrob Agents Chemother* **36**, 77-80 (1992).

48. Apostolos, A.J., Pidgeon, S.E. & Pires, M.M. Remodeling of Cross-bridges Controls Peptidoglycan Cross-linking Levels in Bacterial Cell Walls. *Acs Chem Biol* **15**, 1261-1267 (2020).

49.   Pidgeon, S.E. *et al.* L,D-Transpeptidase Specific Probe Reveals Spatial Activity of Peptidoglycan Cross-Linking. *Acs Chem Biol* **14**, 2185-2196 (2019).

50.   Gautam, S. *et al.* An Activity-Based Probe for Studying Crosslinking in Live Bacteria. *Angew Chem Int Ed Engl* **54**, 10492-10496 (2015).

51.   Gautam, S., Kim, T. & Spiegel, D.A. Chemical probes reveal an extraseptal mode of cross-linking in Staphylococcus aureus. *J Am Chem Soc* **137**, 7441-7447 (2015).

52.   Ngadjeua, F. *et al.* Critical Impact of Peptidoglycan Precursor Amidation on the Activity of l,d-Transpeptidases from Enterococcus faecium and Mycobacterium tuberculosis. *Chemistry* **24**, 5743-5747 (2018).

53.   Welsh, M.A. *et al.* Identification of a Functionally Unique Family of Penicillin-Binding Proteins. *J Am Chem Soc* **139**, 17727-17730 (2017).

54.   Cava, F., de Pedro, M.A., Lam, H., Davis, B.M. & Waldor, M.K. Distinct pathways for modification of the bacterial cell wall by non-canonical D-amino acids. *EMBO J* **30**, 3442-3453 (2011).

55.   Fura, J.M., Kearns, D. & Pires, M.M. D-Amino Acid Probes for Penicillin Binding Protein-based Bacterial Surface Labeling. *J Biol Chem* **290**, 30540-30550 (2015).

56.   Kuru, E. *et al.* In Situ probing of newly synthesized peptidoglycan in live bacteria with fluorescent D-amino acids. *Angew Chem Int Ed Engl* **51**, 12519-12523 (2012).

57.   Lebar, M.D. *et al.* Reconstitution of peptidoglycan cross-linking leads to improved fluorescent probes of cell wall synthesis. *J Am Chem Soc* **136**, 10874-10877 (2014).

58.   Pidgeon, S.E. *et al.* Metabolic Profiling of Bacteria by Unnatural C-terminated D-Amino Acids. *Angew Chem Int Ed Engl* **54**, 6158-6162 (2015).

59.   Sarkar, S., Libby, E.A., Pidgeon, S.E., Dworkin, J. & Pires, M.M. In Vivo Probe of Lipid II-Interacting Proteins. *Angew Chem Int Ed Engl* **55**, 8401-8404 (2016).

60.   Siegrist, M.S. *et al.* (D)-Amino acid chemical reporters reveal peptidoglycan dynamics of an intracellular pathogen. *Acs Chem Biol* **8**, 500-505 (2013).

61.   Feigman, M.J.S. & Pires, M.M. Synthetic Immunobiotics: A Future Success Story in Small Molecule-Based Immunotherapy? *ACS Infect Dis* **4**, 664-672 (2018).

62.   Lu, Y., Sega, E. & Low, P.S. Folate receptor-targeted immunotherapy: induction of humoral and cellular immunity against hapten-decorated cancer cells. *Int J Cancer* **116**, 710-719 (2005).

63.   Handlogten, M.W., Kiziltepe, T., Alves, N.J. & Bilgicer, B. Synthetic allergen design reveals the significance of moderate affinity epitopes in mast cell degranulation. *Acs Chem Biol* **7**, 1796-1801 (2012).

64.   Fillon, Y.A., Anderson, J.P. & Chmielewski, J. Cell penetrating agents based on a polyproline helix scaffold. *J Am Chem Soc* **127**, 11798-11803 (2005).

65.   Nepal, M. *et al.* A Library Approach to Cationic Amphiphilic Polyproline Helices that Target Intracellular Pathogenic Bacteria. *ACS Infect Dis* **4**, 1300-1305 (2018).

66.   Arias, C.A. & Murray, B.E. The rise of the Enterococcus: beyond vancomycin resistance. *Nat Rev Microbiol* **10**, 266-278 (2012).

67.   Mainardi, J.L. *et al.* Balance between two transpeptidation mechanisms determines the expression of beta-lactam resistance in Enterococcus faecium. *J Biol Chem* **277**, 35801-35807 (2002).

68.   Cremniter, J. *et al.* Novel mechanism of resistance to glycopeptide antibiotics in Enterococcus faecium. *J Biol Chem* **281**, 32254-32262 (2006).

69.   Lu, J., Ellsworth, J.L., Hamacher, N., Oak, S.W. & Sun, P.D. Crystal structure of Fcgamma receptor I and its implication in high affinity gamma-immunoglobulin binding. *J Biol Chem* **286**, 40608-40613 (2011).

70.   Schoch, A. *et al.* Charge-mediated influence of the antibody variable domain on FcRn-dependent pharmacokinetics. *Proc Natl Acad Sci U S A* **112**, 5997-6002 (2015).

71.   Antillon, K., Ross, P.A. & Farrell, M.P. Directing CAR NK Cells via the Metabolic Incorporation of CAR Ligands into Malignant Cell Glycans. *Acs Chem Biol* **17**, 1505-1512 (2022).

Chapter 4 Immuno-targeting of Gram-positive Pathogens *via* a Cell Wall Binding Tick Antifreeze Protein

Adapted from: Dalesandro, B. E.; Pires, M. M. Immuno-targeting of Gram-positive Pathogens *via* a Cell Wall Binding Tick Antifreeze Protein. *J. Med. Chem*. **2022,** under revision.

4.1 Abstract

The human immune system employs several mechanisms to defend against pathogenic bacteria. However, pathogenic bacterial cells have evolved means to counter these responses, rendering our immune system less effective. Immunological agents that supplement or modulate the host immune response have proven to have powerful therapeutic potential, although this modality is less explored against bacterial pathogens. We describe the application of a bacterial binding protein to re-engage the immune system towards pathogenic bacteria. More specifically, a hapten was conjugated to a protein expressed by *Ixodes scapularis* ticks, called *Ixodes scapularis* antifreeze glycoprotein (IAFGP), that has high affinity for the D-alanine residue on the peptidoglycan of the bacterial cell wall. We showed that a fragment of this protein retained high surface binding affinity. Moreover, conjugation of a hapten to this peptide led to the display of haptens on the cell surface of vancomycin-resistant *Enterococcus faecalis*. Hapten display then induced the recruitment of antibodies and promoted uptake of bacterial pathogens by immune cells. These results demonstrate the feasibility in using cell wall binding agents as the basis of a class of bacterial immunotherapies against bacterial pathogens.

4.2 Introduction

Findings from over 100 years ago by Emil von Behring demonstrated that a patient's immune system is, in fact, potent enough to reverse the course of severe bacterial infections even at late-stage disease.[1] This serum-based therapy was formulated by

challenging horses with inactivated infectious agents, which yielded potent antiserum that was then administered to diphtheria/tetanus patients. At the time, a rudimentary understanding of the molecular mechanisms underpinning the therapeutic efficacy of convalescent plasma complicated further development of immunotherapy against bacterial infections. Later, biomolecular advances revealed that antibodies in the antiserum contributed directly to the therapeutic effect observed in patients;[2] opsonization of the bacterial cells promoted their clearance *via* phagocytosis and/or complement.

In the years following von Behring's seminal work, there was a large influx of small molecule antibiotics – an era ushered in by the discovery of penicillin. In a short period, small molecule antibiotics became the standard course of treatment against bacterial infections. More recently, traditional antibiotic therapy is starting to become less effective as incidences of drug-resistant bacterial infections rise.[3, 4] This trend can provide a powerful impetus to explore alternative strategies, including modern versions of the early work by von Behring that focuses on harnessing the patient's own immune system for bacterial clearance.[5, 6] The findings by von Behring, therefore, serve as foundational precedence to the development of modern anti-bacterial immunotherapeutic agents, which can provide additional options for patients who are unresponsive to conventional antibiotics.

While modern immunotherapy has blossomed in the areas of oncology and autoimmunity, development of immunotherapies to treat bacterial infections has lagged behind. Nonetheless, in recent years increasing efforts towards this area have been made, and there are several monoclonal antibodies (mAbs) currently being developed against bacterial toxins[7-13] and towards epitopes on the bacterial cell surface.[14-22] One of the strategies being currently explored against cancer cells focuses on tagging cancer cell surfaces with small molecule haptens to promote recognition and subsequent destruction by the immune system.[23-29] For example, Low and coworkers have developed anti-cancer agents, which have undergone clinical evaluation, that are composed of folate linked to the endogenous hapten, dinitrophenol (DNP), to destroy cancer cells displaying high levels of folate receptors.[30-32]

Our group[33-37] and others[38, 39] have developed several classes of molecules that label the surface of bacterial pathogens with small molecule haptens. A principal design consideration for hapten display involves the choice of the targeting moiety to the bacteria cell surface. For Gram-positive pathogens, peptidoglycan (PG) is one of the most exposed targets on the cell surface. PG is a primary component of bacterial cell walls, and, in the case of Gram-positive bacteria, it can reach several nanometers in thickness. There are many structural components that are unique to PG including the inclusion of D-alanine (D-ala) residues within the stem peptide (humans do not biosynthesize D-ala[40, 41]). Herein, we describe the surface tagging of bacterial pathogens based on a peptide derived from a protein found in the innate immune system of *Ixodes scapularis* ticks called *Ixodes scapularis* antifreeze glycoprotein (IAFGP). It was recently found that IAFGP binds to the D-alanine residue within the PG of the bacterial cell wall.[42, 43] Moreover, a fragment of this protein – called P1 – retained its ability to bind to the surface of the bacteria.[44, 45] P1 has also been found to inhibit biofilm formation, potentiate antibiotics, and render mice resistant to septic shock.[28, 46, 47] Given its therapeutic potential, we reasoned that P1 could additionally serve as a selective tagging modality to decorate the surface of bacterial cells. Here, we showed that conjugation of a non-native hapten resulted in high levels of antibody recruitment and immune-cell mediated uptake of bacterial cells (Figure 4.1A).
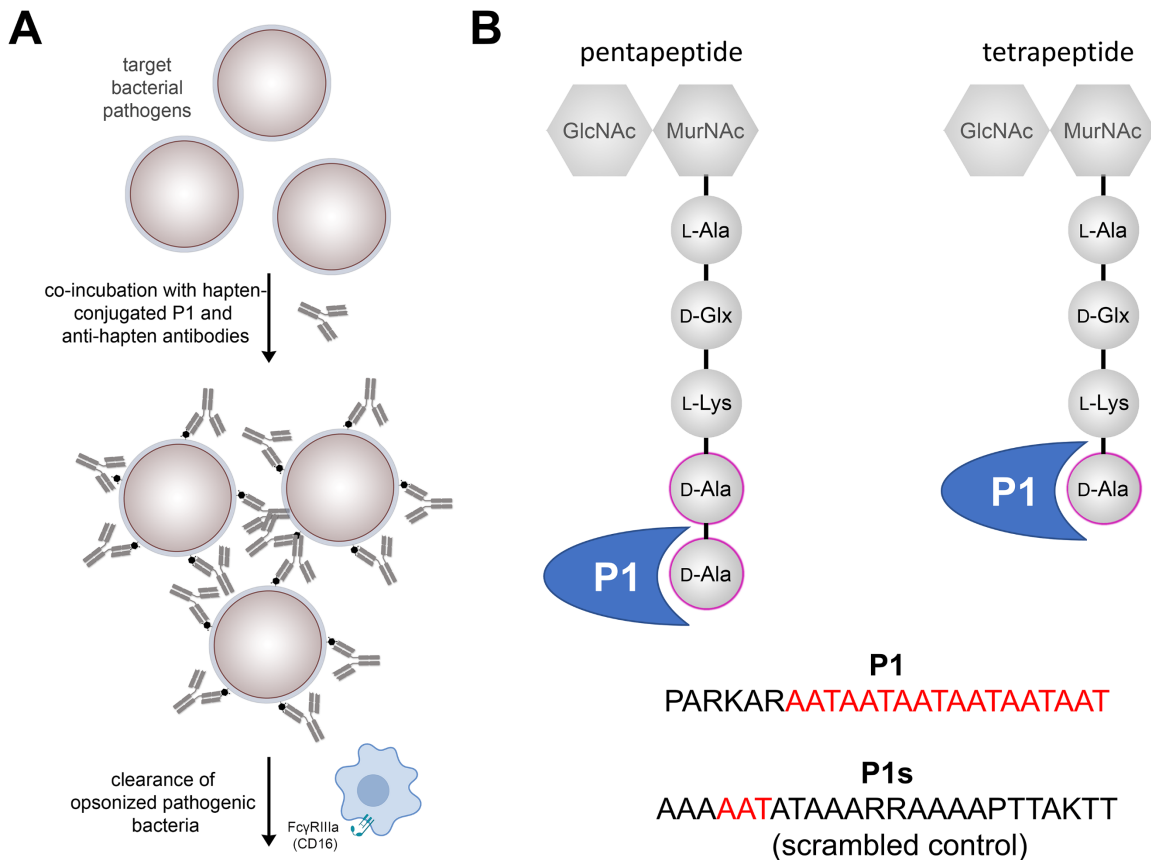
Figure 4.1 *A peptide derived from Ixodes scapularis antifreeze glycoprotein has affinity for D-alanine on bacterial peptidoglycan*

(A) General representation of hapten conjugates tagging the surface of bacteria followed by a specific immune response directed by the hapten. (B) Amino acid sequences of P1 and P1s with a cartoon representation of P1 binding to the D-Ala residue of a pentapeptide or tetrapeptide within the PG of the bacterial cell wall. D-iGlx refers to D-isoGln or D-isoGlu.

4.3 Results and Discussion

4.3.1 Design of immune tags to label live bacteria

Anti-bacterial immunotherapy has thus far been primarily based on the use of small molecule haptens for which humans already have an existing antibody pool (endogenous antibodies).[5, 28, 47] Several different approaches by our group and others have demonstrated that using hapten-modified antibiotics, metabolic tags, and receptor binding polymers can harness this endogenous antibody pool to increase opsonization and subsequent killing of bacterial pathogens.[5, 6, 28, 34, 35, 37-39, 46-54] However, despite such successes, there are several shortcomings associated with endogenous haptens, such as a lack in temporal control of antibody circulation and variable levels of antibodies across a diverse population. Instead, we envisioned that a non-native hapten could overcome these challenges in combination of the cognate exogenous mAbs. We describe a novel bifunctional molecule that associates with epitopes on the surface of pathogenic Gram-positive bacteria and displays an exogenous hapten for mAb recognition. This alternative approach can potentially reduce the necessity to discover and target pathogen-specific epitopes on the surface of Gram-positive bacteria. Targeting of bacterial cell surfaces was mediated by a peptide, P1, that binds to D-ala[42, 43] present exclusively on the PG layers of bacterial cell wall and not within the host (Figure 4.1B). P1 was labeled with a fluorescein moiety to promote the binding of exogenous anti-fluorescein antibodies to the surface of Gram-positive bacterial pathogens.

The cell wall of Gram-positive bacteria has a thick layer of PG on the extracellular side of the cytoplasmic membrane, whereas the PG of Gram-negative bacteria are found in the periplasmic space. The PG scaffold provides physical and chemical stability to the bacterial cell.[55, 56] Generally, the structure of PG is highly conserved between species and is composed of repeating disaccharides connected to a short peptide, often referred to as the stem peptide. While there is variation in the stem peptide primary sequence, the canonical sequence is L-Ala-D-Glx-(L-Lys/m-DAP)-D-Ala-D-Ala where m-DAP is *meso*-diaminopimelic acid (Figure 4.1B). Often, proteins involved in the innate immune system will target the PG for mitigation of potential pathogens (e.g., lysozyme and Peptidoglycan Binding Proteins).[57, 58] Similarly, the presence of the bacterial pathogen *Anaplasma phagocytophilum* in *Ixodes scapularis* ticks induces the host to express IAFGP.[42, 43]

Among the many biological activities related to IAFGP, it possess the ability to bind the terminal D-ala residue within the PG of the invading pathogen to alter bacterial cell permeability and interfere with biofilm formation.[42, 45]

IAFGP is unique in its repetitive nature of trimeric units (AAT) that are purported to bind D-Ala on bacterial PG.[42] We envisioned that a fragment of IAFGP (peptide P1, PARKARAATAATAATAATAATAAT) could serve as a surface homing receptor to graft exogenous haptens onto the PG of the target bacteria (Figure 4.2A). To test the ability of the P1 peptide to bind to bacterial cell surfaces, P1 (and a scramble peptide P1s, AATAATATAAARRAAAAPTTAKTT) were synthesized using solid phase peptide synthesis (SPPS) and modified with a fluorescein on the *N*-terminus (**P1fl** and **P1fls**, respectively) (Figure 4.2B). Cell surface binding of **P1fl** and **P1fls** were evaluated against the Gram-positive bacterial species *Enterococcus faecalis (E. faecalis)* and *Enterococcus faecium (E. faecium)*. We chose to investigate the binding of P1 to *E. faecalis* and *E. faecium* because there are increasing incidences of drug resistant Enterococci infections, thus making it difficult to treat patients with conventional antibiotics.[59, 60] Stationary phase bacterial cells were incubated with **P1fl** and cellular fluorescence was analyzed by flow cytometry, whereby fluorescence levels are expected to correspond with binding of the bacterial cell surface (Figure 4.2C). Additionally, the PG scaffold of these bacterial cells were metabolically labeled with diethylaminocumarin-modified D-amino acid, D-DADA, to easily identify overlapping fluorescence signals between bacterial cells and **P1fl**. Remarkably, high levels of surface labeling were observed for both *E. faecalis* and *E. faecium* when treated with **P1fl**, while incubation with **P1fls** did not result in bacterial surface tagging (Figure 4.2C). Moreover, we found that **P1fl** bound the surface of both *Enterococci* species in a concentration dependent manner (Figure 4.2D, E).
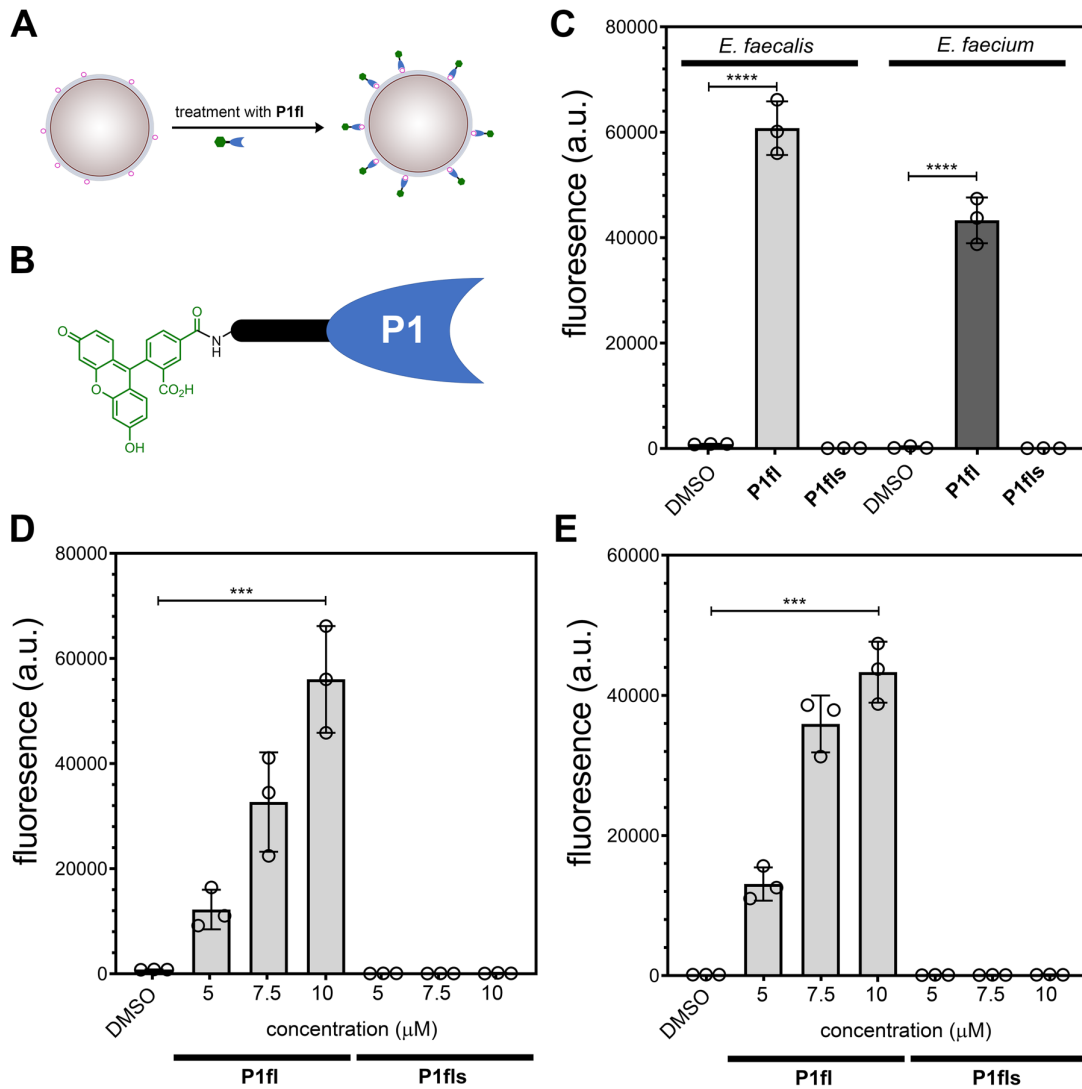
Figure 4.2 *Labeling of live Enterococci cell wall with P1fl*

(A) Schematic of bacterial cells labeled with P1 probes. (B) Chemical structure of fluorescein modified to P1. (C) *E. faecalis* 29212 and *E. faecium* 2127 were treated with 10 μM of P1fl or P1fls and analyzed by flow cytometry. (D) *E. faecalis* 29212 and (E) *E. faecium* 2127 were treated with indicated concentrations of P1 probes and analyzed by flow cytometry. Data are represented as mean ± SD (n= 3). *P*-values were determined by a two-tailed t-test (*p < 0.05, **p < 0.01, ***p < 0.001, ****p < 0.0001, ns = not significant).

Further, we examined how **P1fl** binding would compare to vancomycin, given its well-established ability to bind to the D-ala-D-ala motif on lipid II or within the PG scaffold.[61, 62] We anticipated that **P1fl** and vancomycin would exhibit similar cell labeling patterns being that both are expected to bind D-ala. *E. faecium* was co-incubated with BODIPY conjugated vancomycin (**VBD**)[63] and tetramethyl-rhodamine modified P1 (**P1tam**) then analyzed by confocal microscopy (Figure 4.3). *E. faecium* displayed labeling of **VBD** at both the septal region and the surrounding cell wall as expected.[54, 64-66] On the other hand, **P1tam** demonstrated labeling primarily at the surrounding cell wall, with minimal septal labeling. The septal region has the highest density of lipid II within the cell, as it is the site of PG biosynthesis; therefore, it is expected that vancomycin would display the highest degree of labeling to that region.[65] The surrounding cell wall is primarily composed of enzymatically processed PG which contains mainly tetra- and tri- stem peptides, rather than penta- stem peptides.[67] Moreover, we speculate that **P1tam** binding may be primarily directed to the surrounding cell wall because of its affinity for a singular D-ala motif rather than for D-ala-D-ala as with **VBD**. Additionally, this may be due in part to the limited accessibility of the septal region by P1, as it is larger than vancomycin.

VBD	P1tam	overlay
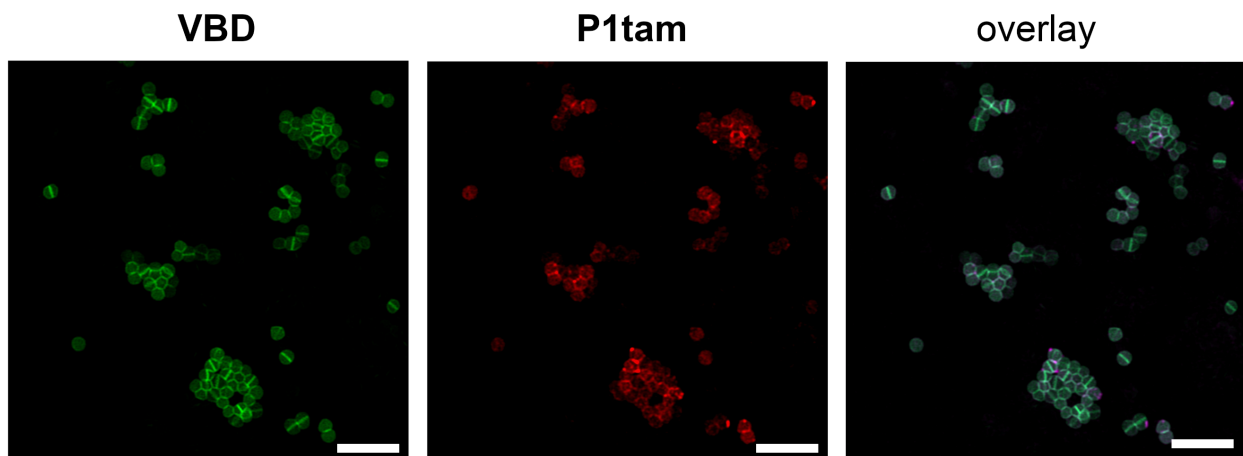
Figure 4.3 Confocal microscopy images of *E. faecium* 2127 treated with 10 μg/mL of VBD and 500 μM of P1tam. Shown is the overlay of channels corresponding to bodipy-Fl and tetramethyl-rhodamine. Scale bar = 3 μm.

4.3.2 FITC modified P1 to bind bacterial sacculi

Our lab has recently demonstrated a novel assay, SaccuFlow, to evaluate binding to bacterial PG using isolated, intact sacculi from a variety of bacterial strains (Figure 4.4A).[68] To further demonstrate the binding specificity of **P1fl** to ᴅ-ala on PG, sacculus from *E. faecalis* and *E. faecium* were isolated and individually incubated with **P1fl** and sacculi binding was assessed *via* flow cytometry (Figure 4.4B). As expected, **P1fl** bound to the sacculi of both *E. faecalis and E. faecium*, with *E. faecium* exhibiting higher binding levels as indicated by a higher fluorescence signal. We also identified that **P1fl** labeled both sacculi in a concentration dependent manner (Figure 4.5A, B)**.** Additionally, incubation of **P1fls** exhibited background levels of fluorescence compared to **P1fl**, indicating that the scramble peptide did not bind to either strain of sacculi (Figure 4.4B). From these data, we were able to further demonstrate the binding propensity of **P1fl** to ᴅ-ala on PG *via* SaccuFlow and provide further evidence that binding indeed occurs with the PG of live bacterial cells.
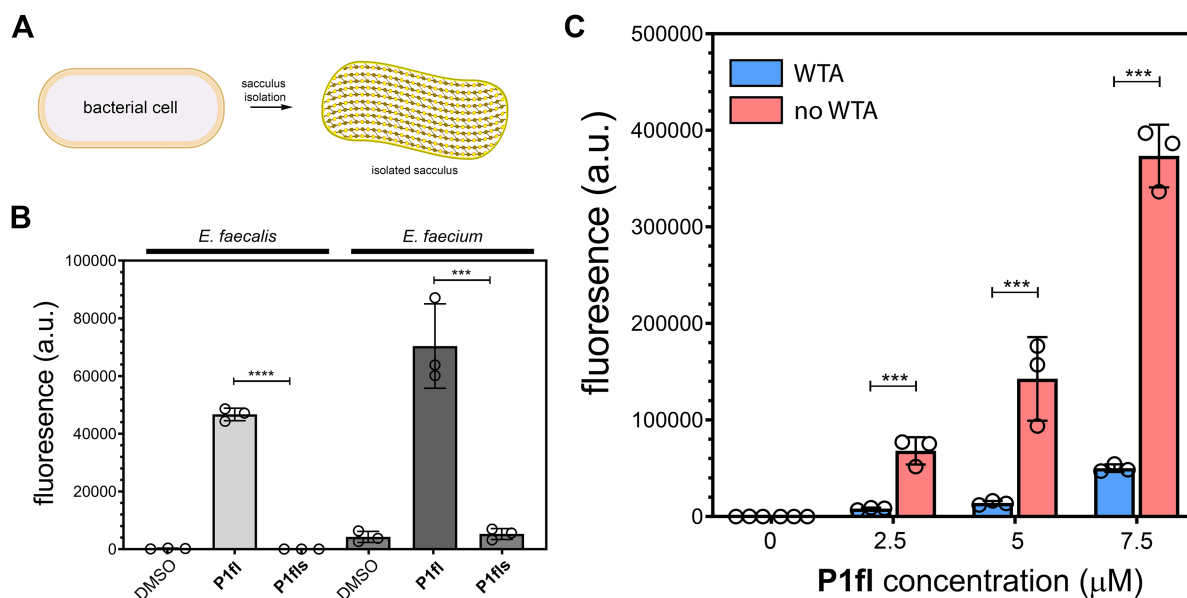
Figure 4.4 *Binding of P1fl to isolated Enterococci sacculi*

(A) Schematic of bacterial cells undergoing treatment to isolate intact bacterial sacculi. (B) *E. faecalis* 21922 and *E. faecium* 2127 sacculi were incubated with 7.5

μM of P1fl or P1fls and analyzed by flow cytometry. (C) *E. faecalis* 21922 sacculi with and without WTA were incubated with indicated concentration of P1fl and analyzed by flow cytometry. Data are represented as mean ± SD (n= 3). *P*-values were determined by a two-tailed t-test (*p < 0.05, **p < 0.01, ***p < 0.001, ****p < 0.0001, ns = not significant).

The accessibility of immune proteins to its bacterial cell wall target is largely mitigated by the presence of large surface polymers, wall teichoic acid (WTA) and lipoteichoic acid (LTA). Our lab,[69] and others,[48, 70-72] have recently demonstrated that WTA play a major contribution to the accessibility of molecules to the PG of bacterial cells; therefore, we aimed to investigate the role that WTA plays on the accessibility of **P1fl** to the surface of *E. faecalis,* as WTA is the most highly abundant glycopolymer on the enterococci cell wall.[73, 74] To achieve this, sacculi isolated from *E. faecalis* were treated with acid to hydrolyze the phosphodiester linkage between WTA and the PG, effectively removing the WTA from the isolated PG. Sacculi with and without WTA were incubated with **P1fl** and **P1fls**, and binding was monitored *via* flow cytometry. As expected, the removal of the WTA resulted in a large increase of cellular fluorescence when treated with **P1fl**, while binding of **P1fls** remained near background levels (Figure 4.4C). The binding of **P1fl** to the bacterial sacculi was observed in a concentration dependent manner for both with and without WTA and labeling was observed at concentrations as low as 2.5 μM.
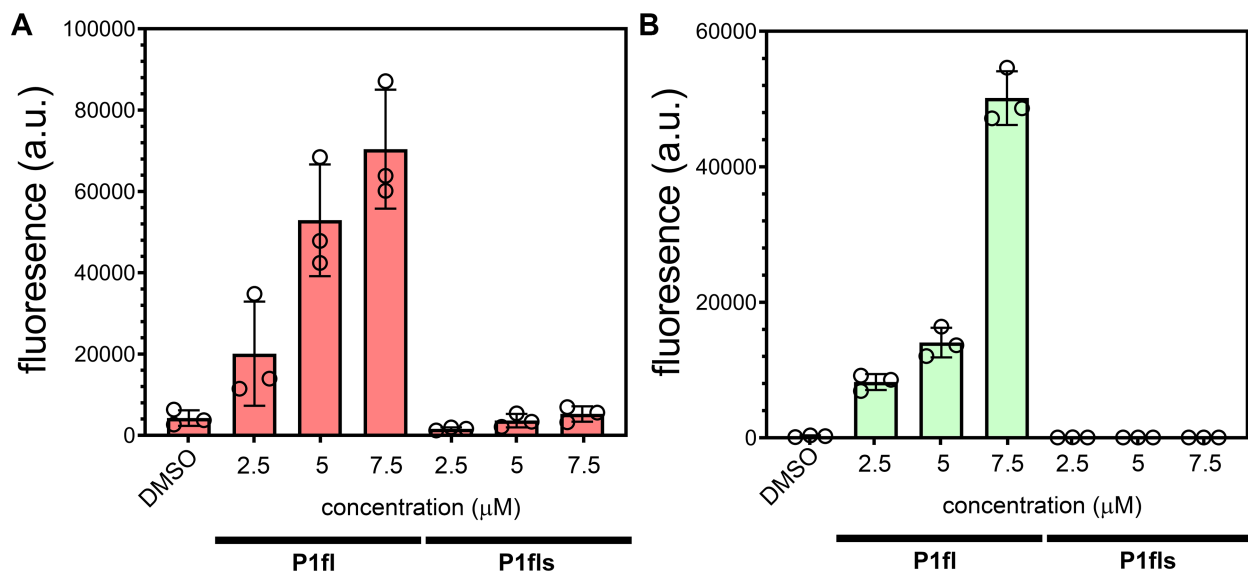
Figure 4.5 (A) *E. faecium* 2127 sacculi and (B) *E. faecalis* 29212 sacculi were treated with indicated concentrations of **P1fl** or **P1fls** and analyzed via flow cytometry. Data are represented as mean ± SD (n= 3). P-values were determined by a two-tailed t-test (*p < 0.05, **p < 0.01, ***p < 0.001, ns = not significant).

4.3.3 FITC modified P1 to opsonize live Enterococci bacteria

Based on our findings that **P1fl** efficiently binds *Enterococci* bacterial cell surfaces, we anticipated that utilizing the fluorescein moiety as an exogenous hapten would result in opsonization of anti-FITC antibodies for a directed immune response to the bacterial cell. The directed opsonization of *E. faecalis* was anticipated to occur *via* two different pathways: a pre-assembly of **P1fl** with anti-FITC prior to bacterial cell binding and/or initial tagging of **P1fl** to the surface of *E. f*aecalis followed by the sequential binding of anti-FITC (Figure 4.6A). We opted to maintain the fluorescein hapten as it has been shown to successfully direct the recruitment of anti-FITC antibodies for killing of cancer cells.[29, 31] Additionally, to improve surface presentation of the hapten to anti-fluorescein antibodies, we positioned the fluorescein moiety to be displayed on the ε-amine of an additional *N*-terminal lysine residue on P1 (Figure 4.6B). We directed our efforts of antibody recruitment towards *E. faecalis*, as **P1fl** demonstrated high levels of cell binding and has

vital clinical applicability, being that some types of drug resistant *E. faecalis* can induce a vancomycin-resistant phenotype.[75, 76] Vancomycin-resistant *Enterococci* (VRE) are identified as serious threat level pathogens by the Centers for Disease Control and Prevention (CDC), as treatment options for these organisms are becoming limited.[77, 78] Vancomycin-sensitive (VSE) *E. faecalis* was incubated with a solution containing **P1fl** or **P1Kfl** and AlexaFluor 647 anti-FITC antibodies, and then analyzed by flow cytometry, where fluorescence levels are expected to correspond with binding of anti-FITC antibodies (Figure 4.6C).[79, 80] VSE *E. faecalis* demonstrated greater levels of antibody recruitment when treated with **P1Kfl** at as low as 5 μM compared to **P1fl,** despite **P1fl** exhibiting much higher cell labeling levels over **P1Kfl** (Figure 4.7). This confirms that hapten presentation to the antibody plays a pivotal role in antibody recognition.
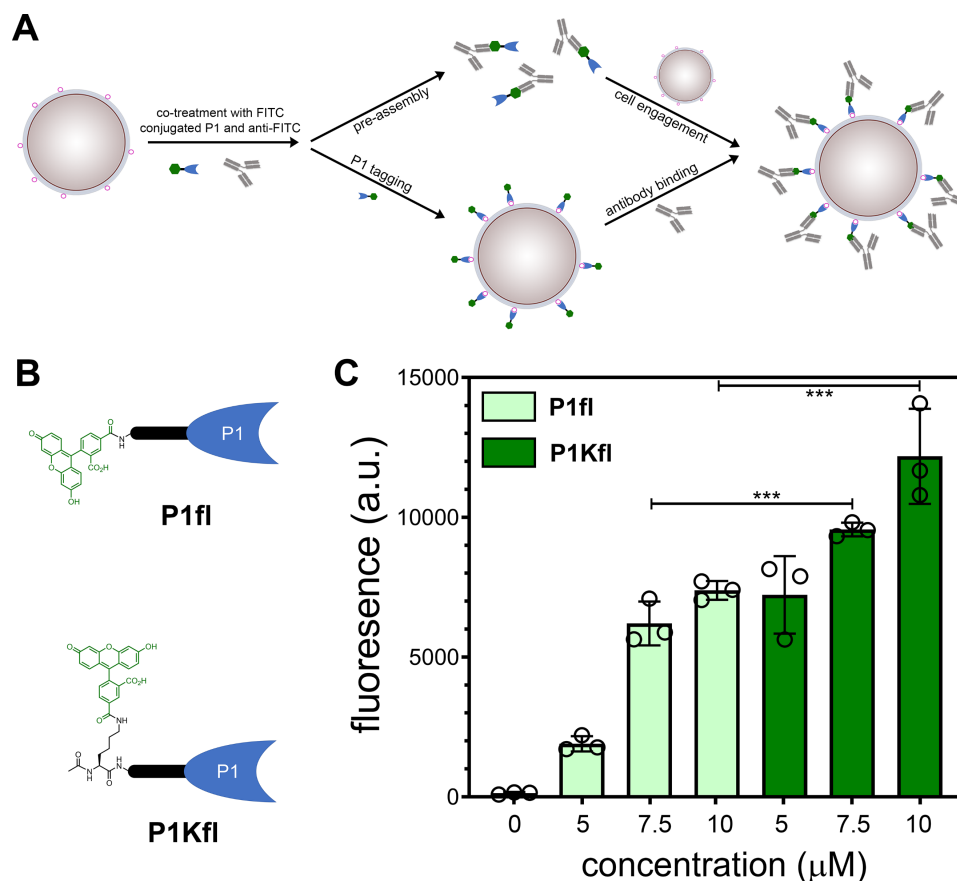
Figure 4.6 *Binding of anti-FITC antibodies to live E. faecalis*

(A) Cartoon representation of co-incubation of bacterial cells with P1 immune tags and anti-FITC antibodies. Cell targeting can occur via two pathways: pre-assembly of **P1fl**/anti-FITC prior to cell engagement or P1 tagging followed by antibody binding. (B) Chemical structures of modifications to P1 peptides. (C) *E. faecalis* 21922 was treated with indicated concentrations of **P1fl** or **P1Kfl** and AlexaFluor 647 anti-FITC antibodies where anti-FITC fluorescence was measured by flow cytometry. Data are represented as mean ± SD (*n*= 3). *P*-values were determined by a two-tailed *t*-test (*$p < 0.05$, **$p < 0.01$, ***$p < 0.001$, ns = not significant).
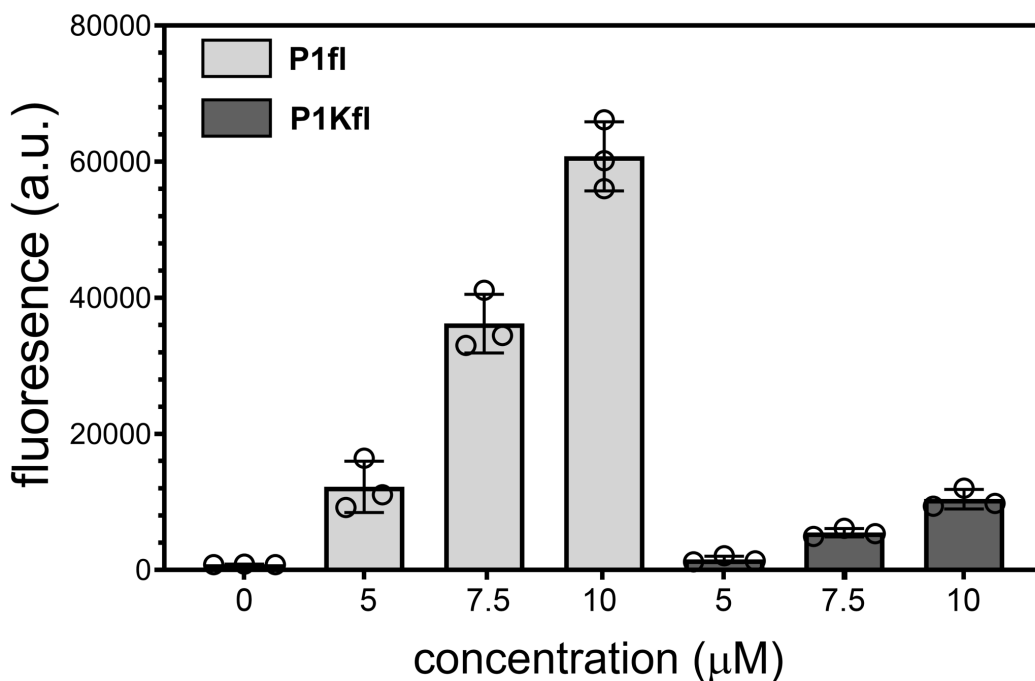
Figure 4.7 *E. faecalis* 29212 was treated with indicated concentrations of **P1fl** or **P1Kfl** and analyzed for cell binding. FITC fluorescence was measured by flow cytometry. Data are represented as mean ± SD (n= 3). P-values were determined by a two-tailed t-test (*$p < 0.05$, **$p < 0.01$, ***$p < 0.001$, ns = not significant).

Next, we wanted to evaluate the cell labeling and antibody recruitment of VSE *E. faecalis* compared to vancomycin- resistant (VRE) *E. faecalis*. When VSE and VRE *E. faecalis* were treated with **P1Kfl** immune tags, VRE *E. faecalis* exhibited much higher levels of

cell labeling compared to VSE, as indicated by a higher fluorescence signal (Figure 4.8A). The same trend in fluorescence was observed for the recruitment of anti-FITC antibodies, whereby **P1Kfl** treatment of VRE *E. faecalis* led to much higher levels of fluorescence relative to VSE (Figure 4.8B). **P1Kfl** also demonstrated superior levels of antibody recruitment to VRE *E. faecalis* compared to when treated with **P1fl**. Further, background fluorescence levels were observed for all scramble P1 control peptides for both cell labeling and antibody recruitment in VRE *E. faecalis* (Figure 4.8A, B). We speculate that the differences in recruitment between VSE and VRE *Enterococci* may be reflective of several variations in surface composition of drug resistant phenotypes including changes to cell surface accessibility. It may be possible that varying amounts of LTA and WTA of VSE and VRE may contribute to **P1Kfl** binding and subsequent anti-FITC recruitment.[73, 74]
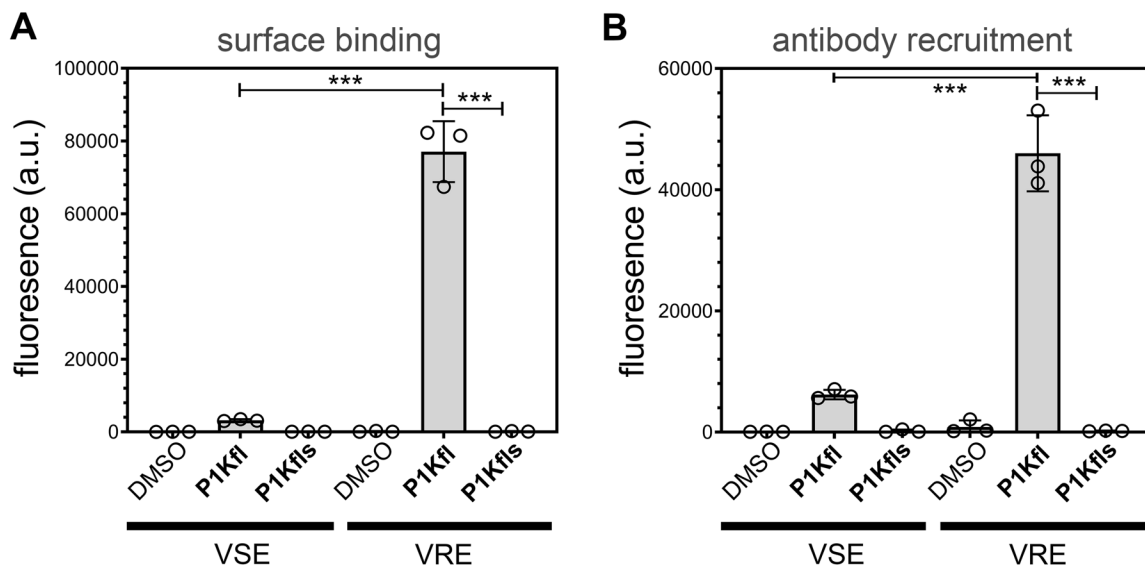
Figure 4.8 *Analysis of P1fl and anti-FITC binding to live vancomycin resistant E. faecalis*

(A) *E. faecalis* 21922 (vancomycin sensitive, VSE) and *E. faecalis* 51922 (vancomycin resistant, VRE) were treated with 7.5 μM of P1 probes and FITC fluorescence was measured by flow cytometry. (B) VSE and VRE *E. faecalis* were treated with 7.5 μM of P1 probes and AlexaFluor 647 anti-FITC antibodies and

anti-FITC fluorescence was measured by flow cytometry. Data are represented as mean ± SD (n= 3). P-values were determined by a two-tailed *t*-test (*p < 0.05, **p < 0.01, ***p < 0.001, ns = not significant).

It has been demonstrated that in order to induce the drug resistant phenotype of E. faecalis, vancomycin must be supplemented to the growth medium.81-83 We set out to examine how the addition of vancomycin to the growth medium would affect binding of P1Kfl and subsequent anti-FITC recruitment. Interestingly, minimal differences in bacterial cell binding and antibody recruitment were observed between induced and non-induced VRE E. faecalis (Figure 4.9A, B). We speculate that the ability of the P1 peptide to bind terminal D-ala, rather than D-ala-D-ala as with vancomycin, would remain unchanged following the induction of the VRE because this would not be expected to change the overall levels of D-ala. Critically, our results show that P1 conjugates would likely not be impacted by this type of VRE drug resistant phenotype.
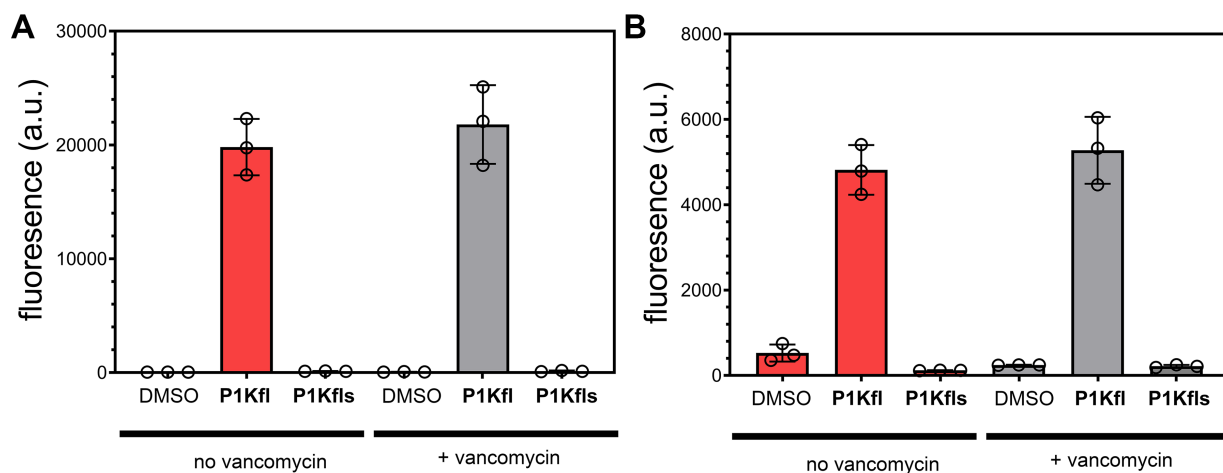
Figure 4.9 *E. faecalis* 51922 cells grown with or without 16 μg/mL of vancomycin and analyzed for (A) cell binding and (B) anti-FITC recruitment when treated with P1Kfl or P1Kfls. Samples were analyzed via flow cytometry. Data are represented as mean ± SD (n= 3). P-values were determined by a two-tailed t-test (*p < 0.05, **p < 0.01, ***p < 0.001, ns = not significant).

The specificity of anti-FITC for **P1Kfl** was further confirmed by treating cells with a mock antibody in place of anti-FITC; background fluorescence levels were observed for both P1 and P1s immune tags in the presence of Alexa Fluor 647 conjugated anti-human IgG (Figure 4.10A). Additionally, anti-FITC recruitment was not disrupted by the presence of pooled human serum, indicating that the **P1Kfl**/anti-FITC complex maintains recognition of the bacterial cell surface in a complex medium (Figure 4.10B). Based on our findings, we can conclude that fluorescein was grafted on the surface of VRE and successfully opsonized with anti-FITC antibodies.
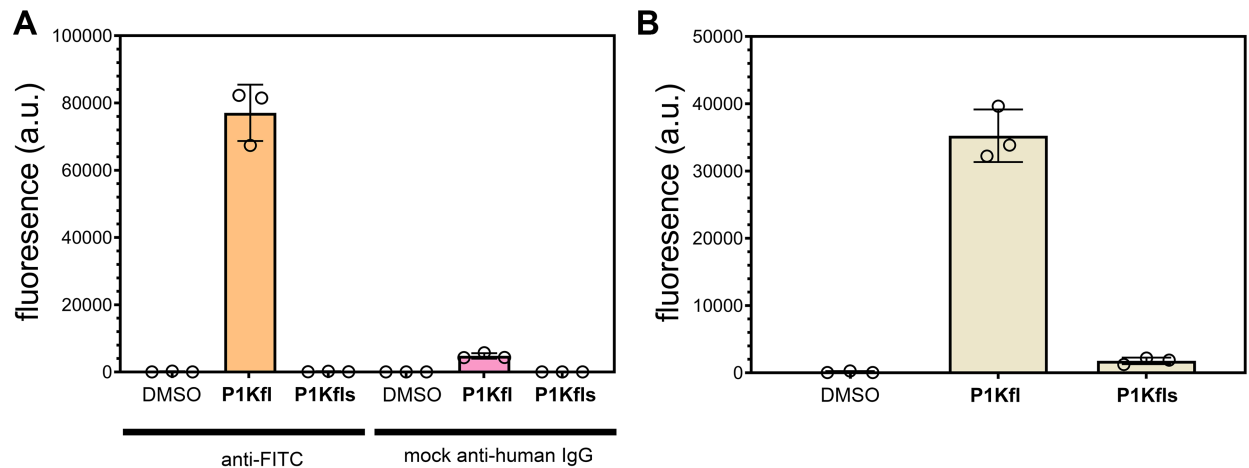
Figure 4.10 Flow cytometry data for *E. faecalis* 51922 cells treated with (A) **P1Kfl** or **P1Kfls** and either anti-FITC or anti-human IgG (mock antibody) and (B) **P1Kfl** or **P1Kfls** + anti-FITC in the presence of human serum. Data are represented as mean ± SD (n= 3). P-values were determined by a two-tailed t-test (*p < 0.05, **p < 0.01, ***p < 0.001, ns = not significant).

4.3.4 DNP modified P1 to opsonize live E. faecalis

To further expand the applicability of the P1 peptide to graft haptens on to the surface of bacterial cells, and show its overall generality in surface tagging, an endogenous hapten,

dinitrophenol (DNP), was used in place of the FITC moiety on P1, resulting in **P1dnp** (Figure 4.11A). Anti-DNP antibodies make up 1-2% of the naturally occurring human antibody pool.[59, 60, 81] Our group[34-37] and others[38, 39] have demonstrated that DNP can be used to recruit anti-DNP antibodies from human serum for bacterial immunotherapy. As expected, when **P1dnp** and anti-DNP were incubated with VRE *E. faecalis,* high fluorescence levels were only observed with **P1dnp** treatment and not with the scrambled sequence **P1dnps** (Figure 4.11B). Based on these results, a hapten modified P1 can function as a surface tagging modality for the recruitment of both exogenous and endogenous antibodies to pathogenic bacteria.
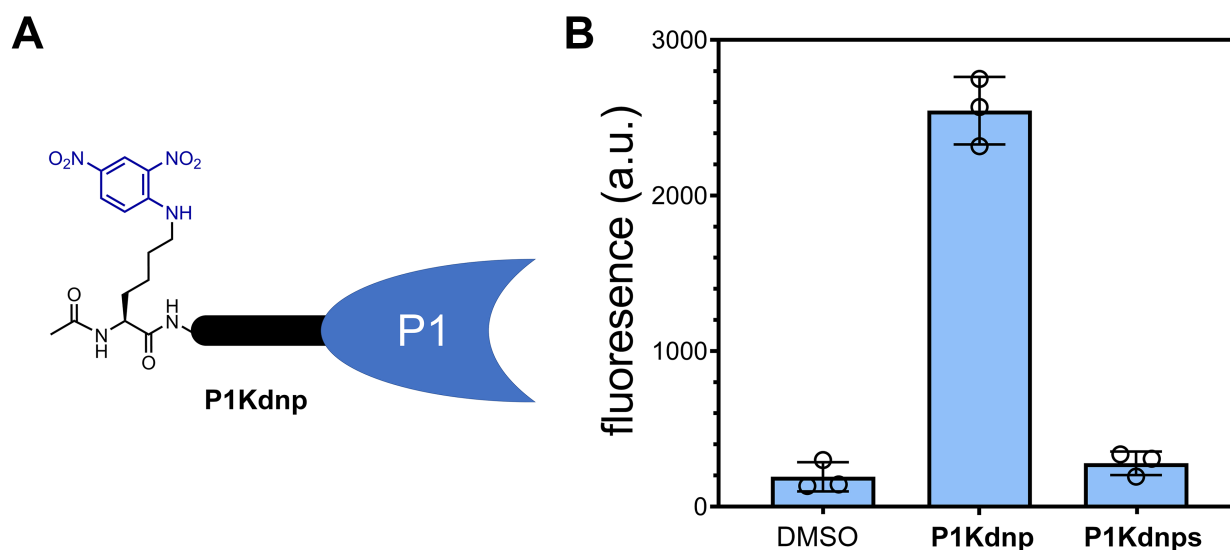
Figure 4.11 (A) Chemical structure of DNP modified to P1K peptide. (B) Flow cytometry analysis of *E. faecalis* 51299 cells treated with 10 μM of **P1dnp** or **P1dnps**. Data are represented as mean ± SD (n= 3). P-values were determined by a two-tailed t-test (*$p < 0.05$, **$p < 0.01$, ***$p < 0.001$, ns = not significant).

4.3.5 FITC modified P1 mediated uptake of live E. faecalis into macrophages

Finally, we set out to determine whether anti-FITC antibodies present on the surface of VRE E. faecalis would increase recognition and phagocytosis of the bacterial cells by

macrophages, as antibody dependent cellular phagocytosis (ADCP) is one of the primary mechanisms for clearance of bacterial pathogens by the immune system.82 Bacterial cells were co-incubated with J774A macrophages in the presence of P1Kfl and anti-FITC antibodies, with phagocytosis of bacterial cells being tracked by flow cytometry. VRE E. faecalis uptake by macrophages increased by 20-fold in the presence of both P1Kfl and anti-Fl antibodies, compared to macrophages co-incubated with VRE E. faecalis treated with P1Kfls. Background levels of phagocytosis were observed when anti-FITC antibodies were omitted for both P1Kfl and P1Kfls (Figure 4.12A, B). Confocal microscopy confirmed that the fluorescent population of bacterial cells were phagocytosed into the macrophages (Figure 4.12C). This demonstrates that increasing antibody opsonization of VRE can enhance phagocytosis and clearance of bacterial pathogens.
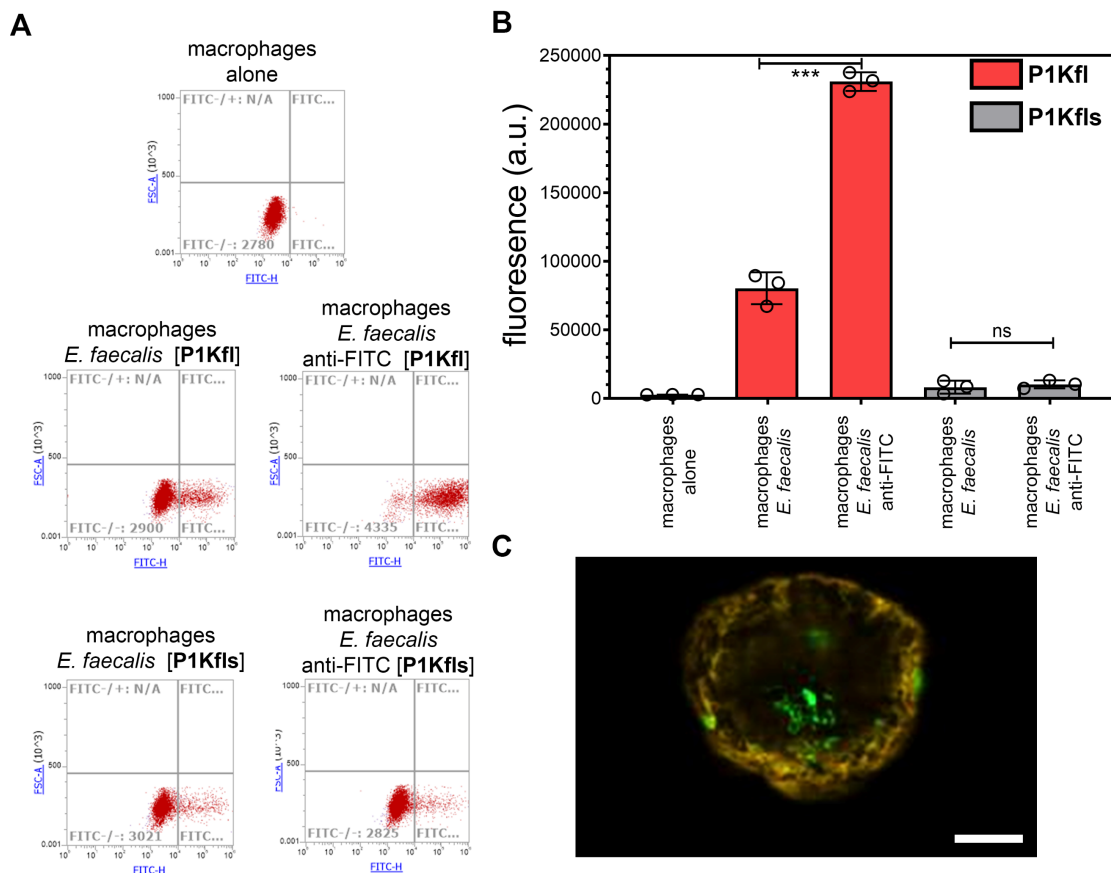
Figure 4.12 *Anti-FITC mediated uptake of live E. faecalis into macrophages*

(A) Representative scatter plots exhibiting changes in fluorescence for the macrophage population co-incubated with **P1Kfl** or **P1Kfls** opsonized *E. faecalis* 51922*. (B) Flow cytometry quantification of *E. faecalis* cells treated with **P1Kfl** or **P1Kfls** and anti-FITC antibodies prior to co-incubation with J774A macrophages. Data are represented as mean ± SD (n= 3). P-values were determined by a two-tailed t-test (*p < 0.05, **p < 0.01, ***p < 0.001, ns = not significant). (C) Confocal microscopy images of *E. faecalis* treated with 7.5 μM **P1Kfl** and anti-FITC phagocytosed into macrophages. Cells were fixed with formaldehyde and treated with tetramethyl-rhodamine-tagged WGA (5 μg/mL) for 30 min. Shown is the overlay of the channels corresponding to FITC and tetramethyl-rhodamine. Scale bar = 10 μm.

4.4 Conclusion

In conclusion, we have shown that **P1fl** is able to bind to whole bacterial cell surfaces in a sequence dependent manner, as a scrambled version of P1 demonstrated no binding propensity towards bacterial cells. We were able to label the surface of two strains of *Enterococci*, *E. faecalis* and *E. faecium*, using **P1fl** as demonstrated by flow cytometry and confocal microscopy. Additionally, **P1Kfl** was able to induce the recruitment of exogenous anti-FITC antibodies to the surface of *E. faecalis* and facilitated a P1-mediated immune cell uptake of the bacterial cells. We demonstrated that the hapten displayed on P1 can be altered to recruit its cognate antibodies, thus demonstrating the broad applicability of P1 to target bacterial cell surfaces with various treatment modalities. Additionally, **P1fl** preferentially targeted the PG of vancomycin resistant *E. faecalis*; therefore, **P1fl** may be used as a therapeutic option in conjunction with antibiotics for the treatment of drug resistant *Enterococci* species.

4.5 Summary and Future Outlook

In Chapter 4, we describe the utilization of a peptide fragment derived from *Ixodes scapularis* antifreeze glycoprotein (IAFGP) to bind D-alanine within the bacterial PG. Installation of an exogenous hapten to the peptide fragment enabled antigen specific recruitment of antibodies to the surface of two drug resistant *Enterococci* species. Further, antibody opsonization enhanced pathogen uptake into immune cells. A key feature of this design is the use of an exogenous hapten for antibody binding. For bacterial immunotherapy, traditional haptens include 2,4-dinitrophenol, L-rhamnose, and α-galactose. All of which are considered endogenous haptens as 1-2% of the natural human antibody pool contains such antibodies. Here, we capitalized on the ability of the exogenous hapten peptide fragment to form an *ex vivo* complex with the antibody prior to bacterial cell incubation; therefore, increasing the clinical applicability of the therapeutic modality, particularly in terms of extending the half-life of the peptide.

This approach has a similar associated drawback as described in Chapter 3, as in, this therapy is a multicomponent system that is dependent on several non-covalent interactions. To improve upon this work, expression of a bispecific protein could limit the dissociation of the participating entities. Bi- or tri- specific antibodies are exhibiting tremendous success in terms of cancer immunotherapeutics, where the variable regions of two antibodies with specificity for two different targets are fused together to create a bifunctional protein.[82] Here, fusion of an Fc receptor specific antibody fragment with the D-alanine binding peptide fragment would create a singular entity that has affinity for both the bacterial cell and the immune cell, effectively bridging to two cell types together for enhanced bacterial cell uptake and killing.

4.6 Materials and Methods

Materials. All peptide related reagents and protected amino acids were purchased from Chem-Impex. 5, 6-carboxyfluorescein was purchased from Chem-Impex. Anti-fluorescein

and anti-human IgG was purchased from Jackson Immuno Research Laboratories. Anti-dinitrophenol KHL was purchased from Thermo Fisher. Pooled Human Serum was purchase from Sigma Aldrich. Dulbecco's Modified Eagle's Medium (DMEM) was purchased from VWR. Fetal Bovine Serum (FBS) was purchased from R&D Systems. Penicillin-Streptomycin was purchased from Sigma-Aldrich. All other organic chemical reagents were purchased from Fisher Scientific or Sigma Aldrich and used without further purification. ALL COMPOUNDS ARE >95% PURE BY HPLC ANALYSIS.

Bacterial Cell Culture. Bacterial cells were cultured in specified media in an aerobic environment while shaking at 250 rpm at 37 °C. *E. faecalis* 29212 (vancomycin- sensitive) and *E. faecalis* 51299 (vancomycin- resistant) were grown in brain heart infusion broth (BHI). *E. faecium* ATCC BAA 2127 (vancoymycin-sensitive) and *E. faecium* ATCC BAA 2317 (vancoymycin-resistant) were grown in Trypticase Soy Broth (TSB). *E. faecalis* 51299 and *E. faccium* 2317 were supplemented with 16 µg/mL vancomycin to induce resistant phenotype. BLS2 organisms should be manipulated using proper protective equipment.

Mammalian Cell Culture. J774A.1 cells were cultured in Dulbecco's modified Eagle's medium (DMEM) supplemented with 10% (v/v) FBS, 50 IU/mL penicillin, 50 ug/mL streptomycin, and 2 mM L-glutamine in a humidified atmosphere of 55 CO_2 at 37 °C.

Fluorescent Labeling of Whole Bacterial Cells with P1 conjugates. Bacterial cells were grown over-night to stationary phase in corresponding growth media while shaking (250 rpm) at 37 °C. Bacterial cells from the overnight growth were used to inoculate BHI (1:100) supplemented with 100 µM D-DADA and incubated at 37 °C with shaking (250 rpm) for 16 h. The bacteria were harvested, washed three times with 1X phosphate buffered saline (PBS). The bacterial cells were resuspended in 1X PBS supplemented with P1- or P1s- fl conjugates **(**7.5 µM or designated concentration) and incubated at 37 °C with shaking (250 rpm) for 30 min. The bacteria were washed two times with 1X PBS, fixed with 2% formaldehyde solution, and analyzed using the Attune NxT Flow Cytometer

(Thermo Fischer) equipped with a 405 nm and a 488 nm laser with 440/50 and 530/30 nm bandpass filter respectively. The data were analyzed using Attune Nxt software.

Confocal Microscopy Analysis. Bacterial cells were grown over-night to stationary phase in corresponding growth media while shaking (250 rpm) at 37 °C. Bacterial cells from the over-night growth were harvested and washed once with 1X PBS. The bacterial cells were resuspended in 1X PBS supplemented with 500 μM of P1tam and 10 μg/mL of vancomycin bodipy Fl conjugate (Invitrogren #V34850, VBD) and incubated at 37°C with shaking (250 rpm) for 30 min. The bacteria were washed three times with 1X PBS, fixed with 2% formaldehyde solution, and imaged using the Zeiss LSM 980 Imaging System with multiplex Airyscan. We acknowledge the Keck Center for Cellular Imaging for the usage of the Zeiss 880/980 multiphoton Airyscan microscopy system (PI- AP: NIH-OD025156).

Peptidoglycan Isolation of *E. faecalis*. *E. faecalis* 29212 (vancomycin sensitive) and *E. faecalis* 51299 (vancomycin resistant) were grown over-night to stationary phase in BHI medium. A 100 mL culture volume in BHI medium was inoculated (1:100) from the stationary phase cultures and allowed to grow for 16 h while shaking (250 rpm) 37 °C. The cultures were harvested, resuspended in 1X PBS, boiled at 100 °C for 25 min, and centrifuged at 14,000 g for 15 min at 4 °C. The cells were placed in 50 mL of 2% (w/v) sodium dodecyl sulfate (SDS) and boiled for 30 min followed by centrifugation at 14,000 g for 15 min at 4 °C. Cells were then washed 6 times DI water to remove all the SDS. After washing, cells were resuspended in 25 mL of 20 mM Tris buffer (pH 8.0). Pellets were treated with 800 μg DNase for 24 hours followed by 800 μg trypsin for another 24 h at 37 °C while shaking (115 rpm). Pellets were boiled for 25 min followed by centrifugation at 14,000 g for 15 min at 4 °C. Pellets were resuspended in 1M HCl for 4 h at 37 °C with shaking to remove wall teichoic acids. The pellet was harvested by centrifugation at 4,000 rpm for 10 min and washed with DI water until the pH of the supernatant reached 5-6. The final pellet was resuspended in 1X PBS, and further diluted for analysis by flow cytometry.

Peptidoglycan Isolation of *E. faecium*. *E. faecium* BAA 2127 (vancomycin sensitive) and *E. faecium* BAA 2317 (vancomycin resistant) were grown over-night to stationary phase in TSB medium. The same protocol was followed as stated prior for peptidoglycan isolation of *E. faecalis*.

Fluorescent Labeling of Bacterial Sacculi. Bacterial sacculi were resuspended in 1X PBS supplemented with P1fl or P1fls (at designated concentration) and incubated at 37°C with shaking (250 rpm) for 30 min. Samples were washed twice with 1X PBS, fixed in a 2% formaldehyde solution, and analyzed by flow cytometry as previously described.

Co-incubation of Bacterial Cells with P1 conjugates and anti-FITC antibodies. Bacterial cells were grown over-night to stationary phase in corresponding growth media while shaking (250 rpm) at 37 °C. Bacterial cells from the overnight growth were used to inoculate BHI (1:100) supplemented with 100 μM DADA and incubated at 37 °C with shaking (250 rpm) for 16 h. The bacteria were harvested, washed three times with 1X PBS. The bacteria were resuspended in 50 μL of PBS containing P1fl and P1fls (7.5 μM or indicated concentration), 10 % (v/v) FBS, and 0.03 μg/mL Alexa Fluor 647-conjugated mouse anti-fluorescein (FITC) (Jackson Immuno Research #200-602-037) and incubated at 37°C for 30 min with shaking (250 rpm) protected from light. Samples were washed twice with 1X PBS, fixed in a 2% formaldehyde solution, and analyzed by flow cytometry (as described above) equipped with a 637 nm laser with 670/14 nm bandpass filter.

Co-incubation of Bacterial Cells with P1 conjugates and anti-DNP antibodies. Bacterial cells were prepared as described prior, with the exception that the bacteria were resuspended in 50 μL of 1X PBS containing P1dnp or P1dnps (10 μM or indicated concentration), 10 % (v/v) FBS, and 0.04 μg/mL Alexa Fluor 488-conjugated rabbit anti-dinitrophenol KHL (Thermo Fischer #A-11097) incubated at 37°C for 30 min with shaking (250 rpm) protected from light. Samples were washed twice with 1X PBS, fixed in a 2% formaldehyde solution, and analyzed using the Attune NxT Flow Cytometer (Thermo Fischer) equipped with a 488 nm laser and 525/40 nm bandpass filter. The data were analyzed using Attune Nxt software.

Incubation of bacterial cells with P1 conjugates and anti-FITC antibodies in human serum. Pooled human serum (PHS, Sigma-Aldrich #H4522) was diluted to 25% in 1x PBS and incubated with bentonite for 20 min at 37 °C to deactivate the lysozyme. The serum supernatant was obtained and diluted to a final concentration of 10% for use in the assay. The bacterial cell labeling and antibody recruitment protocol was followed as previously described, except for the 10% PHS was used rather than 10% FBS.

Incubation of bacterial cells with P1 conjugates and a mock antibody. The same protocol was followed as stated prior but with Alexa Fluor 647 goat anti-human IgG (Jackson Immuno Research #109-605-098) used in place of anti-fluorescein.
.

Phagocytosis of bacterial cells with P1Kfl and anti-Fl antibodies. Vancomycin resistant *E. faecalis* were grown to stationary phase in BHI while shaking (250 rpm) at 37 °C. Bacterial cells from the overnight growth were used to inoculate BHI (1:100) supplemented with 100 μM DADA and incubated at 37 °C with shaking (250 rpm) for 16 h. The bacteria were harvested and washed three times with 1X PBS. The bacteria were resuspended in 50 μL of PBS containing 5 μM of P1Kfl and P1Kfls, 10 % (v/v) FBS, and 0.03 mg/mL IgG fraction monoclonal mouse anti-fluorescein (FITC) (Jackson Immuno Research #200-002-037) and incubated at 37°C for 30 min with shaking (250 rpm) protected from light. The opsonized bacteria were washed with 1× PBS. J774A.1 cells were cultured as described prior. On the day of the experiment, J774A.1 cells were washed with 1X PBS by centrifuging 5 min at 1,000 rpm. The washed J774A cells were then mixed with opsonized *E. faecalis* (MOI 100) in DMEM + 10% FBS containing no antibiotics. The cell mixture was then incubated at 37 °C for 30 min to induce phagocytosis. The cell mixture was centrifuged for 5 min at 1,000 rpm and media was replaced with DMEM + 10% FBS + 300 μg/mL gentamycin and incubated at 4°C for 30 min. The cells were washed three times with 1X PBS and fixed for 30 min with 4% formaldehyde in 1X PBS. Samples were then analyzed by flow cytometry as described above.

4.7 *References*

1. Kaufmann, S.H.E. Remembering Emil von Behring: from Tetanus Treatment to Antibody Cooperation with Phagocytes. *Mbio* **8** (2017).

2. Kaufmann, S.H.E. Immunology's foundation: the 100-year anniversary of the Nobel Prize to Paul Ehrlich and Elie Metchnikoff. *Nat Immunol* **9**, 705-712 (2008).

3. Levy, S.B. & Marshall, B. Antibacterial resistance worldwide: causes, challenges and responses. *Nat Med* **10**, S122-S129 (2004).

4. Lewis, K. Persister cells, dormancy and infectious disease. *Nat Rev Microbiol* **5**, 48-56 (2007).

5. Feigman, M.J.S. & Pires, M.M. Synthetic Immunobiotics: A Future Success Story in Small Molecule-Based Immunotherapy? *Acs Infect Dis* **4**, 664-672 (2018).

6. Motley, M.P., Banerjee, K. & Fries, B.C. Monoclonal antibody-based therapies for bacterial infections. *Curr Opin Infect Dis* **32**, 210-216 (2019).

7. Aguilar, J.L. *et al.* Monoclonal antibodies protect from Staphylococcal Enterotoxin K (SEK) induced toxic shock and sepsis by USA300 Staphylococcus aureus. *Virulence* **8**, 741-750 (2017).

8. Biron, B. *et al.* Efficacy of ETI-204 Monoclonal Antibody as an Adjunct Therapy in a New Zealand White Rabbit Partial Survival Model for Inhalational Anthrax. *Antimicrob Agents Ch* **59**, 2206-2214 (2015).

9. Diep, B.A. *et al.* Targeting Alpha Toxin To Mitigate Its Lethal Toxicity in Ferret and Rabbit Models of Staphylococcus aureus Necrotizing Pneumonia. *Antimicrob Agents Ch* **61** (2017).

10. Gerding, D.N. *et al.* Bezlotoxumab for Prevention of Recurrent Clostridium difficile Infection in Patients at Increased Risk for Recurrence. *Clin Infect Dis* **67**, 649-656 (2018).

11. Iwamoto, R., Senoh, H., Okada, Y., Uchida, T. & Mekada, E. An Antibody That Inhibits the Binding of Diphtheria-Toxin to Cells Revealed the Association of a 27-Kda Membrane-Protein with the Diphtheria-Toxin Receptor. *J Biol Chem* **266**, 20463-20469 (1991).

12. Ortines, R. *et al.* Neutralizing alpha-toxin accelerates healing of Staphylococcus aureus-infected wounds in normal and diabetic mice. *J Invest Dermatol* **138**, S243-S243 (2018).

13. Vu, T.T.T. *et al.* Protective Efficacy of Monoclonal Antibodies Neutralizing Alpha-Hemolysin and Bicomponent Leukocidins in a Rabbit Model of Staphylococcus aureus Necrotizing Pneumonia. *Antimicrob Agents Ch* **64** (2020).

14. Ali, S.O. *et al.* Phase 1 study of MEDI3902, an investigational anti-Pseudomonas aeruginosa PcrV and Psl bispecific human monoclonal antibody, in healthy adults. *Clin Microbiol Infec* **25** (2019).

15. Baer, M. *et al.* An Engineered Human Antibody Fab Fragment Specific for Pseudomonas aeruginosa PcrV Antigen Has Potent Antibacterial Activity. *Infect Immun* **77**, 1083-1090 (2009).

16. Diago-Navarro, E. *et al.* Antibody-Based Immunotherapy To Treat and Prevent Infection with Hypervirulent Klebsiella pneumoniae. *Clin Vaccine Immunol* **24** (2017).

17. Fong, R.N. *et al.* Structural investigation of human S-aureus-targeting antibodies that bind wall teichoic acid. *Mabs-Austin* **10**, 979-991 (2018).

18. Gulati, S. *et al.* Complement alone drives efficacy of a chimeric antigonococcal monoclonal antibody. *Plos Biol* **17** (2019).

19. Nielsen, T.B. *et al.* Monoclonal Antibody Protects Against Acinetobacter baumannii Infection by Enhancing Bacterial Clearance and Evading Sepsis. *J Infect Dis* **216**, 489-501 (2017).

20. Storek, K.M. *et al.* Monoclonal antibody targeting the ss-barrel assembly machine of Escherichia coli is bactericidal. *P Natl Acad Sci USA* **115**, 3692-3697 (2018).

21. Visan, L. *et al.* Antibodies to PcpA and PhtD protect mice against Streptococcus pneumoniae by a macrophage- and complement-dependent mechanism. *Hum Vacc Immunother* **14**, 489-494 (2018).

22. Yi, X.Y. *et al.* Immunization with a peptide mimicking Lipoteichoic acid protects mice against Staphylococcus aureus infection. *Vaccine* **37**, 4325-4335 (2019).

23. Carlson, C.B., Mowery, P., Owen, R.M., Dykhuizen, E.C. & Kiessling, L.L. Selective tumor cell targeting using low-affinity, multivalent interactions. *Acs Chem Biol* **2**, 119-127 (2007).

24. Dubrovska, A. *et al.* A Chemically Induced Vaccine Strategy for Prostate Cancer. *Acs Chem Biol* **6**, 1223-1231 (2011).

25. Murelli, R.P., Zhang, A.X., Michel, J., Jorgensen, W.L. & Spiegel, D.A. Chemical Control over Immune Recognition: A Class of Antibody-Recruiting Small Molecules That Target Prostate Cancer. *J Am Chem Soc* **131**, 17090-+ (2009).

26. Popkov, M., Gonzalez, B., Sinha, S.C. & Barbas, C.F. Instant immunity through chemically programmable vaccination and covalent self-assembly. *P Natl Acad Sci USA* **106**, 4378-4383 (2009).

27. Rader, C., Sinha, S.C., Popkov, M., Lerner, R.A. & Barbas, C.F. Chemically programmed monoclonal antibodies for cancer therapy: Adaptor immunotherapy based on a covalent antibody catalyst. *P Natl Acad Sci USA* **100**, 5396-5400 (2003).

28. Sheridan, R.T.C., Hudon, J., Hank, J.A., Sondel, P.M. & Kiessling, L.L. Rhamnose Glycoconjugates for the Recruitment of Endogenous Anti-Carbohydrate Antibodies to Tumor Cells. *Chembiochem* **15**, 1393-1398 (2014).

29. Wehr, J. *et al.* pH-Dependent Grafting of Cancer Cells with Antigenic Epitopes Promotes Selective Antibody-Mediated Cytotoxicity. *J Med Chem* **63**, 3713-3722 (2020).

30. Lu, Y. *et al.* Folate-targeted dinitrophenyl hapten immunotherapy: Effect of linker chemistry on antitumor activity and allergic potential. *Mol Pharmaceut* **4**, 695-706 (2007).

31. Lu, Y.J. & Low, P.S. Folate targeting of haptens to cancer cell surfaces mediates immunotherapy of syngeneic murine tumors. *Cancer Immunol Immun* **51**, 153-162 (2002).

32. Lu, Y.J. & Low, P.S. Targeted immunotherapy of cancer: development of antibody-induced cellular immunity. *J Pharm Pharmacol* **55**, 163-167 (2003).

33. Dalesandro, B.E. & Pires, M.M. Induction of Endogenous Antibody Recruitment to the Surface of the Pathogen Enterococcus faecium. *Acs Infect Dis* **7**, 1116-1125 (2021).

34. Feigman, M.S. *et al.* Synthetic Immunotherapeutics against Gram-negative Pathogens. *Cell Chem Biol* **25**, 1185-+ (2018).

35. Fura, J.M., Pidgeon, S.E., Birabaharan, M. & Pires, M.M. Dipeptide-Based Metabolic Labeling of Bacterial Cells for Endogenous Antibody Recruitment. *Acs Infect Dis* **2**, 302-309 (2016).

36. Fura, J.M. & Pires, M.M. D-Amino Carboxamide-Based Recruitment of Dinitrophenol Antibodies to Bacterial Surfaces via Peptidoglycan Remodeling. *Biopolymers* **104**, 351-359 (2015).

37. Fura, J.M., Sabulski, M.J. & Pires, M.M. D-Amino Acid Mediated Recruitment of Endogenous Antibodies to Bacterial Surfaces. *Acs Chem Biol* **9**, 1480-1489 (2014).

38. Kaewsapsak, P., Esonu, O. & Dube, D.H. Recruiting the Host's Immune System to Target Helicobacter pylori's Surface Glycans. *Chembiochem* **14**, 721-726 (2013).

39. Kristian, S.A. *et al.* Retargeting pre-existing human antibodies to a bacterial pathogen with an alpha-Gal conjugated aptamer. *J Mol Med* **93**, 619-631 (2015).

40. Kiriyama, Y. & Nochi, H. D-Amino Acids in the Nervous and Endocrine Systems. *Scientifica* **2016** (2016).

41. Lee, C.J., Qiu, T.A. & Sweedler, J.V. D-Alanine: Distribution, origin, physiological relevance, and implications in disease. *Bba-Proteins Proteom* **1868** (2020).

42. Abraham, N.M. *et al.* Pathogen-mediated manipulation of arthropod microbiota to promote infection. *P Natl Acad Sci USA* **114**, E781-E790 (2017).

43. Narasimhan, S. *et al.* Gut Microbiota of the Tick Vector Ixodes scapularis Modulate Colonization of the Lyme Disease Spirochete. *Cell Host Microbe* **15**, 58-71 (2014).

44. Abraham, N.M. *et al.* A Tick Antivirulence Protein Potentiates Antibiotics against Staphylococcus aureus. *Antimicrob Agents Ch* **61** (2017).

45. Heisig, M. *et al.* Antivirulence Properties of an Antifreeze Protein (vol 9, pg 417, 2014). *Cell Rep* **9**, 2344-2344 (2014).

46.   Rother, R.P. & Squinto, S.P. The alpha-galactosyl epitope: A sugar coating that makes viruses and cells unpalatable. *Cell* **86**, 185-188 (1996).

47.   Shokat, K.M. & Schultz, P.G. Redirecting the Immune-Response - Ligand-Mediated Immunogenicity. *J Am Chem Soc* **113**, 1861-1862 (1991).

48.   Gautam, S., Kim, T., Lester, E., Deep, D. & Spiegel, D.A. Wall teichoic acids prevent antibody binding to epitopes within the cell wall of Staphylococcus aureus. *Acs Chem Biol* **11**, 25-30 (2016).

49.   Krishnamurthy, V.M. *et al.* Promotion of opsonization by antibodies and phagocytosis of Gram-positive bacteria by a bifunctional polyacrylamide. *Biomaterials* **27**, 3663-3674 (2006).

50.   Luchansky, S.J. *et al.* Constructing azide-labeled cell surfaces using polysaccharide biosynthetic pathways. *Method Enzymol* **362**, 249-272 (2003).

51.   Metallo, S.J., Kane, R.S., Holmlin, R.E. & Whitesides, G.M. Using bifunctional polymers presenting vancomycin and fluorescein groups to direct anti-fluorescein antibodies to self-assembled monolayers presenting D-alanine-D-alanine groups. *J Am Chem Soc* **125**, 4534-4540 (2003).

52.   Nelson, J.W. *et al.* A Biosynthetic Strategy for Re-engineering the Staphylococcus aureus Cell Wall with Non-native Small Molecules (vol 5, pg 1147, 2010). *Acs Chem Biol* **6**, 971-971 (2011).

53.   Prescher, J.A., Dube, D.H. & Bertozzi, C.R. Chemical remodelling of cell surfaces in living animals. *Nature* **430**, 873-877 (2004).

54.   Sabulski, M.J., Pidgeon, S.E. & Pires, M.M. Immuno-targeting of Staphylococcus aureus via surface remodeling complexes. *Chem Sci* **8**, 6804-6809 (2017).

55.   Vollmer, W. & Bertsche, U. Murein (peptidoglycan) structure, architecture and biosynthesis in Escherichia coli. *Bba-Biomembranes* **1778**, 1714-1734 (2008).

56.   Vollmer, W., Blanot, D. & de Pedro, M.A. Peptidoglycan structure and architecture. *Fems Microbiol Rev* **32**, 149-167 (2008).

57.   Guan, R.J. & Mariuzza, R.A. Peptidoglycan recognition proteins of the innate immune system. *Trends Microbiol* **15**, 127-134 (2007).

58.   Wolf, A.J. & Underhill, D.M. Peptidoglycan recognition by the innate immune system. *Nat Rev Immunol* **18**, 243-254 (2018).

59. Klibi, N. *et al.* Antibiotic resistance and mechanisms implicated in clinical enterococci in a Tunisian hospital. *J Chemotherapy* **18**, 20-26 (2006).

60. Shepard, B.D. & Gilmore, M.S. Antibiotic-resistant enterococci: the mechanisms and dynamics of drug introduction and resistance. *Microbes Infect* **4**, 215-224 (2002).

61. Barna, J.C.J. & Williams, D.H. The Structure and Mode of Action of Glycopeptide Antibiotics of the Vancomycin Group. *Annu Rev Microbiol* **38**, 339-357 (1984).

62. Breukink, E. & de Kruijff, B. Lipid II as a target for antibiotics. *Nat Rev Drug Discov* **5**, 321-332 (2006).

63. DeDent, A.C., McAdow, M. & Schneewind, O. Distribution of protein A on the surface of Staphylococcus aureus. *J Bacteriol* **189**, 4473-4484 (2007).

64. Daniel, R.A. & Errington, J. Control of cell morphogenesis in bacteria: Two distinct ways to make a rod-shaped cell. *Cell* **113**, 767-776 (2003).

65. Jia, Z.G., O'Mara, M.L., Zuegg, J., Cooper, M.A. & Mark, A.E. The Effect of Environment on the Recognition and Binding of Vancomycin to Native and Resistant Forms of Lipid II. *Biophys J* **101**, 2684-2692 (2011).

66. Tiyanont, K. *et al.* Imaging peptidoglycan biosynthesis in Bacillus subtilis with fluorescent antibiotics. *P Natl Acad Sci USA* **103**, 11033-11038 (2006).

67. Irazoki, O., Hernandez, S.B. & Cava, F. Peptidoglycan Muropeptides: Release, Perception, and Functions as Signaling Molecules. *Front Microbiol* **10** (2019).

68. Apostolos, A.J., Ferraro, N.J., Dalesandro, B.E. & Pires, M.M. SaccuFlow: A High-Throughput Analysis Platform to Investigate Bacterial Cell Wall Interactions. *Acs Infect Dis* **7**, 2483-2491 (2021).

69. Ferraro, N.J., Kim, S., Im, W. & Pires, M.M. Systematic Assessment of Accessibility to the Surface of Staphylococcus aureus. *Acs Chem Biol* **16**, 2527-2536 (2021).

70. Bertsche, U. *et al.* Correlation of Daptomycin Resistance in a Clinical Staphylococcus aureus Strain with Increased Cell Wall Teichoic Acid Production and D-Alanylation. *Antimicrob Agents Ch* **55**, 3922-3928 (2011).

71.   Eugster, M.R. & Loessner, M.J. Wall Teichoic Acids Restrict Access of Bacteriophage Endolysin Ply118, Ply511, and PlyP40 Cell Wall Binding Domains to the Listeria monocytogenes Peptidoglycan. *J Bacteriol* **194**, 6498-6506 (2012).

72.   Vaz, F. *et al.* Accessibility to Peptidoglycan Is Important for the Recognition of Gram-Positive Bacteria in Drosophila. *Cell Rep* **27**, 2480-+ (2019).

73.   Fabretti, F. *et al.* Alanine esters of enterococcal lipoteichoic acid play a role in biofilm formation and resistance to antimicrobial peptides. *Infect Immun* **74**, 4164-4171 (2006).

74.   Sava, I.G., Heikens, E. & Huebner, J. Pathogenesis and immunity in enterococcal infections. *Clin Microbiol Infec* **16**, 533-540 (2010).

75.   Arthur, M. & Courvalin, P. Genetics and Mechanisms of Glycopeptide Resistance in Enterococci. *Antimicrob Agents Ch* **37**, 1563-1571 (1993).

76.   Arthur, M., Depardieu, F., Snaith, H.A., Reynolds, P.E. & Courvalin, P. Contribution of Vany D,D-Carboxypeptidase to Glycopeptide Resistance in Enterococcus-Faecalis by Hydrolysis of Peptidoglycan Precursors. *Antimicrob Agents Ch* **38**, 1899-1903 (1994).

77.   Cetinkaya, Y., Falk, P. & Mayhall, C.G. Vancomycin-resistant enterococci. *Clin Microbiol Rev* **13**, 686-+ (2000).

78.   Murray, B.E. Drug therapy: Vancomycin-resistant enterococcal infections. *New Engl J Med* **342**, 710-721 (2000).

79.   Hong, H.F. *et al.* Universal endogenous antibody recruiting nanobodies capable of triggering immune effectors for targeted cancer immunotherapy. *Chem Sci* **12**, 4623-4630 (2021).

80.   Weiner, G.J. Monoclonal antibody mechanisms of action in cancer. *Immunol Res* **39**, 271-278 (2007).

81.   Miller, W.R., Munita, J.M. & Arias, C.A. Mechanisms of antibiotic resistance in enterococci. *Expert Rev Anti-Infe* **12**, 1221-1236 (2014).

82.   Labrijn, A.F., Janmaat, M.L., Reichert, J.M. & Parren, P. Bispecific antibodies: a mechanistic review of the pipeline. *Nat Rev Drug Discov* **18**, 585-608 (2019).

Chapter 5 Systematic Evaluation of the Permeability of Antibiotics to the Peptidoglycan of Intracellular *Staphylococcus aureus*

Adapted from: Dalesandro, B. E.[#]; Kelly, J. J.[#]; Lui, Z.; Chordia, M. D.; Pires, M. M., Systematic Evaluation of the Permeability of Antibiotics to the Peptidoglycan of Intracellular *Staphylococcus aureus*. **2022.** Manuscript in preparation.
[#]authors contributed equally

5.1 Abstract

A major mechanism for antimicrobial resistance in *Staphylococcus aureus* lies in its ability to proliferate and survive within the intracellular compartments of immune cells. Pressure from circulating immune cells drives *S. aureus* to invade host cells, protecting them from immune clearance and reducing antibiotic susceptibility. However, a difficulty arises in uncovering whether antibiotic resistance is due to low antibiotic concentrations within the intracellular compartments, or if the intracellular environment promotes phenotypic changes to the pathogen that renders antibiotics ineffective. To address this, we adapted our labs recently developed Peptidoglycan Accessibility Click-Mediated Assessment (PAC-MAN) strategy to analyze the permeability of antibiotics to target intracellular *S. aureus.* We metabolically labeled *S. aureus* with a D-amino acid containing dibenzocycooctyne (DBCO) to determine the permeability of azide modified antibiotics through macrophage membranes. Our findings enable us to empirically determine differences between the permeability of antibiotics to extra- and intracellular *S. aureus*.

5.2 Introduction

Staphylococcus aureus (*S. aureus*) is a Gram-positive pathogen that rapidly induces drug resistance upon challenge with antibiotics.[1] As a result, the World Health Organization (WHO) has identified *S. aureus* as high priority in terms of developing new antibiotics and therapeutic modalities.[2] One of the primary mechanisms that *S. aureus* escapes pressure from antibiotics and immune recognition is the ability to survive within host cells,

particularly immune cells.[3-9] Upon infection of *S. aureus,* host immune cells, primarily macrophages and neutrophils, phagocytose the bacterium within minutes.[8, 10-13] Typically, the majority of the phagocytosed *S. aureus* will be effectively killed by macrophage clearance mechanisms such as the release of reactive oxygen and nitrogen species (ROS, RNS), the production of antimicrobial peptides and enzymes, and acidification of the phagosome.[14] However, *S. aureus* has evolved means to circumvent this response, enabling bacterial survival inside of the macrophage for days; moreover, bacteria proliferate and lyse the infected macrophage.[10, 11, 15] Not only is intracellular survival of *S. aureus* a large proponent of reoccurring infection, but evidence suggests that the bacterium also undergoes a phenotypic switch in response to the phagosomal environment, further enabling pathogenicity.[5, 16]

The cell wall of *S. aureus* provides a formidable barrier to extracellular threats, including that of antibiotics and immune detection. As a Gram- positive pathogen, the cell wall is primarily comprised of a thick (20-30 nm) layer of peptidoglycan (PG) that displays various surface proteins and extracellular matrices, which are essential to maintaining the overall integrity of the cell.[17] The PG is composed of repeating disaccharide units, *N*-acetylglucosamine (GlcNAc) and *N*-acetylmuramic acid (MurNAc), covalently linked to a short, highly conserved, stem peptide (L-ala-D-glu-L-lys-D-ala-D-ala). The stem peptide strands are crosslinked together by transpeptidase (TPs) enzymes to create a dense, mesh-like scaffold that surrounds the cell.[18-20] As the PG is a critical component to the fitness of the pathogen, many antibiotics target PG biosynthesis enzymes.[21, 22] However, *S. aureus* employs several mechanisms to decrease this antibiotic susceptibility. For example, downregulation of crosslinking thickens the bacterial cell wall to render *S. aureus* resistant to vancomycin, while the expression of β-lactamases employs resistance to β-lactams.[23-25]

The ability of *S. aureus* to survive inside of phagocytotic cells provides an additional escape mechanism from antibiotic killing, presumably due to poor accessibility of the antibiotics to the intracellular compartments of the host cell. To date, *S. aureus* reduced susceptibility to antibiotics*,* in the case of intracellular survival, have been demonstrated

in vitro and *in vivo*.[26-28] However, the case has not been made to differentiate between the susceptibility of intracellular *S. aureus* to antibiotics versus the ability of the antibiotic to reach its intended target within the host cell. Traditionally, antibiotic efficacy is evaluated using a minimum inhibitory concentration (MIC) assay for both extra- and intracellular infections; however, such assays do not have the ability to differentiate between resistance due to poor antibiotic permeation and phenotypic switching. Here, we aim to distinguish between these two instances by systematically determining the permeability of select antibiotics to the PG of intracellular *S. aureus* (Figure 5.1).
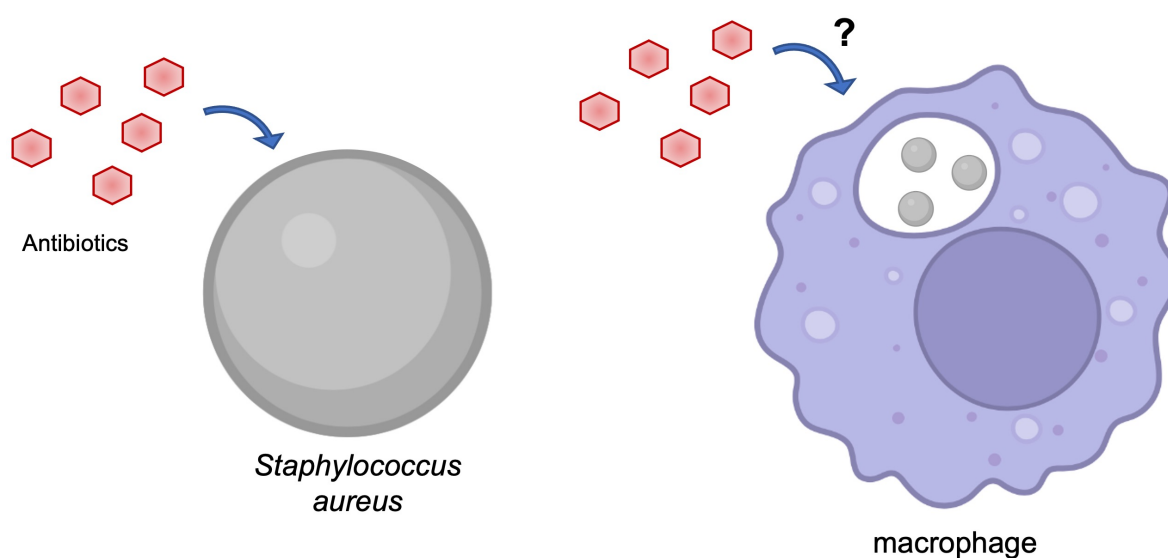
Figure 5.1 *Cartoon representation of antibiotic permeability to extracellular S. aureus (left) and intracellular S. aureus (right).*

Our lab[29-39] and others[40-43] have extensively demonstrated the ability to remodel bacterial PG with synthetic analogs of PG precursors. Further, it has been demonstrated that such analogs can be incorporated *in vivo* into the cell wall of *S. aureus* infected C. elegans[37] and various bacterial species residing in the gut microbiome of a mouse model.[44] Additionally, our lab has applied similar concepts to investigate permeability preferences of large biopolymers and small molecules to the PG of extracellular *S. aureus*[34] and mycobacterium,[45] respectively. Therefore, we reasoned that site-specific metabolic installation of a biorthogonal reactive handle within the PG of *S. aureus* could be utilized

to analyze the permeability of antibiotics through the PG of extracellular *S. aureus* compared to within the context of a phagosome. Our design aims to metabolically label the PG of *S. aureus* with a single D-amino acid containing dibenzocyclooctyne (DBCO) prior to infection of macrophages. Then incubation of the cells with azide-modified antibiotics (azAbx) post infection will result in the reaction between the DBCO and azAbx *via* strain promoted alkyne-azide cycloaddition (SPAAC).[46-48] We anticipate that subsequent incubation with an azide-modified fluorophore will react with any unoccupied DBCO moieties, enabling a fluorescent read out of antibiotic permeability where cellular fluorescence inversely correlates with antibiotic permeability. We expect that our assay will give insight to antibiotic permeability differences between extra- and intracellular *S. aureus* (Figure 5.1).

5.3 Results and Discussion

We recently described a novel assay, Peptidoglycan Accessibility Click-Mediated Assessment (PAC-MAN), that analyzed the permeability of small molecules to reach the PG of *Mycobacterium smegmatis* (*Msm*). *Msm* was treated with the unnatural amino acid D-diaminopimelic acid (D-Dap) modified with a DBCO on the side chain. During bacterial cell growth, supplementation of exogenous D-amino acids to the culture medium are swapped for the terminal D-alanine residue on the 4th or 5th position of the PG stem peptide (Figure 5.2).[35, 49-59] Here, we reasoned that PAC-MAN can be adapted to investigate the permeability of a panel of FDA approved antibiotics to the PG of intracellular *S. aureus* to potentially aid in distinguishing between antibiotic susceptibility and phagosome permeability.
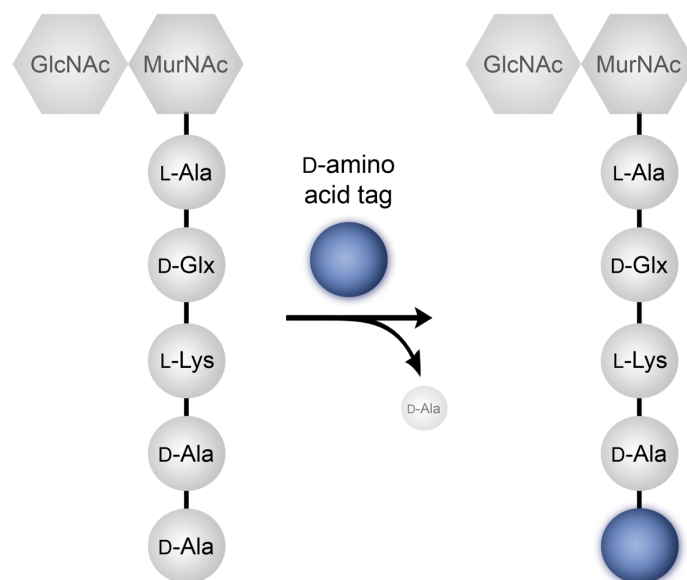
Figure 5.2 *Mode of incorporation of single amino acids into the 5th position of the peptidoglycan stem peptide.*

5.3.1 Optimizing PAC-MAN for S. aureus

Prior to investigating permeability intracellularly, the applicability of our assay must be examined *in vitro*. We synthesized a single amino acid with a DBCO conjugated to the sidechain of ᴅ-Dap (**ᴅ-DapD**). *S. aureus* cells were incubated with **ᴅ-DapD** (and its stereocontrol, **ʟ-DapD**) for metabolic incorporation into the growing PG scaffold. Stationary phase bacteria were washed to remove unincorporated **ᴅ-DapD** or **ʟ-DapD**, and then subject to incubation with azide-modified rhodamine 110 (**R110az**), where cellular fluorescence was measured by flow cytometry (Figure 5.3A). Satisfyingly, the fluorescence associated with *S.* aureus cells metabolically labeled with **ᴅ-DapD** were significantly higher than DMSO treated cells (Figure 5.3B). The stereocontrol, **ʟ-DapD**, exhibited similar fluorescence levels to DMSO treated cells, indicating that the DapD was selectively incorporated in the PG scaffold of *S. aureus* in a stereochemical specific manner, as bacterial enzymes only have tolerability for D-amino acids. Additionally, incubation with **ᴅ-DabD** did not perturb cell growth, as cellular turbidity did not differ from

DMSO treated cells (Figure 5.3C). Finally, we utilized a novel technique recently developed by our lab, SaccuFlow, to further confirm *S. aureus* PG labeling with **D-DapD**, as SaccuFlow enables a fluorescent readout of isolated, intact
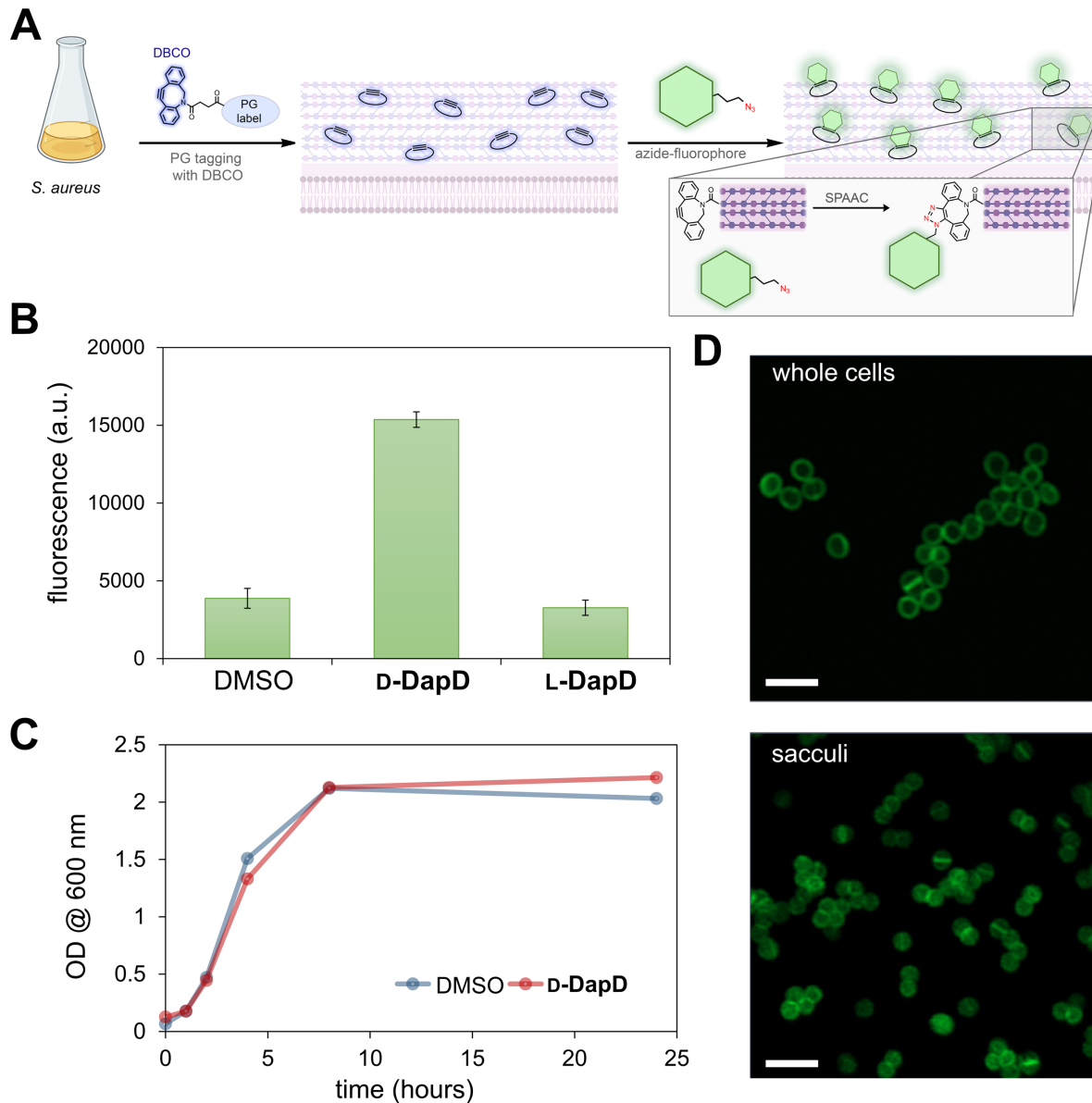
***Figure 5.3** In vitro analysis of S. aureus*

A) Workflow schematic of the PG labeling with a DBCO-displaying agent followed by treatment with an azide-tagged fluorophore. B) Flow cytometry analysis of *S.*

aureus treated overnight with 500 µM of **ᴅ-DapD** and incubated for 30 min with 25 µM of **R110az**. C) Measurement of OD_{600} over time for *S. aureus* cells treated with either DMSO or 500 µM of **ᴅ-DapD**. D) Confocal microscopy analysis of *S. aureus* cells treated with 500 µM of **ᴅ-DapD** followed by incubation with 25 µM of **R110az** for both whole cells (top) and isolated sacculi (bottom). Data are represented as mean ± SD (n= 3). P-values were determined by a two-tailed t-test (*p < 0.05, **p < 0.01, ***p < 0.001, ****p < 0.0001, ns = not significant).

bacterial sacculi *via* flow cytometry or confocal microscopy. *S. aureus* were treated with **ᴅ-DapD** and subsequently reacted with **R110az** as described above. The fluorescently labeled bacterial cells were then subject to sacculi isolation for further analysis by flow cytometry and confocal microscopy. As expected, confocal microscopy analysis revealed that the fluorescently labeled bacterial sacculus was matching in size and shape relative to whole cell *S. aureus* (Figure 5.3D)*.*

In order to optimize PAC-MAN for *S. aureus*, a number of labeling conditions were examined such as **ᴅ-DapD** and **R110az** concentration. Following the same workflow as prior, *S. aureus* cells were grown over-night in the presence of increasing concentrations of **ᴅ-DapD** followed by incubation with 25 µM of **R110az** and analyzed by flow cytometry. As expected, the cellular fluorescence levels of *S. aureus* grown with **ᴅ-DapD** increased in as the concentration of **ᴅ-DapD** increased (Figure 5.4A), indicating that more **ᴅ-DapD** was covalently linked into the growing PG scaffold as more amino acid was supplemented into the growth media. As such, we opted to use 500 µM for continued experimentation, as it exhibited significant labeling levels over background while minimally perturbing cellular growth (Figure 5.3C). Next, we aimed to investigate the optimal concentration of **R110az** to occupy a significant portion of the available DBCO sites anchored within the PG. To do so, *S. aureus* cells were incubated with 500 µM of **ᴅ-DapD**, followed by incubation with increasing concentrations of **R110az** for analysis by flow cytometry.

Similarly, as with increasing concentrations of **ᴅ-DapD**, increasing the concentration of **R110az** resulted increasing cellular fluorescence levels. This trend could indicate that increasing the concentration of **R110az** will result in a plateau of cellular fluorescence when all incorporated **ᴅ-DapD** sites have been occupied. Additionally, cellular labeling levels revealed that 25 μM of **R110az** would be sufficient for further experiments (Figure 5.4B). To ensure the timeframe of the assay on the surface of *S. aureus* will enable completion of the SPAAC reaction, a time course of **R110az** labeling was performed, which indicated that the **R110az** reacted with the majority of available DBCO sites on the peptidoglycan layer within 30 minutes (Figure 5.4C). Lastly, to investigate the permeation effects of the fluorophore itself, we examined two additional azide fluorophores: fluorescein azide (**Flaz**) and coumarin azide (**Coaz**). Both of which demonstrated to be compatible with PAC-MAN for *S. aureus* (Figure 5.4D), as indicated by significant fluorescence signals over cells lacking **ᴅ-DapD**.
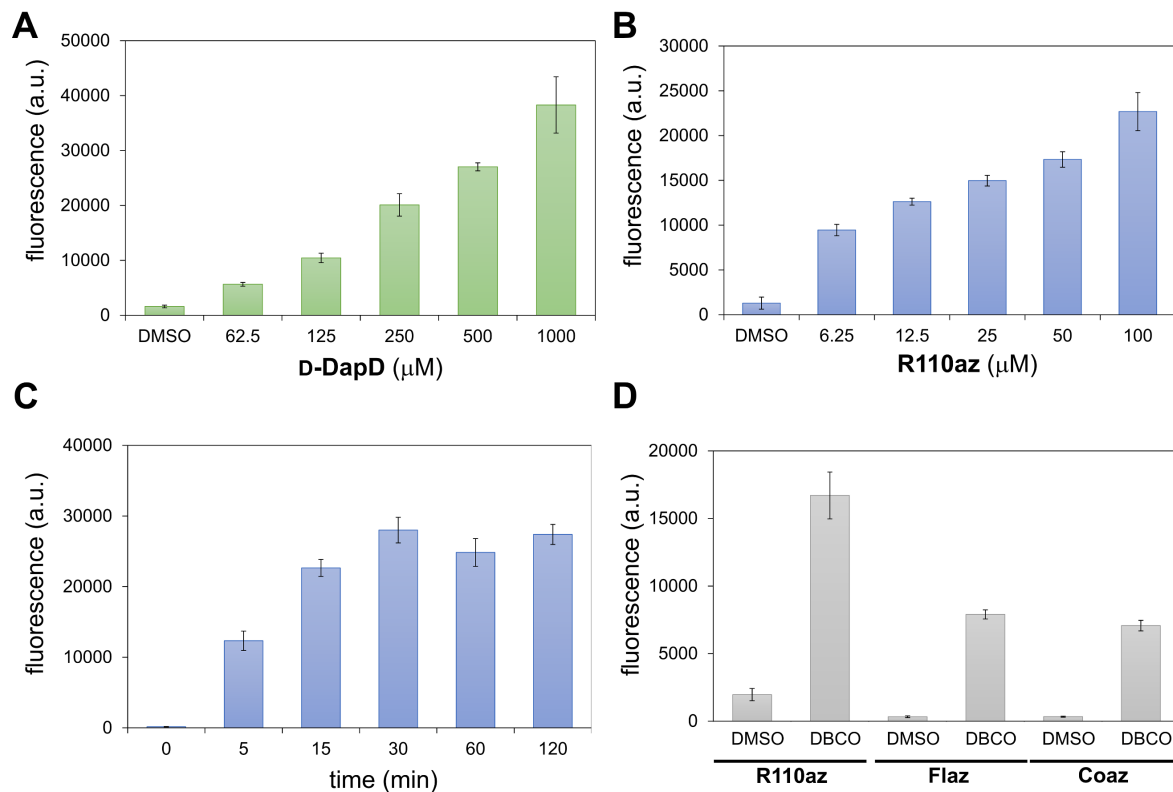
Figure 5.4 *Optimization conditions for S. aureus PAC-MAN*

A) Flow cytometry analysis of *S. aureus* incubated over-night with increasing concentrations of D-DapD, followed by incubation with 25 μM **R110az** for 30 min.

B) Flow cytometry analysis of *S. aureus* incubated over-night with 500 μM D-DapD, followed by incubation with increasing concentrations of **R110az** for 30 min. C) Flow cytometry analysis of *S. aureus* incubated over-night with 500 μM D-DapD, followed by incubation with 25 μM **R110az** over time. D) Flow cyometry analysis of *S. aureus* incubated overnight with 500 μM D-DapD, followed by incubation with **R110az**, 6-azido-fluorescein (**Flaz**), and 3-azido-7-hydroxy coumarin (**Coaz**). Data are represented as mean ± SD (n= 3).

5.3.2 Investigating Antibiotic Permeability to S. aureus in vitro

Next, we wanted to evaluate the ability of a representative panel of FDA approved antibiotics to permeate the PG of *S.* aureus. To this end, antibiotics were modified with an azide moiety (azAbx), on a location known to minimally perturb efficacy, in order to assess the ability of the antibiotic to sieve through the PG layer. We envisioned that treatment of D-DapD displaying *S. aureus* with the azAbx would result in occupation of the DBCO sites in an azAbx permeability dependent manner. Moreover, the occupied DBCO sites would be unavailable to react with a subsequent incubation of **R110az**. Therefore, we expect an inverse relationship between fluorescence intensity and the permeability of the azAbx to sieve the PG layer (Figure 5.5A). To test this idea, we modified a number of FDA approved antibiotics to bear reactive azide handles (Figure 5.5B). The antibiotics selected for this proof-of-concept were rifampicin, erythromycin, linezolid, and ciprofloxacin, which are currently used as a treatment option for *S. aureus.*[60-63] Our library consists solely of antibiotics that have intracellular targets in order to assess how permeability can be related to antibiotic potency. Additionally, the antibiotics have chemical compositions that range in hydrophobicity, polarity, size, and charge to examine how these factors affect the ability of the antibiotic to reach the PG layer. Moreso, we also included two variations of ciprofloxacin: one containing the azide modification off of the pyridinyl group and has an overall net negative charge, and another

that contains the azide in the same location but has an additional methyl ester modification to neutralize the overall charge of the molecule. This modification was done to evaluate the impact of net charge on the permeability of ciprofloxacin to the PG layer.
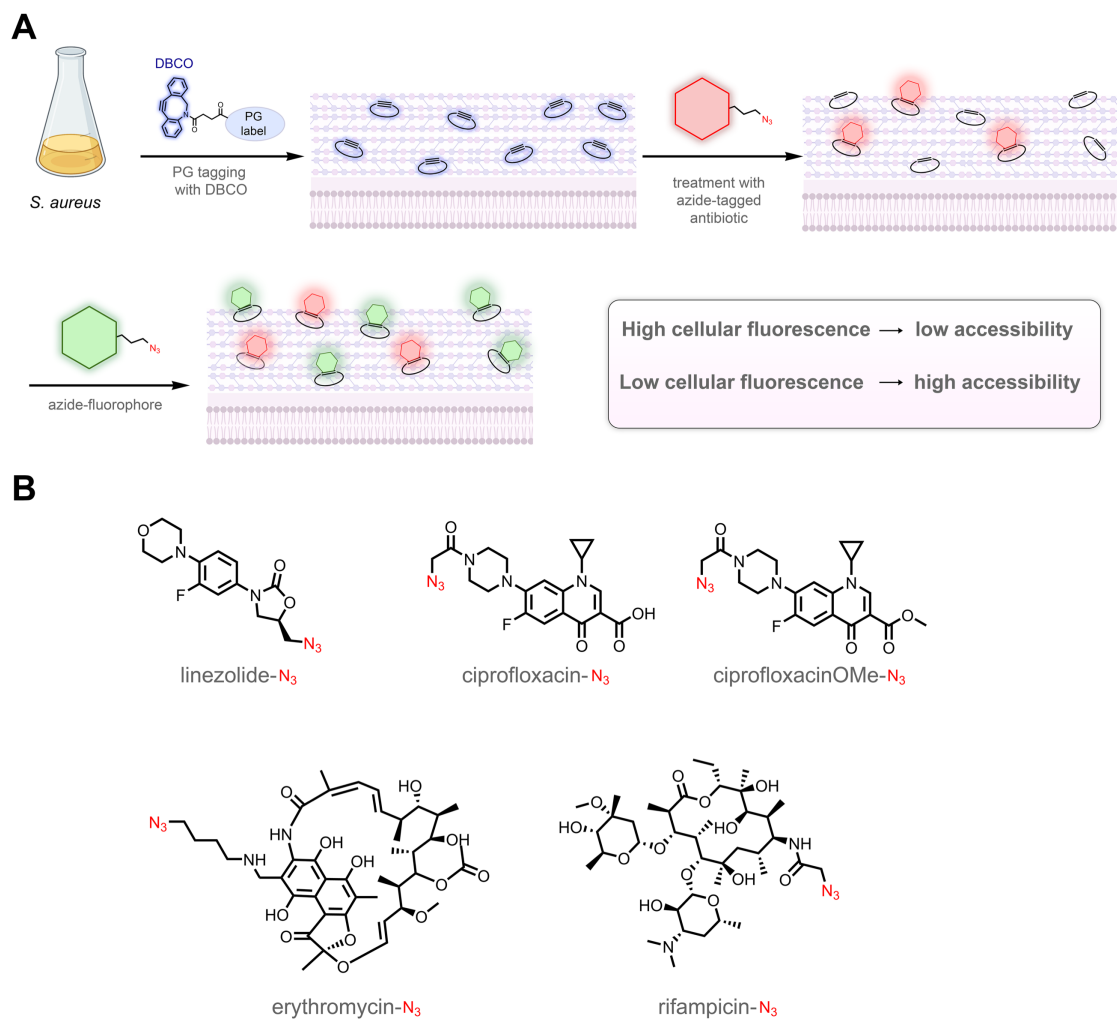
Figure 5.5 *Workflow for in vitro antibiotic competition to S. aureus PG*

A) Schematic of the general workflow for assessing the permeability of antibiotics to the PG of *S. aureus*. B) Chemical structures of azide modified antibiotics.

S. aureus cells were incubated over-night with **D-DapD** then subject to the library of azAbx over time. Following incubation with the azAbx, the excess azAbx was removed from the cells and followed with 25 μM of **R110az** then analyzed by flow cytometry. Nonpolar

antibiotics such as linezolid and rifampicin were able to sieve through the peptidoglycan and fully react with the DBCO modified peptidoglycan within 2 hours, as indicated by a
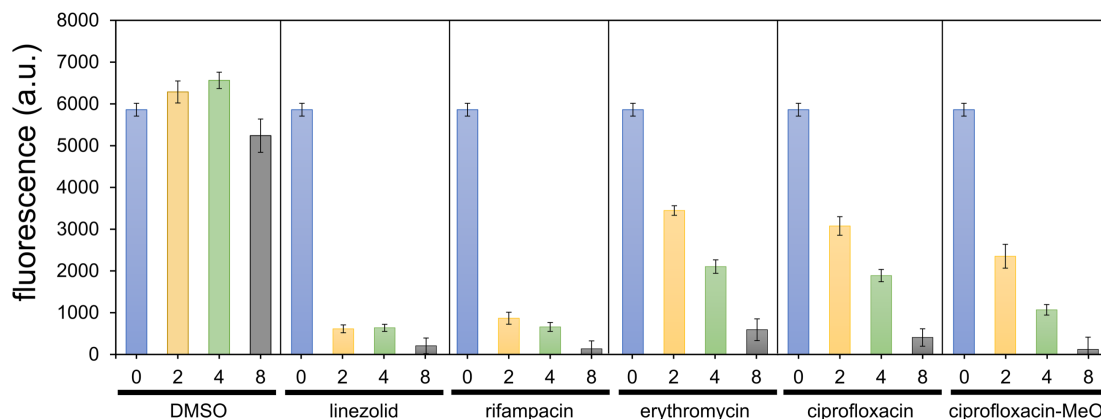
Figure 5.6 *in vitro analysis of antibiotic competition to S. aureus PG*

S. aureus cells were incubated with 500 µM of D-**DapD** over-night followed by incubation with 25 µM of azABx for indicated time points. Following azAbx incubation, the cells were resuspended in 25 mM of **R110az** for 30 min and analyzed by flow cytometry. Data are represented as mean ± SD (n= 3). P-values were determined by a two-tailed t-test (*p < 0.05, **p < 0.01, ***p < 0.001, ****p < 0.0001, ns = not significant).

low fluorescence signal. It is anticipated that the small size of linezolid and the flexible backbone of rifampicin enabled the antibiotic scaffolds to permeate the PG most efficiently of the Abx within azAbx library. However, the increased rigidity of erythromycin and the negative charge of ciprofloxacin appeared to hinder their ability to permeate the PG, as it took nearly 8 hours for both to fully react with the available DBCO moieties on *S. aureus* PG (Figure 5.6), as indicated by decreasing fluorescence levels over time. Additionally, a similar pattern of permeation was observed between the two ciprofloxacin derivatives, indicating that masking the net negative charge of ciprofloxacin had negligible effects in terms of reaching the PG of *S. aureus*. To further ensure whether the SPAAC reaction between the azAbx and D-DapD was complete within the timescale of the assay,

we modified amine-terminated beads to display DBCO epitopes (Figure 5.7A). As these beads are compatible with flow cytometry, this approach will provide a similar workflow as the live cell analysis but without the hinderance of the PG barrier. Our results showed that the antibiotics within the azide-modified panel readily react when not faced with a complex cell wall structure, as indicated by background fluorescence levels observed for all 5 azAbx within 2 hours (Figure 5.7B).
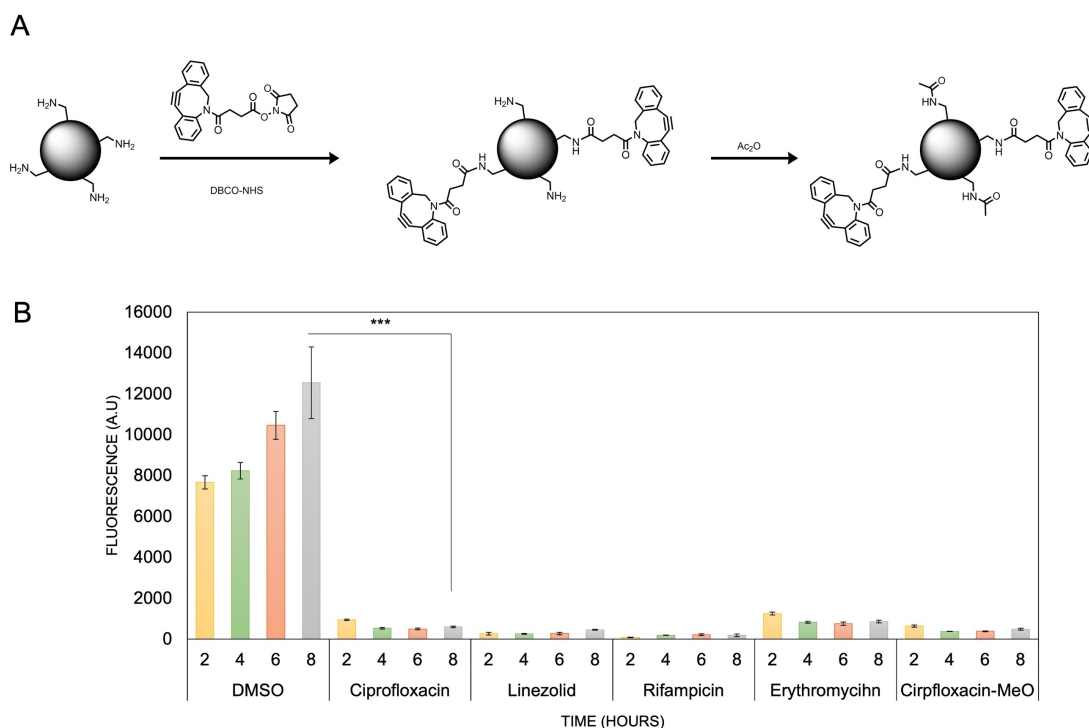
Figure 5.7 *Analysis of azAbx reaction of DBCO modified polystyrene beads*

A) Amine functionalized polystyrene beads were reacted with DBCO-NHS to form DBCO functionalized flow cytometer beads. The beads were further reacted with acetic anhydride to cap the remaining free amines. B) DBCO functionalized beads were incubated with 25 μM of azAbx over time, followed by incubation with 25 μM of **Flaz** for 30 min. Data are represented as mean ± SD (n= 3). P-values were determined by a two-tailed t-test (*p < 0.05, **p < 0.01, ***p < 0.001, ****p < 0.0001, ns = not significant).

5.3.3 Investigating the permeability of antibiotics to MRSA

Next, we tested PAC-MANs ability to determine antibiotic permeability in a methicillin resistant *S. aureus* (MRSA) strain to demonstrate the applicability of this assay across varying degrees of drug resistance. Satisfyingly, treatment of USA 300 *S. aureus* with D-
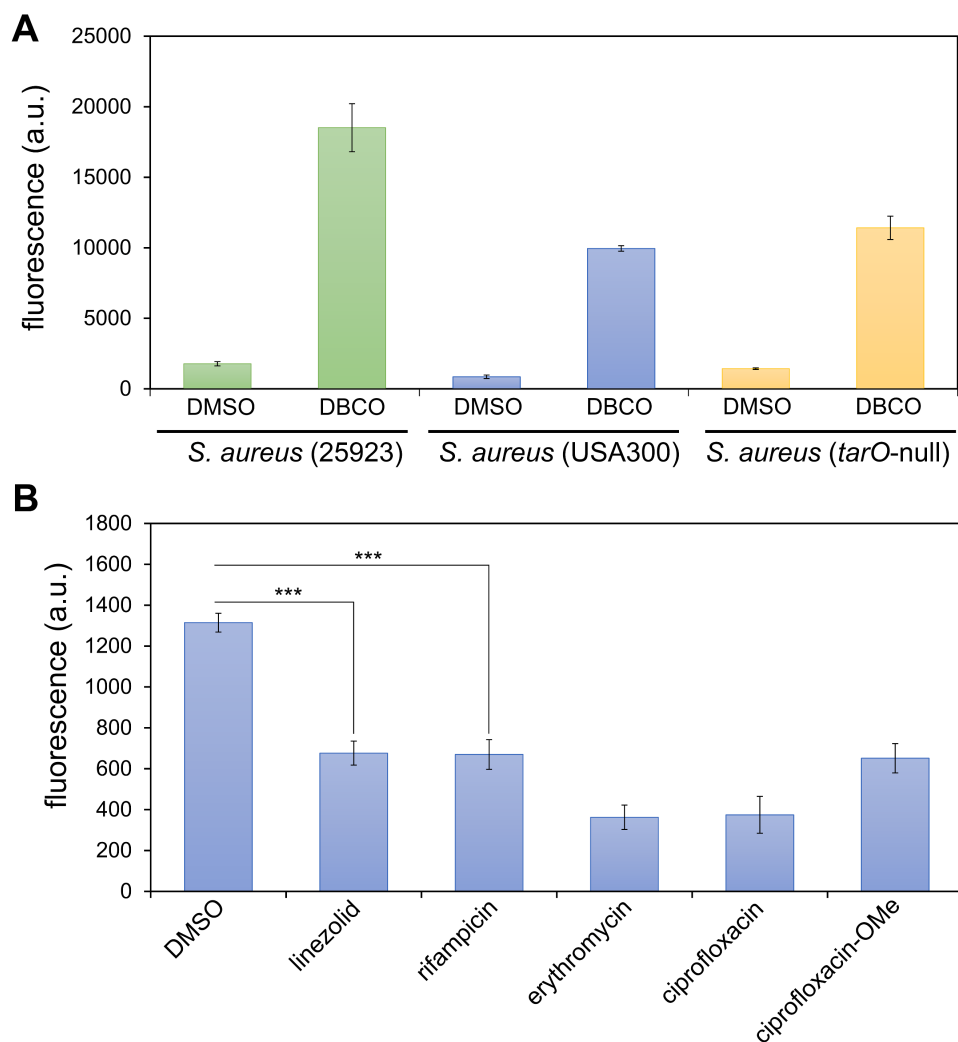
Figure 5.8 *Application of PAC-MAN to methicillin resistant S. aureus*

A) *S. aureus* 25923 (green), USA 300 (blue), a WTA deletion strain, dTarO, (yellow) was incubated overnight with 500 μM D-DapD followed by incubation with 25 μM R110az for 30 min and analyzed by flow cytometry. B) *S. aureus* USA 300 was incubated with 500 μM D-DapD overnight followed by incubation for 25 μM azAbx for 8 hours followed by a 30 min incubation with 25 μM of R110az.

Florescence intensity was then measured by flow cytometry. Data are represented as mean ± SD (n= 3). P-values were determined by a two-tailed t-test (*$p < 0.05$, **$p < 0.01$, ***$p < 0.001$, ****$p < 0.0001$, ns = not significant).

DapD resulted in a high fluorescence signal when incubated with **R110az**, indicating that D-**DapD** was incorporated into the PG layer of a methicillin resistant strain, and readily reacts with an azide molecule (Figure 5.8A). Further, we aimed to investigate the contribution that PG anchored polymers play on permeability. The surface of *S. aureus* is coated with wall teichoic acids (WTAs), anionic glycopolymers known to sterically hinder biomolecules from reaching the surface of the PG.[34, 64, 65] Therefore, we anticipated that removing the WTAs may improve the permeability of **R110az** to the PG layer. However, no significant difference was observed between the USA300 parent strain and TarO deletion strain, which removes WTAs from the surface of *S. aureus*, indicating that WTA do not impinge on the permeability of **R110az**. Further, we went on to investigate azAbx permeability to USA300 PG. After incubating D-**DapD** labeled USA 300 with the azAbx, a similar pattern was observed for all azAbx compared to wild type *S. aureus*, as evidenced by a significant decrease in fluorescence signal compared to DMSO treated cells (Figure 5.8B) after incubation with the azAbx for 8 hours. This indicates that the azAbx were able to sieve through the USA300 PG layer and occupy the majority of the installed DBCO sites located on the PG. Overall, these experiments demonstrate that PAC-MAN can be utilized across multiple S. aureus strains with varying degrees of antibiotic resistance.

5.3.4 Optimizing PAC-MAN for intracellular S. aureus

We next sought to test the permeability of the azAbx to reach the PG of intracellular *S. aureus*. *S. aureus* is known to survive within host immune cells, typically requiring a much higher concentration of the antibiotics to be effective. However, it has been reported that the physiological state of *S. aureus* also changes in the presence of intracellular environments, making it difficult to determine if resistance to antibiotics is induced by poor antibiotic permeability or by induction of a resistant phenotype. We envision that the application of PAC-MAN to intracellular *S. aureus* may provide insight for treating such

infections by solely analyzing antibiotic permeability. To transition the assay to apply to intracellular infections, *S. aureus* will be pre-labeled with D-**DapD** over-night and then infected into macrophages. Following cellular uptake, the macrophages will be incubated with the azAbx library for 8 hours, and then followed with incubation of **R110az** to be analyzed by flow cytometry (Figure 5.9A).
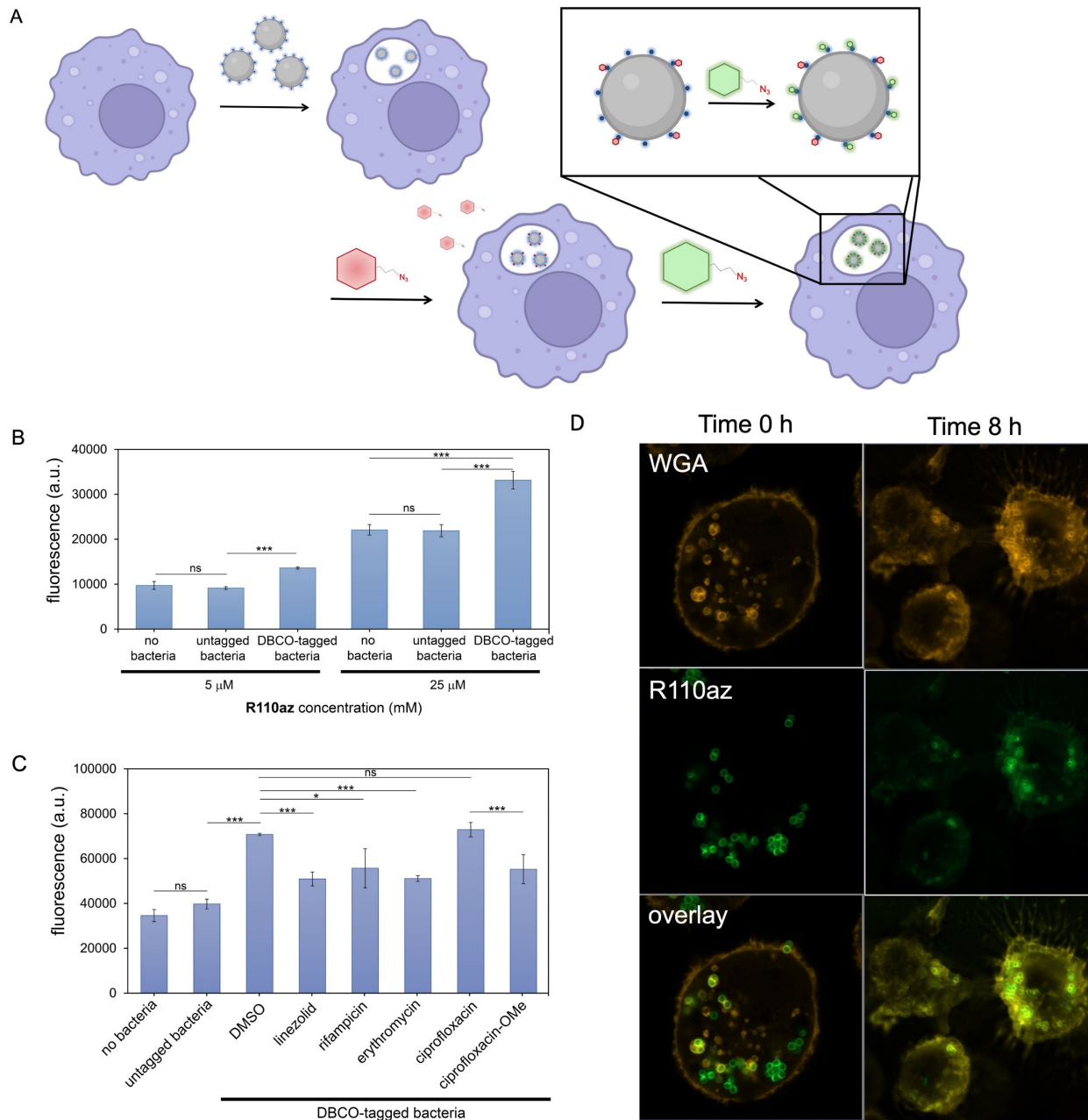
Figure 5.9 *Application of PAC-MAN to intracellular S. aureus*

A) Schematic of the assay workflow. *S. aureus* cells that were grown overnight with **ᴅ-DapD** will be infected into macrophages. The azAbx library will be incubated for 8 hours with *S. aureus* infected macrophages, followed by incubation with **R110az**, and analyzed by flow cytometry. B) *S. aureus* was grown overnight with 500 μM of **ᴅ-DapD** and infected into J774A macrophages at indicated MOI. Following bacterial uptake, varying concentrations of **R110az** were incubated for 30 min and cells were analyzed by flow cytometry. C) *S. aureus* cells were grown overnight with 500 μM of **ᴅ-DapD** and infected into J774A macrophages at an MOI of 100. AzAbx library was incubated with bacteria infected macrophages for 8 hours, followed by incubation with 25 μM of **R110az** and analyzed by flow cytometry. D) Confocal analysis of ᴅ-DapD infected J774A macrophages. *S. aureus* was labeled overnight with 500 μM of ᴅ-DapD and then immediately reacted with 25 μM of **R110az**. Fluorescently labeled *S. aureus* was infected into J774A macrophages at an MOI 100. Immediately following bacterial uptake, time 0 samples were fixed and analyzed by confocal microscopy. Time 8-hour samples were resuspended in PBS for 8 hours, fixed, and analyzed by confocal microscopy. Macrophage membrane was labeled with wheat germ agglutin (WGA) tetramethylrodamine. Data are represented as mean ± SD (n= 3). P-values were determined by a two-tailed t-test (*$p < 0.05$, **$p < 0.01$, ***$p < 0.001$, ****$p < 0.0001$, ns = not significant).

We first performed initial optimization experiments in the absence the azAbx, such as varying of the **R110az** concentration and the multiplicity of infection (MOI) in J774A macrophages. *S. aureus* was labeled over-night with **ᴅ-DapD** and then infected into J774A macrophages. As R110 has been shown to label mitochondria, we performed a concentration scan of **R110az** to analyze any background contribution from the fluorophore, which revealed that 25 μM of **R110az** provided the highest signal to noise ratio between **ᴅ-DapD** labeled and unlabeled (DMSO control) *S. aureus* (Figure 5.9B). Additionally, two different MOI's were investigated to ensure a sufficient number of

bacterial cells are being taken up into the macrophage. It was determined that an MOI of 100 could detect significant changes in **R110az** uptake for D-DapD *S. aureus* over the unlabeled DMSO control, as indicated by a significant change in fluorescence. To analyze the integrity of the bacterial cell within the macrophage within the time frame of the assay, confocal microscopy images were analyzed immediately after bacterial cell uptake and 8 hours post infection (Figure 5.9D). Here, it was revealed that the bacterial cells were intact and exhibited fluorescence labeling at the septal region and surrounding cell wall, which is consistent with confocal images of *S. aureus* alone (Figure 5.3D). Additionally, the fluorescence of the bacterial cell wall remained after surviving within the macrophage for 8 hours. Therefore, it was confirmed by confocal microscopy that the bacteria were intact and remained fluorescent inside the macrophages 8 hours post-phagocytosis.

5.3.5 *Analyzing antibiotic permeability to intracellular S. aureus*

We then asked if PAC-MAN was able to determine relative permeability of the azAbx through the macrophage membrane to reach the PG of intracellular *S. aureus*. After macrophages were allowed to uptake **D-DapD** labeled *S. aureus*, the cells were incubated with the azAbx library over an 8-hour period to distinguish any differences in the antibiotics ability to reach the PG layer (Figure 5.9C). Interestingly, ciprofloxacin was the only antibiotic tested that failed to show any detectable ability to reach the PG layer of intracellular *S. aureus*, as indicated by an indistinguishable difference in fluorescence between **D-DapD** labeled *S. aureus* with and without Ciprofloxacin-N_3 competition. Interestingly, when ciprofloxacin permeability was analyzed against extracellular *S. aureus*, a significant decrease in fluorescence was observed at the 8-hour time point, indicating that the azAbx fully occupied the DBCO sites on the PG (Figure 5.6). However, no detectable fluorescence change was observed when ciprofloxacin was analyzed against intracellular *S. aureus*. We reason that the negative charge of ciprofloxacin severely hindered antibiotic permeation into the macrophage. As anticipated, masking the charge of ciprofloxacin with a methyl ester derivative demonstrated significantly improved permeability of ciprofloxacin to the PG of intracellular *S. aureus*, as the fluorescence for intracellular *S. aureus* treated with ciprofloxacin-MeO was significantly lower than those

treated with ciprofloxacin. Further, this hints that the effect of the negative charge on ciprofloxacin has a significant impact in permeability into the cellular compartments of the macrophage, being that there were indistinguishable differences in fluorescence between the masked and unmasked ciprofloxacin for extracellular *S. aureus*. Additionally, the remaining azAbx demonstrated some ability to transverse the macrophage membrane to reach the surface of *S. aureus*, as indicated by near background fluorescence levels. Furthermore, we successfully demonstrated the applicability of PAC-MAN to empirically analyze the permeability of antibiotics to the surface of intracellular *S. aureus.* We anticipate that this platform can serve as foundational precedence to address the permeability of other classes of antibiotics to aid developing effective treatments for persisting intracellular *S. aureus* infections.

5.4 Conclusion

Here, we demonstrated that PAC-MAN is a suitable approach to assess the permeability of antibiotics to the surface of a Gram-positive pathogen *in vitro* and in the context of a macrophage. A select group of FDA approved antibiotics were successfully modified with an azide handle to covalently react with DBCO moieties embedded within the PG of *S. aureus* to give a direct read out of antibiotic permeability. Understanding the ability of antibiotics to penetrate both the mammalian cell membrane and phagosome are critical in terms of treating intracellular *S. aureus* infections. With our approach, we were able to identify that the overall efficacy of certain classes of antibiotics against intracellular *S. aureus* may be largely impacted by the membrane barrier provided by the phagocytic cell. Therefore, it is critical to consider additional membrane components when it comes to treating intracellular bacterial infections. However, in cases which antibiotic permeability is not the primary cause of resistance, additional factors including phenotypic changes of the pathogen, such as dormancy or persistence, should be evaluated as alternative causes for antimicrobial resistance. We anticipate PAC-MAN will be valuable in distinguishing the root cause of antibiotic resistance in intracellular pathogens.

5.5 Summary and Future Outlook

There is a rising crisis in terms of treating infections that are rendered resistant to antibiotics. In addition to traditional resistance mechanisms, *S. aureus* has evolved to escape both antibiotic and immune cell pressure by surviving within the contents of host cells. Chapter 5 details the novel application of our lab's recently developed Peptidoglycan Accessibility Click-Mediated Assessment (PAC-MAN) to the context of intracellular pathogens. Here, it was demonstrated that we can embed reactive DBCO moieties within the surface of intracellular *S. aureus* PG to react *via* SPAAC with azide modified antibiotics to assess antibiotic permeation to an intracellular target. We showed that only ciprofloxacin demonstrated poor permeability when comparing between extra- and intracellular *S. aureus*. We anticipate that this technique can be used to develop a more effective antibiotic treatment for intracellular *S. aureus* tailored around improving antibiotic efficacy through improved permeability.

As this application was demonstrated with a small panel of antibiotics, we aim to further develop this assay to include a broader range of antibiotics and continue investigating the effects of masking detrimental permeability factors to improve antibiotic uptake, as was demonstrated by masking the negative charge of ciprofloxacin with a methyl ester. Additionally, this technique may be beneficial to solicit chemical motifs that may aid in or hinder mammalian cell permeability. For instance, our lab has access to a library of azide modified small molecules; therefore, identifying chemical entities that exhibit high permeability may guide antibiotic design. Further, the application of PAC-MAN can be applied to analyze the permeability of antibiotics against other intracellular pathogens, such as gonorrhea and chlamydia.

5.6 Materials and Methods

Materials. All peptide related reagents and protected amino acids were purchased from Chem-Impex. DBCO-NHS (Catelog # BP-22231) was purchased from Broad Pharm. Deacetamide Linezolid Azide was purchased from Toronto Research Chemicals (Cat #:

D195600). Dulbecco's Modified Eagle's Medium (DMEM) was purchased from VWR. Fetal Bovine Serum (FBS) was purchased from R&D Systems. Penicillin-Streptomycin was purchased from Sigma-Aldrich. All other organic chemical reagents were purchased from Fisher Scientific or Sigma Aldrich and used without further purification.

Bacterial Cell Culture. Bacterial cells were cultured in specified media in an aerobic environment while shaking at 250 rpm at 37°C. *Staphylococcus aureus* (*S. aureus*) ATCC 25923 and *S. aureus* USA 300 were grown in Tryptic Soy Broth (TSB). BLS2 organisms should be manipulated using proper protective equipment.

Mammalian Cell Culture. J774A.1 cells were cultured in Dulbecco's modified Eagle's medium (DMEM) supplemented with 10% (v/v) FBS, 50 IU/mL penicillin, 50 ug/mL streptomycin, and 2 mM L-glutamine in a humidified atmosphere of 55 CO_2 at 37°C.

Labeling of Whole Bacterial Cells with D-DapD. *S. aureus* was grown over-night to stationary phase in TSB while shaking (250 rpm) at 37°C. Bacterial cells from the overnight growth were used to inoculate TSB (1:100) supplemented with 500 µM D-DapD (or indicated concentration) and incubated at 37°C with shaking (250 rpm) for 16 h. The bacteria were harvested, washed three times with 1X phosphate buffered saline (PBS). The bacterial cells were resuspended in 1X PBS supplemented with 25 µM (or indicated concentration) of either 6-azido-rhodamine 110 (R110az, Lumiprobe #D5230), 6-azido-fluorescein (Flaz, Lumiprobe #D1530), or 3-azido-7-hydroxy coumarin (Coaz, Sigma Aldrich #909513) in 1X PBS and incubated at 37°C for 30 min. The bacteria were spun down to remove excess dye, immediately fixed with a 2% formaldehyde solution in 1X PBS, and analyzed using the Attune NxT Flow Cytometer (Thermo Fisher) equipped with a 488 nm laser with 530/30 nm bandpass filter. The data were analyzed using Attune Nxt software.

Peptidoglycan Isolation of *S. aureus*. *S. aureus* ATCC 25923 was grown over-night to stationary phase in TSB medium. A 2 mL culture volume containing either DMSO or 500

μM D-DapD in TSB medium was inoculated (1:100) from the stationary phase cultures and allowed to grow for 16 h while shaking (250 rpm) 37°C. The cultures were harvested, resuspended in 25 μM of R110az in 1X PBS for 30 min at 37°C, and washed thrice with 1X PBS. The samples were boiled at 100 °C for 25 min and centrifuged at 14,000 g for 5 min at 4°C. The cells were placed in 2 mL of 2% (w/v) sodium dodecyl sulfate (SDS) and boiled for 30 min followed by centrifugation at 14,000 g for 5 min at 4°C. Cells were then washed 6 times with DI water to remove the SDS. After washing, cells were resuspended in 2 mL of 20 mM Tris buffer (pH 8.0). Pellets were treated with 800 μg DNase for 24 h followed by 800 μg trypsin for another 24 h at 37°C while shaking (115 rpm). Pellets were boiled for 25 min followed by centrifugation at 14,000 g for 5 min at 4°C. The pellet was harvested by centrifugation at 16,000 g for 5 min, resuspended in 1X PBS, and further diluted for analysis by flow cytometry and confocal imaging.

Azide- Antibiotic (Abx) competition of Whole Bacterial Cells with D-DapD. *S. aureus* was grown over-night to stationary phase in TSB while shaking (250 rpm) at 37°C. Bacterial cells from the overnight growth were used to inoculate TSB (1:100) supplemented with 500 μM D-DapD and incubated at 37°C with shaking (250 rpm) for 16 h. The bacteria were harvested, washed three times with 1X PBS. The bacterial cells were resuspended in 1X PBS supplemented with 25 μM of azide- Abx for the indicated amount of time at 37°C. The bacteria were spun down to remove excess antibiotics and were resuspended in 1X PBS supplemented with 25 μM 6-azido-rhodamine 110 (R110az, Lumiprobe #D5230) in 1X PBS and incubated at 37°C for 30 min. The bacteria were spun down to remove excess dye, immediately fixed with a 2% formaldehyde solution in 1X PBS, and analyzed using the Attune NxT Flow Cytometer (Thermo Fisher) equipped with a 488 nm laser with 530/30 nm bandpass filter. The data were analyzed using Attune Nxt software.

Confocal Microscopy Analysis of Whole Bacterial Cells and Bacterial Sacculi. Glass microscope slides were spotted with a 1% agarose pad and 2 μL of the fixed bacterial samples were deposited onto the agarose. Samples were covered with a micro cover

glass and imaged using a Zeiss 880/990 multiphoton Airyscan microscopy system (63x oil-immersion lens) equipped with a 488 nm laser. Images were obtained and analyzed via Zeiss Zen software. We acknowledge the Keck Center for Cellular Imaging and for the usage of the Zeiss 880/980 multiphoton Airyscan microscopy system (PI- AP: NIH-OD025156).

DBCO Modification of Polystyrene Beads. 100 μL amino functionalized polystyrene beads (5% w/v, 5 mg) were spun down at 21000 g for 10 min in a 1.7 mL ebb tube and washed with 1 mL deionized water before use. The beads were then spun down and resuspended in 1 mL 20 mM sodium borate buffer pH 9 with 2 μg/mL DBCO-NHS and reacted in 37℃ for 2 h with shaking. The resulting beads were spun down at 21000 g for 10 min, washed once and resuspended in sodium borate buffer. 20 μL acetic anhydride was added to the suspension and reacted in 37°C for 2h with shaking. The resulting product was then spun down and washed twice with 1 mL PBS and resuspend in 1 mL PBS for further use. Control beads were acetylated with acetic anhydride directly after wash with deionized water in the same conditions.

Competition with Azide-Abx on DBCO Modified Polystyrene Beads. DBCO modified and acetylated polystyrene beads were 1 to 1 diluted in PBS before adding to the assay. To a 96-well plate added 5 μL beads each well to 25 μM of each azide-abx in the library with a final volume of 100 μL in multiplicity of 12. The plate was incubated in 37°C for 2 h, 4 h, 6 h, 8 h. At each time point, 3 wells of the beads in each group were transferred to a 0.45 mm MultiScreen HV Filter Plate (Sigma, Cat # MSHVN4510) and vacuum filtered. The beads were then washed with 200 mL PBS two times to remove the residue azide-abx and resuspended in 100 μL PBS until next reaction. After collection of the last time point, 100 μL of 25 mM **Fl-Az** was added to each well and the plate was then incubated in 37℃ for 30 min. The samples were then vacuum filtered and washed twice with 200 μL PBS and then resuspended in 200 μL PBS. The samples were then analyzed by Attune™ NxT Flow Cytometer (Thermo Fisher) equipped with a 488 nm laser with 530/30 nm bandpass filter. The data were analyzed using Attune Nxt software.

Azide- Abx Competition to Intracellular *S. aureus*. *S. aureus* ATCC 25923 was grown to stationary phase in TSB while shaking (250 rpm) at 37 °C. Bacterial cells from the overnight growth were used to inoculate TSB (1:100) supplemented with 500 µM ᴅ-DapD and incubated at 37 °C with shaking (250 rpm) for 16 h. The bacteria were harvested, washed three times with 1X PBS. The bacterial cells were resuspended with 1X PBS to the original culture volume. J774A.1 cells were cultured as described above. On the day prior to the experiment, J774A.1 cells were seeded into a 48- well plate and allowed to adhere. On the day of the experiment, J774A.1 cells were washed with 1X PBS by centrifuging 5 min at 100 *g*. The washed J774A cells were then mixed with ᴅ-DapD labeled *S. aureus* (MOI 100) in DMEM + 10% FBS containing no antibiotics. The cell mixture was then incubated at 37 °C for 1 hour to induce phagocytosis. The cell mixture was centrifuged for 5 min at 100 *g* and media was replaced with DMEM + 10% FBS + 300 µg/mL gentamycin and incubated at 4°C for 30 min. The cells were washed three times with 1X PBS and incubated with either a solution containing 25 µM R110az (for no Abx competition samples) or 25 µM azide- Abx + 300 µg/mL gentamycin in 1X PBS for indicated amounts of time at 37°C. The Abx medium was removed, and the cells were incubated with a solution of 25 µM R110az in 1X PBS for 30 min at 37°C.The cells were washed thrice with 1X PBS and fixed for 30 min with 4% formaldehyde in 1X PBS. Samples were then removed from the well plate by scraping and analyzed *via* flow cytometry as described above.

Confocal Analysis of *S. aureus* Infection of Macrophages. *S. aureus* was grown overnight to stationary phase in TSB while shaking (250 rpm) at 37 °C. Bacterial cells from the overnight growth were used to inoculate TSB (1:100) supplemented with 500 µM ᴅ-DapD and incubated at 37 °C with shaking (250 rpm) for 16 h. The bacteria were harvested, washed three times with 1X PBS. The bacterial cells were resuspended in 1X PBS supplemented with 25 µM of R110az in 1X PBS and incubated at 37°C for 30 min. The bacteria were washed thrice and resuspended in in 1X PBS to the original culture volume. J774A.1 cells were cultured as described above. On the day prior to the experiment, J774A.1 cells were seeded into 35 mm glass bottom microwell dishes and

allowed to adhere. On the day of the experiment, J774A.1 cells were washed with 1X PBS by centrifuging 5 min at 100 *g*. The washed J774A cells were then mixed with ᴅ-DapD labeled *S. aureus* (MOI 100) in DMEM + 10% FBS containing no antibiotics. The cell mixture was then incubated at 37°C for 1 hour to induce phagocytosis. The cell mixture was centrifuged for 5 min at 100 *g* and media was replaced with DMEM + 10% FBS + 300 μg/mL gentamycin and incubated at 4°C for 30 min. The cells were washed thrice with 1X PBS and fixed for 30 min with 4% formaldehyde in 1X PBS. J774A.1 macrophages were then treated with 5 μg/mL of TMR-tagged Wheat Germ Agglutinin (Vector Laboratories, RL-1022) for 30 min at 4°C and imaged using a Zeiss 880/990 multiphoton Airyscan microscopy system (63x oil-immersion lens) equipped with 488 nm and 550 nm lasers. Images were obtained and analyzed via Zeiss Zen software. We acknowledge the Keck Center for Cellular Imaging and for the usage of the Zeiss 880/980 multiphoton Airyscan microscopy system (PI- AP: NIH-OD025156).

5.7 *References*

1. Lowy, F.D. Antimicrobial resistance: the example of Staphylococcus aureus. *J Clin Invest* **111**, 1265-1273 (2003).

2. Lee, A.S. *et al.* Methicillin-resistant Staphylococcus aureus. *Nat Rev Dis Primers* **4**, 18033 (2018).

3. Anwar, S., Prince, L.R., Foster, S.J., Whyte, M.K. & Sabroe, I. The rise and rise of Staphylococcus aureus: laughing in the face of granulocytes. *Clin Exp Immunol* **157**, 216-224 (2009).

4. Fraunholz, M. & Sinha, B. Intracellular Staphylococcus aureus: live-in and let die. *Front Cell Infect Microbiol* **2**, 43 (2012).

5. Garzoni, C. & Kelley, W.L. Return of the Trojan horse: intracellular phenotype switching and immune evasion by Staphylococcus aureus. *EMBO Mol Med* **3**, 115-117 (2011).

6. Gresham, H.D. *et al.* Survival of Staphylococcus aureus inside neutrophils contributes to infection. *J Immunol* **164**, 3713-3722 (2000).

7. Kapral, F.A. & Shayegani, M.G. Intracellular survival of staphylococci. *J Exp Med* **110**, 123-138 (1959).

8. Rogers, D.E. Studies on bacteriemia. I. Mechanisms relating to the persistence of bacteriemia in rabbits following the intravenous injection of staphylococci. *J Exp Med* **103**, 713-742 (1956).

9. Thwaites, G.E. & Gant, V. Are bloodstream leukocytes Trojan Horses for the metastasis of Staphylococcus aureus? *Nat Rev Microbiol* **9**, 215-222 (2011).

10. Hamza, T. & Li, B. Differential responses of osteoblasts and macrophages upon Staphylococcus aureus infection. *BMC Microbiol* **14**, 207 (2014).

11. Kubica, M. *et al.* A potential new pathway for Staphylococcus aureus dissemination: the silent survival of S. aureus phagocytosed by human monocyte-derived macrophages. *PLoS One* **3**, e1409 (2008).

12. Schnaith, A. *et al.* Staphylococcus aureus subvert autophagy for induction of caspase-independent host cell death. *J Biol Chem* **282**, 2695-2706 (2007).

13. Tuchscherr, L. *et al.* Staphylococcus aureus phenotype switching: an effective bacterial strategy to escape host immune response and establish a chronic infection. *EMBO Mol Med* **3**, 129-141 (2011).

14. Pidwill, G.R., Gibson, J.F., Cole, J., Renshaw, S.A. & Foster, S.J. The Role of Macrophages in Staphylococcus aureus Infection. *Front Immunol* **11**, 620339 (2020).

15. Flannagan, R.S., Heit, B. & Heinrichs, D.E. Intracellular replication of Staphylococcus aureus in mature phagolysosomes in macrophages precedes host cell death, and bacterial escape and dissemination. *Cell Microbiol* **18**, 514-535 (2016).

16. Peyrusson, F., Tulkens, P.M. & Van Bambeke, F. Cellular Pharmacokinetics and Intracellular Activity of Gepotidacin against Staphylococcus aureus Isolates with Different Resistance Phenotypes in Models of Cultured Phagocytic Cells. *Antimicrob Agents Chemother* **62** (2018).

17. Sharif, S., Singh, M., Kim, S.J. & Schaefer, J. Staphylococcus aureus peptidoglycan tertiary structure from carbon-13 spin diffusion. *J Am Chem Soc* **131**, 7023-7030 (2009).

18. Vollmer, W. Structural variation in the glycan strands of bacterial peptidoglycan. *FEMS Microbiol Rev* **32**, 287-306 (2008).

19. Vollmer, W. & Bertsche, U. Murein (peptidoglycan) structure, architecture and biosynthesis in Escherichia coli. *Biochim Biophys Acta* **1778**, 1714-1734 (2008).

20. Vollmer, W., Blanot, D. & de Pedro, M.A. Peptidoglycan structure and architecture. *FEMS Microbiol Rev* **32**, 149-167 (2008).

21. Reed, P. *et al.* Staphylococcus aureus Survives with a Minimal Peptidoglycan Synthesis Machine but Sacrifices Virulence and Antibiotic Resistance. *PLoS Pathog* **11**, e1004891 (2015).

22. Salamaga, B. *et al.* Demonstration of the role of cell wall homeostasis in Staphylococcus aureus growth and the action of bactericidal antibiotics. *Proc Natl Acad Sci U S A* **118** (2021).

23. Sieradzki, K., Pinho, M.G. & Tomasz, A. Inactivated pbp4 in highly glycopeptide-resistant laboratory mutants of Staphylococcus aureus. *J Biol Chem* **274**, 18942-18946 (1999).

24. Wang, M., Buist, G. & van Dijl, J.M. Staphylococcus aureus cell wall maintenance - the multifaceted roles of peptidoglycan hydrolases in bacterial growth, fitness and virulence. *FEMS Microbiol Rev* (2022).

25. Loskill, P. *et al.* Reduction of the peptidoglycan crosslinking causes a decrease in stiffness of the Staphylococcus aureus cell envelope. *Biophys J* **107**, 1082-1089 (2014).

26. Barcia-Macay, M., Seral, C., Mingeot-Leclercq, M.P., Tulkens, P.M. & Van Bambeke, F. Pharmacodynamic evaluation of the intracellular activities of antibiotics against Staphylococcus aureus in a model of THP-1 macrophages. *Antimicrob Agents Chemother* **50**, 841-851 (2006).

27. Lehar, S.M. *et al.* Novel antibody-antibiotic conjugate eliminates intracellular S. aureus. *Nature* **527**, 323-328 (2015).

28. Sandberg, A., Hessler, J.H., Skov, R.L., Blom, J. & Frimodt-Moller, N. Intracellular activity of antibiotics against Staphylococcus aureus in a mouse peritonitis model. *Antimicrob Agents Chemother* **53**, 1874-1883 (2009).

29. Apostolos, A.J., Kelly, J.J., Ongwae, G.M. & Pires, M.M. Structure Activity Relationship of the Stem Peptide in Sortase A Mediated Ligation from Staphylococcus aureus. *Chembiochem* **23**, e202200412 (2022).

30. Apostolos, A.J. *et al.* Facile Synthesis and Metabolic Incorporation of m-DAP Bioisosteres Into Cell Walls of Live Bacteria. *ACS Chem Biol* **15**, 2966-2975 (2020).

31. Apostolos, A.J. *et al.* Metabolic Processing of Selenium-Based Bioisosteres of meso-Diaminopimelic Acid in Live Bacteria. *Biochemistry* **61**, 1404-1414 (2022).

32. Apostolos, A.J., Pidgeon, S.E. & Pires, M.M. Remodeling of Cross-bridges Controls Peptidoglycan Cross-linking Levels in Bacterial Cell Walls. *ACS Chem Biol* **15**, 1261-1267 (2020).

33. Dalesandro, B.E. & Pires, M.M. Induction of Endogenous Antibody Recruitment to the Surface of the Pathogen Enterococcus faecium. *ACS Infect Dis* **7**, 1116-1125 (2021).

34. Ferraro, N.J., Kim, S., Im, W. & Pires, M.M. Systematic Assessment of Accessibility to the Surface of Staphylococcus aureus. *ACS Chem Biol* **16**, 2527-2536 (2021).

35. Fura, J.M., Kearns, D. & Pires, M.M. D-Amino Acid Probes for Penicillin Binding Protein-based Bacterial Surface Labeling. *J Biol Chem* **290**, 30540-30550 (2015).

36. Pidgeon, S.E. *et al.* L,D-Transpeptidase Specific Probe Reveals Spatial Activity of Peptidoglycan Cross-Linking. *ACS Chem Biol* **14**, 2185-2196 (2019).

37. Pidgeon, S.E. & Pires, M.M. Cell Wall Remodeling of Staphylococcus aureus in Live Caenorhabditis elegans. *Bioconjug Chem* **28**, 2310-2315 (2017).

38. Pidgeon, S.E. & Pires, M.M. Cell Wall Remodeling by a Synthetic Analog Reveals Metabolic Adaptation in Vancomycin Resistant Enterococci. *ACS Chem Biol* **12**, 1913-1918 (2017).

39. Pidgeon, S.E. & Pires, M.M. Vancomycin-Dependent Response in Live Drug-Resistant Bacteria by Metabolic Labeling. *Angew Chem Int Ed Engl* **56**, 8839-8843 (2017).

40. Gautam, S. *et al.* An Activity-Based Probe for Studying Crosslinking in Live Bacteria. *Angew Chem Int Ed Engl* **54**, 10492-10496 (2015).

41. Gautam, S., Kim, T. & Spiegel, D.A. Chemical probes reveal an extraseptal mode of cross-linking in Staphylococcus aureus. *J Am Chem Soc* **137**, 7441-7447 (2015).

42. Ngadjeua, F. *et al.* Critical Impact of Peptidoglycan Precursor Amidation on the Activity of l,d-Transpeptidases from Enterococcus faecium and Mycobacterium tuberculosis. *Chemistry* **24**, 5743-5747 (2018).

43. Welsh, M.A. *et al.* Identification of a Functionally Unique Family of Penicillin-Binding Proteins. *J Am Chem Soc* **139**, 17727-17730 (2017).

44. Apostolos, A.J., Chordia, M.D., Kolli, S.H., Rutkowski, M.R. & Pires, M.M. Non-invasive Fluorescence Imaging of Gut Commensal Bacteria in Live Mice. *bioRxiv*, 2022.2005.2005.489569 (2022).

45. Liu, Z. *et al.* Permeation Across the Mycomembrane in Live Mycobacteria. *bioRxiv*, 2022.2010.2012.509737 (2022).

46. Baskin, J.M. *et al.* Copper-free click chemistry for dynamic in vivo imaging. *Proc Natl Acad Sci U S A* **104**, 16793-16797 (2007).

47. Jewett, J.C., Sletten, E.M. & Bertozzi, C.R. Rapid Cu-free click chemistry with readily synthesized biarylazacyclooctynones. *J Am Chem Soc* **132**, 3688-3690 (2010).

48. Agard, N.J., Prescher, J.A. & Bertozzi, C.R. A strain-promoted [3 + 2] azide-alkyne cycloaddition for covalent modification of biomolecules in living systems. *J Am Chem Soc* **126**, 15046-15047 (2004).

49. Caparros, M., Aran, V. & de Pedro, M.A. Incorporation of S-[3H]methyl-D-cysteine into the peptidoglycan of ether-treated cells of Escherichia coli. *FEMS Microbiol Lett* **72**, 139-146 (1992).

50. Kuru, E. *et al.* In Situ probing of newly synthesized peptidoglycan in live bacteria with fluorescent D-amino acids. *Angew Chem Int Ed Engl* **51**, 12519-12523 (2012).

51. Kuru, E., Tekkam, S., Hall, E., Brun, Y.V. & Van Nieuwenhze, M.S. Synthesis of fluorescent D-amino acids and their use for probing peptidoglycan synthesis and bacterial growth in situ. *Nat Protoc* **10**, 33-52 (2015).

52. Lebar, M.D. *et al.* Reconstitution of peptidoglycan cross-linking leads to improved fluorescent probes of cell wall synthesis. *J Am Chem Soc* **136**, 10874-10877 (2014).

53. Lupoli, T.J. *et al.* Transpeptidase-mediated incorporation of D-amino acids into bacterial peptidoglycan. *J Am Chem Soc* **133**, 10748-10751 (2011).

54. Siegrist, M.S., Swarts, B.M., Fox, D.M., Lim, S.A. & Bertozzi, C.R. Illumination of growth, division and secretion by metabolic labeling of the bacterial cell surface. *FEMS Microbiol Rev* **39**, 184-202 (2015).

55. Siegrist, M.S. *et al.* (D)-Amino acid chemical reporters reveal peptidoglycan dynamics of an intracellular pathogen. *ACS Chem Biol* **8**, 500-505 (2013).

56. Fura, J.M., Pidgeon, S.E., Birabaharan, M. & Pires, M.M. Dipeptide-Based Metabolic Labeling of Bacterial Cells for Endogenous Antibody Recruitment. *ACS Infect Dis* **2**, 302-309 (2016).

57. Cava, F., Lam, H., de Pedro, M.A. & Waldor, M.K. Emerging knowledge of regulatory roles of D-amino acids in bacteria. *Cell Mol Life Sci* **68**, 817-831 (2011).

58. de Pedro, M.A., Quintela, J.C., Holtje, J.V. & Schwarz, H. Murein segregation in Escherichia coli. *J Bacteriol* **179**, 2823-2834 (1997).

59. Schouten, J.A. *et al.* Fluorescent reagents for in vitro studies of lipid-linked steps of bacterial peptidoglycan biosynthesis: derivatives of UDPMurNAc-pentapeptide containing d-cysteine at position 4 or 5. *Mol Biosyst* **2**, 484-491 (2006).

60. Baldoni, D., Haschke, M., Rajacic, Z., Zimmerli, W. & Trampuz, A. Linezolid alone or combined with rifampin against methicillin-resistant Staphylococcus aureus in experimental foreign-body infection. *Antimicrob Agents Chemother* **53**, 1142-1148 (2009).

61. Gidari, A. *et al.* Tedizolid-Rifampicin Combination Prevents Rifampicin-Resistance on in vitro Model of Staphylococcus aureus Mature Biofilm. *Front Microbiol* **11**, 2085 (2020).

62. Rayner, C. & Munckhof, W.J. Antibiotics currently used in the treatment of infections caused by Staphylococcus aureus. *Intern Med J* **35 Suppl 2**, S3-16 (2005).

63. Wu, C.Y. & Lee, P.I. Antibiotic-lock therapy and erythromycin for treatment of catheter-related Candida parapsilosis and Staphylococcus aureus infections. *J Antimicrob Chemoth* **60**, 706-707 (2007).

64. Brown, S., Santa Maria, J.P., Jr. & Walker, S. Wall teichoic acids of gram-positive bacteria. *Annu Rev Microbiol* **67**, 313-336 (2013).

65. Gautam, S., Kim, T., Lester, E., Deep, D. & Spiegel, D.A. Wall teichoic acids prevent antibody binding to epitopes within the cell wall of Staphylococcus aureus. *ACS Chem Biol* **11**, 25-30 (2016).

Summary and Future Outlook

Antibiotic resistance has presented a serious burden on healthcare systems worldwide, as the majority of pathogenic bacteria have been identified to exhibit some form of antimicrobial resistance. The Golden Age of Antibiotics gave rise to several classes of antibiotics that are still used today; however, the emergence of resistance to such antibiotics has left us with limited means of eradicating unresponsive infections. As a result, society has come to realize within the past several years that antibiotic treatment as the sole mean to eradicate bacterial infections has been rendered ineffective. Therefore, there is a critical need to develop alternative therapies that can provide therapeutic options to those infected by a multi-drug resistant pathogen.

Chapter 1 details the discovery and development of different classes of antibiotics, their drug targets, the biology of the bacterial cell wall, and the mechanisms of antimicrobial resistance. To develop effective therapeutic modalities, understanding the underlying physical and chemical motifs that encompass the bacteria is essential. Most importantly, it is critical to analyze the chemical entities that comprise the metabolic mechanisms that provide the bacterial cell wall with the essential components to remain structurally and functionally sound. The enzymes involved in cell wall synthesis have been extensively exploited to metabolically incorporate unnatural chemical entities into the bacterial cell wall to investigate enzyme dynamics. More specifically, the utilization of enzymatic probes to uncover enzyme substrate specificity and tolerability can be further utilized to develop effective antimicrobials.

In addition, a potential solution to the problem of antibacterial resistance may lie within harnessing a patient's own immune system to rid the body of an infection. Bacterial immunotherapy or enhancing the immune response against bacterial infections, has been heavily utilized within the past several decades as a means to combat resistant infections. Chapter 2 describes the advances made to date in terms of applying immunotherapeutic techniques to target both Gram-positive and Gram-negative bacterial infections. A benefit to such therapy lies within utilizing pre-existing bacterial clearance mechanisms by the immune system to enhance the antibacterial effects. By installing immune modulators

onto the bacterial cell, components of the immune system will redirect to bacterial cells that may have undergone immune evasion mechanisms and enhance targeted killing of the pathogen. A potential pitfall with bacterial immunotherapy arise in the ability to selectively enhance an immune response towards pathogenic bacteria over commensal bacteria, which can cause dysbiosis of the gut microbiome leading to adverse health events. Although there may not be specificity for particular strains of bacteria, the adverse effects would not be significant compared to that of antibiotic therapy. The work demonstrated in chapters 3 and 4 of this thesis hint at a selectivity of particular immune modulators to preferentially recognize vancomycin-resistant *Enterococci* over vancomycin-sensitive strains. Therefore, preferential direction towards resistant strains may limit off target effects of the therapy. Additionally, it may be the case that bacterial immunotherapy may not completely solve the ever-growing problem of resistance; however, it is believed that a multidisciplinary approach may aim to relieve this healthcare burden. Therefore, a combination therapy of antibiotic treatment and reinforced immune stimulation to the bacterial infection may provide an effective modality to combat high priority infections.

In chapter 3, we describe novel immune-modulators that tag and direct the bacterial pathogen, *Enterococcus faecium,* for phagocytic uptake by macrophages. A synthetic tetrapeptide analog modified with a hapten, 2,4- dinitrophenol (DNP), was crosslinked into the growing peptidoglycan scaffold of live *E. faecium* by transpeptidase enzymes. Hapten presentation on the surface of vancomycin-resistant *E. faecium* enhanced recognition, opsonization, and phagocytic activity of macrophages in culture. In this chapter, we aimed to further improve upon the immunotherapy concepts directed towards bacterial pathogens developed previously in the Pires Lab. Prior work demonstrated the use of hapten modified D-amino acids to label bacterial PG and elicit an immune response for enhanced bacterial cell uptake. Although this work was pivotal to the field, a reoccurring drawback was the necessity of millimolar concentrations of the probe to achieve effective probe labeling, of which is not clinically applicable. The D-amino acid is installed into the PG scaffold by TPs, where the unnatural amino acid is swapped for the

terminal D-alanine residue of the stem peptide. However, the process of PG crosslinking involves a sacrifice of the terminal D-alanine for the formation of crosslinks between neighboring PG strands; therefore, this event will result in hydrolysis of the installed unnatural amino acid. As a result, higher concentrations of the D-amino acid are required for effective labeling. To address this problem, a transition from a single D-amino acid to a synthetic mimic of the PG stem peptide improved substrate specificity for TPs; therefore, promoting higher degrees of labeling at lower, more physiologically relevant concentrations.

A key element of Chapter 3 was the utilization of stem peptide mimics to selectively label the cell wall of bacterial cells with an endogenous hapten. Although this approach demonstrated success *in vitro*, it is imperative to rationalize whether this approach will have applicability for *in vivo* studies. In order for the stem peptide mimics to be effectively incorporated into the bacterial cell wall, the bacterial cells must be actively crosslinking their PG. Due to the difficulty in determining the metabolic state of an existing bacterial infection, it can be challenging to determine whether our therapeutic modality will be successfully crosslinked into the PG scaffold. However, recent work done in the Pires Lab has demonstrated the ability to incorporate synthetic tetrapeptide mimics into the gut microbiome of live mouse models. As a result, targeting a pathogen such as *E. faecium,* that exists as part of the gut microbiome, should successfully metabolically incorporate the hapten modified tetrapeptide in its PG.

In Chapter 4, we describe the utilization of a peptide fragment derived from *Ixodes scapularis* antifreeze glycoprotein (IAFGP) to bind D-alanine within the bacterial PG. Installation of an exogenous hapten to the peptide fragment enabled antigen specific recruitment of antibodies to the surface of two drug resistant *Enterococci* species. Further, antibody opsonization enhanced pathogen uptake into immune cells. A key feature of this design is the use of an exogenous hapten for antibody binding. For bacterial immunotherapy, traditional haptens include 2,4-dinitrophenol, L-rhamnose, and α-

galactose. All of which are considered endogenous haptens as 1-2% of the natural human antibody pool contain such antibodies. Here, we capitalized on the ability of the exogenous hapten peptide fragment to form an *ex vivo* complex with the antibody prior to bacterial cell incubation; therefore, increasing the clinical applicability of the therapeutic modality, particularly in terms of extending the half-life of the peptide. A potential pitfall with peptide therapeutics lies within the ability of proteases to degrade the peptide drug. A solution to increase the stability of the peptide would be to use mirror image retro-inverso, where the peptide is sequenced in reverse; however, utilizing D-amino acids, rather than canonical L-amino acids, to reduce proteolytic degradation. Although this approach may work in theory, the peptide must first be re-examined in terms of bacterial cell binding and antibody recruitment prior to use *in vivo*.

In addition to traditional resistance mechanisms, *S. aureus* has evolved to escape both antibiotic and immune cell pressure by surviving within the contents of host cells. Chapter 5 details the novel application of our lab's recently developed Peptidoglycan Accessibility Click-Mediated Assessment (PAC-MAN) to the context of intracellular pathogens. PAC-MAN was utilized to compare the permeability of antibiotics to the PG of *S. aureus* with and without the context of intracellular survival. It was demonstrated that we can embed reactive DBCO moieties within the surface of intracellular *S. aureus* PG to react *via* SPAAC with azide modified antibiotics to assess antibiotic permeation to an intracellular target. We showed that only ciprofloxacin demonstrated poor permeability when comparing between extra- and intracellular *S. aureus* presumably due to the net negative charge associated with the carboxylic acid on ciprofloxacin. We anticipate that this technique can be used to develop a more effective antibiotic treatment for intracellular *S. aureus* tailored around improving antibiotic efficacy through improved permeability.

As this application was demonstrated with a small panel of antibiotics, we aim to further develop this assay to include a broader range of antibiotics and continue investigating the effects of masking detrimental permeability factors to improve antibiotic uptake, as was demonstrated by masking the negative charge of ciprofloxacin with a methyl ester. Additionally, this technique may be beneficial to solicit chemical motifs that may aid in or

hinder mammalian cell permeability to treat intracellular infections. For instance, our lab has access to a library of azide modified small molecules; therefore, identifying chemical entities that exhibit high permeability may guide antibiotic design. Further, the application of PAC-MAN can be applied to analyze the permeability of antibiotics against other Gram-positive intracellular pathogens, such as *Listeria monocytogenes*.

The intracellular environment of immune cells undergoes drastic changes in response to uptake of a pathogen. For instance, macrophages will initiate the generation of reactive oxygen and nitrogen species, and acidification of the phagosome. As a result, the physiology of the bacterial cell surface may adapt in response to such attacks. As PAC-MAN does not address changes to the bacterial cell surface in response to the intracellular environment, a technique that aims at addressing this phenomenon could be the utilization of beads in place of the pathogen. For instance, polystyrene beads can be modified with a reactive DBCO motif and engulfed into macrophages. Upon uptake, treatment with the azAbx library will enable a further evaluation of the changes made to the bacterial cell surface in response to the host cell environment.

Overall, the novel work done in this thesis (Chapters 3 and 4) contributes to advancing the field of bacterial immunotherapy by developing new techniques to increase an immune response against drug resistant pathogens. Finally, Chapter 5 serves to assess antibiotic permeability to intracellular pathogens; therefore, providing a basis for the development of more effective moieties to target pathogens that proliferate within host cell compartments. It is anticipated that the work demonstrated in this thesis can aid in the further development of both immunotherapeutic techniques and antibiotics to treat drug resistant pathogens.

Appendix

*Note: All chromatograms for HPLC analysis were observed at 220 nm.

A.3 *Synthesis and Characterization of Compounds in Chapter 3*

Scheme S1. Synthesis of D-Lys-DNP
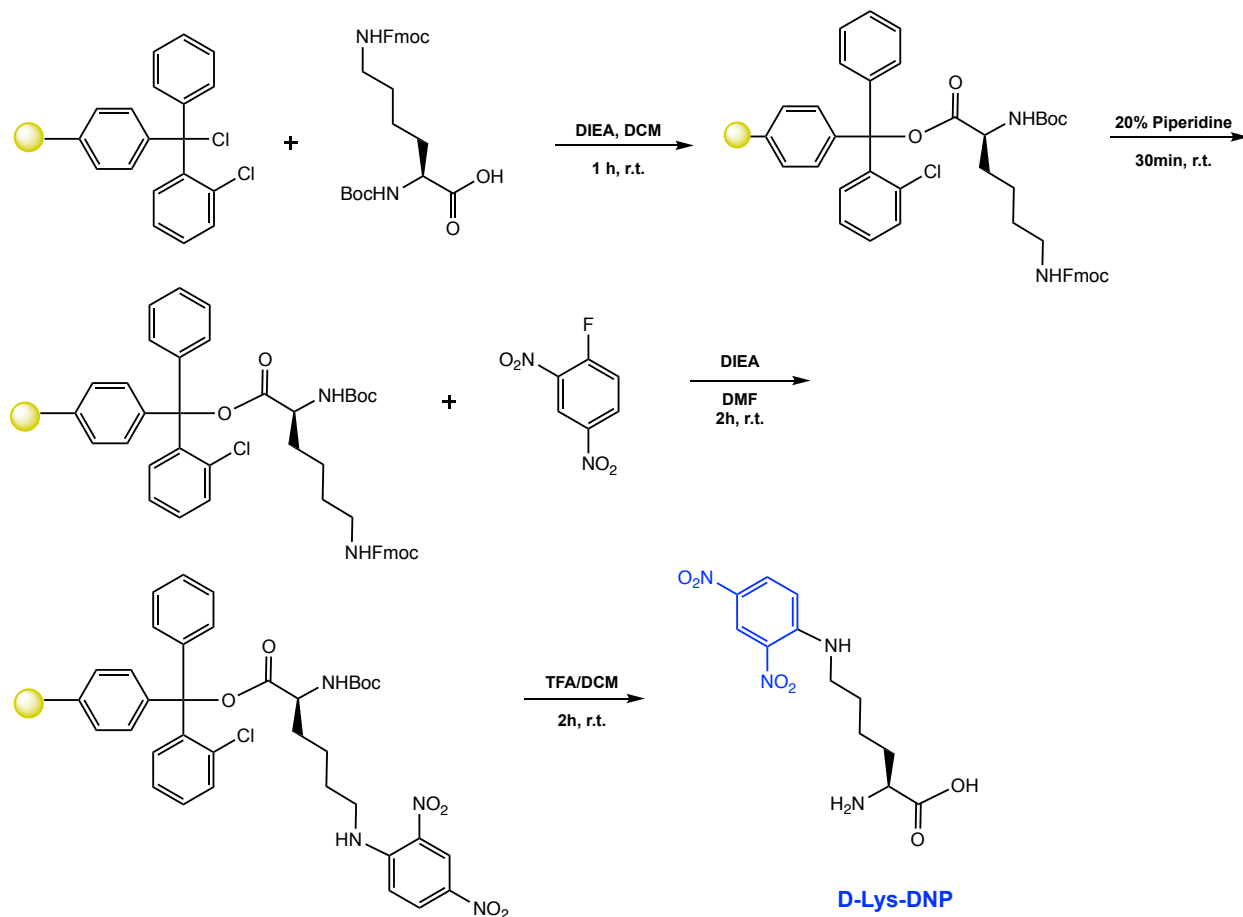
A 25 mL synthetic vessel charged with 500 mg (0.55 mmol) of 2-Chlorotrityl chloride resin was added Boc-D-Lysine(Fmoc)-OH (1.1 eq, 283 mg, 0.605 mmol) and N,N-diisopropylethylamine (DIEA) (4.4 eq, 420 uL, 2.42 mmol) in dry dichloromethane (DCM) (15 mL). The resin was agitated for 1 hour at ambient temperature and washed with methanol (MeOH) and DCM (3 x 15 mL each). The Fmoc protecting group was removed

with a 20% piperidine in N,N-dimethylformamide (DMF) solution (15 mL) for 30 minutes at ambient temperature, then washed as previously stated. 2,4-dinitrofluorobenzene (3 eq, 207 uL, 1.65 mmol) and DIEA (6 eq, 574 uL, 3.3 mmol) in DMF (15 mL) was agitated with the resin for 2 hours protected from light. The resin was then washed as previous stated. To remove the peptide from resin, a trifluoroacetic acid (TFA) cocktail solution (95 % TFA, 2.5% TIPS, and 2.5 % DCM) was added to the resin with agitation for 2 hours protected from light. The resin was filtered and resulting solution was concentrated *in vacuo*. The peptide was trituated with cold diethyl ether and purified using reverse phase high performance liquid chromatography (HPLC) using H_2O/MeOH to yield **D-Lys(DNP)**. The sample was analyzed for purity using a Waters 1525 Binary HPLC Pump using a Phenomenex Luna 5u C8(2) 100A (250 x 4.60 mm) column; gradient elution with H_2O/CH_3CN. Molecular weight was confirmed using a Shimadzu MALDI-TOF Mass Spectrometer (MALDI-8020).
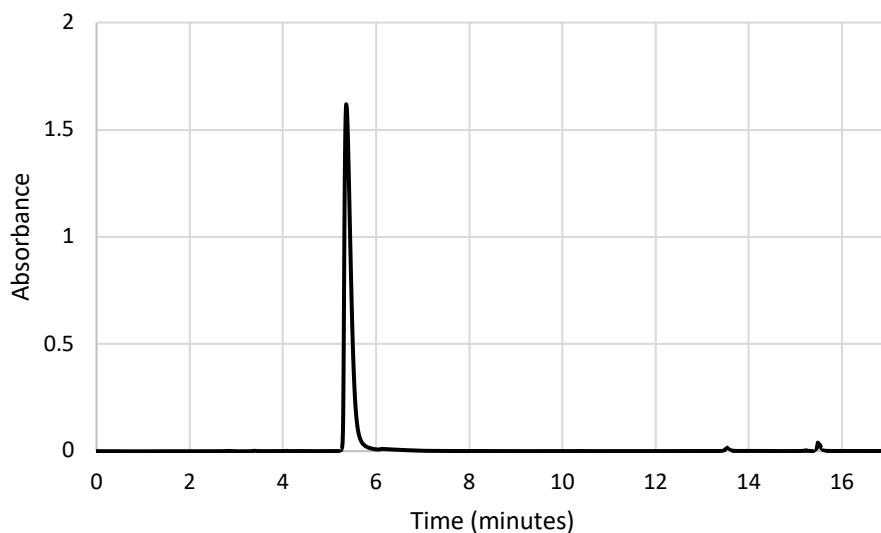
ESI-MS calculated: 313.1148, found: 313.1143

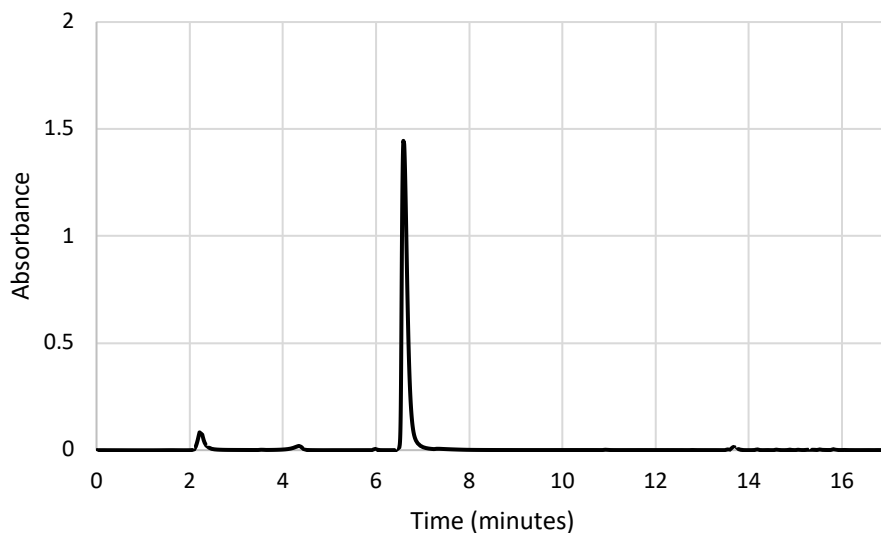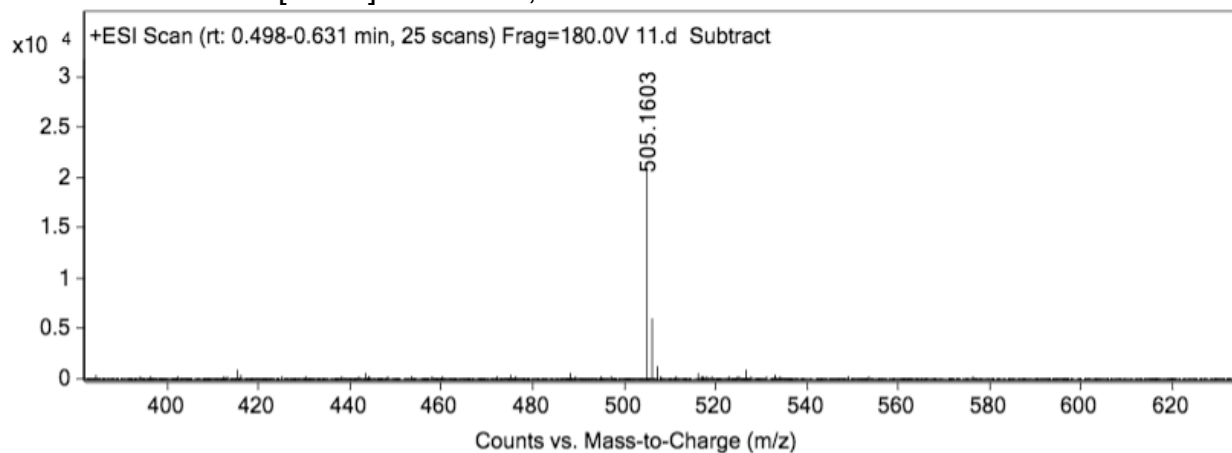+ESI Scan (rt: 0.926-0.987 min, 12 scans) Frag=180.0V 1.d Subtract
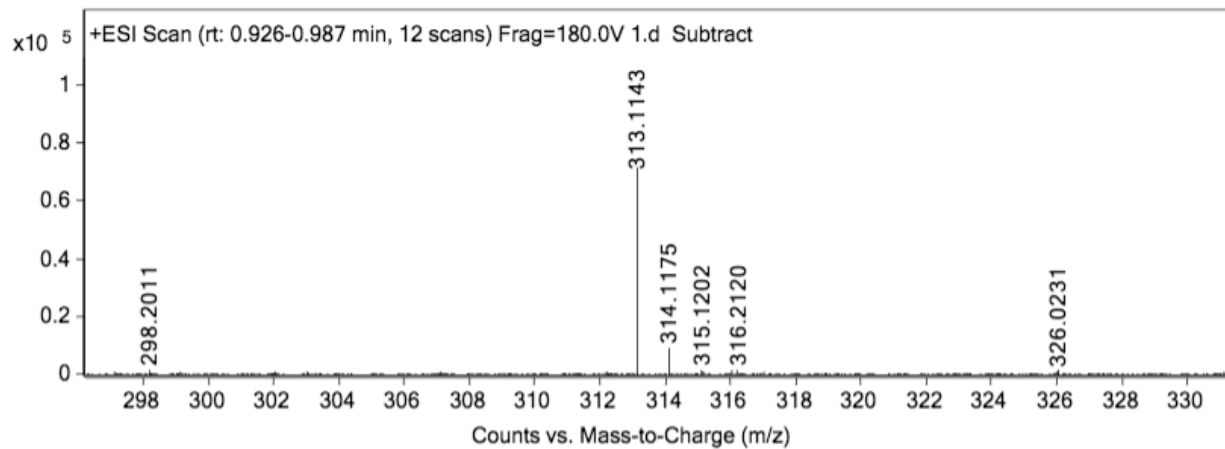
Scheme S2. Synthesis of DNP-Tetra
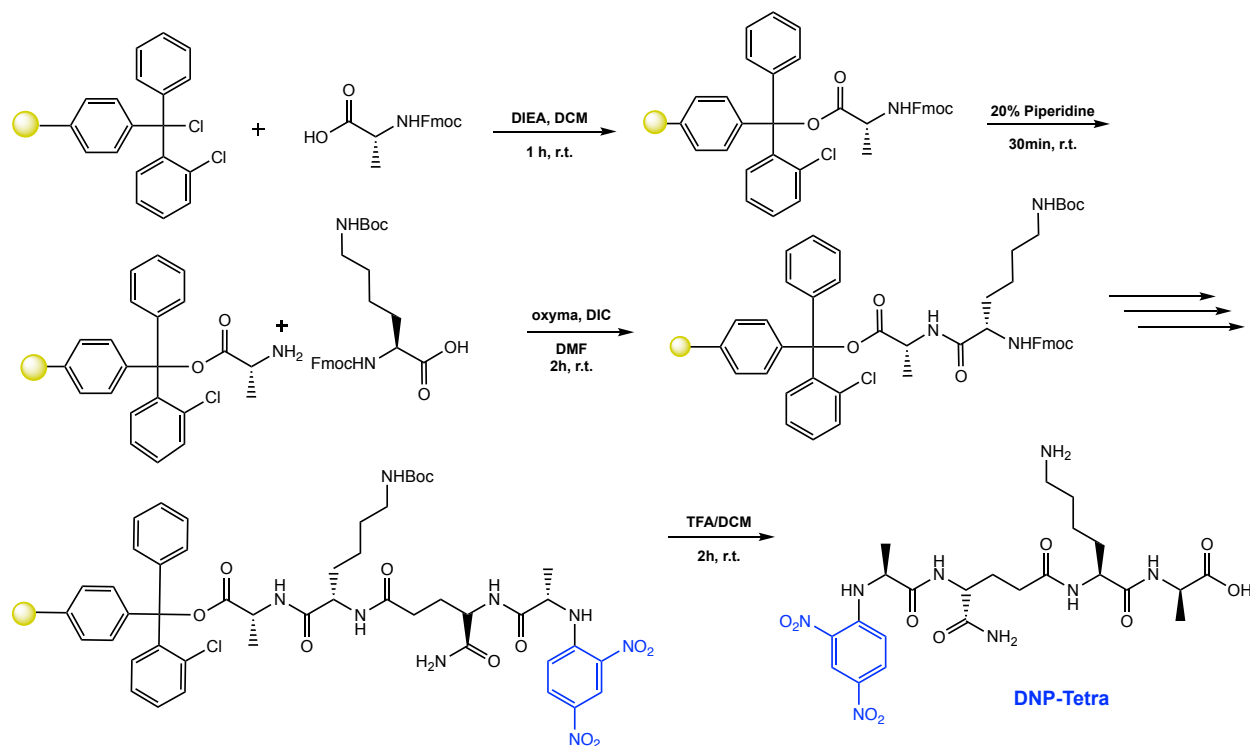
A 25 mL synthetic vessel charged with 500 mg (0.55 mmol) of 2-Chlorotrityl chloride resin was added Fmoc-D-alanine (1.1 eq, 188 mg, 0.605 mmol) and DIEA (4.4 eq, 420 uL, 2.42 mmol) in dry DCM (15 mL). The resin was agitated for 1 hour at ambient temperature and washed with MeOH and DCM (3 x 15 mL each). The Fmoc protecting group was removed with a 20% piperidine in DMF solution (15 mL) for 30 minutes at ambient temperature, then washed as previously stated. Fmoc-L-Lys(Boc)-OH (3 eq, 257 mg, 1.65 mmol), Oxyma (3 eq, 243 mg, 1.65 mmol), and N,N-diisopropylcarbodiimide (DIC) (3 eq, 257 uL, 1.65 mmol) in DMF (15 mL) were added to the reaction flask and agitated for 2 hours at ambient temperature. The Fmoc removal and coupling procedure was repeated as before using the same equivalencies with Fmoc-D-glutamic acid α-amide and Fmoc-L-alanine. The Fmoc group of L-alanine was removed and resin was coupled with 2,4-dinitrofluorobenzene (3 eq, 207 uL, 1.65 mmol) and DIEA (6 eq, 574 uL, 3.3 mmol) in DMF (15 mL) by agitating for 2 hours protected from light. The resin was then washed as previously stated. To remove the peptide from resin, a TFA cocktail solution (95 % TFA,

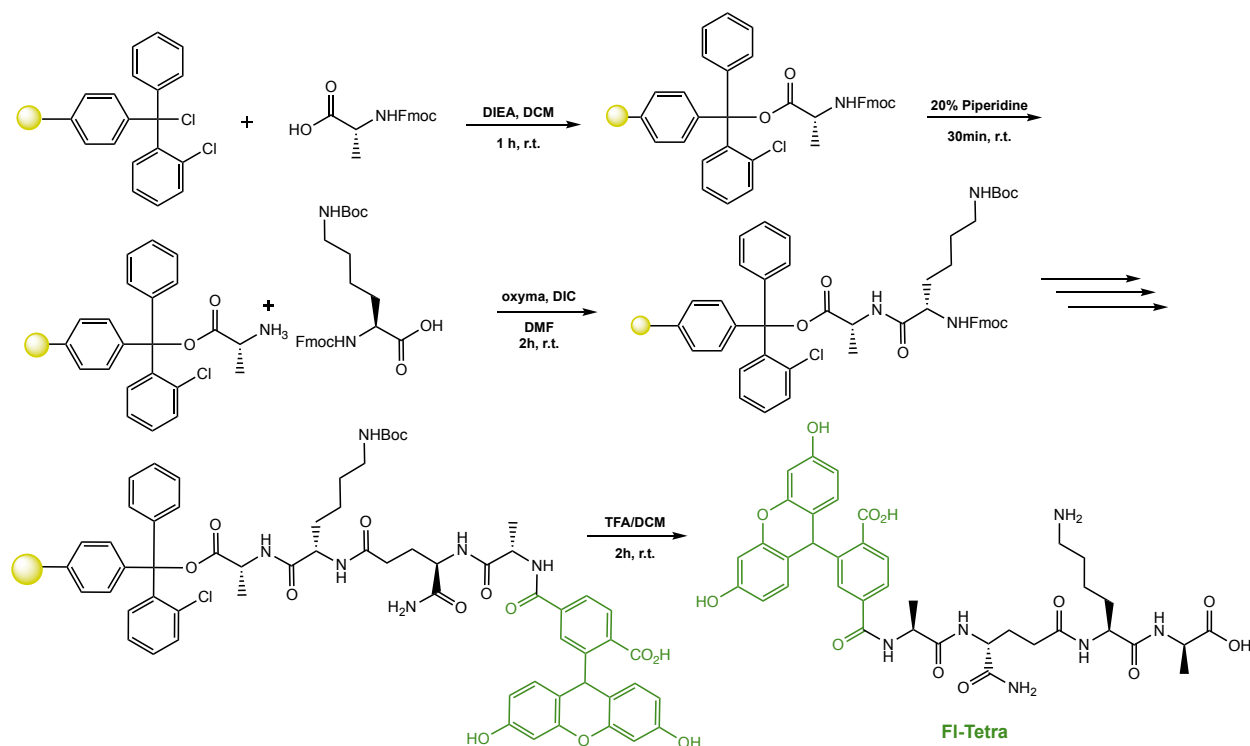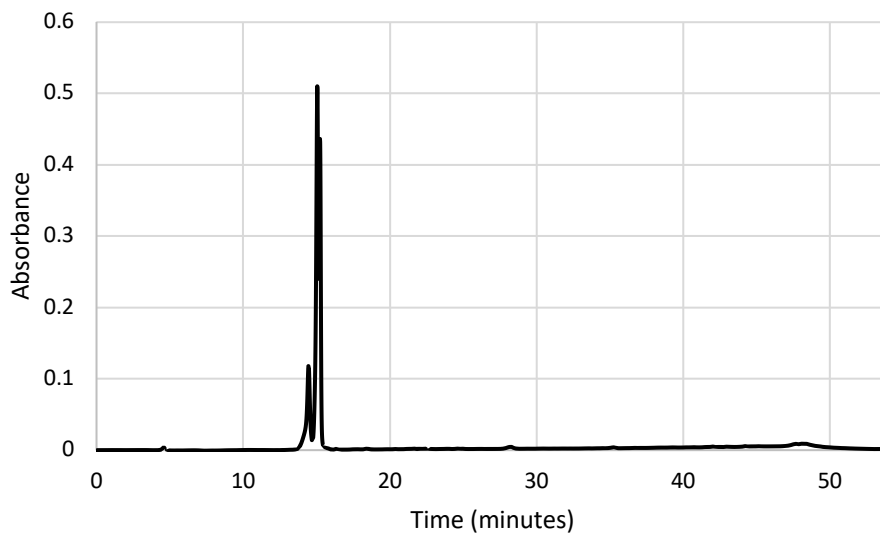2.5% TIPS, and 2.5 % DCM) was added to the resin with agitation for 2 hours protected from light. The resin was filtered and resulting solution was concentrated *in vacuo*. The peptide was trituated with cold diethyl ether and purified using reverse phase HPLC using H_2O/MeOH to yield **DNP-Tetra**. The sample was analyzed for purity using a Waters 1525 Binary HPLC Pump using a Phenomenex Luna 5u C8(2) 100A (250 x 4.60 mm) column; gradient elution with H_2O/CH_3CN.
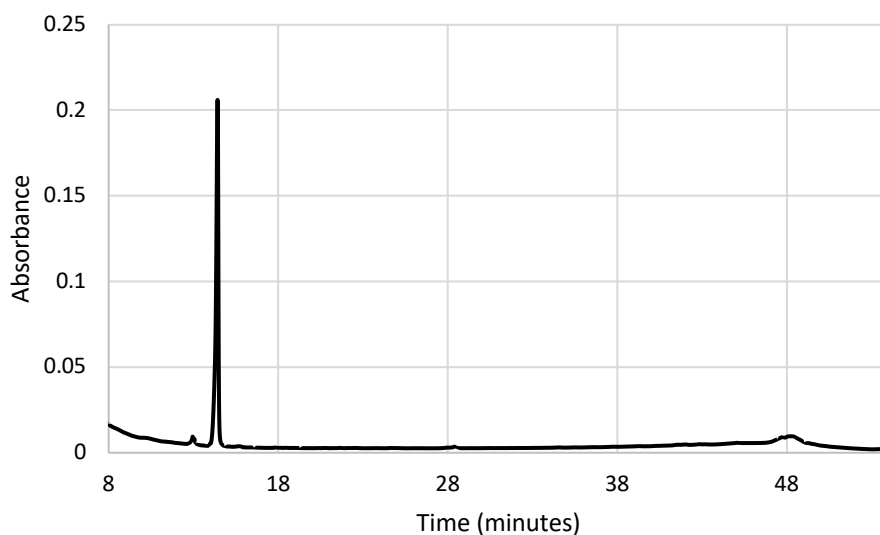
ESI-MS calculated [M+H$^+$]: 583.2476, found: 583.2469
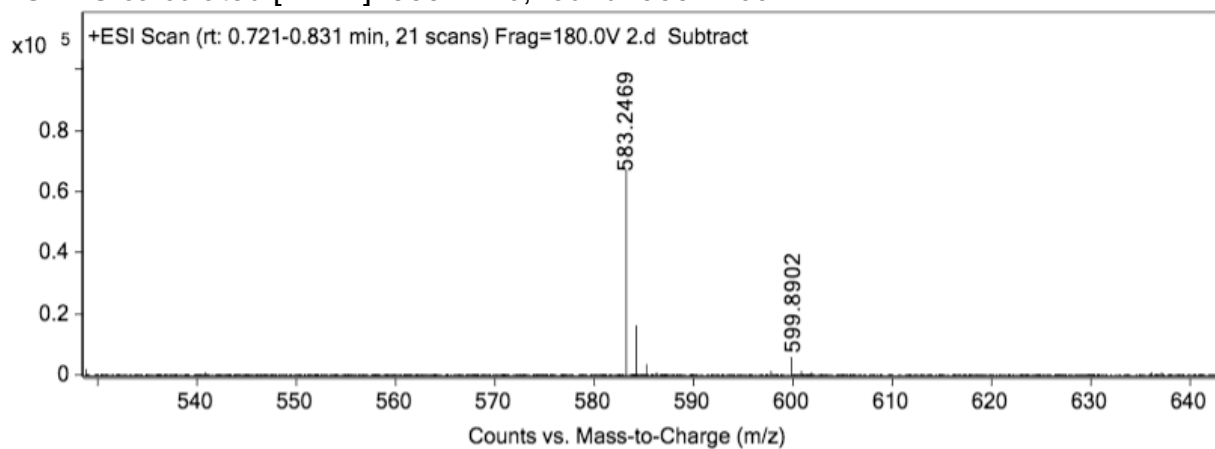
Scheme S3. Synthesis of K(DNP)-Tetra

A 25 mL synthetic vessel was charged with 500 mg (0.35 mmol) of Fmoc-D-Alanine-Wang resin. The Fmoc group was removed using a 20% piperidine in DMF solution (15 mL). The flask was agitated for 30 minutes and the piperidine solution was drained. The resin was washed with DCM and MeOH (3 x 15 mL). Fmoc-L-Lysine(Boc)-OH (3 eq, 491 mg, 1.05 mmol), Oxyma (3 eq, 149 mg, 1.05 mmol), and DIC (3 eq, 164 uL, 1.05 mmol) in DMF (15 mL) were added to the reaction flask and agitated for 2 hours at ambient temperature. The Fmoc removal and coupling procedure was repeated as before using the same equivalencies with Fmoc-D-Glutamic acid α-amide, and Fmoc-L-Alanine. The Fmoc group of L-alanine was removed and resin coupled with Fmoc-L-Lysine(Mtt)-OH (3 eq, 655 mg, 1.05 mmol). The N-terminus of the peptide was acetylated by removing the Fmoc group and then agitating the resin for 1 hour with a solution of 5% acetic anhydride (0.5 mL), 8.5% DIEA (0.85 mL), and 86.5% DMF (8.65 mL). The Mtt protecting group of L-Lysine(Mtt)-OH was removed by adding 10 mL of a TFA cocktail solution (1% TFA, 2% TIPS in DCM) to the resin and agitating for 10 minutes protected from light. The solution was drained, and this procedure was repeated five additional times. The solution was then drained, rinsed with DMF, and washed as previously described. Upon Mtt removal,

2,4-dinitrofluorobenzene (3 eq, 131 uL, 1.05 mmol) and DIEA (6 eq, 365 uL, 1.05 mmol) in DMF (15 mL) was agitated with the resin for 2 hours protected from light. The resin was then washed as previous stated. To remove the peptide from resin, a TFA cocktail solution (95 % TFA, 2.5% TIPS, and 2.5 % DCM) was added to the resin with agitation for 2 hours protected from light. The resin was filtered and resulting solution was concentrated *in vacuo*. The peptide was trituated with cold diethyl ether and purified using reverse phase HPLC using H_2O/MeOH to yield **K(DNP)-Tetra**. The sample was analyzed for purity using a Waters 1525 Binary HPLC Pump using a Phenomenex Luna 5u C8(2) 100A (250 x 4.60 mm) column; gradient elution with H_2O/CH_3CN.
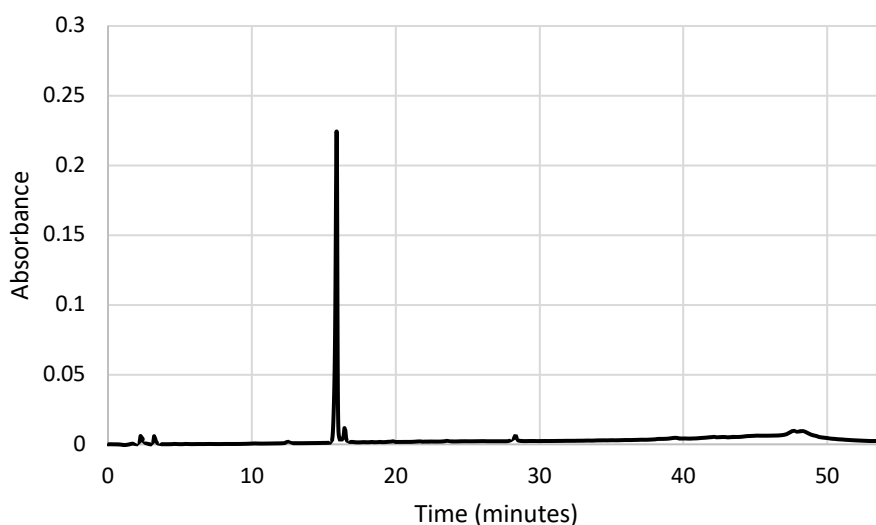
ESI-MS calculated [M+H⁺]: 753.3531, found: 753.3523
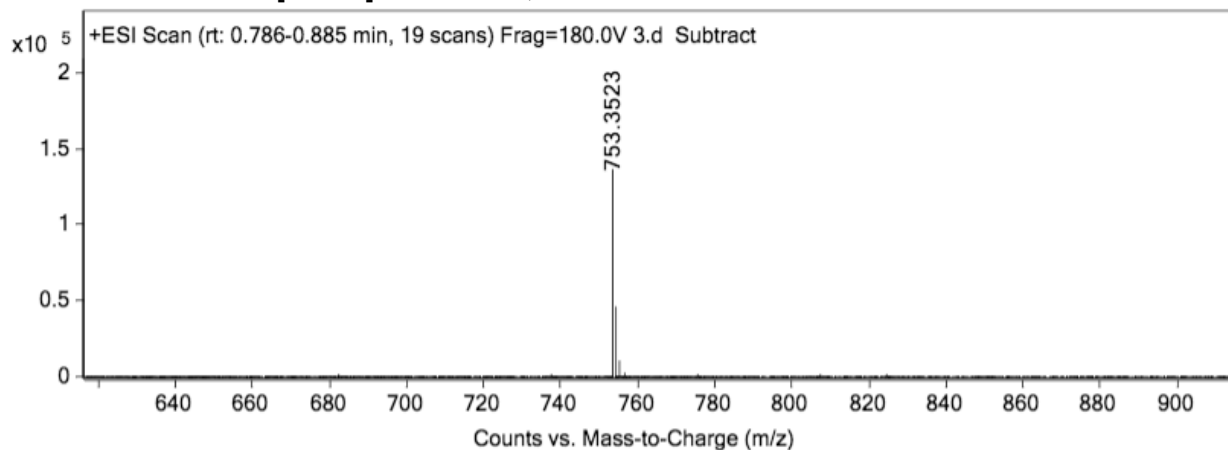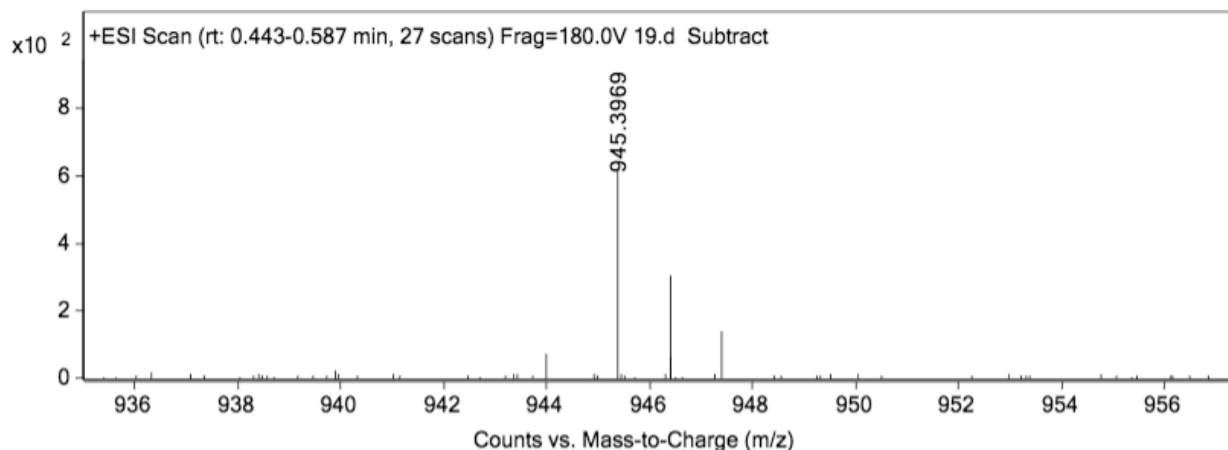
Scheme S4. Synthesis of K(DNP)-Tri

A 25 mL synthetic vessel was charged with 500 mg (0.35 mmol) of Fmoc-D-Alanine-Wang resin. The Fmoc group was removed using a 20% piperidine in DMF solution (15 mL). The flask was agitated for 30 minutes and the piperidine solution was drained. The resin was washed with DCM and MeOH (3 x 15 mL). Fmoc-L-Lysine(Boc)-OH (3 eq, 491 mg, 1.05 mmol), Oxyma (3 eq, 149 mg, 1.05 mmol), and DIC (3 eq, 164 uL, 1.05 mmol) in DMF (15 mL) were added to the reaction flask and agitated for 2 hours at ambient temperature. The Fmoc removal and coupling procedure was repeated as before using the same equivalencies with Fmoc-D-Glutamic acid α-amide and Fmoc-L-Lysine(Mtt)-OH (3 eq, 655 mg, 1.05 mmol). The N-terminus of the peptide was acetylated by removing the Fmoc group and then agitating the resin for 1 hour with a solution of 5% acetic anhydride (0.5 mL), 8.5% DIEA (0.85 mL), and 86.5% DMF (8.65 mL). The Mtt group of L-Lysine(Mtt) was removed by adding 10 mL of a TFA cocktail solution (1% TFA, 2% TIPS in DCM) to the resin and agitating for 10 minutes protected from light. The solution was drained, and this procedure wa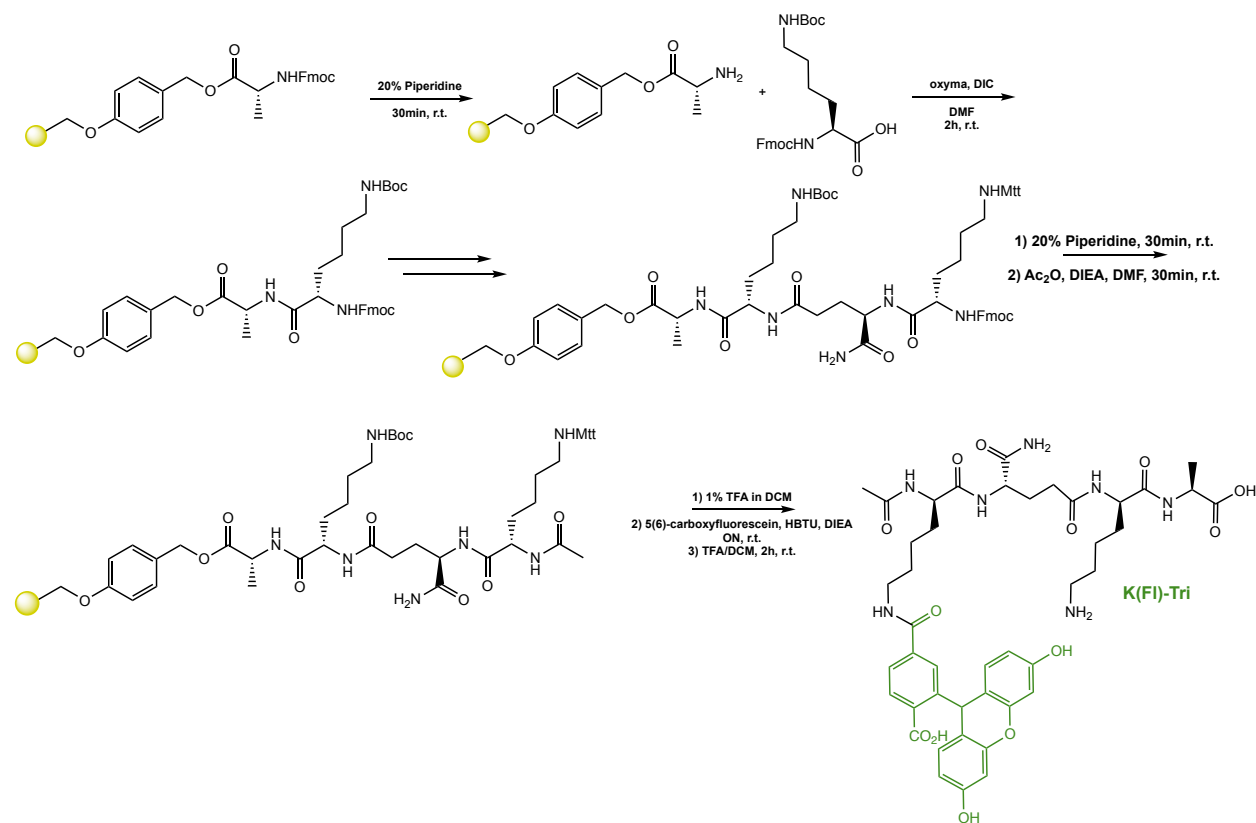s repeated five additional times. The solution was then drained and washed as previously described. Upon Mtt removal, 2,4-dinitrofluorobenzene (3 eq, 131 uL, 1.05 mmol) and DIEA (6 eq, 365 uL, 1.05 mmol) in DMF (15 mL) was agitated with the resin for 2 hours protected from light. The resin was then washed as previous stated. To remove the peptide from resin, a TFA cocktail solution

(95 % TFA, 2.5% TIPS, and 2.5 % DCM) was added to the resin with agitation for 2 hours protected from light. The resin was filtered and resulting solution was concentrated *in vacuo*. The peptide was trituated with cold diethyl ether and purified using reverse phase HPLC using H_2O/MeOH to yield **K(DNP)-Tri**. The sample was analyzed for purity using a Waters 1525 Binary HPLC Pump using a Phenomenex Luna 5u C8(2) 100A (250 x 4.60 mm) column; gradient elution with H_2O/CH_3CN.
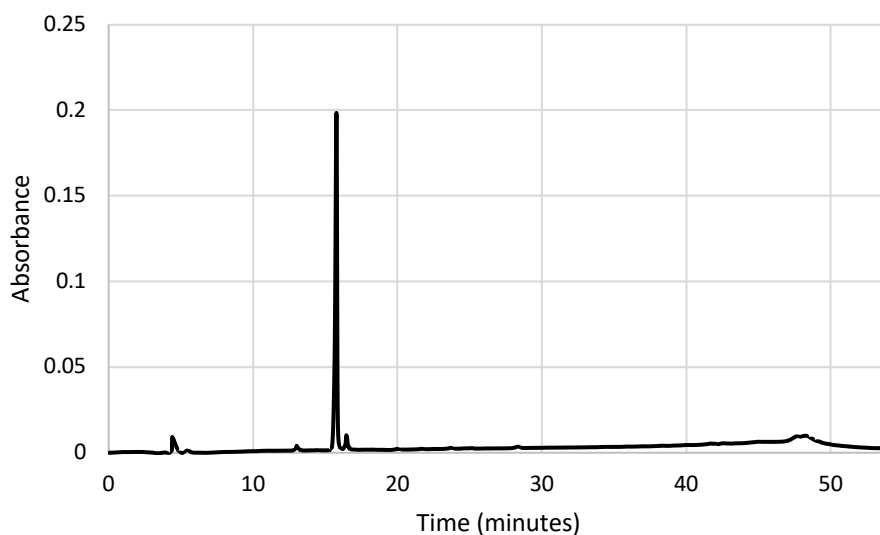

ESI-MS calculated [M+H$^+$]: 682.3160, found: 682.3150
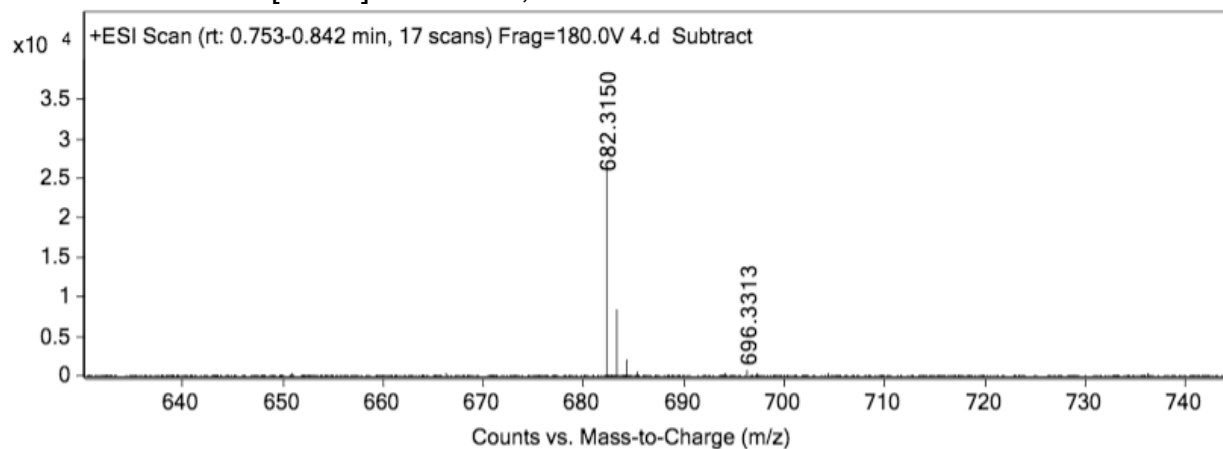
Scheme S5. Synthesis of D-Lys-FITC
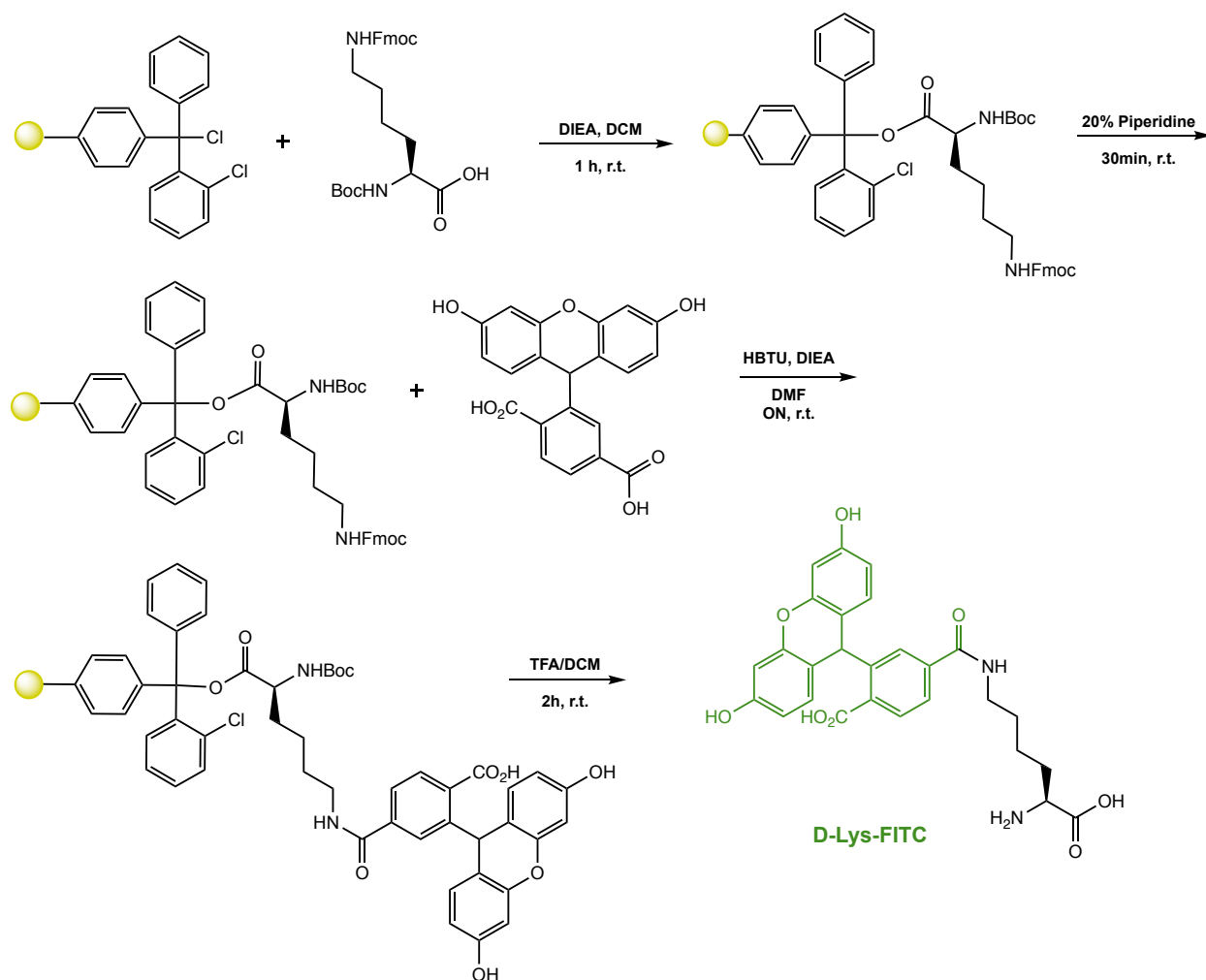
A 25 mL synthetic vessel charged with 500 mg (0.55 mmol) of 2-Chlorotrityl chloride resin was added Boc-D-Lysine(Fmoc)-OH (1.1 eq, 283 mg, 0.605 mmol) and DIEA (4.4 eq, 420 uL, 2.42 mmol) in dry DCM (15 mL). The resin was agitated for 1 hour at ambient temperature and washed with MeOH and DCM (3 x 15 mL each). The Fmoc protecting group was removed with a 20% piperidine in DMF solution (15 mL) for 30 minutes at ambient temperature, then washed as previously stated. The resin was coupled with 5,6-carboxyfluorescein (2 eq, 413 mg, 1.1 mmol), HBTU (2 eq, 416 mg, 1.1 mmol), and DIEA (6 eq, 574 uL, 3.3 mmol) in DMF (15 mL) shaking over-night. The resin was washed as previously described. To remove the peptide from resin, a TFA cocktail solution (95 % TFA, 2.5% TIPS, and 2.5 % DCM) was added to the resin with agitation for 2 hours

protected from light. The resin was filtered and resulting solution was concentrated *in vacuo*. The peptide was trituated with cold diethyl ether and purified using reverse phase HPLC using H_2O/MeOH to yield **D-Lys(Fl)**.

ESI-MS calculated [M+H$^+$]: 505.1611, found: 505.1603

Scheme S6. Synthesis of Fl-Tetra

Fl-Tetra

A 25 mL synthetic vessel charged with 500 mg (0.55 mmol) of 2-Chlorotrityl chloride resin was added Fmoc-D-Alanine (1.1 eq, 188 mg, 0.605 mmol) and DIEA (4.4 eq, 420 uL, 2.42 mmol) in dry DCM (15 mL). The resin was agitated for 1 hour at ambient temperature and washed with MeOH and DCM (3 x 15 mL each). The Fmoc protecting group was removed with a 20% piperidine in DMF solution (15 mL) for 30 minutes at ambient temperature, then washed as previously stated. Fmoc-L-Lysine(Boc)-OH (3 eq, 257 mg, 1.65 mmol), Oxyma (3 eq, 243 mg, 1.65 mmol), and DIC (3 eq, 257 uL, 1.65 mmol) in DMF (15 mL) were added to the reaction flask and agitated for 2 hours at ambient temperature. The Fmoc removal and coupling procedure was repeated as before using the same equivalencies with Fmoc-D-Glutamic acid α-amide and Fmoc-L-Alanine-OH. The Fmoc group of L-alanine was deprotected and resin coupled with 5,6-carboxyfluorescein (2 eq, 413 mg, 1.1 mmol), HBTU (2 eq, 416 mg, 1.1 mmol), and DIEA (6 eq, 574 uL, 3.3 mmol) in DMF (15 mL) shaking over-night. The resin was washed as previously described. To remove the peptide from resin, a TFA cocktail solution (95 % TFA, 2.5% TIPS, and 2.5 % DCM) was added to the resin with agitation for 2 hours

protected from light. The resin was filtered and resulting solution was concentrated *in vacuo*. The peptide was trituated with cold diethyl ether and purified using reverse phase HPLC using H_2O/MeOH to yield **Fl-Tetra**. The sample was analyzed for purity using a Waters 1525 Binary HPLC Pump using a Phenomenex Luna 5u C8(2) 100A (250 x 4.60 mm) column; gradient elution with H_2O/CH_3CN.
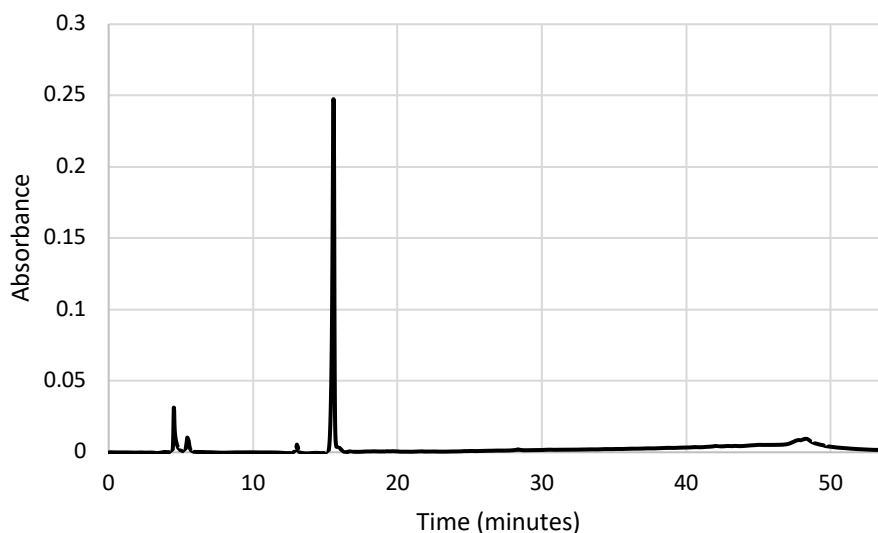

ESI-MS calculated [M+H⁺]: 775.2940, found: 775.2931
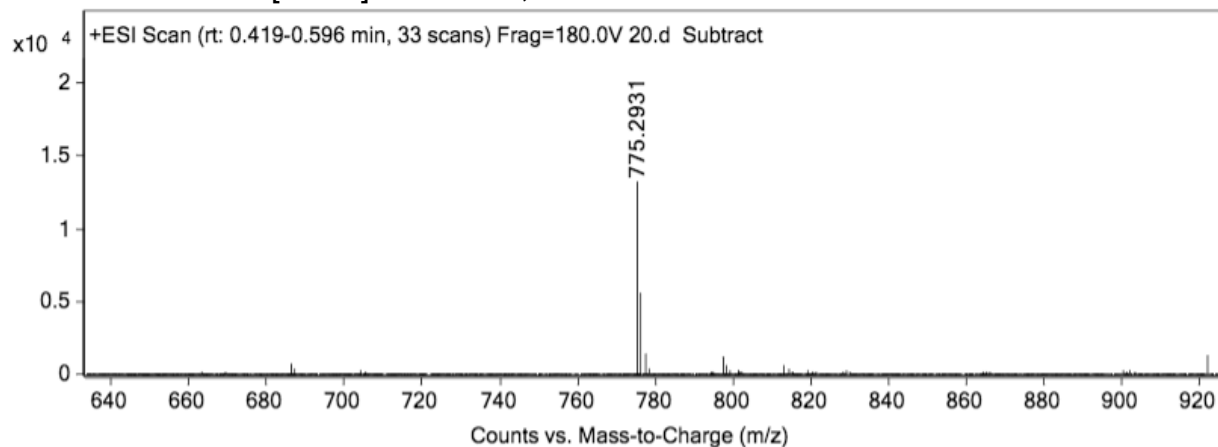
Scheme S7. Synthesis of K(Fl)-Tetra
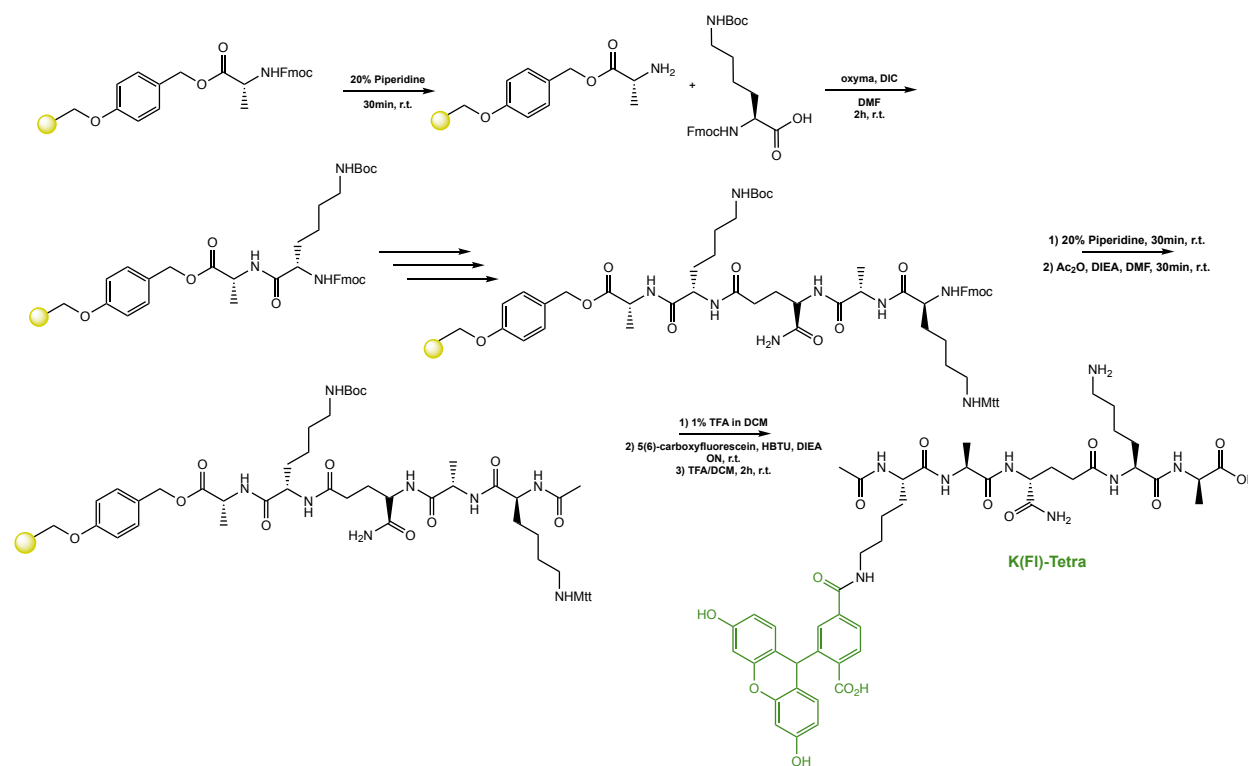
A 25 mL synthetic vessel was charged with 500 mg (0.35 mmol) of Fmoc-D-Alanine-Wang resin. The Fmoc group was removed in a 20% piperidine in DMF solution (15 mL). The flask was agitated for 30 minutes and the piperidine solution was drained. The resin was washed with DCM and MeOH (3 x 15 mL). Fmoc-L-Lys(Boc)-OH (3 eq, 491 mg, 1.05 mmol), Oxyma (3 eq, 149 mg, 1.05 mmol), and DIC (3 eq, 164 uL, 1.05 mmol) in DMF (15 mL) were added to the reaction flask and agitated for 2 hours at ambient temperature. The Fmoc removal and coupling procedure was repeated as before using the same equivalencies with Fmoc-D-Glutamic acid α-amide, and Fmoc-L-Alanine-OH. The Fmoc group o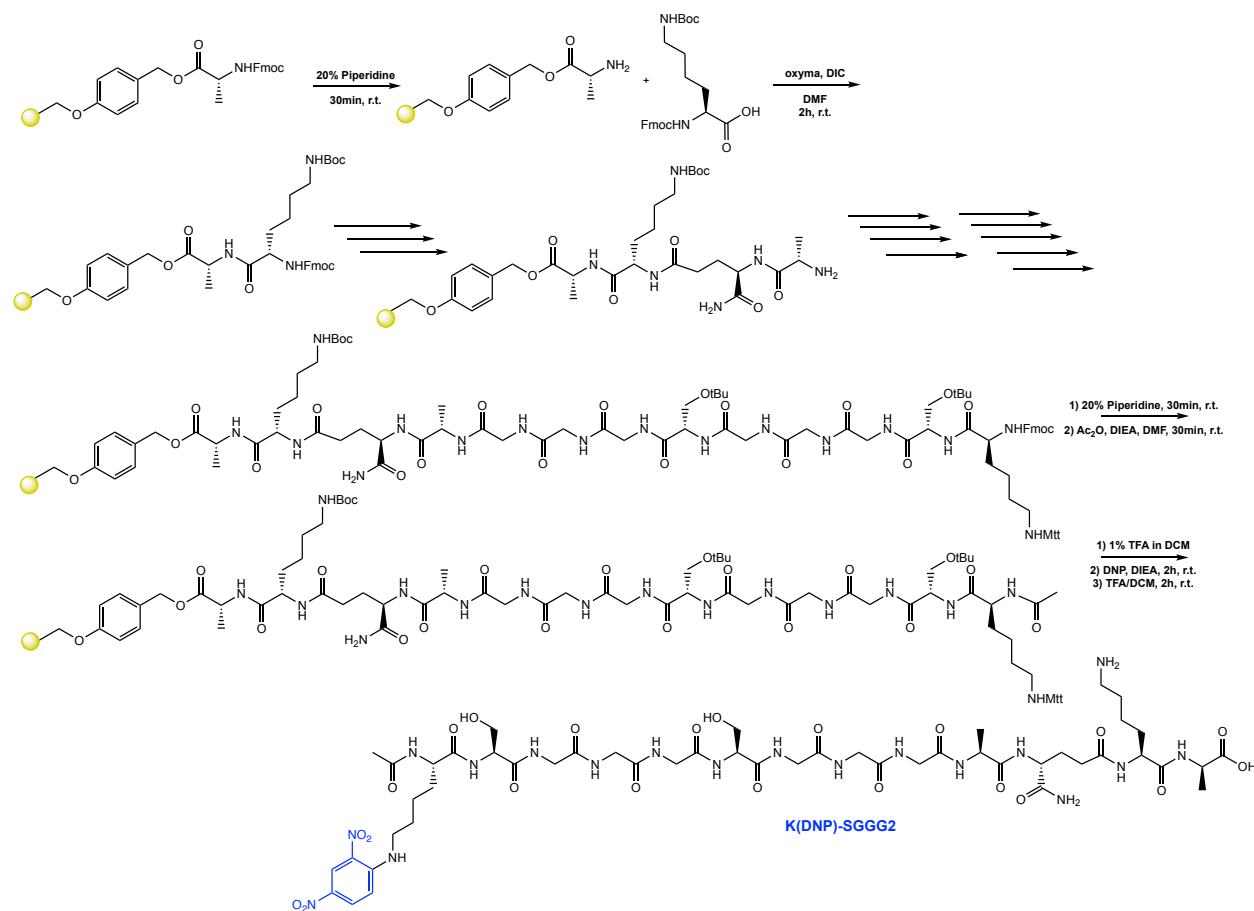f L-Alanine was removed and resin coupled with Fmoc-L-Lysine(Mtt)-OH (3 eq, 655 mg, 1.05 mmol). The N-terminus of the peptide was acetylated by removing the Fmoc group and then agitating the resin for 1 hour with a solution of 5% acetic anhydride (0.5 mL), 8.5% DIEA (0.85 mL), and 86.5% DMF (8.65 mL). The Mtt group of the L-Lysine(Mtt)-OH was removed by adding 10 mL of a TFA cocktail solution (1% TFA, 2% TIPS in DCM) to the resin and agitating for 10 minutes protected from light. The solution was drained, and this procedure was repeated five additional times. The solution was

then drained, rinsed with DMF, and washed as previously described. Upon Mtt removal, the resin was coupled with 5,6-carboxyfluorescein (2 eq, 263 mg, 0.7 mmol), HBTU (2 eq, 265 mg, 0.7 mmol), and DIEA (4 eq, 243 uL, 1.4 mmol) in DMF (15 mL) shaking over-night. The resin was washed as previously described. To remove the peptide from resin, a TFA cocktail solution (95 % TFA, 2.5% TIPS, and 2.5 % DCM) was added to the resin with agitation for 2 hours protected from light. The resin was filtered and resulting solution was concentrated *in vacuo*. The peptide was trituated with cold diethyl ether and purified using reverse phase HPLC using H_2O/MeOH to yield **K(Fl)-Tetra**. The sample was analyzed for purity using a Waters 1525 Binary HPLC Pump using a Phenomenex Luna 5u C8(2) 100A (250 x 4.60 mm) column; gradient elution with H_2O/CH_3CN.
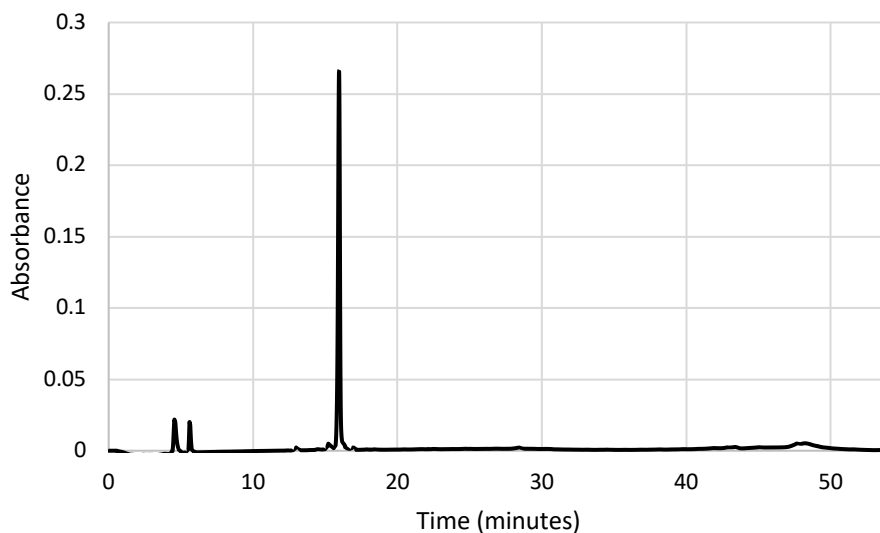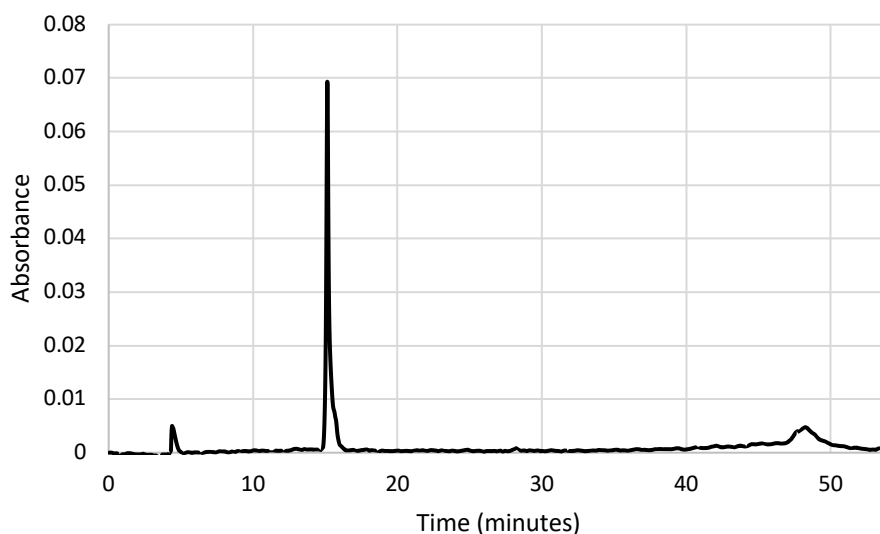

ESI-MS calculated [M+H$^+$]: 945.3994, found: 945.3969

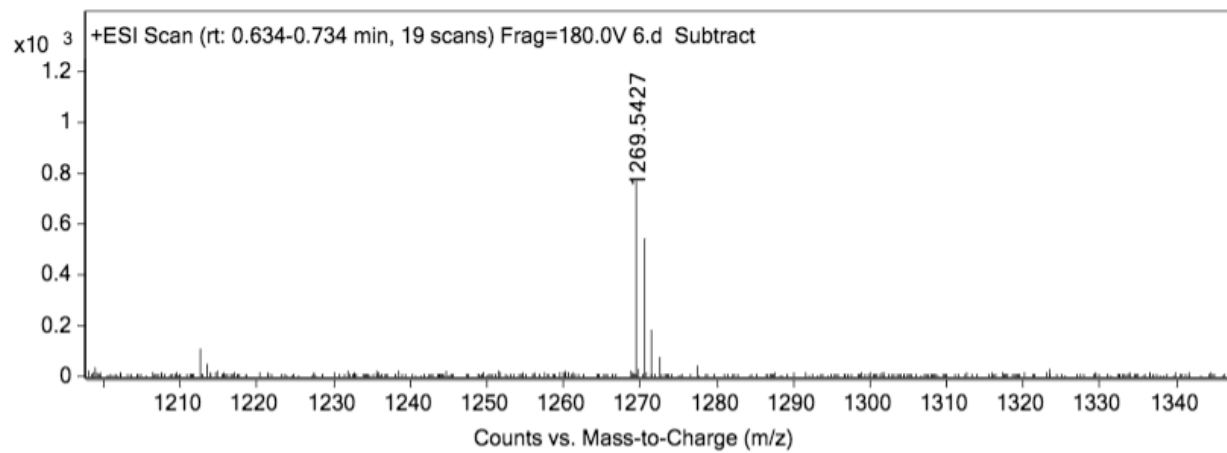**Scheme S8.** Synthesis of K(FI)-Tri

A 25 mL synthetic vessel was charged with 500 mg (0.35 mmol) of Fmoc-D-Alanine-Wang resin. The Fmoc group was removed in a 20% piperidine in DMF solution (15 mL). The flask was agitated for 30 minutes and the piperidine solution was drained. The resin was washed with DCM and MeOH (3 x 15 mL). Fmoc-L-Lysine(Boc)-OH (3 eq, 491 mg, 1.05 mmol), Oxyma (3 eq, 149 mg, 1.05 mmol), and DIC (3 eq, 164 uL, 1.05 mmol) in DMF (15 mL) were added to the reaction flask and agitated for 2 hours at ambient temperature. The Fmoc removal and coupling procedure was repeated as before using the same equivalencies with Fmoc-D-Glutamic acid α-amide and Fmoc-L-Lysine(Mtt)-OH (3 eq, 655 mg, 1.05 mmol). The N-terminus of the peptide was acetylated by removing the Fmoc group then agitating the resin for 1 hour with a solution of 5% acetic anhydride (0.5 mL), 8.5% DIEA (0.85 mL), and 86.5% DMF (8.65 mL). The Mtt group of the L-Lysine(Mtt) was removed by adding 10 mL of a TFA cocktail solution (1% TFA, 2% TIPS in DCM) to the resin and agitating for 10 minutes protected from light. The solution was drained, and this procedure was repeated five additional times. The solution was then drained and washed

as previously described. Upon Mtt deprotection, the resin was coupled with 5,6-carboxyfluorescein (2 eq, 263 mg, 0.7 mmol), HBTU (2 eq, 265 mg, 0.7 mmol), and DIEA (4 eq, 243 uL, 1.4 mmol) in DMF (15 mL) shaking over-night. The resin was washed as previously described. To remove the peptide from resin, a TFA cocktail solution (95 % TFA, 2.5% TIPS, and 2.5 % DCM) was added to the resin with agitation for 2 hours protected from light. The resin was filtered and resulting solution was concentrated *in vacuo*. The peptide was trituated with cold diethyl ether and purified using reverse phase HPLC using H_2O/MeOH to yield **K(Fl)-Tri**. The sample was analyzed for purity using a Waters 1525 Binary HPLC Pump using a Phenomenex Luna 5u C8(2) 100A (250 x 4.60 mm) column; gradient elution with H_2O/CH_3CN.
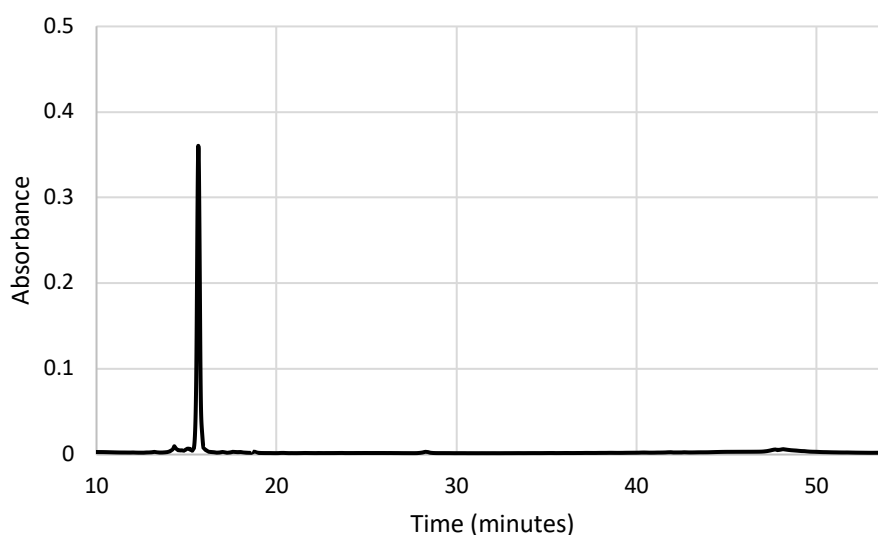
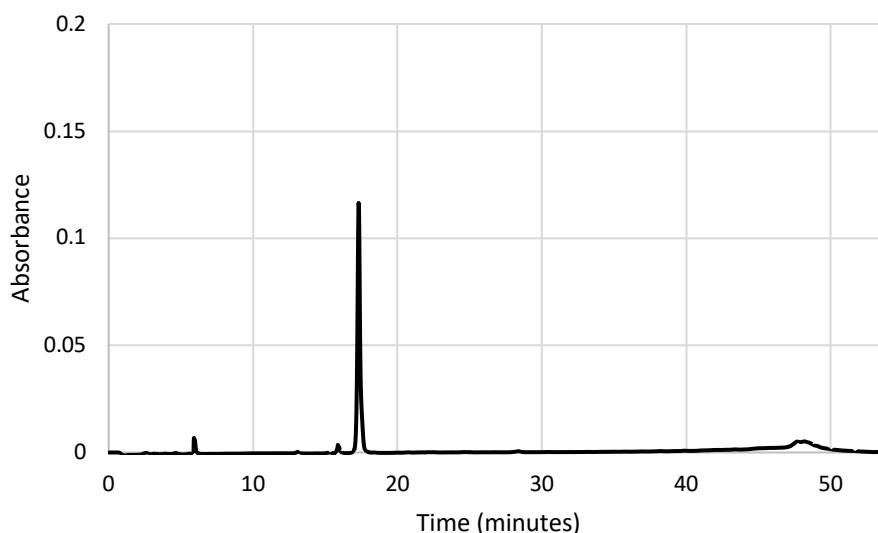ESI-MS calculated [M+2H$^+$]: 437.6851, found: 437.6847
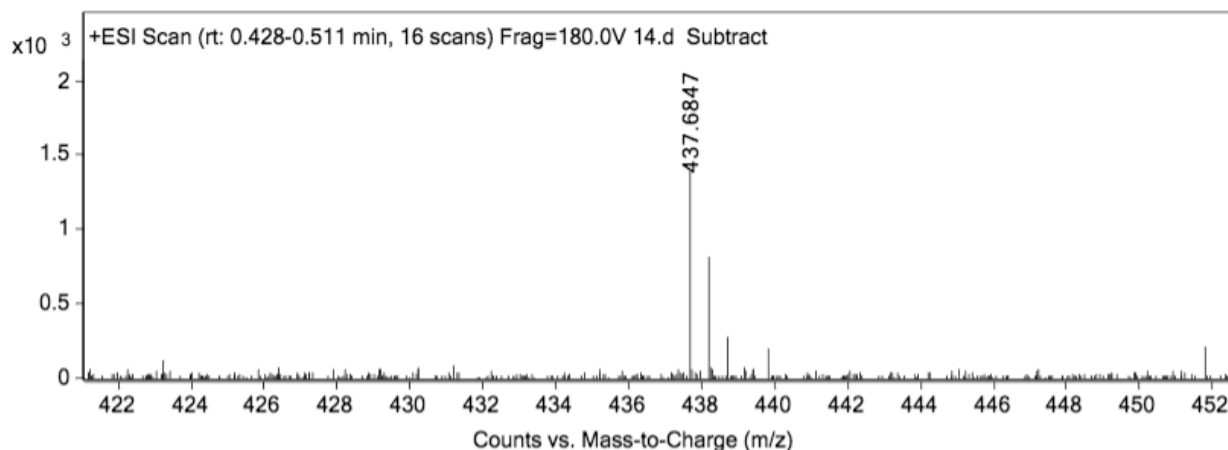
Scheme S9. Synthesis of K(DNP)-SGGG1
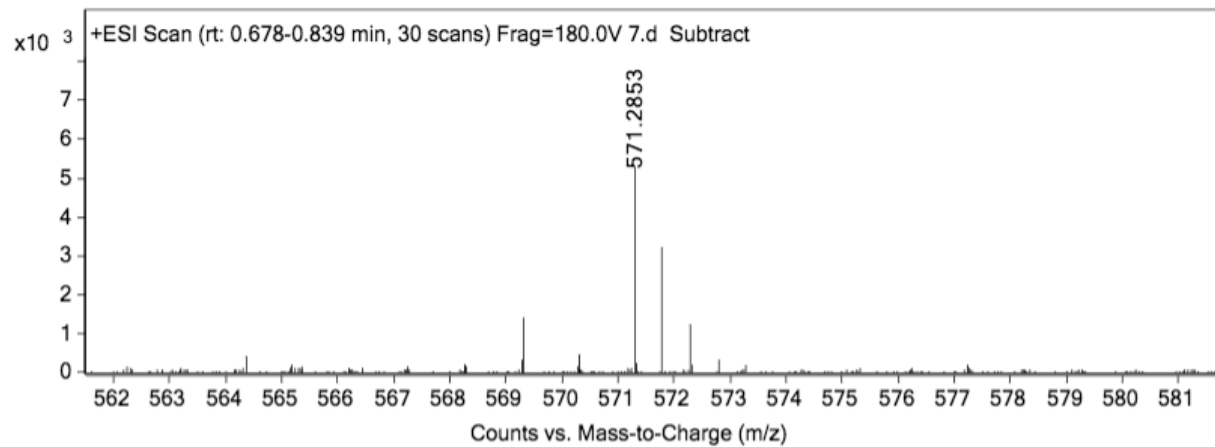

K(DNP)-SGGG1

A 25 mL synthetic vessel was charged with 500 mg (0.35 mmol) of Fmoc-D-Alanine-Wang resin. The Fmoc group was removed in a 20% piperidine in DMF solution (15 mL). The flask was agitated for 30 minutes and the piperidine solution was drained. The resin was washed with DCM and MeOH (3 x 15 mL). Fmoc-L-Lysine(Boc)-OH (3 eq, 491 mg, 1.05 mmol), Oxyma (3 eq, 149 mg, 1.05 mmol), and DIC (3 eq, 164 uL, 1.05 mmol) in DMF (15 mL) were added to the reaction flask and agitated for 2 hours at ambient temperature. The Fmoc removal and coupling procedure was repeated as before using the same equivalencies with Fmoc-D-Glutamic acid α-amide, and Fmoc-L-Alanine-OH. The Fmoc

removal and coupling procedure was repeated using three Fmoc-Glycine-OH (3 eq, 490 mg, 1.65 mmol) residues followed by Fmoc-Serine(tBu)-OH (3 eq, 631 mg, 1.65 mmol) to yield Fmoc-SGGG-Tetra. The Fmoc 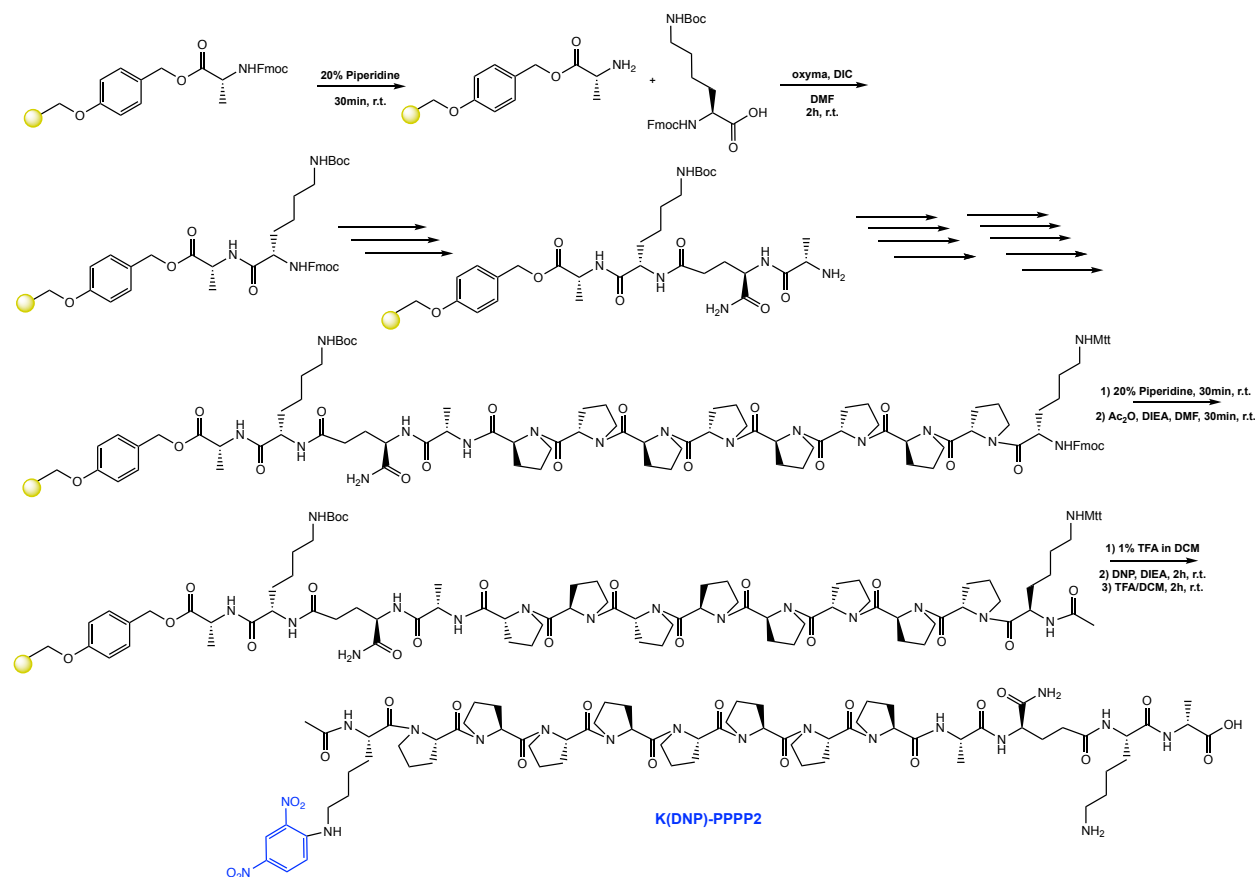group of the N-terminal serine was removed and resin coupled with Fmoc-L-Lysine(Mtt)-OH (3 eq, 655 mg, 1.05 mmol). The N-terminus of the peptide was acetylated by removing the Fmoc group and then agitating the resin for 1 hour with a solution of 5% acetic anhydride (0.5 mL), 8.5% DIEA (0.85 mL), and 86.5% DMF (8.65 mL). The Mtt group of the L-Lysine(Mtt) was removed by adding 10 mL of a TFA cocktail solution (1% TFA, 2% TIPS in DCM) to the resin and agitating for 10 minutes protected from light. The solution was drained, and this procedure was repeated five additional times. The solution was then drained, rinsed with DMF, and washed as previously described. Upon Mtt deprotection, 2,4-dinitrofluorobenzene (3 eq, 131 uL, 1.05 mmol) and DIEA (6 eq, 365 uL, 1.05 mmol) in DMF (15 mL) was agitated with the resin for 2 hours protected from light. The resin was then washed as previous stated. To remove the peptide from resin, a TFA cocktail solution (95 % TFA, 2.5% TIPS, and 2.5 % DCM) was added to the resin with agitation for 2 hours protected from light. The resin was filtered and resulting solution was concentrated *in vacuo*. The peptide was trituated with cold diethyl ether and purified using reverse phase HPLC using H_2O/MeOH to yield **K(DNP)-SGGG1**. The sample was analyzed for purity using a Waters 1525 Binary HPLC Pump using a Phenomenex Luna 5u C8(2) 100A (250 x 4.60 mm) column; gradient elution with H_2O/CH_3CN.

ESI-MS calculated [M+H$^+$]: 1011.4495, found: 1011.4447

+ESI Scan (rt: 0.673-0.711 min, 8 scans) Frag=180.0V 5.d Subtract
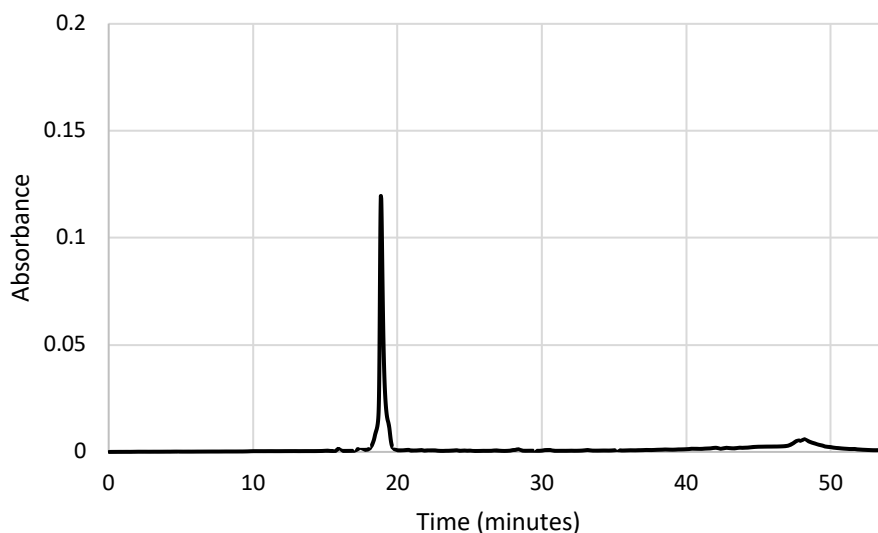
x10 2

1011.4447

Counts vs. Mass-to-Charge (m/z)
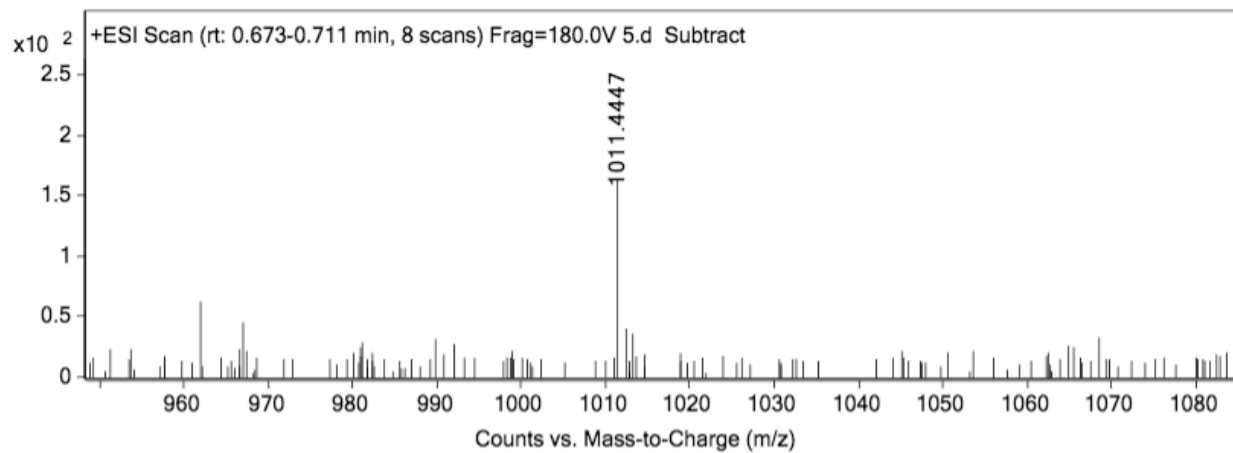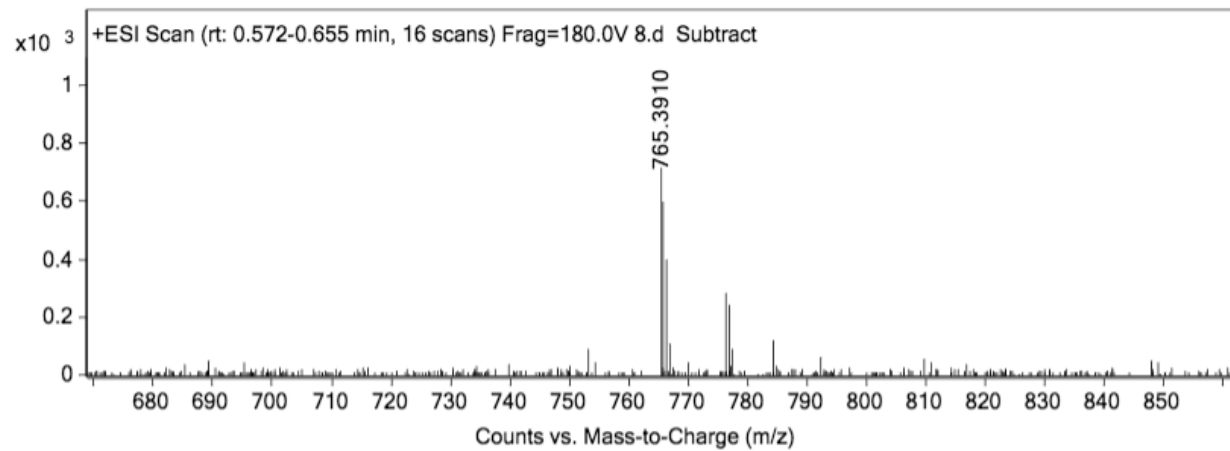
Scheme S10. Synthesis of K(DNP)-SGGG2

A 25 mL synthetic vessel was charged with 500 mg (0.35 mmol) of Fmoc-D-Alanine-Wang resin. The Fmoc group was removed in a 20% piperidine in DMF solution (15 mL). The flask was agitated for 30 minutes and the piperidine solution was drained. The resin was washed with DCM and MeOH (3 x 15 mL). Fmoc-L-Lysine(Boc)-OH (3 eq, 491 mg, 1.05 mmol), Oxyma (3 eq, 149 mg, 1.05 mmol), and DIC (3 eq, 164 uL, 1.05 mmol) in DMF (15 mL) were added to the reaction flask and agitated for 2 hours at ambient temperature. The Fmoc removal and coupling procedure was repeated as before using the same equivalencies with Fmoc-D-Glutamic acid α-amide, and Fmoc-L-Alanine-OH. The Fmoc removal and coupling procedure was repeated using three Fmoc-Glycine-OH (3 eq, 490 mg, 1.65 mmol) residues followed by Fmoc-Serine(tBu)-OH (3 eq, 631 mg, 1.65 mmol) and another three Fmoc-Glycine-OH (3 eq, 490 mg, 1.65 mmol) residues followed by

Fmoc-Serine(tBu)-OH (3 eq, 631 mg, 1.65 mmol) to yield Fmoc-SGGG-SGGG-Tetra. The Fmoc group of the N-terminal serine was removed and resin coupled with Fmoc-L-Lysine(Mtt)-OH (3 eq, 655 mg, 1.05 mmol). The N-terminus of the peptide was acetylated by removing the Fmoc group and then agitating the resin for 1 hour with a solution of 5% acetic anhydride (0.5 mL), 8.5% DIEA (0.85 mL), and 86.5% DMF (8.65 mL). The Mtt group of the L-Lysine(Mtt) was removed by adding 10 mL of a TFA cocktail solution (1% TFA, 2% TIPS in DCM) to the resin and agitating for 10 minutes protected from light. The solution was drained, and this procedure was repeated five additional times. The solution was then drained, rinsed with DMF, and washed as previously described. Upon Mtt deprotection, 2,4-dinitrofluorobenzene (3 eq, 131 uL, 1.05 mmol) and DIEA (6 eq, 365 uL, 1.05 mmol) in DMF (15 mL) was agitated with the resin for 2 hours protected from light. The resin was then washed as previous stated. To remove the peptide from resin, a TFA cocktail solution (95 % TFA, 2.5% TIPS, and 2.5 % DCM) was added to the resin with agitation for 2 hours protected from light. The resin was filtered and resulting solution was concentrated *in vacuo*. The peptide was trituated with cold diethyl ether and purified using reverse phase HPLC using H_2O/MeOH to yield **K(DNP)-SGGG2**. The sample was analyzed for purity using a Waters 1525 Binary HPLC Pump using a Phenomenex Luna 5u C8(2) 100A (250 x 4.60 mm) column; gradient elution with H_2O/CH_3CN.

ESI-MS calculated [M+H$^+$]: 1269.5460, found: 1269.5427

+ESI Scan (rt: 0.634-0.734 min, 19 scans) Frag=180.0V 6.d Subtract

x10 3

1269.5427

Counts vs. Mass-to-Charge (m/z)

Scheme S11. Synthesis of K(DNP)-PPPP1

K(DNP)-PPPP1

A 25 mL synthetic vessel was charged with 500 mg (0.35 mmol) of Fmoc-D-Alanine-Wang resin. The Fmoc group was removed in a 20% piperidine in DMF solution (15 mL). The flask was agitated for 30 minutes and the piperidine solution was drained. The resin was washed with DCM and MeOH (3 x 15 mL). Fmoc-L-Lysine(Boc)-OH (3 eq, 491 mg, 1.05 mmol), Oxyma (3 eq, 149 mg, 1.05 mmol), and DIC (3 eq, 164 uL, 1.05 mmol) in DMF (15 mL) were added to the reaction flask and agitated for 2 hours at ambient temperature. The Fmoc removal and coupling procedure was repeated as before using the same equivalencies with Fmoc-D-Glutamic acid α-amide, and Fmoc-L-Alanine-OH. The Fmoc removal and coupling was repeated four times using Fmoc-Proline-OH (3 eq, 556 mg, 1.65 mmol) to yield Fmoc-PPPP-Tetra. The Fmoc group of the N-terminal proline was
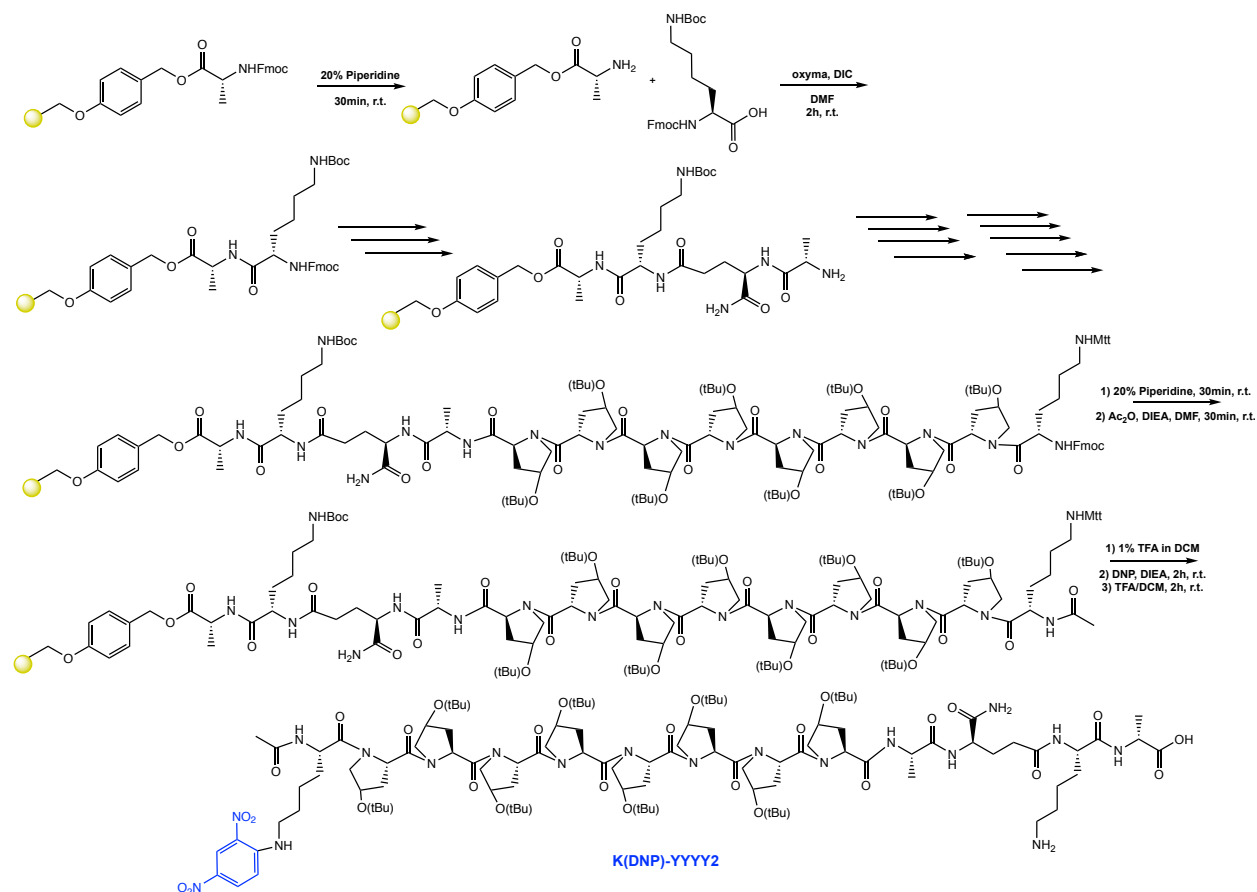
removed and resin coupled with Fmoc-L-Lysine(Mtt)-OH (3 eq, 655 mg, 1.05 mmol). The N-terminus of the peptide was acetylated by removing the Fmoc group and then agitating the resin for 1 hour with a solution of 5% acetic anhydride (0.5 mL), 8.5% DIEA (0.85 mL), and 86.5% DMF (8.65 mL). The Mtt group of the L-Lysine(Mtt) was removed by adding 10 mL of a TFA cocktail solution (1% TFA, 2% TIPS in DCM) to the resin and agitating for 10 minutes protected from light. The solution was drained, and this procedure was repeated five additional times. The solution was then drained, rinsed with DMF, and washed as previously described. Upon Mtt deprotection, 2,4-dinitrofluorobenzene (3 eq, 131 uL, 1.05 mmol) and DIEA (6 eq, 365 uL, 1.05 mmol) in DMF (15 mL) was agitated with the resin for 2 hours protected from light. The resin was then washed as previous stated. To remove the peptide from resin, a TFA cocktail solution (95 % TFA, 2.5% TIPS, and 2.5 % DCM) was added to the resin with agitation for 2 hours protected from light. The resin was filtered and resulting solution was concentrated *in vacuo*. The peptide was trituated with cold diethyl ether and purified using reverse phase HPLC using H_2O/MeOH to yield **K(DNP)-PPPP1**. The sample was analyzed for purity using a Waters 1525 Binary HPLC Pump using a Phenomenex Luna 5u C8(2) 100A (250 x 4.60 mm) column; gradient elution with H_2O/CH_3CN.

ESI-MS calculated [M+2H⁺]: 571.2860, found: 571.2853

+ESI Scan (rt: 0.678-0.839 min, 30 scans) Frag=180.0V 7.d Subtract

Scheme S12. Synthesis of K(DNP)-PPPP2


K(DNP)-PPPP2

A 25 mL synthetic vessel was charged with 500 mg (0.35 mmol) of Fmoc-D-Alanine-Wang resin. The Fmoc group was removed in a 20% piperidine in DMF solution (15 mL). The flask was agitated for 30 minutes and the piperidine solution was drained. The resin was washed with DCM and MeOH (3 x 15 mL). Fmoc-L-Lysine(Boc)-OH (3 eq, 491 mg, 1.05 mmol), Oxyma (3 eq, 149 mg, 1.05 mmol), and DIC (3 eq, 164 uL, 1.05 mmol) in DMF (15 mL) were added to the reaction flask and agitated for 2 hours at ambient temperature. The Fmoc removal and coupling procedure was repeated as before using the same equivalencies with Fmoc-D-Glutamic acid α-amide, and Fmoc-L-Alanine-OH. The Fmoc removal and coupling was repeated eight times using Fmoc-Proline-OH (3 eq, 556 mg, 1.65 mmol) to yield Fmoc-PPPPPPPP-Tetra. The Fmoc group of the N-terminal proline was removed and resin coupled with Fmoc-L-Lysine(Mtt)-OH (3 eq, 655 mg, 1.05 mmol). The N-terminus of the peptide was ac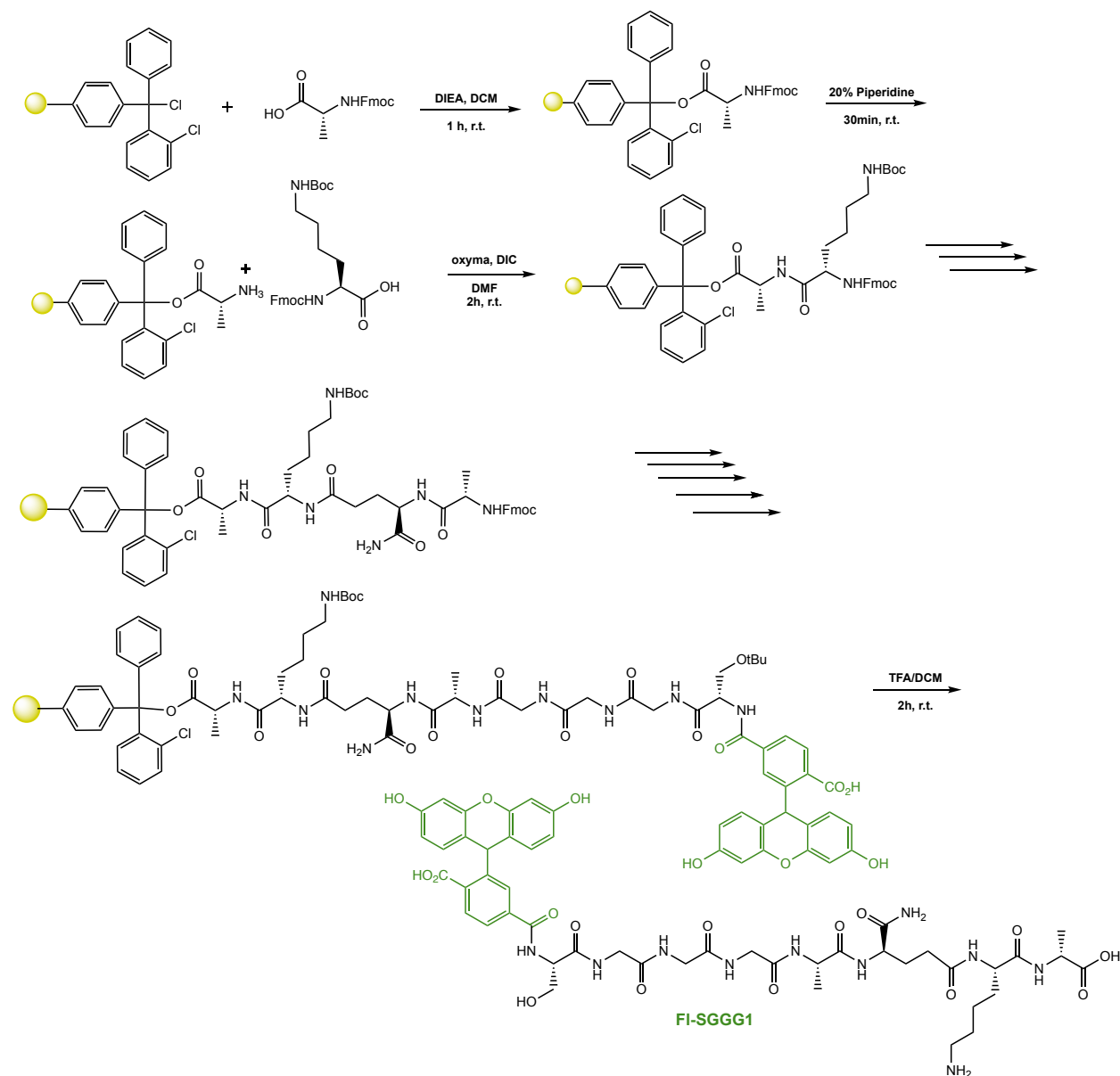etylated by removing the Fmoc group and then agitating the resin for 1 hour with a solution of 5% acetic anhydride (0.5 mL), 8.5% DIEA

(0.85 mL), and 86.5% DMF (8.65 mL). The Mtt group of the L-Lysine(Mtt) was removed by adding 10 mL of a TFA cocktail solution (1% TFA, 2% TIPS in DCM) to the resin and agitating for 10 minutes protected from light. The solution was drained, and this procedure was repeated five additional times. The solution was then drained, rinsed with DMF, and washed as previously described. Upon Mtt deprotection, 2,4-dinitrofluorobenzene (3 eq, 131 uL, 1.05 mmol) and DIEA (6 eq, 365 uL, 1.05 mmol) in DMF (15 mL) was agitated with the resin for 2 hours protected from light. The resin was then washed as previous stated. To remove the peptide from resin, a TFA cocktail solution (95 % TFA, 2.5% TIPS, and 2.5 % DCM) was added to the resin with agitation for 2 hours protected from light. The resin was filtered and resulting solution was concentrated *in vacuo*. The peptide was trituated with cold diethyl ether and purified using reverse phase HPLC using H_2O/MeOH to yield **K(DNP)-PPPP2**. The sample was analyzed for purity using a Waters 1525 Binary HPLC Pump using a Phenomenex Luna 5u C8(2) 100A (250 x 4.60 mm) column; gradient elution with H_2O/CH_3CN.

ESI-MS calculated [M+2H$^+$]: 765.3915, found: 765.3910

+ESI Scan (rt: 0.572-0.655 min, 16 scans) Frag=180.0V 8.d Subtract

x10 3

765.3910

Counts vs. Mass-to-Charge (m/z)

Scheme S13. Synthesis of K(DNP)-YYYY1

K(DNP)-YYYY1

A 25 mL synthetic vessel was charged with 500 mg (0.35 mmol) of Fmoc-D-Alanine-Wang resin. The Fmoc group was removed in a 20% piperidine in DMF solution (15 mL). The flask was agitated for 30 minutes and the piperidine solution was drained. The resin was washed with DCM and MeOH (3 x 15 mL). Fmoc-L-Lysine(Boc)-OH (3 eq, 491 mg, 1.05 mmol), Oxyma (3 eq, 149 mg, 1.05 mmol), and DIC (3 eq, 164 uL, 1.05 mmol) in DMF (15 mL) were added t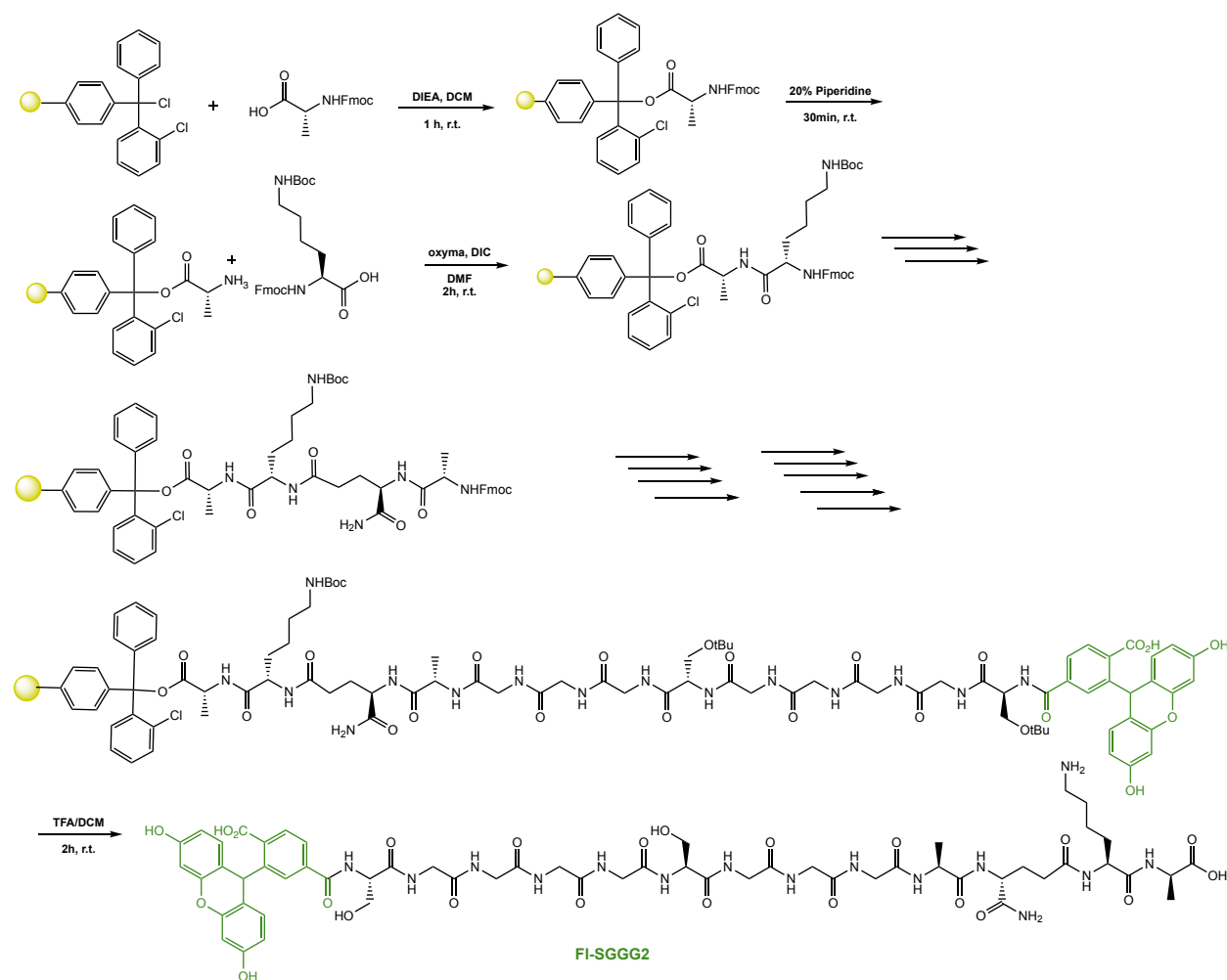o the reaction flask and agitated for 2 hours at ambient temperature. The Fmoc removal and coupling procedure was repeated as before using the same equivalencies with Fmoc-D-Glutamic acid α-amide, and Fmoc-L-Alanine-OH. The Fmoc removal and coupling was repeated four times using Fmoc-L-Hyp(tBu)-OH (3 eq, 647 mg, 1.65 mmol) to yield Fmoc-YYYY-Tetra. The Fmoc group of the N-terminal hydroxyproline

was removed and resin coupled with Fmoc-L-Lysine(Mtt)-OH (3 eq, 655 mg, 1.05 mmol). The N-terminus of the peptide was acetylated by removing the Fmoc group and then agitating the resin for 1 hour with a solution of 5% acetic anhydride (0.5 mL), 8.5% DIEA (0.85 mL), and 86.5% DMF (8.65 mL). The Mtt group of the L-Lysine(Mtt) was removed by adding 10 mL of a TFA cocktail solution (1% TFA, 2% TIPS in DCM) to the resin and agitating for 10 minutes protected from light. The solution was drained, and this procedure was repeated five additional times. The solution was then drained, rinsed with DMF, and washed as previously described. Upon Mtt deprotection, 2,4-dinitrofluorobenzene (3 eq, 131 uL, 1.05 mmol) and DIEA (6 eq, 365 uL, 1.05 mmol) in DMF (15 mL) was agitated with the resin for 2 hours protected from light. The resin was then washed as previous stated. To remove the peptide from resin, a TFA cocktail solution (95 % TFA, 2.5% TIPS, and 2.5 % DCM) was added to the resin with agitation for 2 hours protected from light. The resin was filtered and resulting solution was concentrated *in vacuo*. The peptide was trituated with cold diethyl ether and purified using reverse phase HPLC using H_2O/MeOH to yield **K(DNP)-YYYY1**. The sample was analyzed for purity using a Waters 1525 Binary HPLC Pump using a Phenomenex Luna 5u C8(2) 100A (250 x 4.60 mm) column; gradient elution with H_2O/CH_3CN.
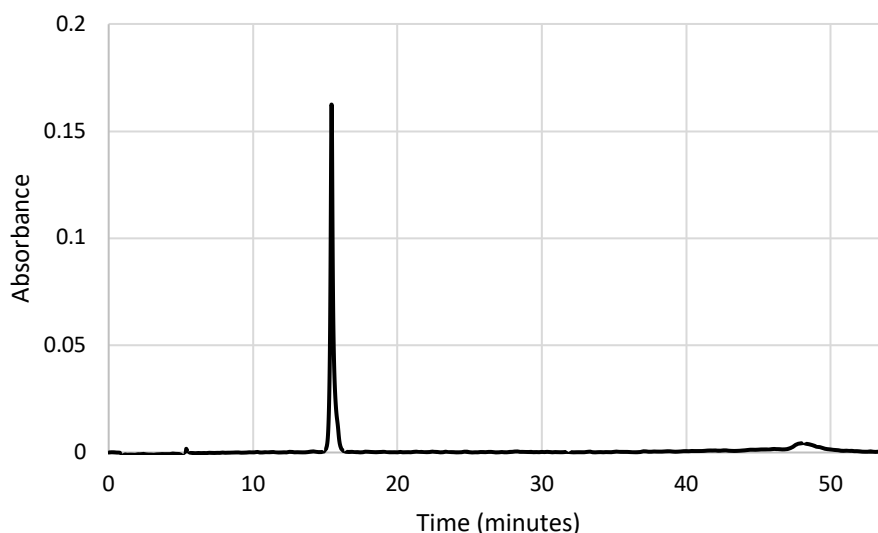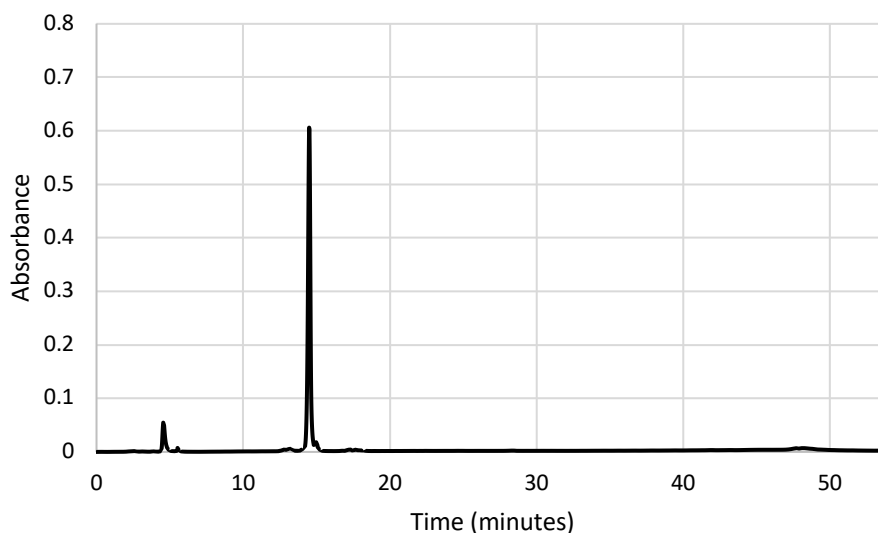
ESI-MS calculated [M+H$^+$]: 1205.5438, found: 1205.5419

+ESI Scan (rt: 0.463-0.563 min, 19 scans) Frag=180.0V 9.d Subtract
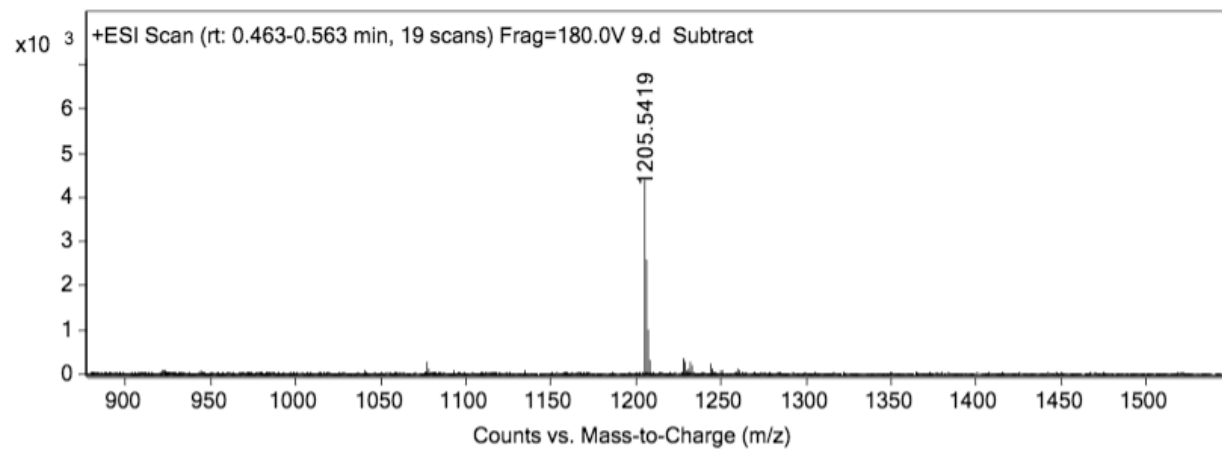
Scheme S14. Synthesis of K(DNP)-YYYY2

K(DNP)-YYYY2

A 25 mL synthetic vessel was charged with 500 mg (0.35 mmol) of Fmoc-D-Alanine-Wang resin. The Fmoc group was removed in a 20% piperidine in DMF solution (15 mL). The flask was agitated for 30 minutes and the piperidine solution was drained. The resin was washed with DCM and MeOH (3 x 15 mL). Fmoc-L-Lysine(Boc)-OH (3 eq, 491 mg, 1.05 mmol), Oxyma (3 eq, 149 mg, 1.05 mmol), and DIC (3 eq, 164 uL, 1.05 mmol) in DMF (15 mL) were added to the reaction flask and agitated for 2 hours at ambient temperature. The Fmoc removal and coupling procedure was repeated as before using the same equivalenci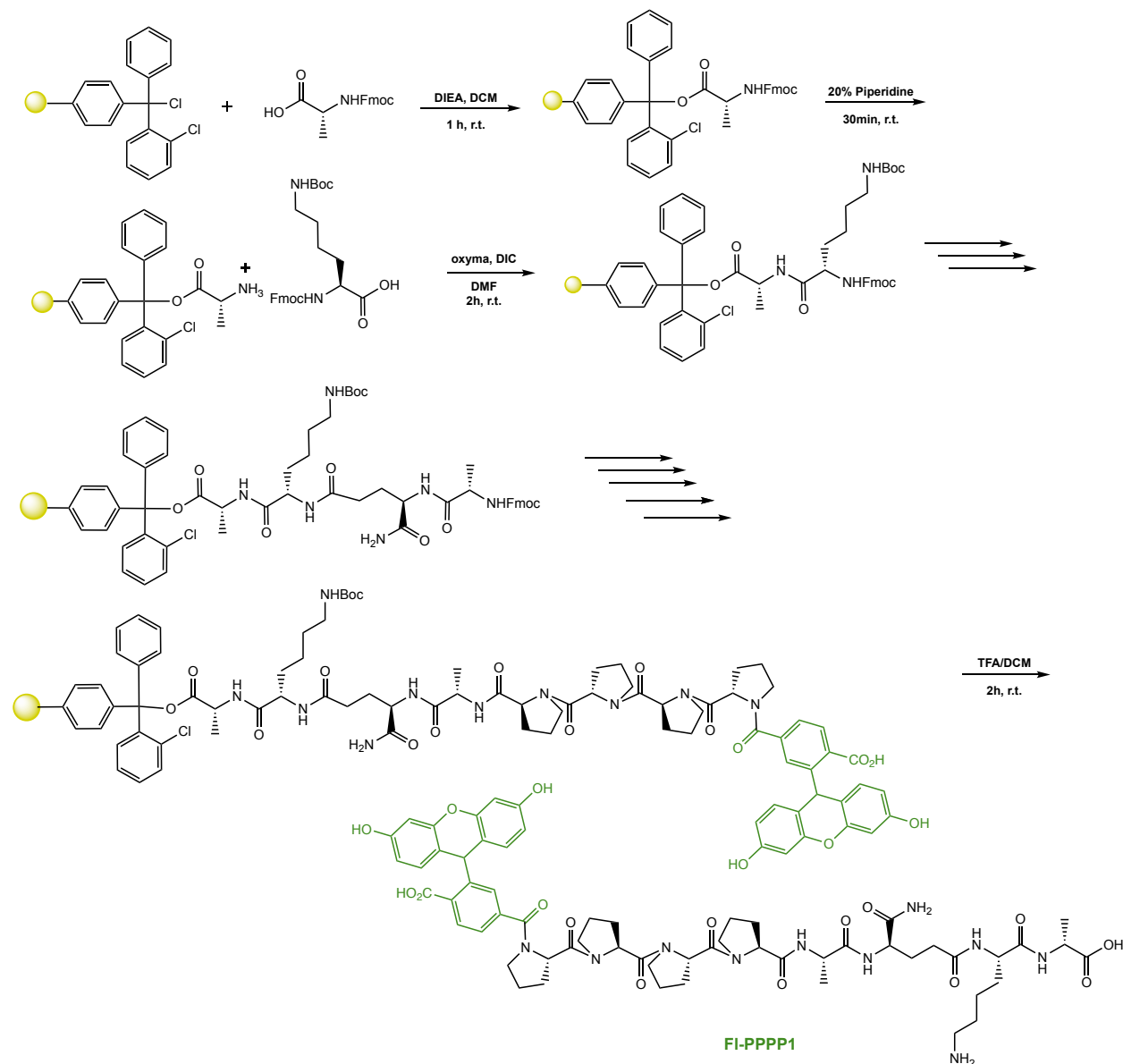es with Fmoc-D-Glutamic acid α-amide, and Fmoc-L-Alanine-OH. The Fmoc removal and coupling was repeated eight times using Fmoc-L-Hyp(tBu)-OH (3 eq, 647 mg, 1.65 mmol) to yield Fmoc-YYYYYYYY-Tetra. The Fmoc group of the N-terminal hydroxyproline was removed and resin coupled with Fmoc-L-Lysine(Mtt)-OH (3 eq, 655 mg, 1.05 mmol). The N-terminus of the peptide was acetylated by removing the Fmoc

group and then agitating the resin for 1 hour with a solution of 5% acetic anhydride (0.5 mL), 8.5% DIEA (0.85 mL), and 86.5% DMF (8.65 mL). The Mtt group of the L-Lysine(Mtt) was removed by adding 10 mL of a TFA cocktail solution (1% TFA, 2% TIPS in DCM) to the resin and agitating for 10 minutes protected from light. The solution was drained, and this procedure was repeated five additional times. The solution was then drained, rinsed with DMF, and washed as previously described. Upon Mtt deprotection, 2,4-dinitrofluorobenzene (3 eq, 131 uL, 1.05 mmol) and DIEA (6 eq, 365 uL, 1.05 mmol) in DMF (15 mL) was agitated with the resin for 2 hours protected from light. The resin was then washed as previous stated. To remove the peptide from resin, a TFA cocktail solution (95 % TFA, 2.5% TIPS, and 2.5 % DCM) was added to the resin with agitation for 2 hours protected from light. The resin was filtered and resulting solution was concentrated *in vacuo*. The peptide was trituated with cold diethyl ether and purified using reverse phase HPLC using H_2O/MeOH to yield **K(DNP)-YYYY2**. The sample was analyzed for purity using a Waters 1525 Binary HPLC Pump using a Phenomenex Luna 5u C8(2) 100A (250 x 4.60 mm) column; gradient elution with H_2O/CH_3CN.
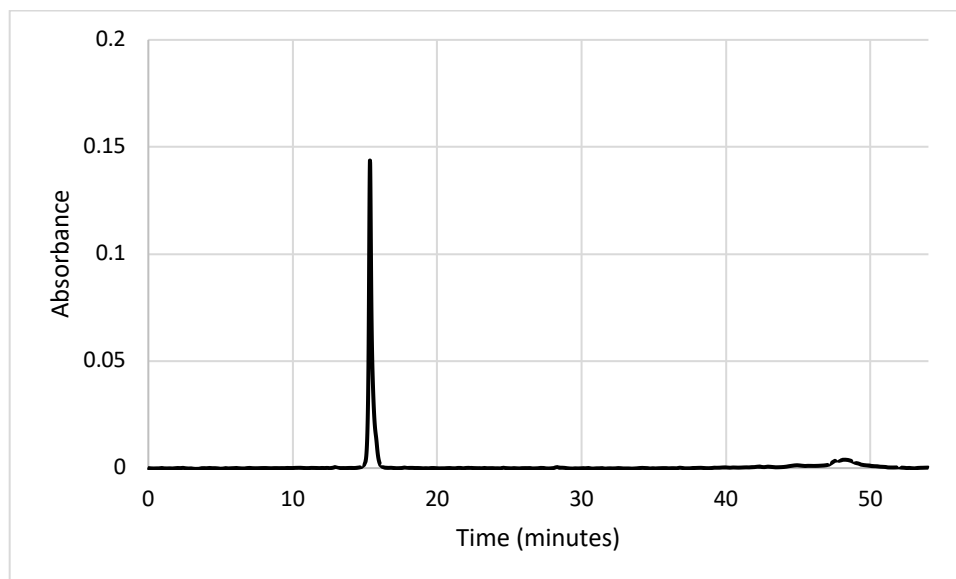
ESI-MS calculated [M+2H$^+$]: 829.3712, found: 829.3699

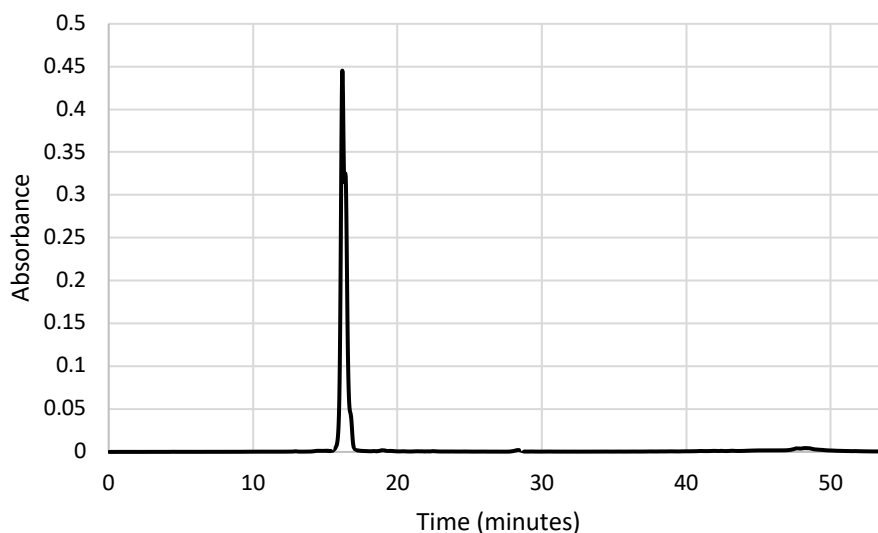+ESI Scan (rt: 0.436-0.547 min, 21 scans) Frag=180.0V 10.d Subtract
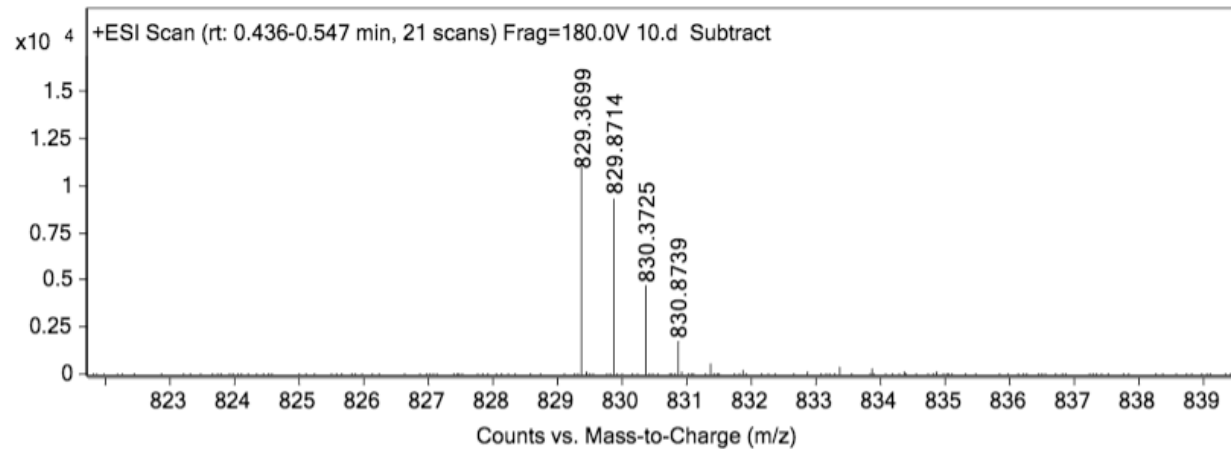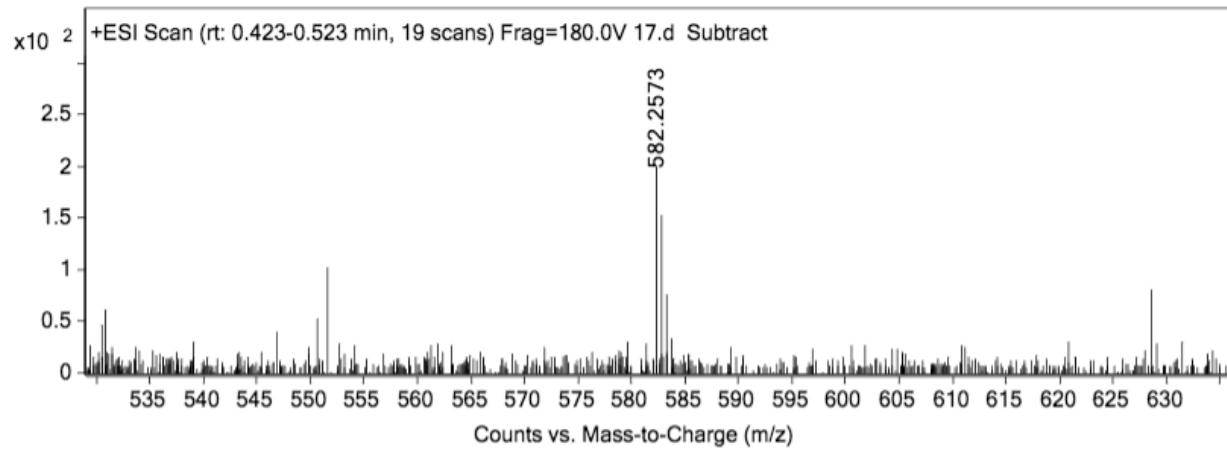
Scheme S15. Synthesis of Fl-SGGG1

A 25 mL synthetic vessel charged with 500 mg (0.55 mmol) of 2-Chlorotrityl chloride resin was added Fmoc-D-Alanine-OH (1.1 eq, 188 mg, 0.605 mmol) and DIEA (4.4 eq, 420 uL, 2.42 mmol) in dry DCM (15 mL). The resin was agitated for 1 hour at ambient temperature and washed with MeOH and DCM (3 x 15 mL each). The Fmoc protecting group was removed with a 20% piperidine in DMF solution (15 mL) for 30 minutes at ambient temperature, then washed as previously stated. Fmoc-L-Lysine(Boc)-OH (3 eq, 257 mg, 1.65 mmol), Oxyma (3 eq, 243 mg, 1.65 mmol), and DIC (3 eq, 257 uL, 1.65 mmol) in
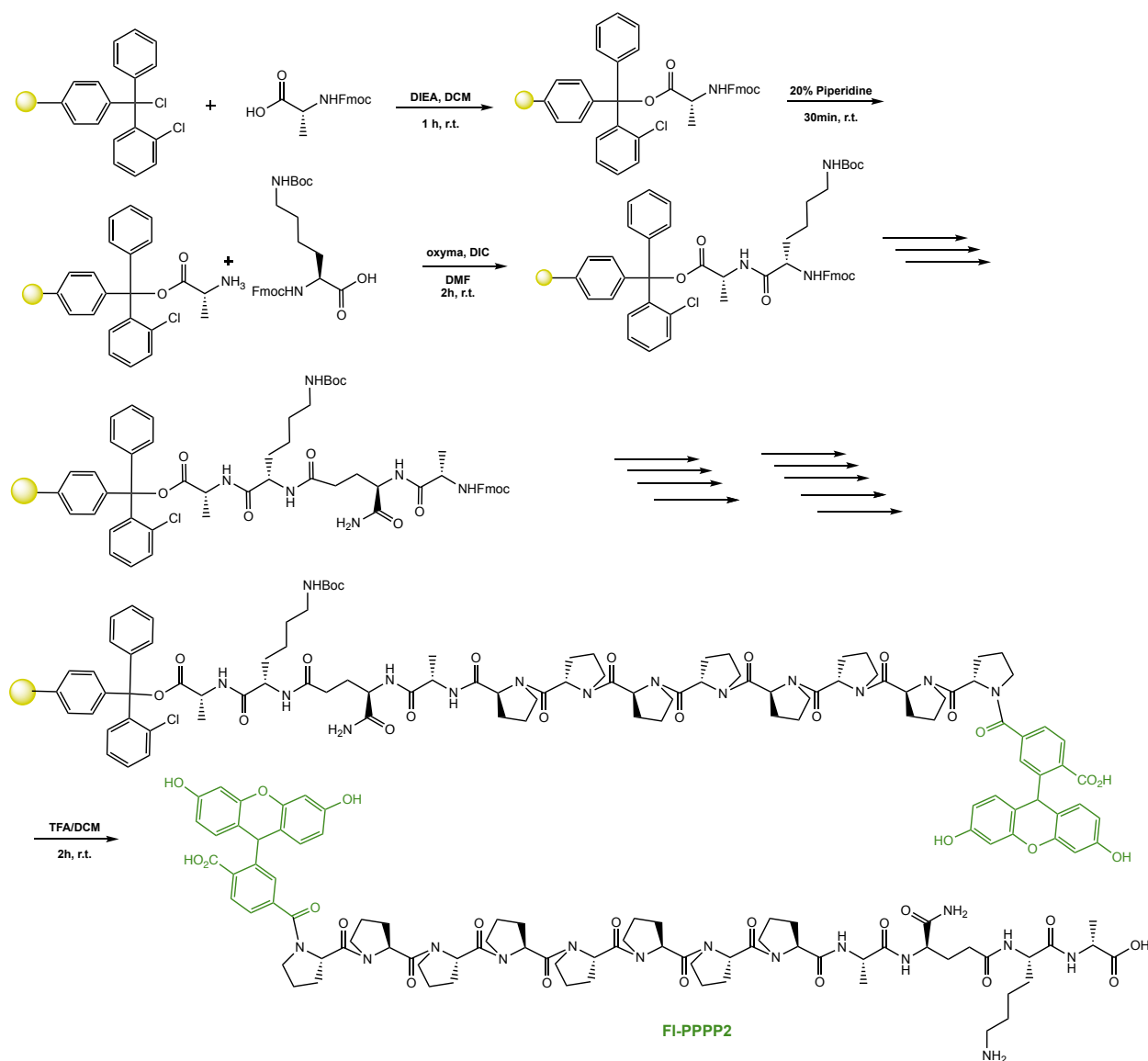
DMF (15 mL) were added to the reaction flask and agitated for 2 hours at ambient temperature. The Fmoc removal and coupling procedure was repeated as before using the same equivalencies with Fmoc-D-Glutamic acid α-amide and Fmoc-L-Alanine-OH. The Fmoc removal and coupling procedure was repeated using three Fmoc-Glycine-OH (3 eq, 490 mg, 1.65 mmol) residues followed by Fmoc-Serine(tBu)-OH (3 eq, 631 mg, 1.65 mmol) to yield Fmoc-SGGG-Tetra. The Fmoc group was removed and resin coupled with 5,6-carboxyfluorescein (2 eq, 413 mg, 1.1 mmol), HBTU (2 eq, 416 mg, 1.1 mmol), and DIEA (6 eq, 574 uL, 3.3 mmol) in DMF (15 mL) shaking over-night. The resin was washed as previously described. To remove the peptide from resin, a TFA cocktail solution (95 % TFA, 2.5% TIPS, and 2.5 % DCM) was added to the resin with agitation for 2 hours protected from light. The resin was filtered and resulting solution was concentrated *in vacuo*. The peptide was trituated with cold diethyl ether and purified using reverse phase HPLC using H_2O/MeOH to yield **FI-SGGG1**. The sample was analyzed for purity using a Waters 1525 Binary HPLC Pump using a Phenomenex Luna 5u C8(2) 100A (250 x 4.60 mm) column; gradient elution with H_2O/CH_3CN.
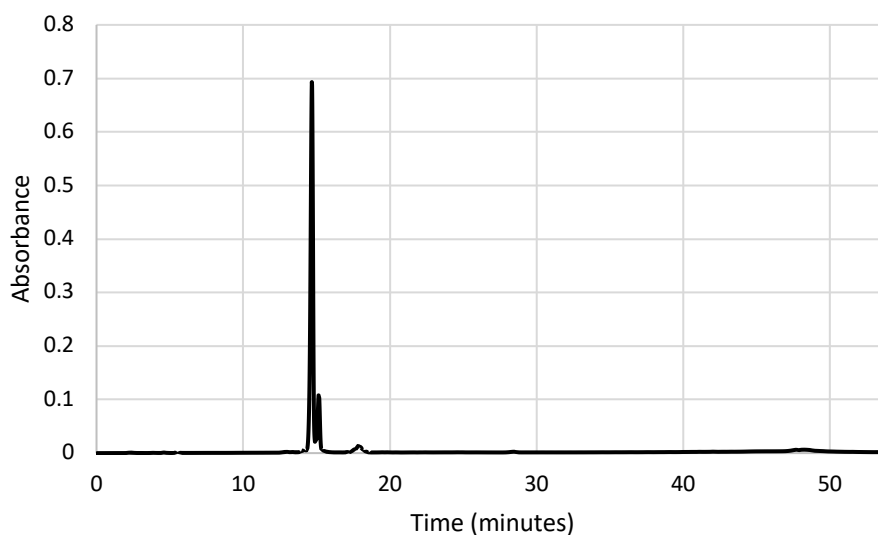
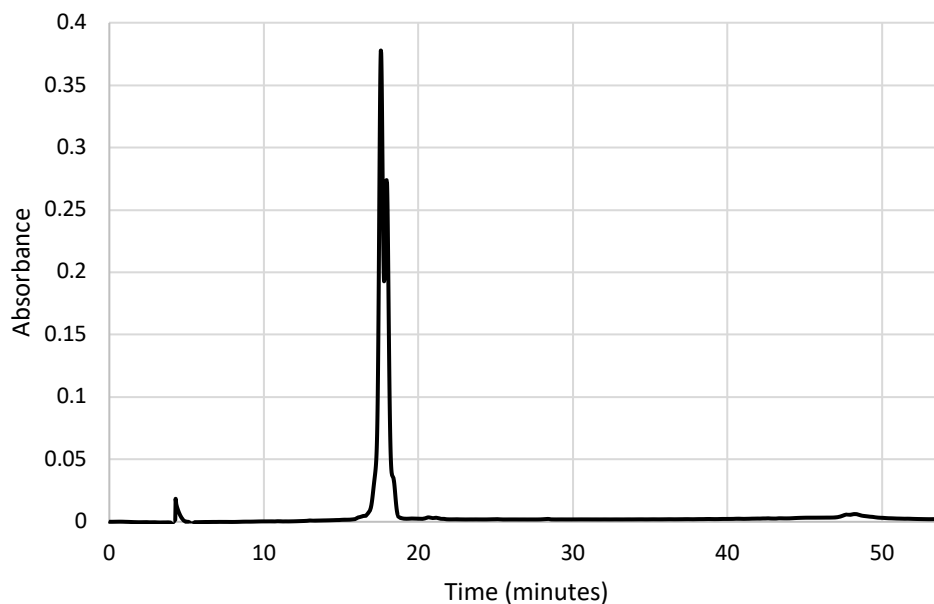ESI-MS calculated [M+2H$^+$]: 517.1991, found (M+2): 517.1984
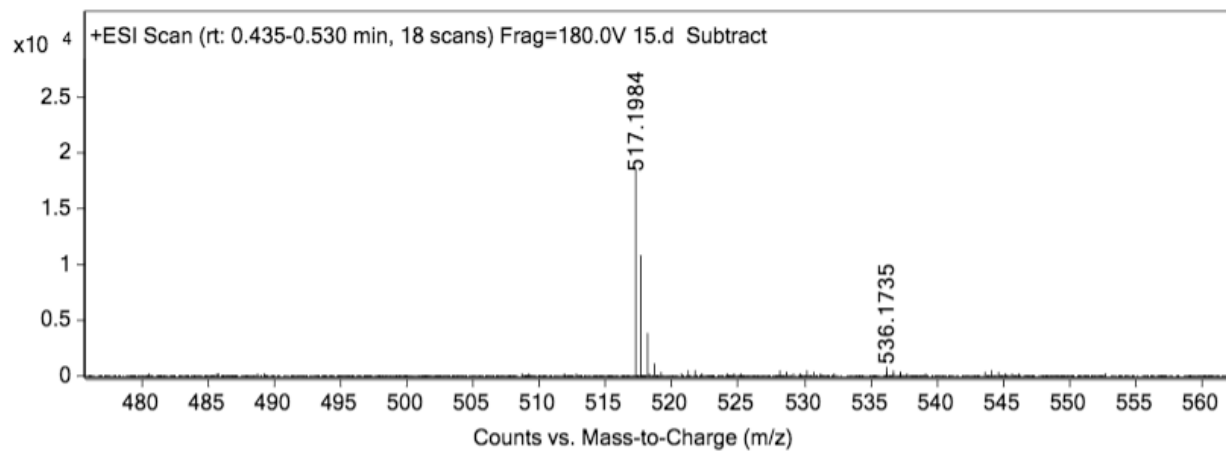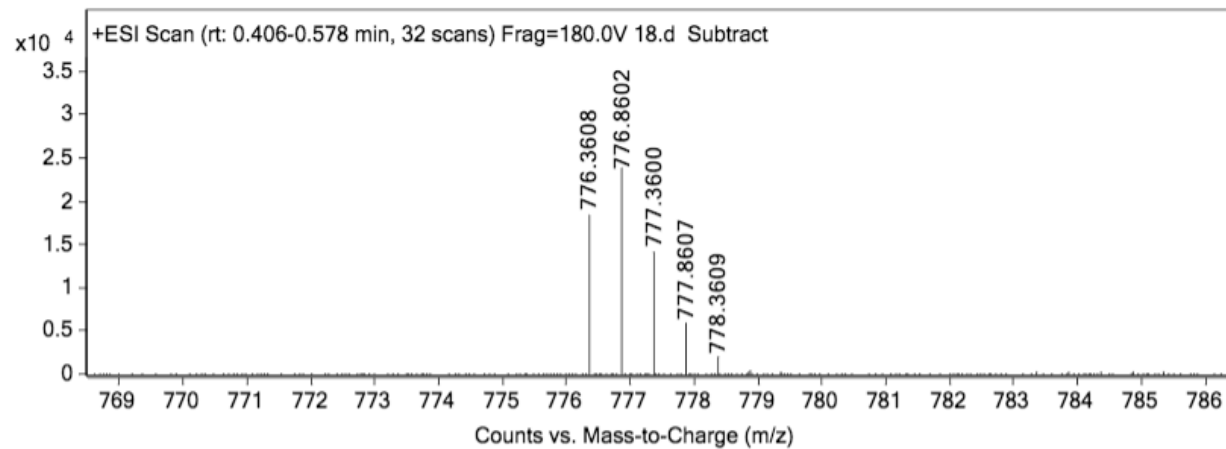
Scheme S16. Synthesis of Fl-SGGG2

A 25 mL synthetic vessel charged with 500 mg (0.55 mmol) of 2-Chlorotrityl chloride resin was added Fmoc-D-Alanine-OH (1.1 eq, 188 mg, 0.605 mmol) and DIEA (4.4 eq, 420 uL, 2.42 mmol) in dry DCM (15 mL). The resin was agitated for 1 hour at ambient temperature and washed with MeOH and DCM (3 x 15 mL each). The Fmoc protecting group was removed with a 20% piperidine in DMF solution (15 mL) for 30 minutes at ambient temperature, then washed as previously stated. Fmoc-L-Lysine(Boc)-OH (3 eq, 257 mg, 1.65 mmol), Oxyma (3 eq, 243 mg, 1.65 mmol), and DIC (3 eq, 257 uL, 1.65 mmol) in DMF (15 mL) were added to the reaction flask and agitated for 2 hours at ambient temperature. The Fmoc removal and coupling procedure was repeated as before using the same equivalencies with Fmoc-D-Glutamic acid α-amide and Fmoc-L-Alanine-OH.

The Fmoc removal and coupling procedure was repeated using three Fmoc-Glycine-OH (3 eq, 490 mg, 1.65 mmol) residues followed by Fmoc-Serine(tBu)-OH (3 eq, 631 mg, 1.65 mmol) and another three Fmoc-Glycine-OH (3 eq, 490 mg, 1.65 mmol) residues followed by Fmoc-Serine(tBu)-OH (3 eq, 631 mg, 1.65 mmol) to yield Fmoc-SGGG-SGGG-Tetra. The Fmoc group was removed and resin coupled with 5,6-carboxyfluorescein (2 eq, 413 mg, 1.1 mmol), HBTU (2 eq, 416 mg, 1.1 mmol), and DIEA (6 eq, 574 uL, 3.3 mmol) in DMF (15 mL) shaking over-night. The resin was washed as previously described. To remove the peptide from resin, a TFA cocktail solution (95 % TFA, 2.5% TIPS, and 2.5 % DCM) was added to the resin with agitation for 2 hours protected from light. The resin was filtered and resulting solution was concentrated *in vacuo*. The peptide was trituated with cold diethyl ether and purified using reverse phase HPLC using H_2O/MeOH to yield **Fl-SGGG2**. The sample was analyzed for purity using a Waters 1525 Binary HPLC Pump using a Phenomenex Luna 5u C8(2) 100A (250 x 4.60 mm) column; gradient elution with H_2O/CH_3CN.
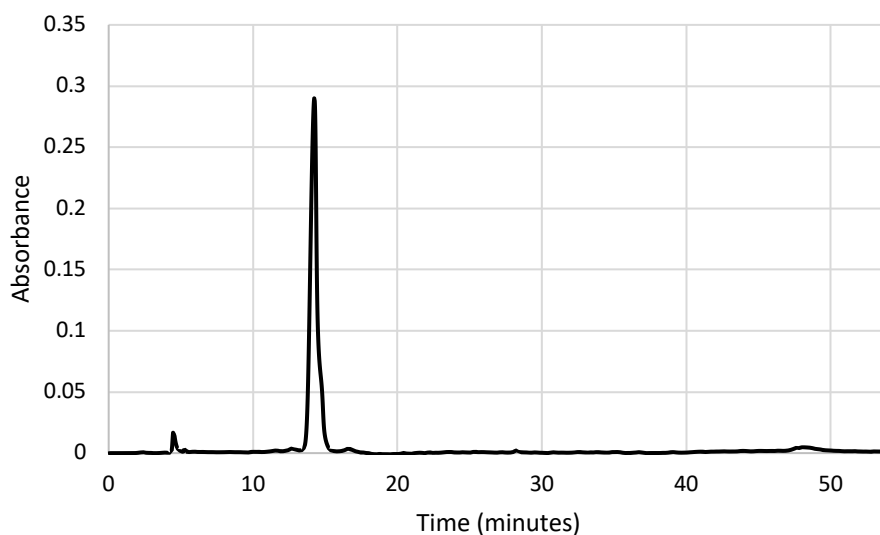
ESI-MS calculated [M+2H$^+$]: 646.2473, found: 646.2468

+ESI Scan (rt: 0.418-0.502 min, 16 scans) Frag=180.0V 16.d Subtract

Counts vs. Mass-to-Charge (m/z)
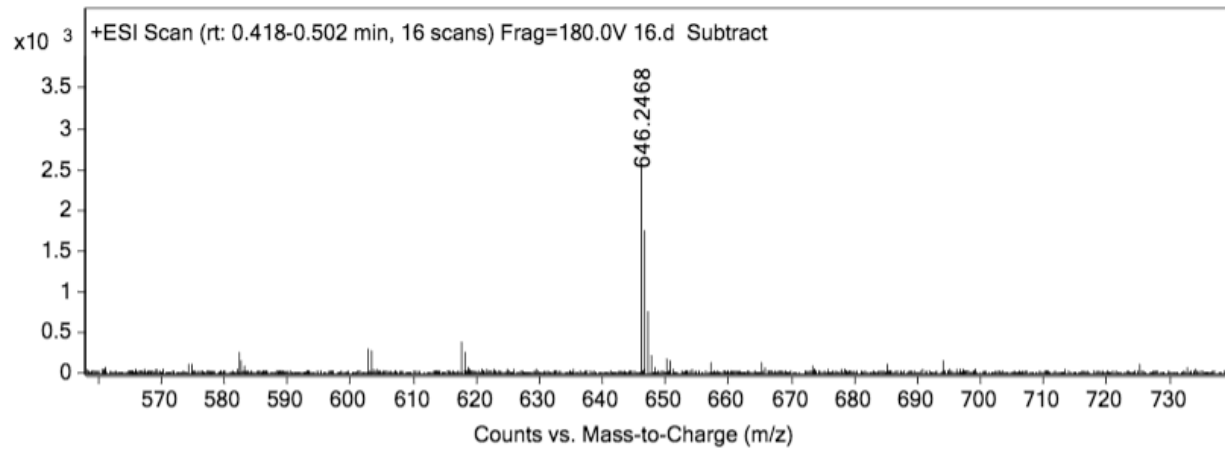
Scheme S17. Synthesis of Fl-PPPP1

Fl-PPPP1

A 25 mL synthetic vessel charged with 500 mg (0.55 mmol) of 2-Chlorotrityl chloride resin was added Fmoc-D-Alanine-OH (1.1 eq, 188 mg, 0.605 mmol) and DIEA (4.4 eq, 420 uL, 2.42 mmol) in dry DCM (15 mL). The resin was agitated for 1 hour at ambient temperature and washed with MeOH and DCM (3 x 15 mL each). The Fmoc protecting group was removed with a 20% piperidine in DMF solution (15 mL) for 30 minutes at ambient temperature, then wa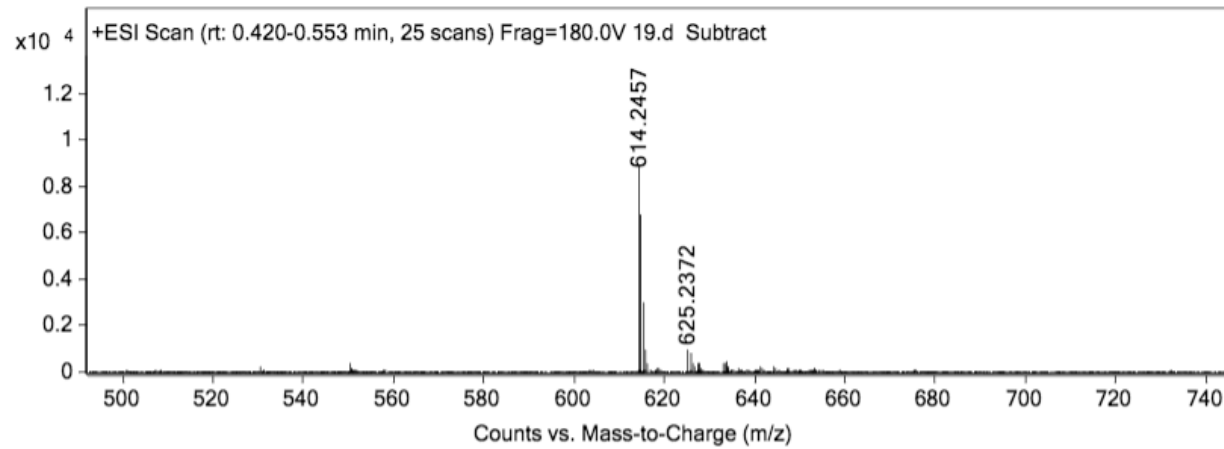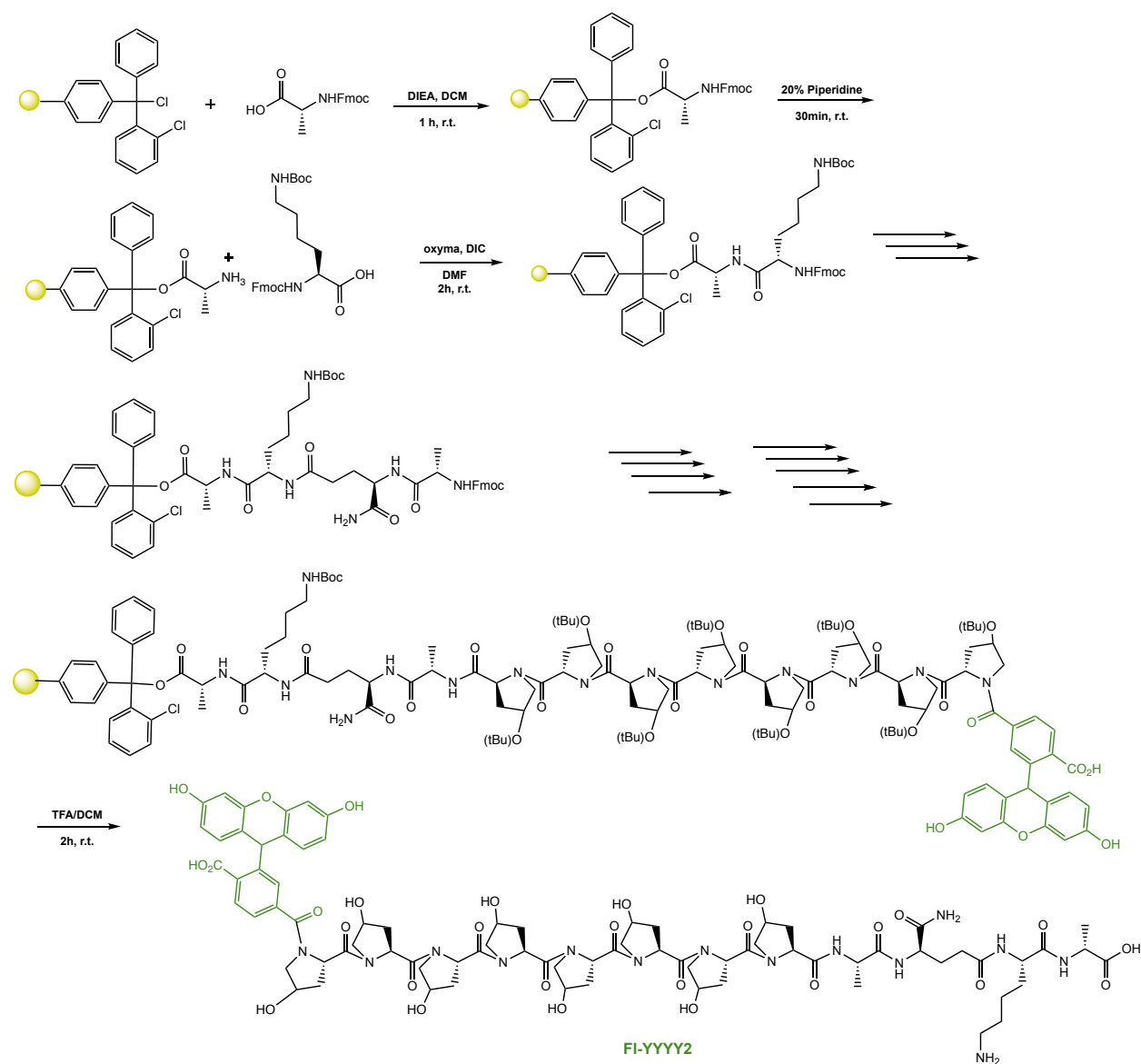shed as previously stated. Fmoc-L-Lysine(Boc)-OH (3 eq, 257 mg, 1.65 mmol), Oxyma (3 eq, 243 mg, 1.65 mmol), and DIC (3 eq, 257 uL, 1.65 mmol) in

DMF (15 mL) were added to the reaction flask and agitated for 2 hours at ambient temperature. The Fmoc removal and coupling procedure was repeated as before using the same equivalencies with Fmoc-D-Glutamic acid α-amide and Fmoc-L-Alanine-OH. The Fmoc removal and coupling was repeated using four Fmoc-Proline-OH (3 eq, 556 mg, 1.65 mmol) residues to yield Fmoc-PPPP-Tetra. The Fmoc group was removed and resin coupled with 5,6-carboxyfluorescein (2 eq, 413 mg, 1.1 mmol), HBTU (2 eq, 416 mg, 1.1 mmol), and DIEA (6 eq, 574 uL, 3.3 mmol) in DMF (15 mL) shaking over-night. The resin was washed as previously described. To remove the peptide from resin, a TFA cocktail solution (95 % TFA, 2.5% TIPS, and 2.5 % DCM) was added to the resin with agitation for 2 hours protected from light. The resin was filtered and resulting solution was concentrated *in vacuo*. The peptide was trituated with cold diethyl ether and purified using reverse phase HPLC using H_2O/MeOH to yield **Fl-PPPP1**. The sample was analyzed for purity using a Waters 1525 Binary HPLC Pump using a Phenomenex Luna 5u C8(2) 100A (250 x 4.60 mm) column; gradient elution with H_2O/CH_3CN.

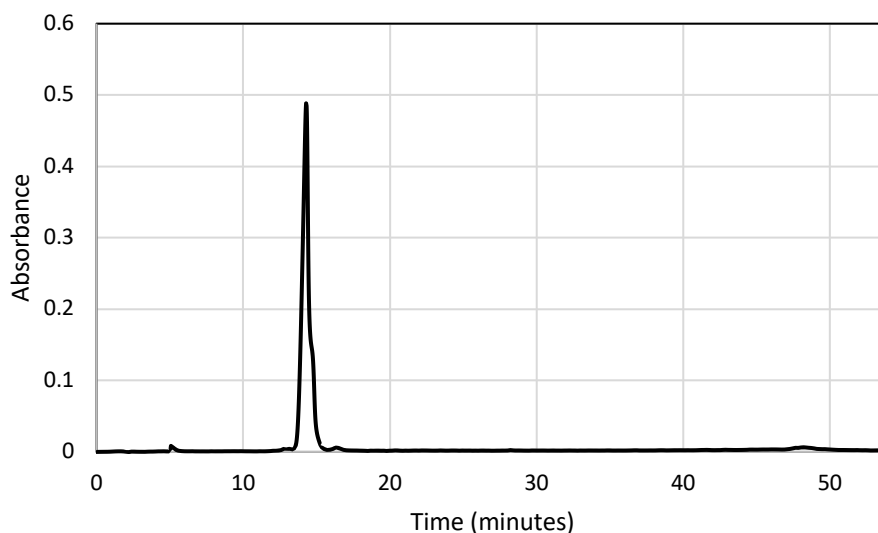ESI-MS calculated [M+2H$^+$]: 582.2564, found: 582.2573

Scheme S18. Synthesis of Fl-PPPP2

A 25 mL synthetic vessel charged with 500 mg (0.55 mmol) of 2-Chlorotrityl chloride resin was added Fmoc-D-Alanine-OH (1.1 eq, 188 mg, 0.605 mmol) and DIEA (4.4 eq, 420 uL, 2.42 mmol) in dry DCM (15 mL). The resin was agitated for 1 hour at ambient temperature and washed with MeOH and DCM (3 x 15 mL each). The Fmoc protecting group was removed with a 20% piperidine in DMF solution (15 mL) for 30 minutes at ambient temperature, then washed as previously stated. Fmoc-L-Lysine(Boc)-OH (3 eq, 257 mg, 1.65 mmol), Oxyma (3 eq, 243 mg, 1.65 mmol), and DIC (3 eq, 257 uL, 1.65 mmol) in

DMF (15 mL) were added to the reaction flask and agitated for 2 hours at ambient temperature. The Fmoc removal and coupling procedure was repeated as before using the same equivalencies with Fmoc-D-Glutamic acid α-amide and Fmoc-L-Alanine-OH. The Fmoc removal and coupling was repeated using eight Fmoc-Proline-OH (3 eq, 556 mg, 1.65 mmol) residues to yield Fmoc-PPPPPPPP-Tetra. The Fmoc group was removed and resin coupled with 5,6-carboxyfluorescein (2 eq, 413 mg, 1.1 mmol), HBTU (2 eq, 416 mg, 1.1 mmol), and DIEA (6 eq, 574 uL, 3.3 mmol) in DMF (15 mL) shaking over-night. The resin was washed as previously described. To remove the peptide from resin, a TFA cocktail solution (95 % TFA, 2.5% TIPS, and 2.5 % DCM) was added to the resin with agitation for 2 hours protected from light. The resin was filtered and resulting solution was concentrated *in vacuo*. The peptide was trituated with cold diethyl ether and purified using reverse phase HPLC using H_2O/MeOH to yield **Fl-PPPP2**. The sample was analyzed for purity using a Waters 1525 Binary HPLC Pump using a Phenomenex Luna 5u C8(2) 100A (250 x 4.60 mm) column; gradient elution with H_2O/CH_3CN.
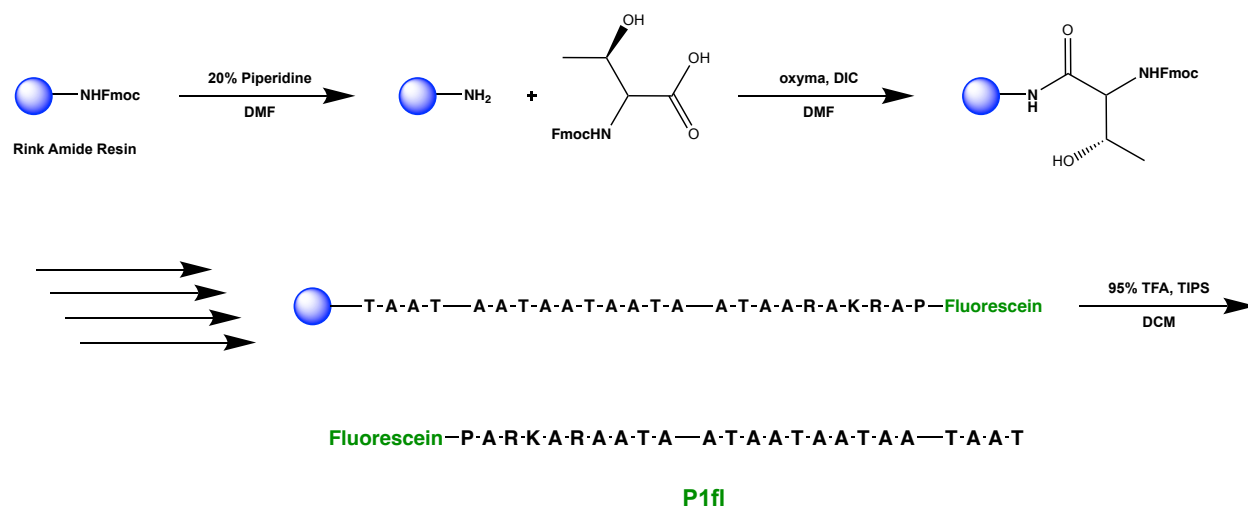
ESI-MS calculated [M+2H$^+$]: 776.3619, found: 776.3608
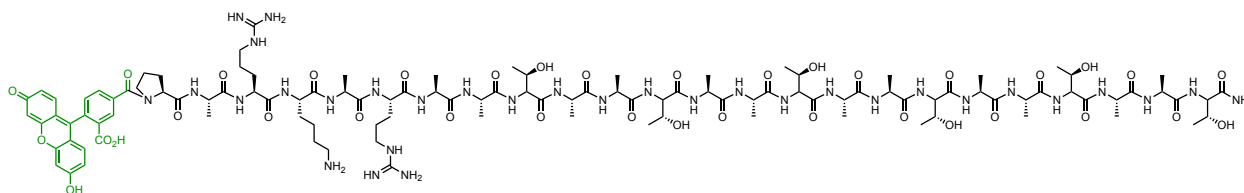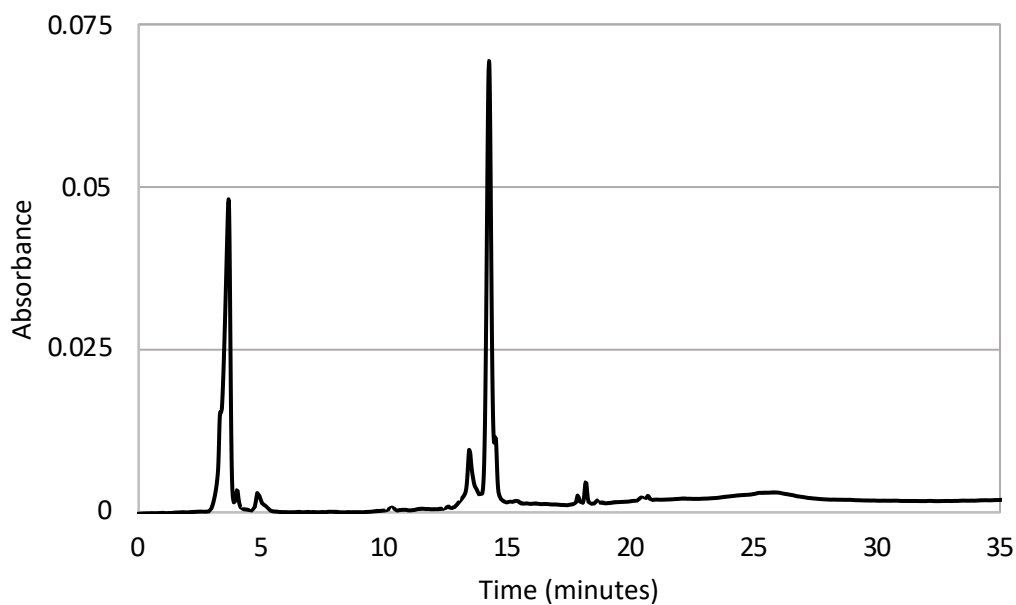
+ESI Scan (rt: 0.406-0.578 min, 32 scans) Frag=180.0V 18.d Subtract

x10 4

776.3608
776.8602
777.3600
777.8607
778.3609

Counts vs. Mass-to-Charge (m/z)

Scheme S19. Synthesis of Fl-YYYY1

Fl-YYYY1

A 25 mL synthetic vessel charged with 500 mg (0.55 mmol) of 2-Chlorotrityl chloride resin was added Fmoc-D-Alanine-OH (1.1 eq, 188 mg, 0.605 mmol) and DIEA (4.4 eq, 420 uL, 2.42 mmol) in dry DCM (15 mL). The resin was agitated for 1 hour at ambient temperature and washed with MeOH and DCM (3 x 15 mL each). The Fmoc protecting group was removed with a 20% piperidine in DMF solution (15 mL) for 30 minutes at ambient temperature, then washed as previously stated. Fmoc-L-Lysine(Boc)-OH (3 eq, 257 mg,

1.65 mmol), Oxyma (3 eq, 243 mg, 1.65 mmol), and DIC (3 eq, 257 uL, 1.65 mmol) in DMF (15 mL) were added to the reaction flask and agitated for 2 hours at ambient temperature. The Fmoc removal and coupling procedure was repeated as before using the same equivalencies with Fmoc-D-Glutamic acid α-amide and Fmoc-L-Alanine-OH. The Fmoc removal and coupling procedure was repeated using four Fmoc-L-Hyp(tBu)-OH (3 eq, 647 mg, 1.65 mmol) to yield Fmoc-YYYY-Tetra. The Fmoc group was removed and resin coupled with 5,6-carboxyfluorescein (2 eq, 413 mg, 1.1 mmol), HBTU (2 eq, 416 mg, 1.1 mmol), and DIEA (6 eq, 574 uL, 3.3 mmol) in DMF (15 mL) shaking over-night. The resin was washed as previously described. To remove the peptide from resin, a TFA cocktail solution (95 % TFA, 2.5% TIPS, and 2.5 % DCM) was added to the resin with agitation for 2 hours protected from light. The resin was filtered and resulting solution was concentrated *in vacuo*. The peptide was trituated with cold diethyl ether and purified using reverse phase HPLC using H_2O/MeOH to yield **Fl-YYYY1**. The sample was analyzed for purity using a Waters 1525 Binary HPLC Pump using a Phenomenex Luna 5u C8(2) 100A (250 x 4.60 mm) column; gradient elution with H_2O/CH_3CN.
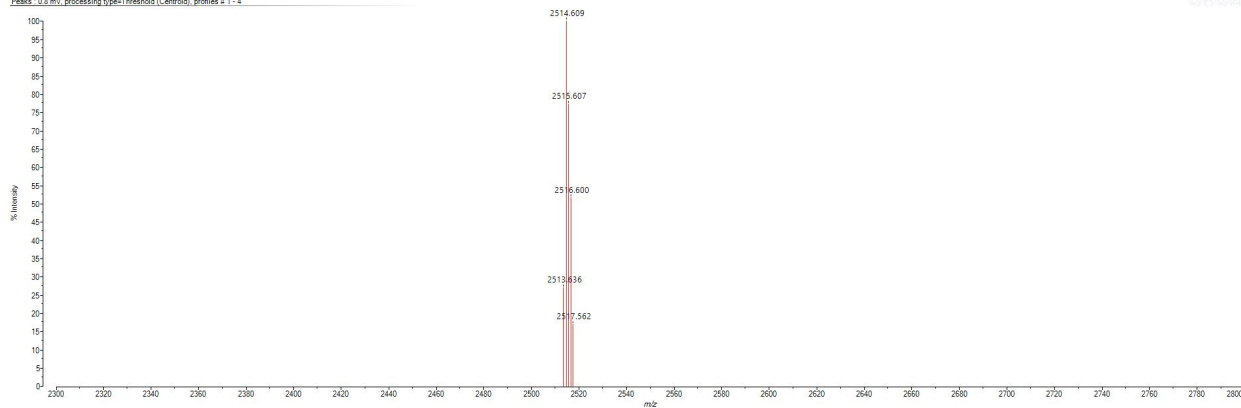
ESI-MS calculated [M+2H$^+$]: 614.2462, found: 614.2457

+ESI Scan (rt: 0.420-0.553 min, 25 scans) Frag=180.0V 19.d Subtract

Scheme S20. Synthesis of Fl-YYYY2

FI-YYYY2

A 25 mL synthetic vessel charged with 500 mg (0.55 mmol) of 2-Chlorotrityl chloride resin was added Fmoc-D-Alanine-OH (1.1 eq, 188 mg, 0.605 mmol) and DIEA (4.4 eq, 420 uL, 2.42 mmol) in dry DCM (15 mL). The resin was agitated for 1 hour at ambient temperature and washed with MeOH and DCM (3 x 15 mL each). The Fmoc protecting group was removed with a 20% piperidine in DMF solution (15 mL) for 30 minutes at ambient temperature, then washed as previously stated. Fmoc-L-Lysine(Boc)-OH (3 eq, 257 mg, 1.65 mmol), Oxyma (3 eq, 243 mg, 1.65 mmol), and DIC (3 eq, 257 uL, 1.65 mmol) in

DMF (15 mL) were added to the reaction flask and agitated for 2 hours at ambient temperature. The Fmoc removal and coupling procedure was repeated as before using the same equivalencies with Fmoc-D-Glutamic acid α-amide and Fmoc-L-Alanine-OH. The Fmoc removal and coupling procedure was repeated using eight Fmoc-L-Hyp(tBu)-OH (3 eq, 647 mg, 1.65 mmol) to yield Fmoc-YYYYYYYY-Tetra. The Fmoc group was removed and resin coupled with 5,6-carboxyfluorescein (2 eq, 413 mg, 1.1 mmol), HBTU (2 eq, 416 mg, 1.1 mmol), and DIEA (6 eq, 574 uL, 3.3 mmol) in DMF (15 mL) shaking over-night. The resin was washed as previously described. To remove the peptide from resin, a TFA cocktail solution (95 % TFA, 2.5% TIPS, and 2.5 % DCM) was added to the resin with agitation for 2 hours protected from light. The resin was filtered and resulting solution was concentrated *in vacuo*. The peptide was trituated with cold diethyl ether and purified using reverse phase HPLC using H_2O/MeOH to yield **Fl-YYYY2**. The sample was analyzed for purity using a Waters 1525 Binary HPLC Pump using a Phenomenex Luna 5u C8(2) 100A (250 x 4.60 mm) column; gradient elution with H_2O/CH_3CN.

ESI-MS calculated [M+2H$^+$]: 840.3416, found: 840.8410

+ESI Scan (rt: 0.431-0.509 min, 15 scans) Frag=180.0V 20.d Subtract
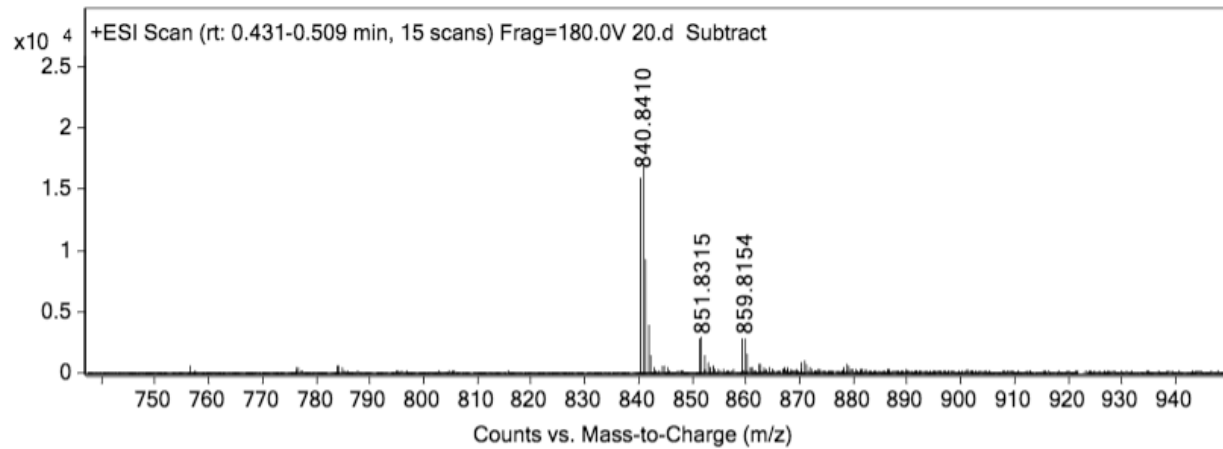
A.4 Synthesis and Characterization of Compounds in Chapter 3

Scheme S1. Synthesis of P1fl

Fluorescein—P·A·R·K·A·R·A·A·T·A—A·T·A·A·T·A·A·T·A·A—T·A·A·T

P1fl

A 25 mL vessel of a CEM Discover Bio Manual Peptide Synthesizer was charged with 500 mg (0.27 mmol) of Rink Amide resin. The Fmoc group was removed using a 20% piperidine in DMF solution (10 mL). Using Synergy software, the deprotection protocol was run. The piperidine solution was drained and the resin was washed with DMF (4 x 10 mL). Fmoc-Thr(tBu)-OH (5 eq, 321 mg, 1.35 mmol), 1 M Oxyma (5 eq, 1.35 mmol), and 1 M DIC (5 eq, 1.35 mmol) in DMF (10 mL) were added to the reaction flask and the coupling protocol was run. The amino acid solution was drained, and the resin was washed with DMF (2 x 10 mL). The Fmoc removal and coupling procedure was repeated as before using the same equivalencies for the following amino acids: AATAATAATAATAATAARAKRAP. The Fmoc group of Proline was removed, and resin was transferred to a 25 mL synthetic peptide vessel and coupled 5,6-carboxyfluorescein (3 eq, 304 mg, 0.81 mmol), HBTU (3 eq, 301 mg, 0.81 mmol), and DIEA (6 eq, 281 uL, 1.62 mmol) in DMF (15 mL) shaking over-night. The resin was washed with DCM and MeOH (3 x 15 mL each). To remove the peptide from resin, a TFA cocktail solution (95 % TFA, 2.5% TIPS, and 2.5 % DCM) was added to the resin with agitation for 2 hours protected from light. The resin was filtered and resulting solution was concentrated *in vacuo*. The peptide was trituated with cold diethyl ether and purified using reverse phase HPLC using H_2O/MeOH to yield **P1fl**. The sample was analyzed for purity using a Waters 1525 Binary HPLC Pump using a Phenomenex Luna 5u C8(2) 100A (250 x 4.60 mm)

column; gradient elution with H_2O/CH_3CN. Molecular weight was confirmed using a Shimadzu MALDI-TOF Mass Spectrometer (MALDI-8020).
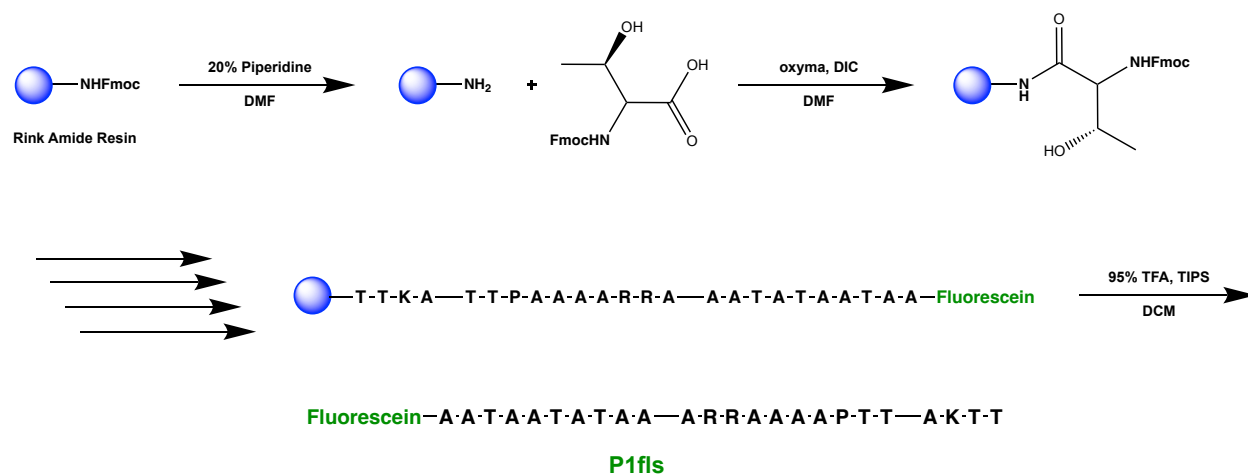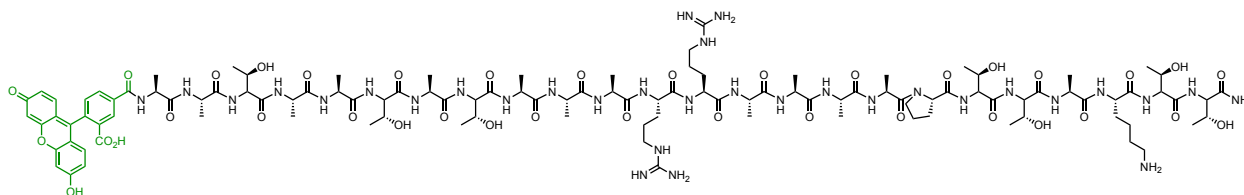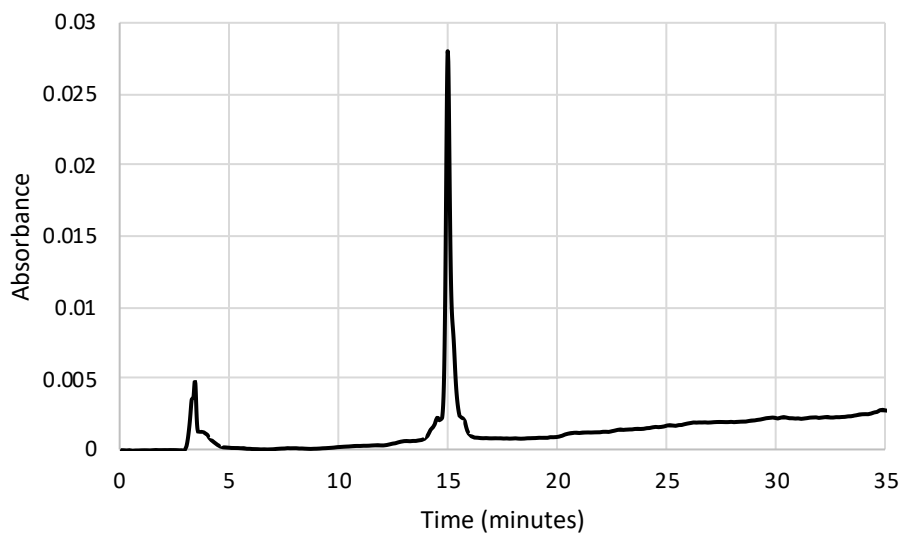

m/z calculated: 2514.223, found: 2514.609
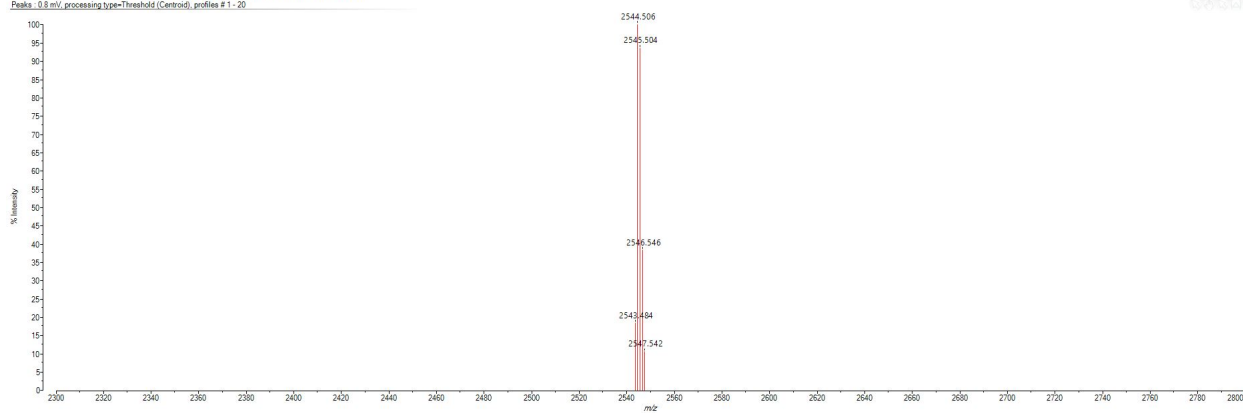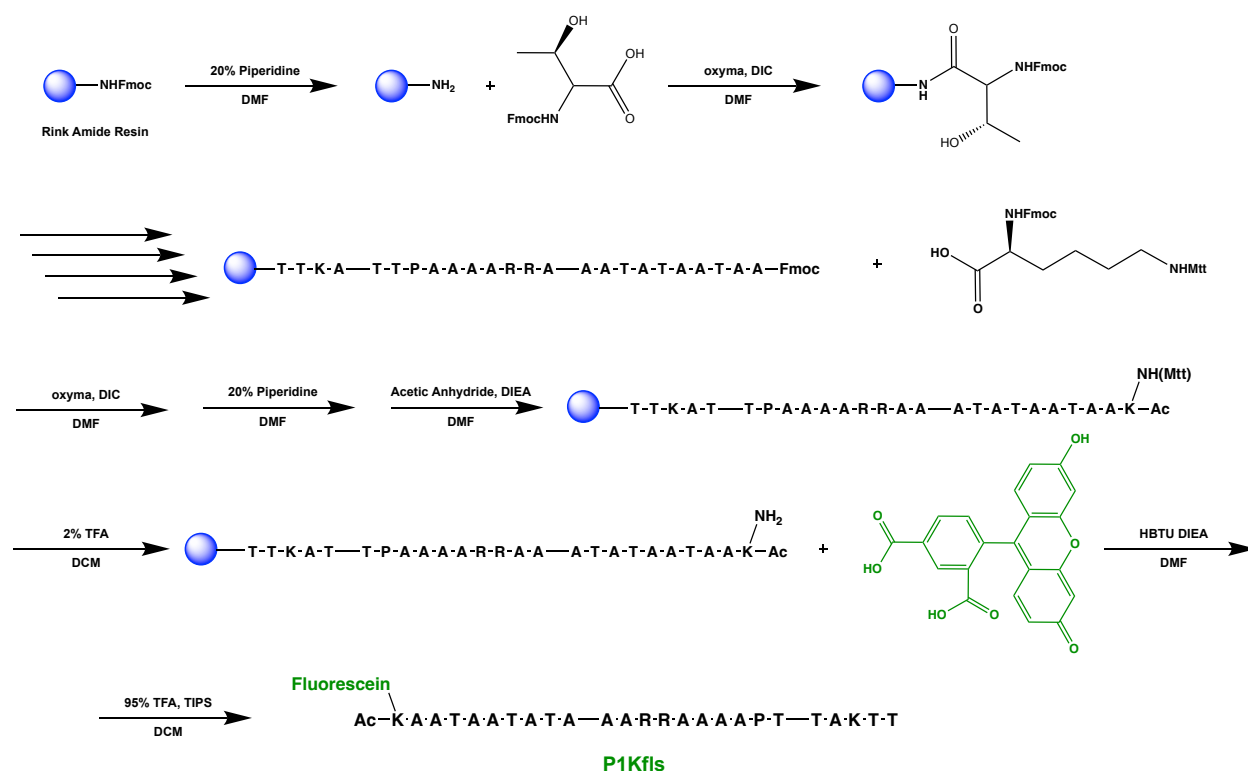
Scheme S2. Synthesis of P1Kfl

A 25 mL vessel of a CEM Discover Bio Manual Peptide Synthesizer was charged with 500 mg (0.27 mmol) of Rink Amide resin. The Fmoc group was removed using a 20% piperidine in DMF solution (10 mL). Using Synergy software, the deprotection protocol was run. The piperidine solution was drained and the resin was washed with DMF (4 x 10 mL). Fmoc-Thr(tBu)-OH (5 eq, 321 mg, 1.35 mmol), 1 M Oxyma (5 eq, 1.35 mmol), and 1 M DIC (5 eq, 1.35 mmol) in DMF (10 mL) were added to the reaction flask and the coupling protocol was run. The amino acid solution was drained, and the resin was washed with DMF (2 x 10 mL). The Fmoc removal and coupling procedure was repeated as before using the same equivalencies for the following amino acids: AATAATAATAATAATAARAKRAP. The Fmoc group of Proline was removed and Fmoc-L-Lysine(Mtt)-OH (5 eq, 505 mg, 1.35 mmol) was coupled. The resin was transferred to a 25 mL synthetic vessel and the N-terminus of the peptide was acetylated by removing the Fmoc group and then agitating the resin for 1 hour with a solution of 5% acetic anhydride (0.5 mL), 8.5% DIEA (0.85 mL), and 86.5% DMF (8.65 mL). The Mtt protecting group of L-Lysine(Mtt)-OH was removed by adding 10 mL of a TFA cocktail solution (1%

TFA, 2% TIPS in DCM) to the resin and agitating for 10 minutes protected from light. The solution was drained, and this procedure was repeated five additional times. The solution was then drained, rinsed with DMF, and washed as previously described. Upon Mtt removal, 5,6-carboxyfluorescein (3 eq, 304 mg, 0.81 mmol), HBTU (3 eq, 301 mg, 0.81 mmol), and DIEA (6 eq, 281 uL, 1.62 mmol) in DMF (15 mL) was agitated with the resin over-night. The resin was washed with DCM and MeOH (3 x 15 mL each). To remove the peptide from resin, a TFA cocktail solution (95 % TFA, 2.5% TIPS, and 2.5 % DCM) was added to the resin with agitation for 2 hours protected from light. The resin was filtered and resulting solution was concentrated *in vacuo*. The peptide was trituated with cold diethyl ether and purified using reverse phase HPLC using H_2O/MeOH to yield **P1Kfl**. The sample was analyzed for purity using a Waters 1525 Binary HPLC Pump using a Phenomenex Luna 5u C8(2) 100A (250 x 4.60 mm) column; gradient elution with H_2O/CH_3CN. Molecular weight was confirmed using a Shimadzu MALDI-TOF Mass Spectrometer (MALDI-8020).

m/z calculated: 2684.339, found: 2684.046

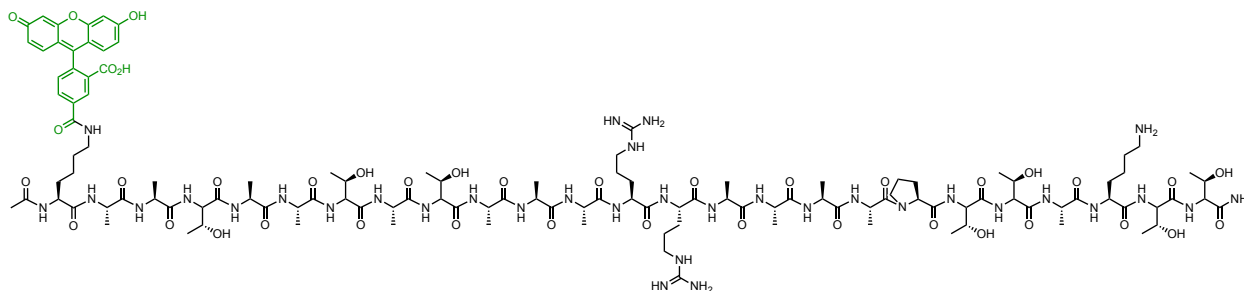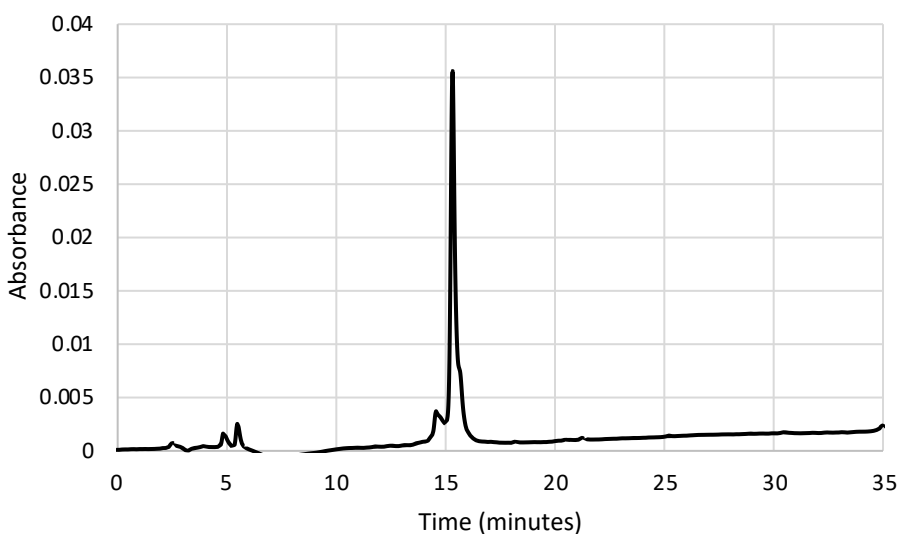**Scheme S3.** Synthesis of P1fls

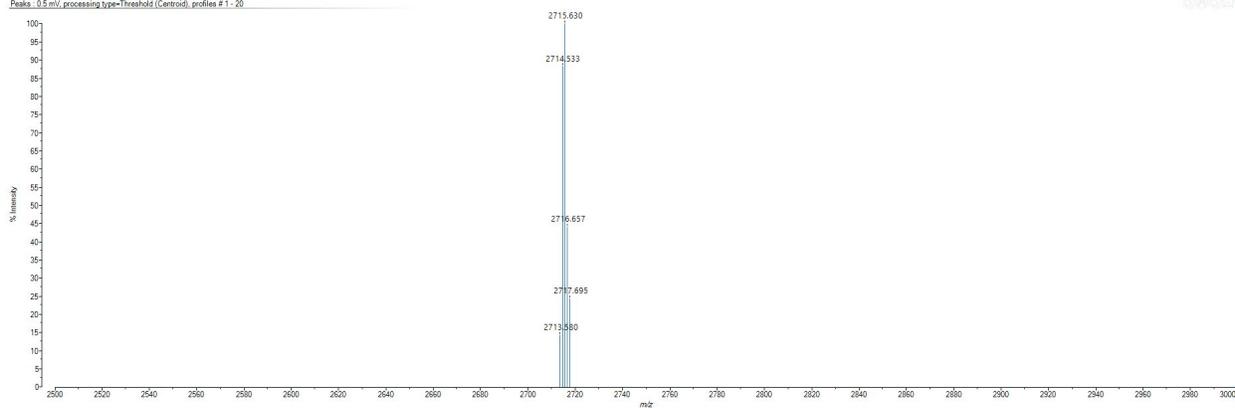Fluorescein—A·A·T·A·A·T·A·T·A·A—A·R·R·A·A·A·A·P·T·T—A·K·T·T

P1fls

A 25 mL vessel of a CEM Discover Bio Manual Peptide Synthesizer was charged with 500 mg (0.27 mmol) of Rink Amide resin. The Fmoc group was removed using a 20% piperidine in DMF solution (10 mL). Using Synergy software, the deprotection protocol was run. The piperidine solution was drained and the resin was washed with DMF (4 x 10 mL). Fmoc-Thr(tBu)-OH (5 eq, 321 mg, 1.35 mmol), 1 M Oxyma (5 eq, 1.35 mmol), and 1 M DIC (5 eq, 1.35 mmol) in DMF (10 mL) were added to the reaction flask and the coupling protocol was run. The amino acid solution was drained, and the resin was washed with DMF (2 x 10 mL). The Fmoc removal and coupling procedure was repeated as before using the same equivalencies for the following amino acids: TKATTPAAAARRAAATATAATAA. The Fmoc group of Alanine was removed, and resin was transferred to a 25 mL synthetic peptide vessel and coupled 5,6-carboxyfluorescein (3 eq, 304 mg, 0.81 mmol), HBTU (3 eq, 301 mg, 0.81 mmol), and DIEA (6 eq, 281 uL, 1.62 mmol) in DMF (15 mL) shaking over-night. The resin was washed with DCM and MeOH (3 x 15 mL each). To remove the peptide from resin, a TFA cocktail solution (95 % TFA, 2.5% TIPS, and 2.5 % DCM) was added to the resin with agitation for 2 hours protected from light. The resin was filtered and resulting solution was concentrated *in vacuo*. The peptide was trituated with cold diethyl ether and purified using reverse phase HPLC using H_2O/MeOH to yield P1fls. The sample was analyzed for purity using a Waters 1525 Binary HPLC Pump using a Phenomenex Luna 5u C8(2) 100A (250 x 4.60 mm) column; gradient elution with H_2O/CH_3CN. Molecular weight was confirmed using a Shimadzu MALDI-TOF Mass Spectrometer (MALDI-8020).
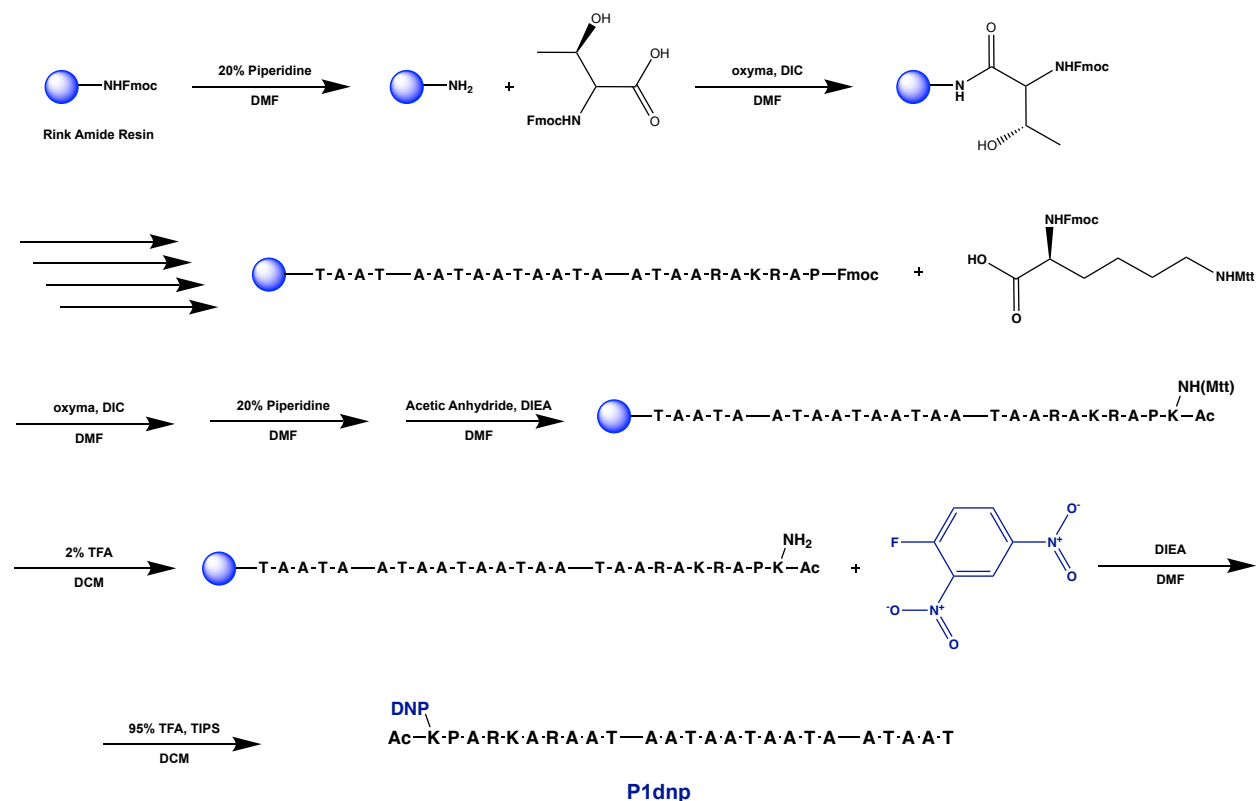
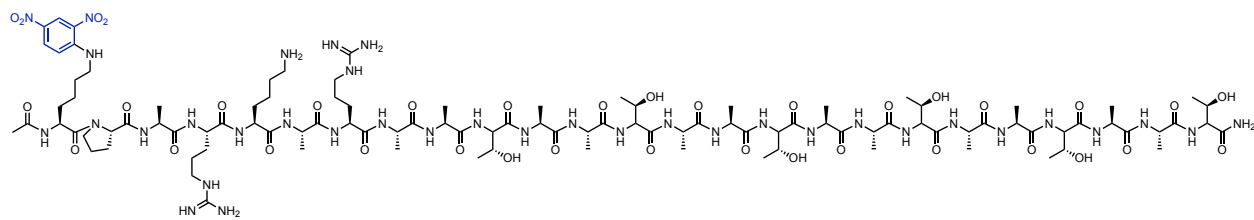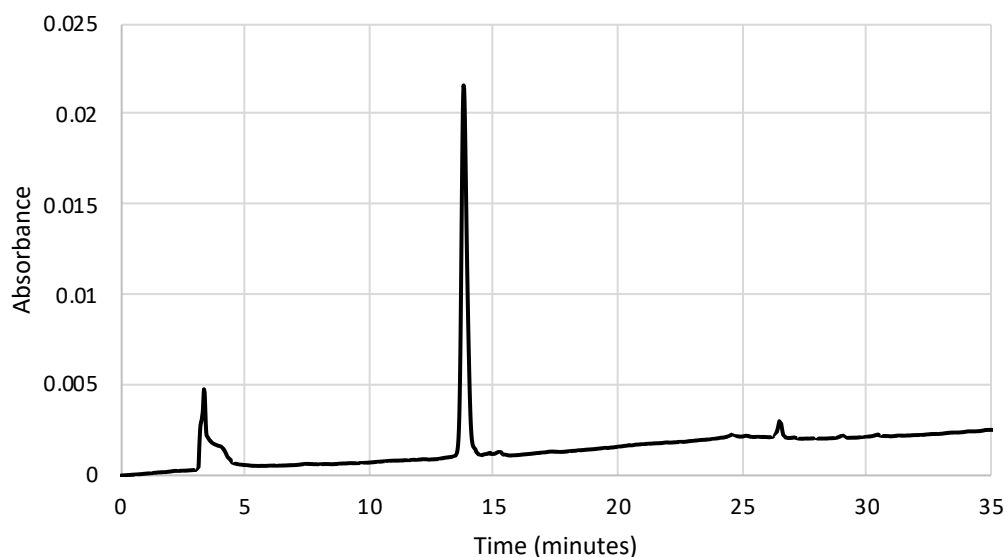*m/z* calculated: 2544.249, found: 2544.506
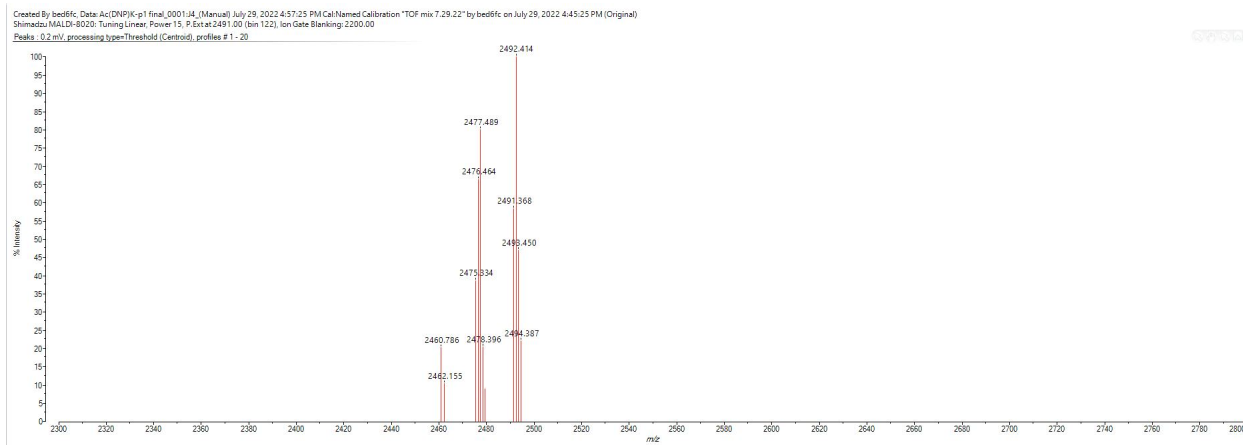
Scheme S4. Synthesis of P1Kfls

P1Kfls

A 25 mL vessel of a CEM Discover Bio Manual Peptide Synthesizer was charged with 500 mg (0.27 mmol) of Rink Amide resin. The Fmoc group was removed using a 20% piperidine in DMF solution (10 mL). Using Synergy software, the deprotection protocol was run. The piperidine solution was drained and the resin was washed with DMF (4 x 10 mL). Fmoc-Thr(tBu)-OH (5 eq, 321 mg, 1.35 mmol), 1 M Oxyma (5 eq, 1.35 mmol), and 1 M DIC (5 eq, 1.35 mmol) in DMF (10 mL) were added to the reaction flask and the coupling protocol was run. The amino acid solution was drained, and the resin was washed with DMF (2 x 10 mL). The Fmoc removal and coupling procedure was repeated as before using the same equivalencies for the following amino acids: TKATTPAAAARRAAATATAATAA. The Fmoc group of Alanine was removed and Fmoc-L-Lysine(Mtt)-OH (5 eq, 505 mg, 1.35 mmol) was coupled. The resin was transferred to a 25 mL synthetic vessel and the N-terminus of the peptide was acetylated by removing the Fmoc group and then agitating the resin for 1 hour with a solution of 5% acetic anhydride (0.5 mL), 8.5% DIEA (0.85 mL), and 86.5% DMF (8.65 mL). The Mtt protecting group of L-Lysine(Mtt)-OH was removed by adding 10 mL of a TFA cocktail solution (1%
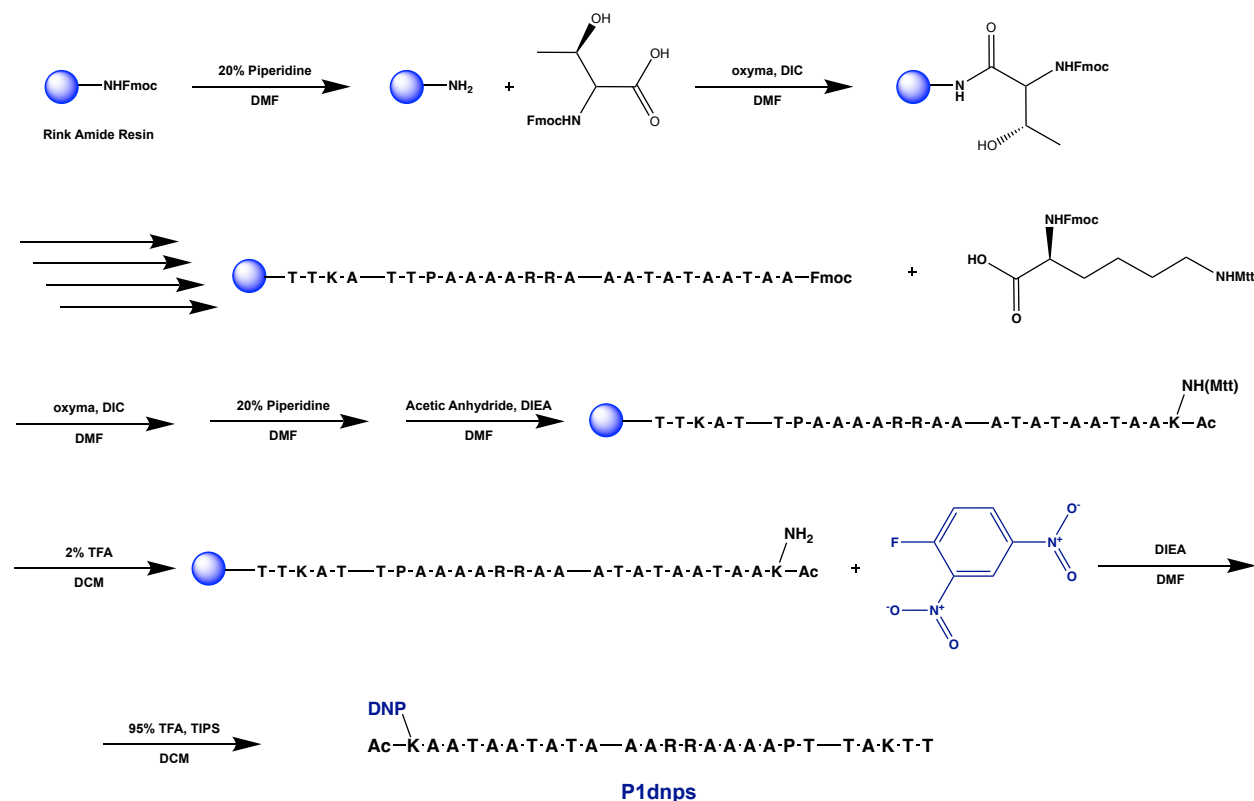
TFA, 2% TIPS in DCM) to the resin and agitating for 10 minutes protected from light. The solution was drained, and this procedure was repeated five additional times. The solution was then drained, rinsed with DMF, and washed as previously described. Upon Mtt removal, 5,6-carboxyfluorescein (3 eq, 304 mg, 0.81 mmol), HBTU (3 eq, 301 mg, 0.81 mmol), and DIEA (6 eq, 281 uL, 1.62 mmol) in DMF (15 mL) was agitated with the resin over-night. The resin was washed with DCM and MeOH (3 x 15 mL each). To remove the peptide from resin, a TFA cocktail solution (95 % TFA, 2.5% TIPS, and 2.5 % DCM) was added to the resin with agitation for 2 hours protected from light. The resin was filtered and resulting solution was concentrated *in vacuo*. The peptide was trituated with cold diethyl ether and purified using reverse phase HPLC using H_2O/MeOH to yield **P1Kfls**. The sample was analyzed for purity using a Waters 1525 Binary HPLC Pump using a Phenomenex Luna 5u C8(2) 100A (250 x 4.60 mm) column; gradient elution with H_2O/CH_3CN. Molecular weight was confirmed using a Shimadzu MALDI-TOF Mass Spectrometer (MALDI-8020).

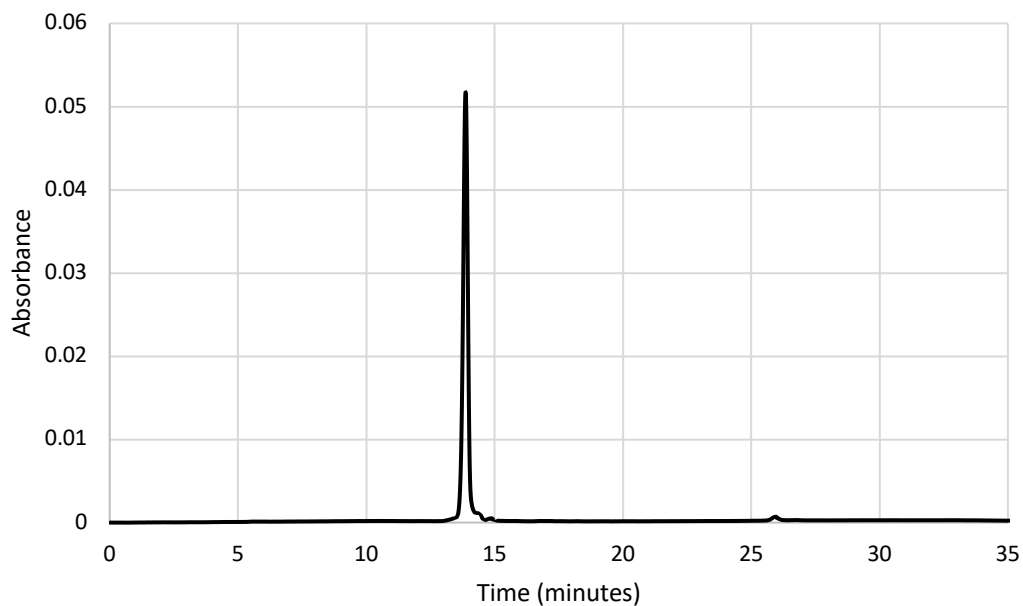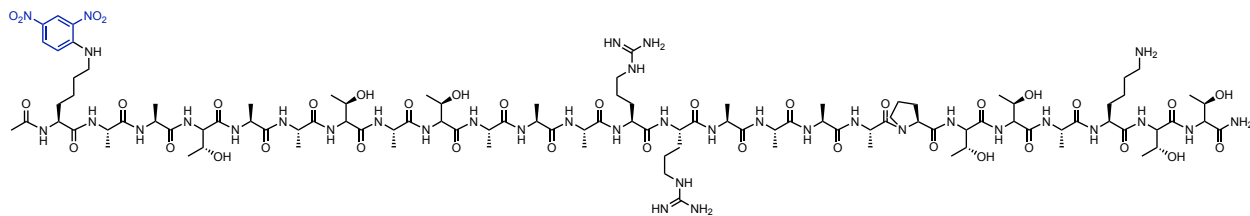*m/z* calculated: 2714.350, found: 2714.533

Scheme S5. Synthesis of P1dnp

P1dnp

A 25 mL vessel of a CEM Discover Bio Manual Peptide Synthesizer was charged with 500 mg (0.27 mmol) of Rink Amide resin. The Fmoc group was removed using a 20% piperidine in DMF solution (10 mL). Using Synergy software, the deprotection protocol was run. The piperidine solution was drained and the resin was washed with DMF (4 x 10 mL). Fmoc-Thr(tBu)-OH (5 eq, 321 mg, 1.35 mmol), 1 M Oxyma (5 eq, 1.35 mmol), and 1 M DIC (5 eq, 1.35 mmol) in DMF (10 mL) were added to the reaction flask and the coupling protocol was run. The amino acid solution was drained, and the resin was washed with DMF (2 x 10 mL). The Fmoc removal and coupling procedure was repeated as before using the same equivalencies for the following amino acids: AATAATAATAATAATAARAKRAP. The Fmoc group of Proline was removed and Fmoc-L-Lysine(Mtt)-OH (5 eq, 505 mg, 1.35 mmol) was coupled. The resin was transferred to a 25 mL synthetic vessel and the N-terminus of the peptide was acetylated by removing the Fmoc group and then agitating the resin for 1 hour with a solution of 5% acetic anhydride (0.5 mL), 8.5% DIEA (0.85 mL), and 86.5% DMF (8.65 mL). The Mtt protecting group of L-Lysine(Mtt)-OH was removed by adding 10 mL of a TFA cocktail solution (1%

TFA, 2% TIPS in DCM) to the resin and agitating for 10 minutes protected from light. The solution was drained, and this procedure was repeated five additional times. The solution was then drained, rinsed with DMF, and washed as previously described. Upon Mtt removal, 2,4-dinitrofluorobenzene (3 eq, 100 uL, 1.35 mmol) and DIEA (6 eq, 467 uL, 1.62 mmol) in DMF (15 mL) was agitated with the resin for 2 hours protected from light. The resin was washed with DCM and MeOH (3 x 15 mL each). To remove the peptide from resin, a TFA cocktail solution (95 % TFA, 2.5% TIPS, and 2.5 % DCM) was added to the resin with agitation for 2 hours protected from light. The resin was filtered and resulting solution was concentrated *in vacuo*. The peptide was trituated with cold diethyl ether and purified using reverse phase HPLC using H_2O/MeOH to yield **P1dnp**. The sample was analyzed for purity using a Waters 1525 Binary HPLC Pump using a Phenomenex Luna 5u C8(2) 100A (250 x 4.60 mm) column; gradient elution with H_2O/CH_3CN. Molecular weight was confirmed using a Shimadzu MALDI-TOF Mass Spectrometer (MALDI-8020).

m/z calculated: 2492.293, found: 2492.414

Created By bed6fc, Data: Ac(DNP)K-p1 final_0001:J4_(Manual) July 29, 2022 4:57:25 PM Cal:Named Calibration "TOF mix 7.29.22" by bed6fc on July 29, 2022 4:45:25 PM (Original)
Shimadzu MALDI-8020: Tuning Linear, Power 15, P.Ext at 2491.00 (bin 122), Ion Gate Blanking: 2200.00
Peaks : 0.2 mV, processing type=Threshold (Centroid), profiles # 1 - 20

Scheme S6. Synthesis of P1dnps

A 25 mL vessel of a CEM Discover Bio Manual Peptide Synthesizer was charged with 500 mg (0.27 mmol) of Rink Amide resin. The Fmoc group was removed using a 20% piperidine in DMF solution (10 mL). Using Synergy software, the deprotection protocol was run. The piperidine solution was drained and the resin was washed with DMF (4 x 10 mL). Fmoc-Thr(tBu)-OH (5 eq, 321 mg, 1.35 mmol), 1 M Oxyma (5 eq, 1.35 mmol), and 1 M DIC (5 eq, 1.35 mmol) in DMF (10 mL) were added to the reaction flask and the coupling protocol was run. The amino acid solution was drained, and the resin was washed with DMF (2 x 10 mL). The Fmoc removal and coupling procedure was repeated as before using the same equivalencies for the following amino acids: TKATTPAAAARRAAATATAATAA. The Fmoc group of Alanine was removed and Fmoc-L-Lysine(Mtt)-OH (5 eq, 505 mg, 1.35 mmol) was coupled. The resin was transferred to a 25 mL synthetic vessel and the N-terminus of the peptide was acetylated by removing the Fmoc group and then agitating the resin for 1 hour with a solution of 5% acetic anhydride (0.5 mL), 8.5% DIEA (0.85 mL), and 86.5% DMF (8.65 mL). The Mtt protecting group of L-Lysine(Mtt)-OH was removed by adding 10 mL of a TFA cocktail solution (1%

TFA, 2% TIPS in DCM) to the resin and agitating for 10 minutes protected from light. The solution was drained, and this procedure was repeated five additional times. The solution was then drained, rinsed with DMF, and washed as previously described. Upon Mtt removal, 2,4-dinitrofluorobenzene (3 eq, 100 uL, 1.35 mmol) and DIEA (6 eq, 467 uL, 1.62 mmol) in DMF (15 mL) was agitated with the resin for 2 hours protected from light. The resin was washed with DCM and MeOH (3 x 15 mL each). To remove the peptide from resin, a TFA cocktail solution (95 % TFA, 2.5% TIPS, and 2.5 % DCM) was added to the resin with agitation for 2 hours protected from light. The resin was filtered and resulting solution was concentrated *in vacuo*. The peptide was trituated with cold diethyl ether and purified using reverse phase HPLC using H_2O/MeOH to yield **P1dnps**. The sample was analyzed for purity using a Waters 1525 Binary HPLC Pump using a Phenomenex Luna 5u C8(2) 100A (250 x 4.60 mm) column; gradient elution with H_2O/CH_3CN. Molecular weight was confirmed using a Shimadzu MALDI-TOF Mass Spectrometer (MALDI-8020).

m/z calculated: 2522.303, found: 2522.186

Scheme S7. Synthesis of P1tam

TAMRA−P·A·R·K·A·R·A·A·T·A—A·T·A·A·T·A·A·T·A·A—T·A·A·T
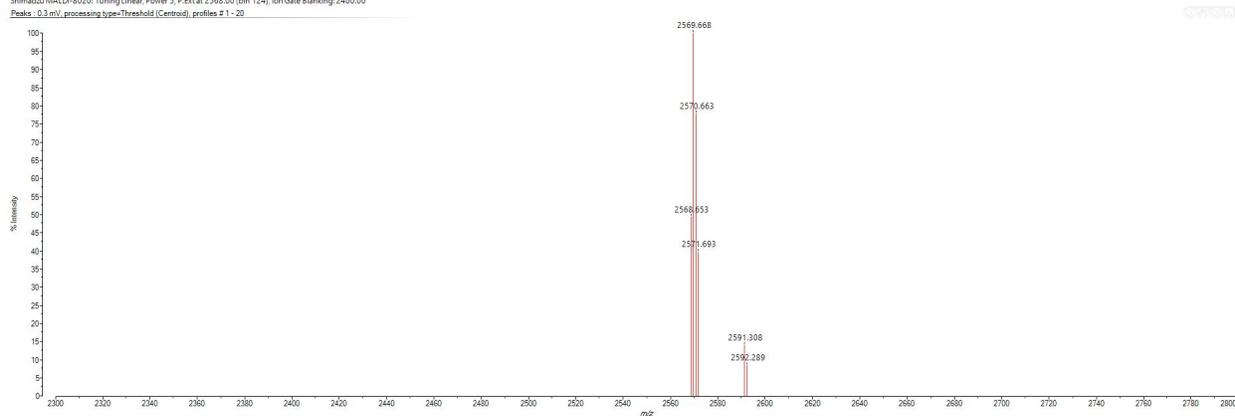
P1tam

A 25 mL vessel of a CEM Discover Bio Manual Peptide Synthesizer was charged with 500 mg (0.27 mmol) of Rink Amide resin. The Fmoc group was removed using a 20% piperidine in DMF solution (10 mL). Using Synergy software, the deprotection protocol was run. The piperidine solution was drained and the resin was washed with DMF (4 x 10 mL). Fmoc-Thr(tBu)-OH (5 eq, 321 mg, 1.35 mmol), 1 M Oxyma (5 eq, 1.35 mmol), and 1 M DIC (5 eq, 1.35 mmol) in DMF (10 mL) were added to the reaction flask and the coupling protocol was run. The amino acid solution was drained, and the resin was washed with DMF (2 x 10 mL). The Fmoc removal and coupling procedure was repeated as before using the same equivalencies for the following amino acids: AATAATAATAATAATAARAKRAP. The Fmoc group of Proline was removed, and resin was transferred to a 25 mL synthetic peptide vessel and coupled 5,6-carboxy-tetramethylrhodamine (3 eq, 304 mg, 0.81 mmol), HBTU (3 eq, 301 mg, 0.81 mmol), and DIEA (6 eq, 281 uL, 1.62 mmol) in DMF (15 mL) shaking over-night. The resin was washed with DCM and MeOH (3 x 15 mL each). To remove the peptide from resin, a TFA cocktail solution (95 % TFA, 2.5% TIPS, and 2.5 % DCM) was added to the resin with agitation for 2 hours protected from light. The resin was filtered and resulting solution was concentrated *in vacuo*. The peptide was trituated with cold diethyl ether and purified using reverse phase HPLC using H_2O/MeOH to yield **P1tam**. The sample was analyzed for purity using a Waters 1525 Binary HPLC Pump using a Phenomenex Luna 5u C8(2) 100A

(250 x 4.60 mm) column; gradient elution with H_2O/CH_3CN. Molecular weight was confirmed using a Shimadzu MALDI-TOF Mass Spectrometer (MALDI-8020).
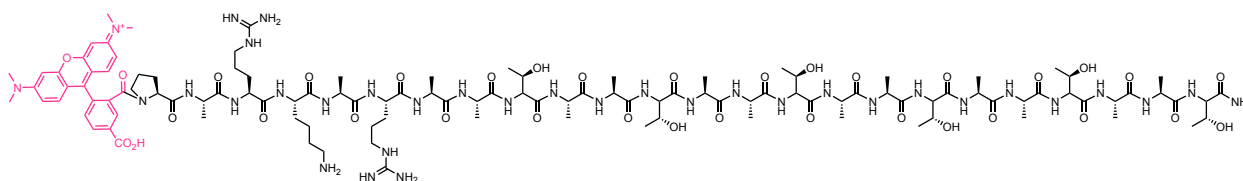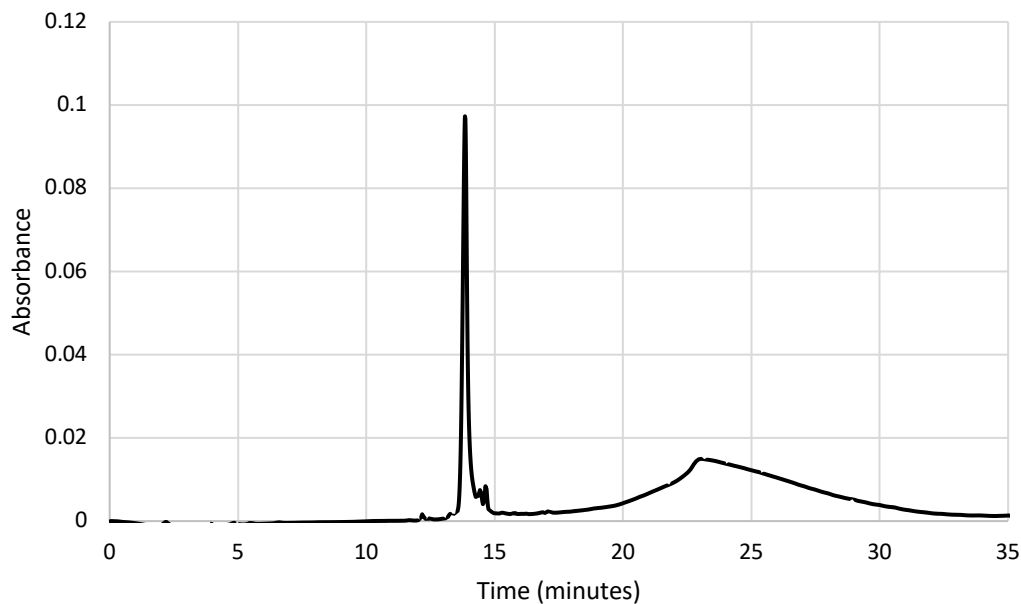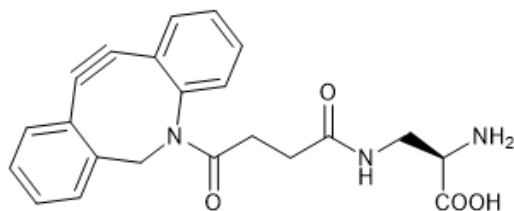

m/z calculated: 2569.335, found: 2569.668

A.5 Synthesis and Characterization of Compounds in Chapter 5

Scheme S1. Synthesis of D-DapD

To a 25 mL peptide synthesis vessel with 100 mg 2-Chlorotrityl chloride resin (0.142 mmol) resuspended in 15 mL dry dichloromethane, was added Nα-Boc-Nβ-Fmoc-D-2,3-diaminopropionic acid (D-Dap, 67 mg, 1.1 eq, 0.16 mmol), and DIEA (4.4 eq, 0.11 mL, 0.62 mmol). The resin was shaken for 1 hour at room temperature and washed with methanol and dichloromethane (3 times and 15 mL each). Fmoc protecting group was removed with 6M piperazine in N, N-Dimethylformamide (DMF, 15 mL) for 30 min at room temperature and washed as before. DBCO was coupled on the side chain of D-Dap on resin. 25-30 mg DBCO-NHS was dissolved in 1 mL dry DMF and added to the 25 mL peptide synthesis vessel with 100 mg equivalent 2-Chlorotrityl chloride resin with D-Dap resuspended in 2 mL DMF. The resin was shaken overnight at room temperature and washed with methanol and dichloromethane (3 times and 15 mL each). The resin was then added 20% trifluoroacetic acid (TFA) in dichloromethane after wash and shaken in room temperature for 1 h. The liquid phase was filtered and concentrated with nitrogen flow and added icy ether to precipitate the peptide. The ether layer was decanted, and the resulting solid was washed with icy ether and air dried. The crude material was purified with reverse phased high performance liquid chromatography (RP-HPLC) using a 40 to 100% linear gradient of methanol in H_2O/MeOH with 0.1% TFA to yield **D-DapD**. The sample was analyzed for purity using a Waters 1525 with a Phenomenex Luna 5μ C8(2) 100 Å (250 x 4.6 mm) column; gradient elution with H_2O/CH_3CN. Molecular weight was confirmed using an Agilent LC-QTOF (Agilent 1260 Infinity II Prime LC with Agilent 6545B QTOF).
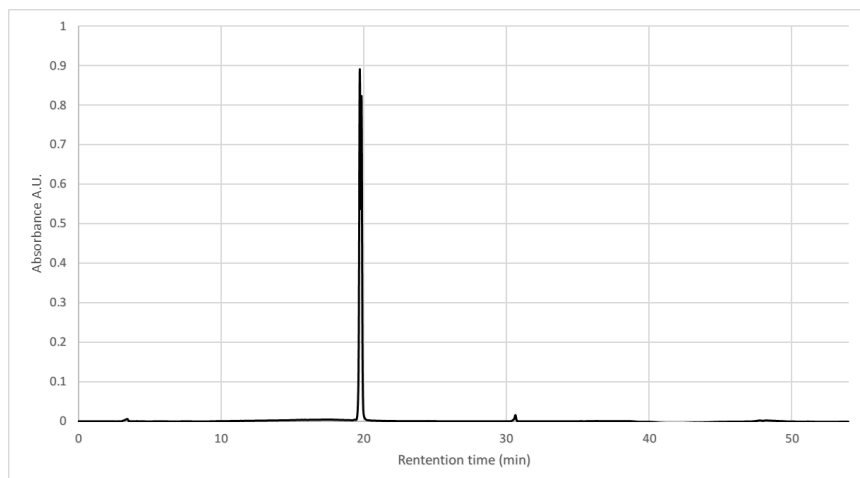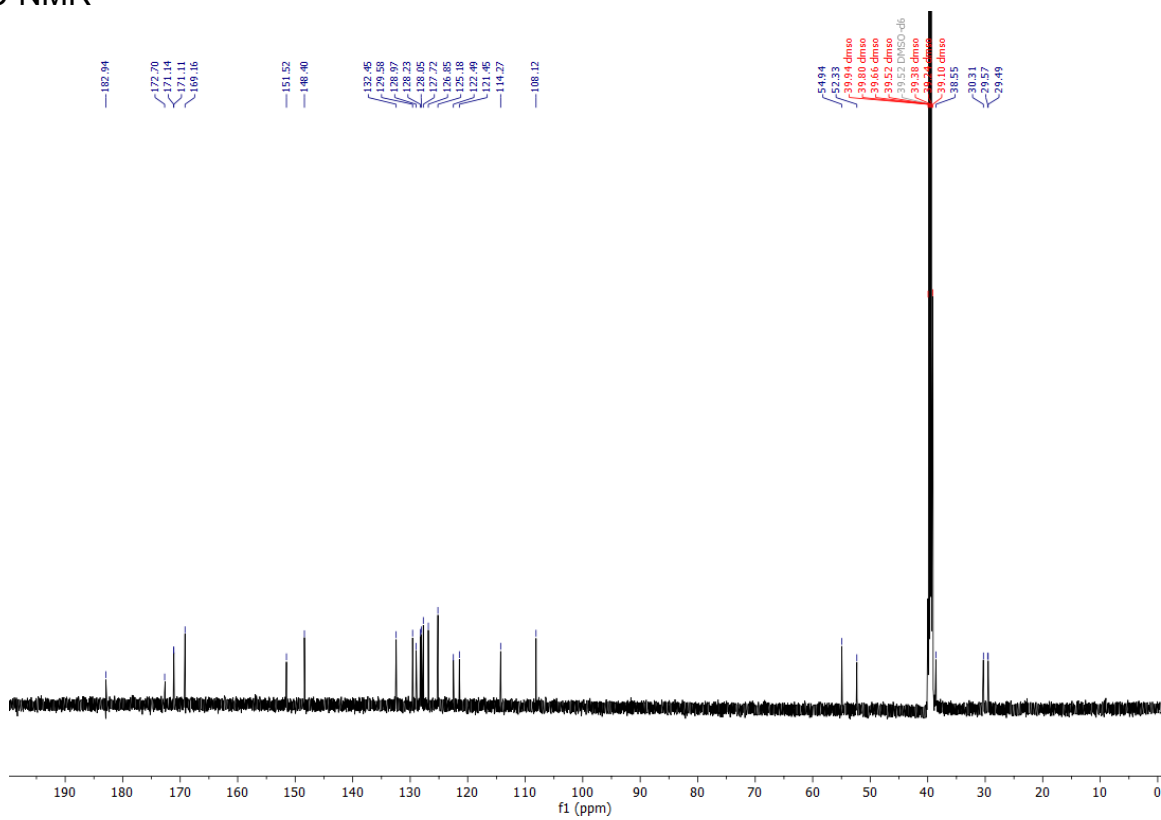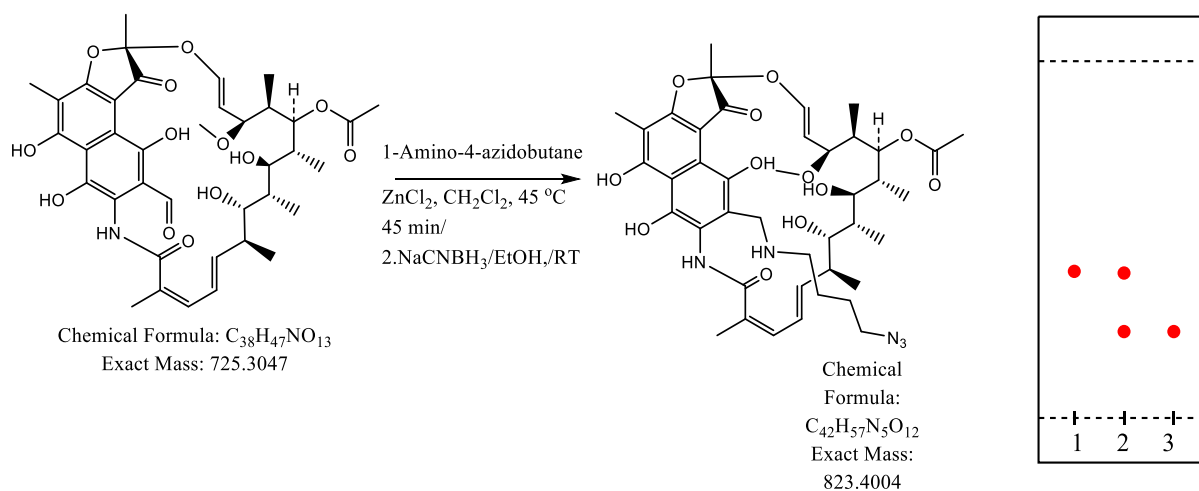
Calculated $(M+H)^+$, 392.1605, found: $(M+H)^+$ 392.1607.

Sample Name	D-Dap-DBCO	Position	P1-A1	Instrument Name	Instrument 1
User Name		Inj Vol	2	InjPosition	
Sample Type	Sample	IRM Calibration Status	All Ions Missed	Data Filename	D-Dap-DBCO-MW392-3.d
ACQ Method	Acq 100 MeOH Iso-ESI.m	Comment		Acquired Time	9/30/2022 3:53:18 PM (UTC-04:00)
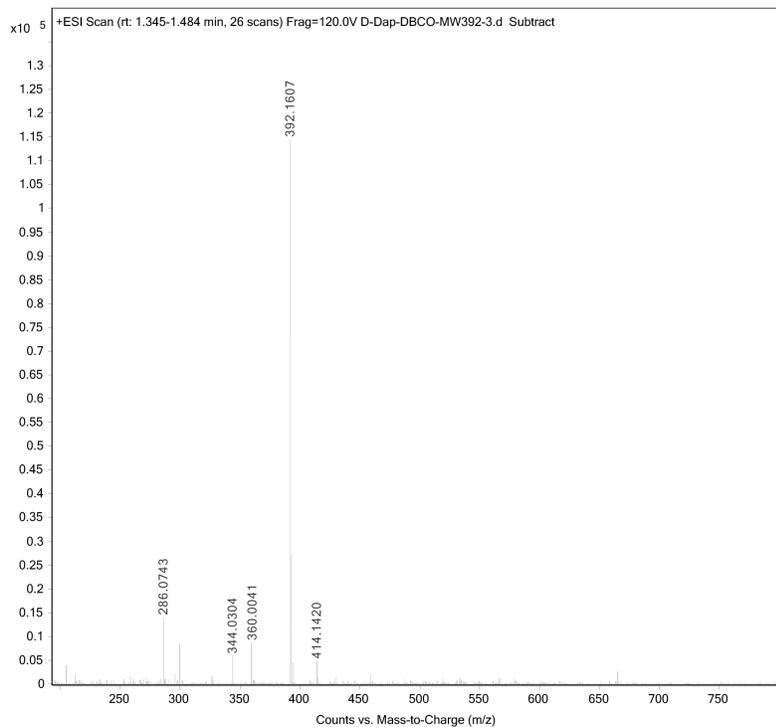
*Note: ^1H and ^{13}C-NMR spectra for all new compounds and intermediates for characterization were acquired on a Varian 600MHz spectrophotometer. All NMR spectra were analyzed using MestreNova software. Residual solvent signal from $CDCl_3$, CD_3OD and DMSO-d6 referenced to tetramethylsilane (TMS) were used as reference standards for defining chemical shifts of ^1H or ^{13}C spectra of compounds. Chemical

shifts are reported in δ ppm and coupling constants (J) are reported in Hertz [Hz]. Deuterated solvents were used as received from Cambridge Isotopes.

^{1}H-NMR

^{13}C-NMR

Scheme S2. Synthesis of Rifampicin-azidobutane

Chemical Formula: $C_{38}H_{47}NO_{13}$
Exact Mass: 725.3047

1-Amino-4-azidobutane
$ZnCl_2$, CH_2Cl_2, 45 °C
45 min/
2.$NaCNBH_3$/EtOH,/RT

Chemical Formula: $C_{42}H_{57}N_5O_{12}$
Exact Mass: 823.4004

Rifamycine aldehyde (72.5mg. 0.1 mmol) dissolved in 5.0mL of anhydrous methylene chloride in 50 mL RB flask equipped with reflux condenser, to this solution was added 1-amino-4-azidobutane (17.1 mg, 0.15 mmol), followed by $ZnCl_2$ (11.0mg, at room temperature and the mixture was refluxed at 45 °C in an oil bath for 45 minutes. The mixture was the allowed cooled to room temperature. The solvents were evaporated, and crude material as is used for reduction of iminium. The crude material was dissolved in ethanol (200% proof, 2.5mL), sodium cyanoborohydride (10.7 mg, 0.17mmol) was added to it and stirred the mixture at room temperature for 2 hr. TLC analysis of crude material indicated complete conversion starting material (Rt ~0.4) to polar new compound (Rt ~0.2) in EtOAc:methanol (95:5) . The volatiles were removed under vacuo using rotary evaporator. The remaining residue was dissolved in EtOAc and purified by column chromatography over silica gel using gradient ranging from ethyl acetate to 3% methanol EtOAc. Fractions showing homogeneity on TLC were combined and concentrated under reduced pressure to yield red solid (65.1 mg, 79%). Further purification with reverse phase HPLC (80:20; Water;Methanol) afforded pure compound used for assay.

Molecular weight was confirmed using an Agilent LC-QTOF (Agilent 1260 Infinity II Prime LC with Agilent 6545B QTOF).
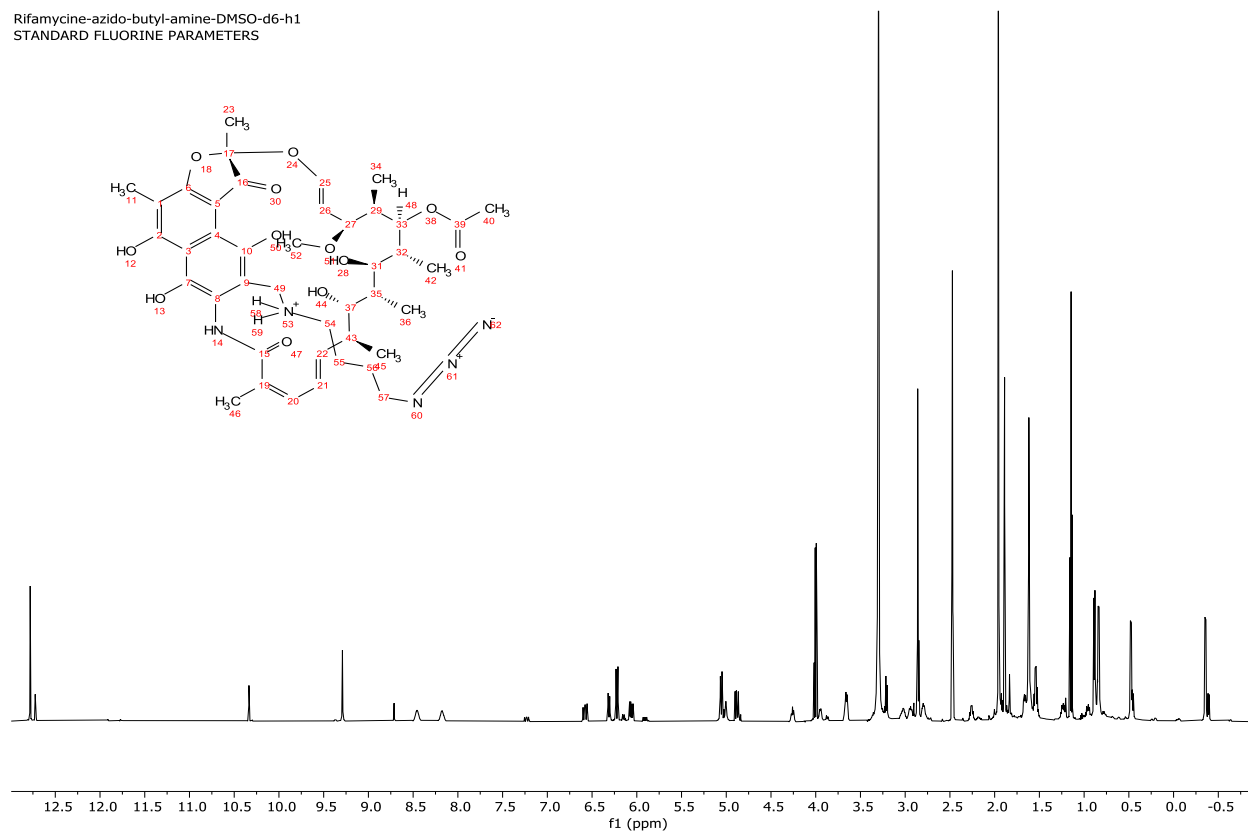
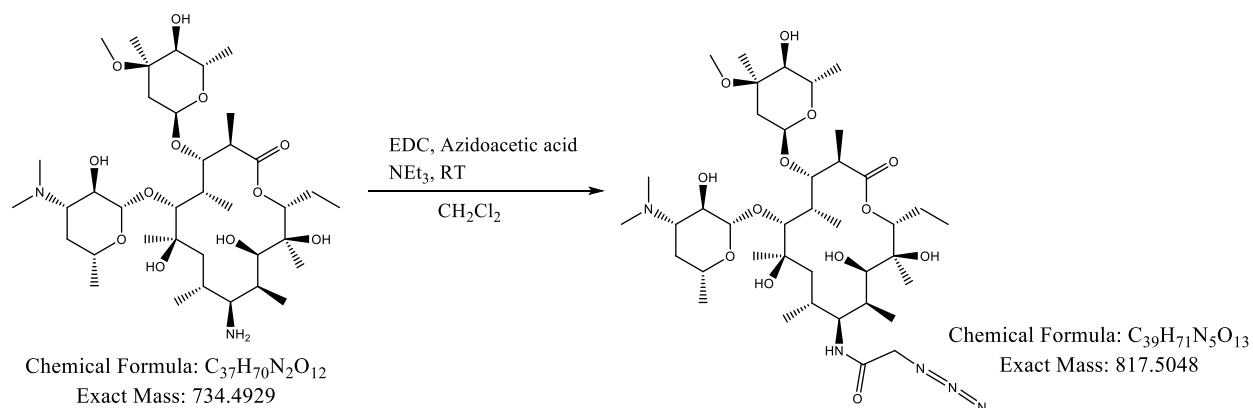Calculated m/z,824.534, found m/z, 824.4131

Sample Name	MDC Rifampicin azide	Position	P1-A4	Instrument Name	Instrument 1
User Name		Inj Vol	1	InjPosition	
Sample Type	Sample	IRM Calibration Status	Success	Data Filename	MDC rifampicin azide 1.3ul injection.d
ACQ Method	Acq 80_20 MeOH_H2O Iso.m	Comment		Acquired Time	8/26/2022 2:37:15 PM (UTC-04:00)

+ESI Scan (rt: 0.586-0.985 min, 73 scans) Frag=175.0V MDC rifampicin azide 1.3ul injection.d Subtract
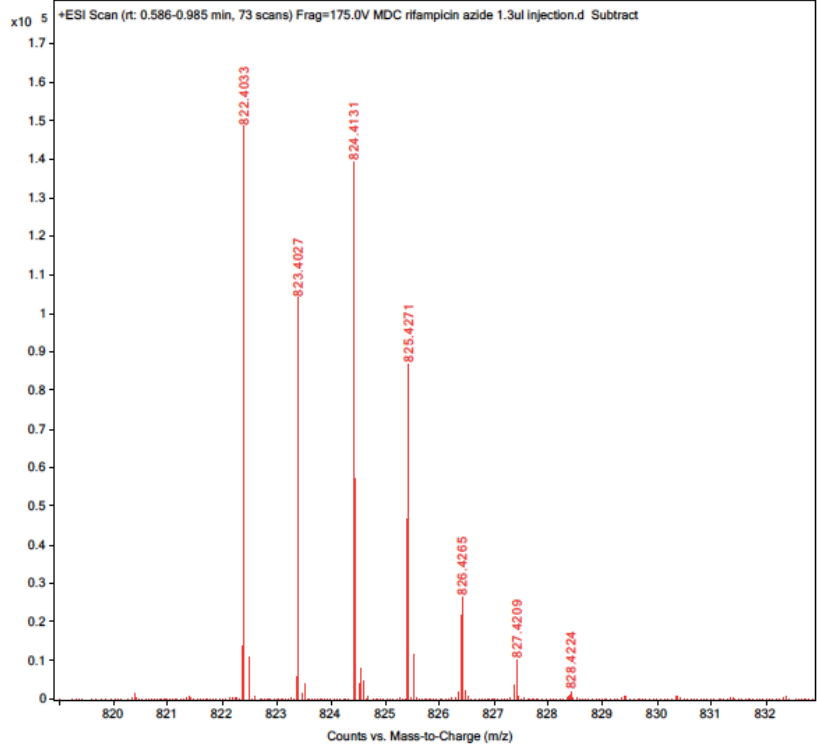
^{1}H-NMR

Rifamycine-azido-butyl-amine-DMSO-d6-h1
STANDARD FLUORINE PARAMETERS

Scheme S3. Synthesis of Erythromycin-azidoacetamide

EDC, Azidoacetic acid
NEt$_3$, RT

CH$_2$Cl$_2$

Chemical Formula: $C_{37}H_{70}N_2O_{12}$
Exact Mass: 734.4929

Chemical Formula: $C_{39}H_{71}N_5O_{13}$
Exact Mass: 817.5048

Erythromycin (25.1 mg, 0.034mmol) was dissolved in methylene chloride (5 mL), subsequently azido acetic acid (3.9 mg, 0.0386 mmol), EDC (11.5 mg) and triethyl amine (25.0ul) were added and mixture was stirred at room temperature for overnight (16hr). Next day, the solvents were evaporated under reduced pressure using rotary evaporator, the leftover crude material was purified by gradient reverse phase HPLC (C8, Water:MeOH; 95:5). The homogenous fractions collected at 205nm, were concentrated to yield pure compound.

Molecular weight was confirmed using an Agilent LC-QTOF (Agilent 1260 Infinity II Prime LC with Agilent 6545B QTOF).
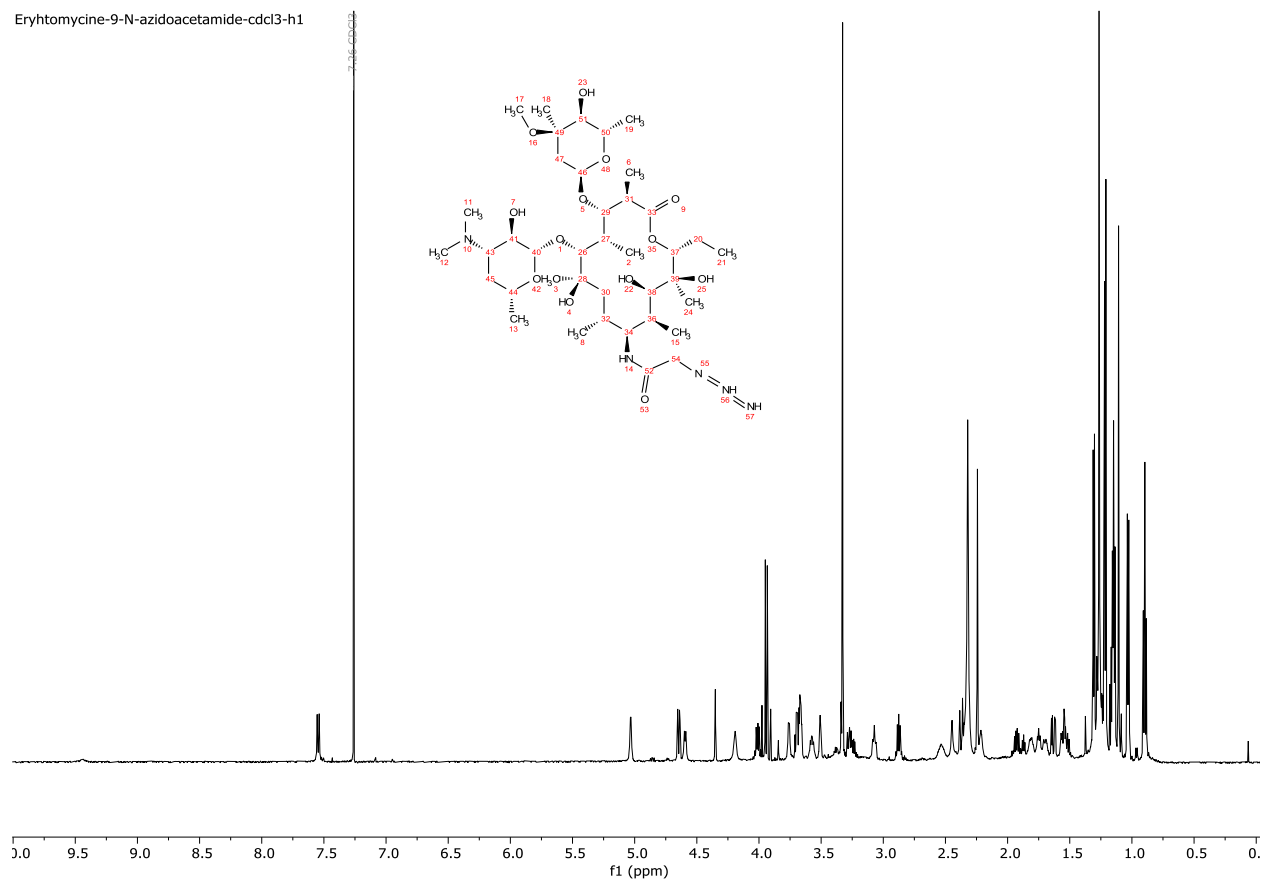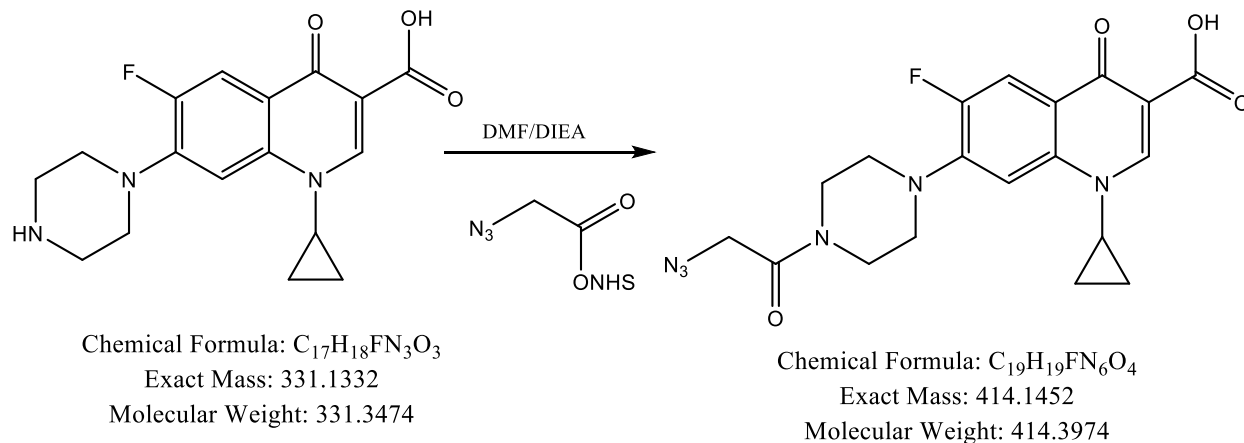
Calculated (M+D)$^+$, 819.5208, found (M+D)$^+$, 819.5321

Sample Name	MDC erythromycin azide	Position	P1-A3	Instrument Name	Instrument 1
User Name		Inj Vol	1	InjPosition	
Sample Type	Sample	IRM Calibration Status	Success	Data Filename	MDC erythro 1uL 8.26.22.d
ACQ Method	Acq 80_20 MeOH_H2O Iso.m	Comment		Acquired Time	8/26/2022 12:29:12 PM (UTC-04:00)

+ESI Scan (rt: 0.546-0.773 min, 42 scans) Frag=175.0V MDC erythro 1uL 8.26.22.d Subtract
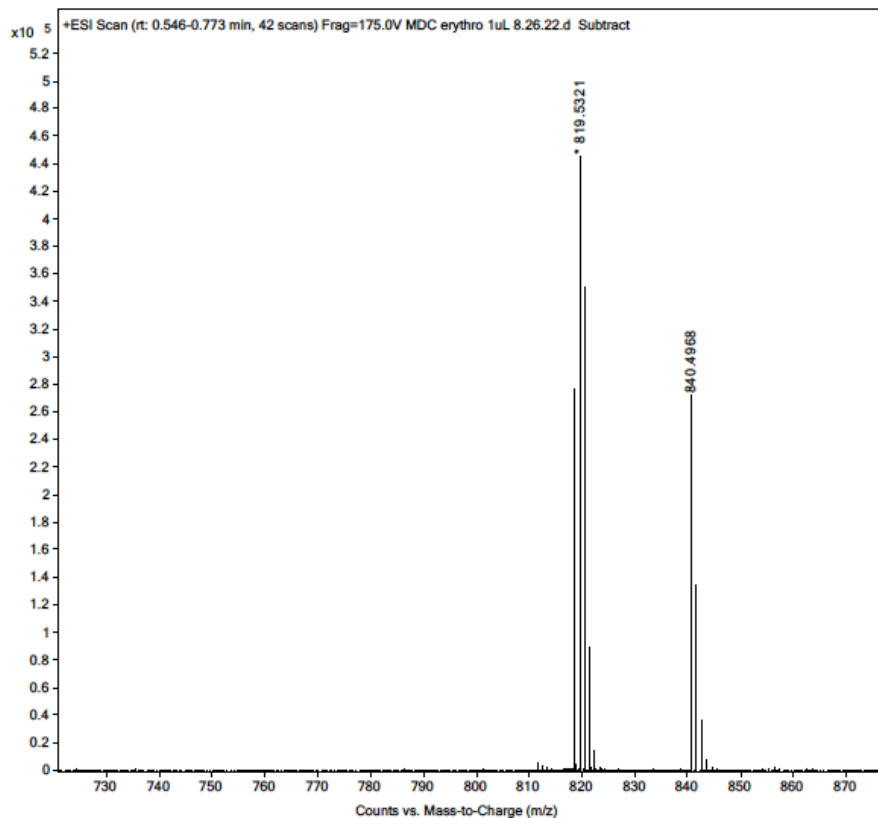
^{1}H-NMR

Eryhtomycine-9-N-azidoacetamide-cdcl3-h1

Scheme S4. Synthesis of N-azidoacetyl-Ciprofloxacin

Chemical Formula: $C_{17}H_{18}FN_3O_3$
Exact Mass: 331.1332
Molecular Weight: 331.3474

Chemical Formula: $C_{19}H_{19}FN_6O_4$
Exact Mass: 414.1452
Molecular Weight: 414.3974

Ciprofloxacin (33.1mg, 0.1 mmol) suspended in anhydrous DMF (1.0mL), to which first DIEA (50uL) was added the stirred for minute prior to addition of Azido-N-hydroxy succinate (20.3mg, 0.102mmol) and the mixture was stirred at room temperature for overnight. Some white fine solid remained undissolved in the mixture. 15.0mL of ethyl acetate was added to reaction mixture followed by 10.0mL of water. The ethyl acetate layer was pale yellow colored while water layer was brownish colored. The ethyl acetate layer was separated, the aq. Layer was once more extracted with ethyl acetate 5.0mL. The combined ethyl acetate layer wash washed with brine, dried over $MgSO_4$ and concentrated on rotary evaporator under reduced pressure. The left-over residue was triturated with ether to obtained white solid. 1H-NMR of white solid indicated presence of unreacted azido acetic acid. The solid was dissolved in 0.5 mL DMSO and diluted with water to total volume of 10 mL. The analytical HPLC showed desired compound at Rt = min. Preparative HPLC using Water:CH_3CN gradient (95:5 from 5 min. 25 min, 100% B for 5 min., total of 35 min run) purified to homogeneity by collected peak at Rt=23.4 min. (monitored at 280 and 320nm) as fractions. Combined fractions were concentrated first on rotary evaporator and then by lyophilized to obtain off white solid (14.7mg).

Molecular weight was confirmed using an Advion Expression® CMS mass spectrometer.
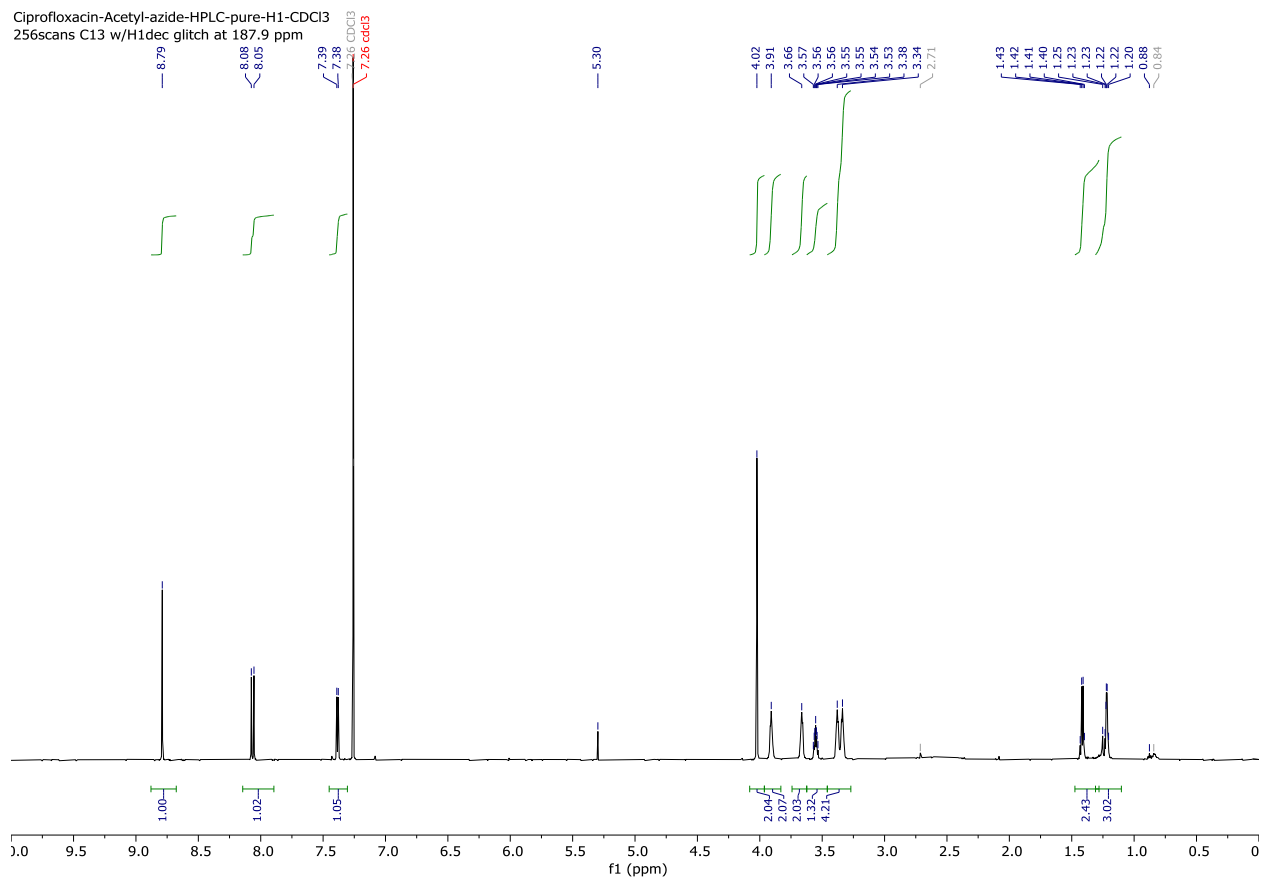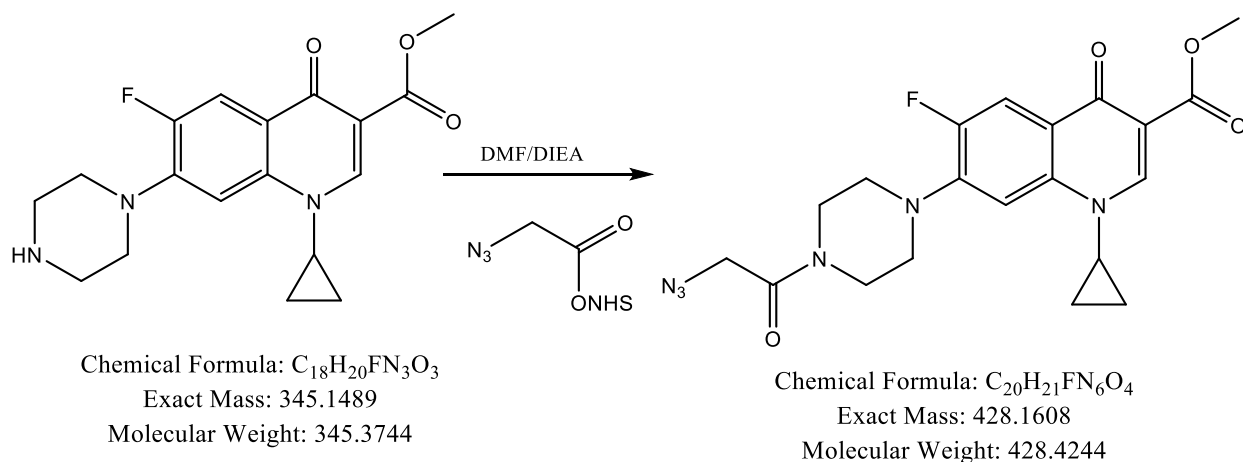
Calculated m/z, 414.4, found m/z, 415.2

Spectrum RT 1.14 - 2.00 {72 scans} - Background Subtracted 0.04 - 1.04
Cipro-N-Azidocarboxyamide-MW414.datx 2022.09.28 20:30:29 Type in summary here;
ESI + Settings for tune mix using source type ESI Positive.   Max: 5E5
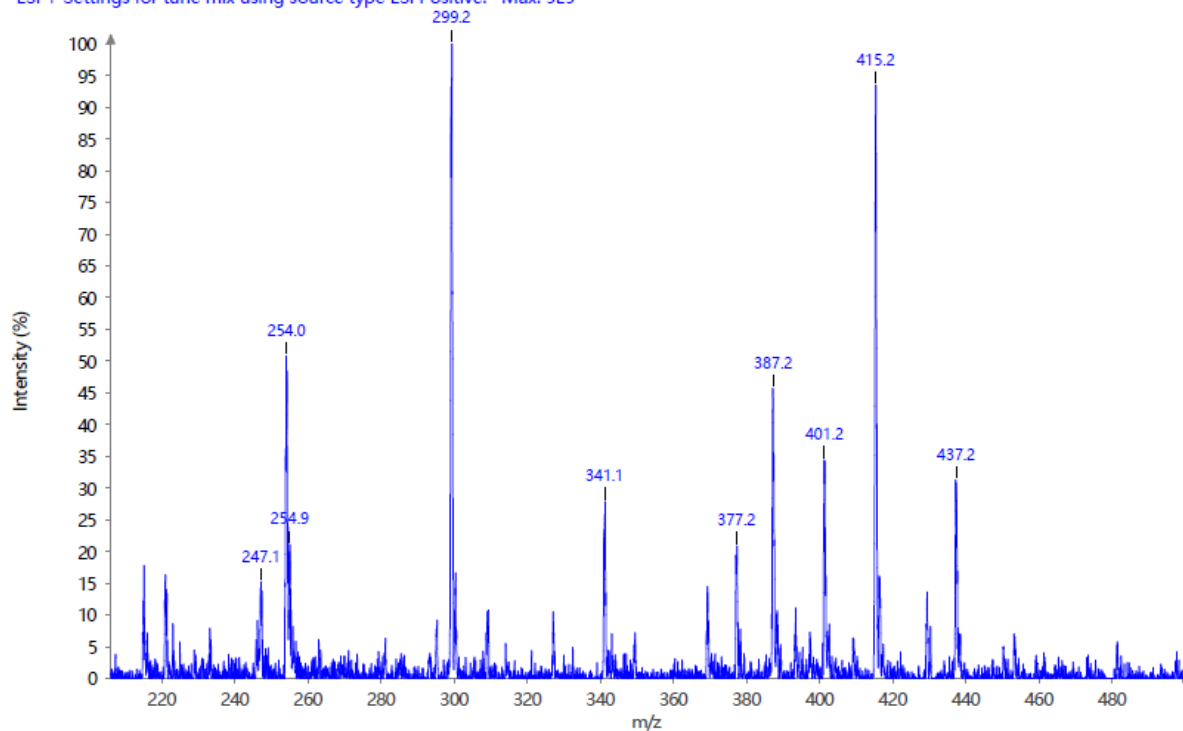
^{1}H-NMR

Ciprofloxacin-Acetyl-azide-HPLC-pure-H1-CDCl3
256scans C13 w/H1dec glitch at 187.9 ppm

8.79
8.08
8.05
7.39
7.38
7.26 CDCl3
7.26 cdcl3
5.30
4.02
3.91
3.66
3.57
3.56
3.55
3.54
3.53
3.38
3.34
2.71
1.43
1.42
1.41
1.40
1.25
1.23
1.22
1.20
0.88
0.84

1.00
1.02
1.05
2.04
2.07
2.03
1.32
4.21
2.43
3.02

f1 (ppm)

Scheme S5. Synthesis of Ciprofloxacin-azidoacetyl methyl ester

Chemical Formula: $C_{18}H_{20}FN_3O_3$
Exact Mass: 345.1489
Molecular Weight: 345.3744

Chemical Formula: $C_{20}H_{21}FN_6O_4$
Exact Mass: 428.1608
Molecular Weight: 428.4244

Ciprofloxacin-methyl ester as white solid was synthesized and characterized as per reported procedure using MeOH, SOCl$_2$. The ciprofloxacin-methyl ester (34.5 mg, 0.1mmol) was dissolved in anhydrous DMF (1.0 mL) and DIEA (50.0uL), followed by Azido-acetic acid NHS ester (25.3mg, 0.13 mmol) were added to it at room temperature and stirred for 4 hr. The TLC analysis indicated formation of new compound. The mixture was then diluted with chloroform (15.0mL), transferred to separatory funnel and washed thoroughly with water, and dil. HCl (0.1M). The organic layer was finally washed with brine, dried over Na$_2$SO$_4$ and concentrated under reduced pressure to yield crude material, which was purified with silica gel column chromatography using chloroform:methanol gradient (98:2), Homogenous fractions as analyzed by TLC were combined and concentrated on rotary evaporator, to afford white solid (32.5mg, 76%),

Molecular weight was confirmed using an Advion Expression® CMS mass spectrometer.

Calculated m/z, 428.4, found m/z, 429.2

Spectrum RT 8.94 - 9.06 {13 scans} - Background Subtracted 6.01 - 8.70
MDC-Ciprofloxacin-Acetylazide1 2021.10.27 18:25:31 Type in summary here;
ESI + Settings for compounds with typical temperature and fragmentation stability using source type ESI Positive. Max: 1.2E7
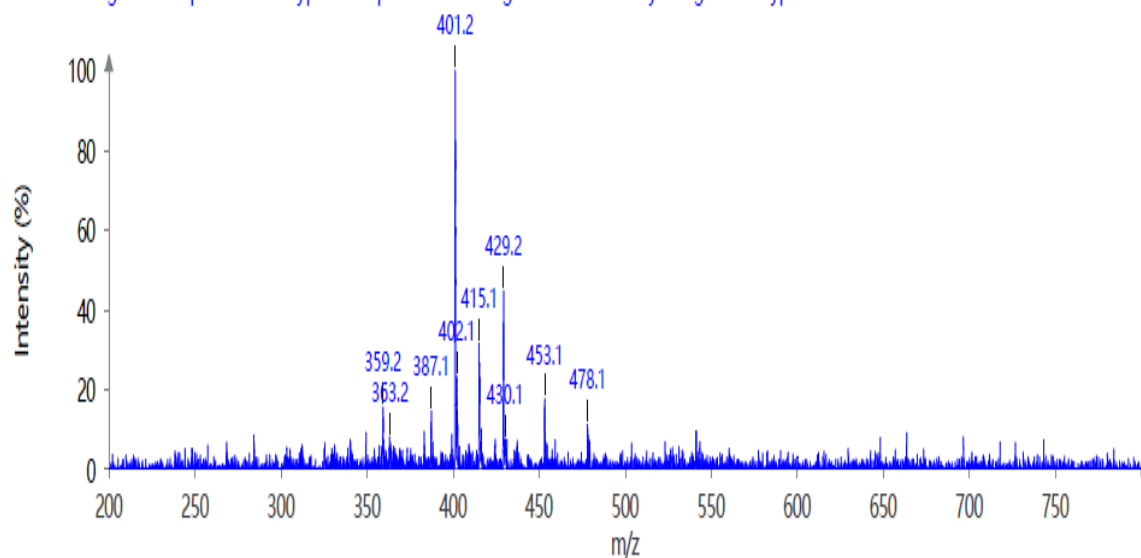
^{1}H-NMR

Ciprofloxacin-Acetyl-azide-pure-2nd-H1-DMSO
256scans C13 w/H1dec glitch at 187.9 ppm